Bifurcations In Reversible Systems With Application To The Michelson System

Kevin N. Webster

August 2003

Bifurcations In Reversible Systems With Application To The Michelson System

A thesis presented for the degree of

Doctor of Philosophy of the University of London

and the

Diploma of Membership for Imperial College

by

Kevin N. Webster

Department of Mathematics

Imperial College London

180 Queen's Gate, London SW7 2AZ

United Kingdom

August 2003

Abstract

This thesis forms a contribution to the development of reversible-equivariant bifurcation theory. Codimension one local and global bifurcations are studied in the setting of purely reversible systems. The work is also partially motivated by the Michelson system,

$$x_{ttt} = c^2 - \frac{1}{2}x^2 - x_t,$$

a reversible dynamical system exhibiting much of the phenomena that are studied. This system is moreover volume-preserving, and many of the results presented in this thesis also extend to the reversible, volume-preserving class.

In particular, the normal forms for the reversible 'Hopf-zero' bifurcation—a local codimension one bifurcation—are computed, and a number of cases identified. This bifurcation occurs in the Michelson system at $c = 0$, and the normal form is computed up to the desired order. It is shown that for small c, the asymptotic form of the system can be computed analytically using the method of multiple time scales.

In a C^2-open subset of vector fields (which include the Michelson system), the formal normal form of the Hopf-zero bifurcation is shown to admit a degenerate family of heteroclinic cycles. It is shown that many heteroclinic cycle bifurcations occur in the unfolding of the singularity in a generic set of one parameter families of such reversible systems. To prove this result, a new Kupka-Smale type theorem for this class of reversible systems is used.

The heteroclinic cycle bifurcation is then studied in the general reversible case, and it is shown that such a heteroclinic cycle generically leads to very rich and complicated dynamics. These results offer explanation for previously numerically observed behaviour in the Michelson system. Two methods are utilised and compared in the analysis: a geometrical approach, using surfaces of section and return maps; as well as deriving explicit bifurcation equations through a function analytic approach using ideas and techniques first introduced by X.-B. Lin.

Acknowledgements

I would like to thank both my supervisors John Elgin and Jeroen Lamb for their enthusiasm, support, ideas and generosity of time. Without their help, this thesis could not have been written.

I would also like to express my gratitude to Jürgen Knobloch of TU-Ilmenau, Germany, for sharing his expertise on the principles and application of Lin's method.

I gratefully acknowledge the support of the Engineering and Physical Sciences Research Council, for financing this three years work.

Finally, thanks to my family and to Franziska for support and encouragement throughout my years at university. Thanks also to friends in and around university, for taking my mind off mathematics every now and then.

Contents

Chapter 1

Introduction

The dynamical behaviour of systems of first order ordinary differential equations can be strongly influenced by special structures appearing in the equations. In this thesis, the consequences of an involutory reversing symmetry are examined for three dimensional vector fields, with an application to the study of simple solutions of the one-dimensional Kuramoto-Sivashinsky equation, see equation (‡).

A system of first order differential equations

$$\dot{x} = f(x), \quad x \in \mathbb{R}^n \tag{$*$}$$

is said to be equivariant if there exists a compact Lie group Γ acting linearly on the $\mathbb{R}^n$ such that if $x(t)$ is a trajectory for the system, then so is $\gamma x(t)$ for all $\gamma \in \Gamma$. It is easy to show that this definition is equivalent to the condition that $\gamma f(x) = f(\gamma x)$, $\forall x \in \mathbb{R}^n$.

The study of equivariant systems is now commonly generalised to reversible-equivariant systems. These are systems which, together with equivariant symmetries as above, may also contain symmetries that reverse the direction of time—that is, if $x(t)$ is a solution of $(*)$ then so is $\tilde{\gamma}x(-t)$, for $\tilde{\gamma}$ in some compact Lie group $\tilde{\Gamma}$. This is equivalent to the condition $\tilde{\gamma}f(x) = -f(\tilde{\gamma}(x))$ for all $\tilde{\gamma} \in \tilde{\Gamma}$.

Symmetries—including equivariance and reversibility—often play an important role in determining the behaviour of a dynamical system. Local steady state bifurcations in the general (dissipative) case typically require to be codimension two in order to admit complicated (chaotic) dynamics. However, in the presence of additional structure, a degenerate phenomenon in the dissipative case may become generic, and it is possible for codimension one bifurcations to exhibit complicated dynamics. Equivariant symmetries in ordinary differential equations have been studied extensively in connection with bifurcation theory [37, 42, 43, 44, 93, 109]. The study of reversible symmetries in dynamical systems has had a more recent development. A common example of systems with symmetries arises in Hamiltonian systems, in the case where the Hamiltonian $H(p, q)$ satisfies $H(p, q) = H(-p, q)$. In this case the $\mathbb{Z}_2$ representation $R = \text{diag}(-I, I)$ is a reversing symmetry for the equations of motion. In fact many of the properties associated specifically with Hamiltonian systems have been shown to arise also in even-dimensional reversible systems [31, 83, 95, 96, 110].

A more general reversible-equivariant bifurcation theory is currently being developed [68, 69, 70, 71]. The strategy in this research is to study first steady state bifurcation in the presence of a general reversible-equivariant symmetry group. It is then possible to reduce the problem of periodic orbit (and relative periodic orbit) bifurcation to the steady state problem, see [70]. It remains to study bifurcations of homoclinic and heteroclinic orbits in the same manner. The work in this thesis also contributes to this end.

This thesis is also partially motivated by the study of the Michelson system,

$$y_{ttt} = c^2 - \frac{1}{2}y^2 - y_t, \tag{†}$$

which is derived from the study of travelling wave solutions of the Kuramoto-Sivashinsky (K-S) equation,

$$u_t + u_{xxxx} + u_{xx} + uu_x = 0. \tag{‡}$$

The K-S equation has been extensively studied in an effort to understand the complex dynamical behaviour exhibited in nonlinear partial differential equations. Equation (‡) models various physical processes such as propagation of concentration waves in Belousov-Zhabotinsky chemical reactions [67]; thin viscous film flow down inclined planes [19, 20] and flame fronts in combustion [81, 99]. Solutions are often sought in the case of periodic boundary conditions, that is, $u(x+L,t) = u(x,t)$ for any t, with the period L as a control parameter.

This thesis is organised as follows:

Chapter 2. Here we introduce the Michelson system, and give an overview of work undertaken and what is known about the system. We show how it may be derived from the Kuramoto-Sivashinsky equation in the study of simple solution types, as travelling wave or steady state solutions. Basic properties of the system are presented, together with some important consequences of these properties. We collect together previous results for the Michelson system, including a useful global perspective of the dynamics in a certain parameter range by Lau [73]. There, the effects of a tangle of heteroclinic orbits in the system is studied, and numerical evidence is given for the existence of a Smale horseshoe. This numerical work explains the previous numerical observation of a near-simultaneous creation of many periodic orbits, not all of which can be explained by local bifurcations. We also identify other numerically observed phenomena that will be studied in this thesis.

Chapter 3. In this chapter we present an account of the reversible Hopf-Zero bifurcation, where a steady state, invariant under the reversing symmetry action, has a zero and a purely imaginary pair of eigenvalues. This situation typically arises in one parameter families of purely reversible vector fields, such as the Michelson system at $c = 0$. The theory here is also presented for the cases of volume-preserving, and reversible volume-preserving vector fields.

This work is a natural extension of existing theory—the analysis for the dissipative and volume preserving case is contained in [13, 14, 29, 39, 49]. For each case considered here, the formal normal form displays a degenerate family of heteroclinic cycles up to arbitrarily high order in an open set of unfoldings. We use the method of multiple time scales to show that the Michelson system has a particularly simple solution structure in the normal form, and that it is possible to provide asymptotic analytic forms for all bounded orbits in the Michelson system for small c. Techniques of 'flat' perturbation theory (as in [14]) are then adapted to the reversible case and applied to show that typical unfoldings of this singularity under the asserted open conditions lead to a cascade of heteroclinic and homoclinic bifurcations, see Theorems 3.4.1 and 3.4.2. This proof requires a new modified Kupka-Smale type theorem, and an account of this is given, together with further generic properties of purely reversible, and reversible volume-preserving three dimensional systems, see Theorems 3.5.4 and 3.5.5. This work is a generalisation of results presented in [91] for the case of volume-preserving systems.

Chapter 4. The heteroclinic cycle bifurcation found to exist typically in the unfolding of the Hopf-Zero bifurcation is independently studied in this chapter, using geometrical methods. We set up convenient Poincaré sections around the configuration, and derive return maps for the study of the local dynamics about such a cycle under generic (open and dense) conditions. This analysis is original to the study of the heteroclinic cycle bifurcation in reversible systems, although some results presented here have been obtained for the general (dissipative) case, see [16, 17]. It is shown that there locally exists very rich dynamics, including cascades of infinitely many more heteroclinic and homoclinic orbits, as well as the existence of countably many one parameter families of periodic orbits, see Theorems 4.1.1–4.1.4. An organising centre for the dynamics is given by the presence of a 'symmetric horseshoe' at the critical parameter value— for any given $n \in \mathbb{N}$, there exists a uniformly hyperbolic set which is setwise invariant under the reversing symmetry action, indecomposable and topologically conjugate to a full Bernoulli shift on n symbols, see Theorem 4.1.5. Each of these sets is structurally stable. However, the union of all of these sets is not uniformly hyperbolic (due to a singular point in the return maps), and countably many of these sets are destroyed with an arbitrarily small perturbation.

Chapter 5. Here the same heteroclinic cycle bifurcation is studied using an alternative, analytical approach. This is based on ideas first developed by X.-B. Lin [74], but exploits more recent results in the development of Lin's method and adapts them to the reversible case. This method also sets up surfaces of section around the heteroclinic cycle, but uses a function analytic approach to prove the existence and uniqueness of piecewise smooth solutions that spend a given time between sections, and which have a possible discontinuity (or 'jump') in the sections, in a specified direction. This principle can be used to derive explicit bifurcation equations for all bounded orbits close to the heteroclinic cycle. The analysis of the bifurcation equations shows that the existence of homoclinic, heteroclinic and periodic orbits can be deduced, as well as the existence of a set of orbits which are topologically conjugate to a full shift on n symbols, for any $n \in \mathbb{N}$. These results are summarised in Theorem 5.6.2.

Chapter 2

The Michelson System

In this chapter we study the properties of the third order equation

$$x_{ttt} = c^2 - \frac{1}{2}x^2 - x_t, \tag{2.1}$$

where the suffix t denotes differentiation with respect to time, and c is a parameter. This equation is usefully cast as the following third order dynamical system:

$$\begin{aligned} \dot{x} &= y, \\ \dot{y} &= z, \\ \dot{z} &= c^2 - \frac{1}{2}x^2 - y, \end{aligned} \tag{2.2}$$

where here the dot denotes differentiation with respect to time. This system has become known as the Michelson system, following the first thorough analysis of the system in 1986 [80]. The dynamics of (2.2) vary from simple behaviour to a diverse solution structure including a wealth of homoclinic, heteroclinic, periodic and aperiodic solutions and chaotic dynamics. We first provide the importance of the system as a derivation from the Kuramoto-Sivashinsky equation.

2.1 The Kuramoto-Sivashinsky Equation

The one-dimensional Kuramoto-Sivashinsky (K-S) equation

$$u_t + uu_x + u_{xx} + u_{xxxx} = 0 \tag{2.3}$$

has been studied extensively in the effort to understand the complicated dynamics in nonlinear partial differential equations (PDEs). We will consider equation (2.3) on periodic boundary conditions, $u(x,t) = u(x+L,t)$ (with L as a parameter). There is a rigorous proof of an inertial manifold [38, 85] for equation (2.3) which makes this equation effectively equivalent to a finite-dimensional system for long time behaviour. Estimates of the dimension of the latter are discussed in [85]. This, together with the fact that it is a scalar equation, makes it a paradigm for the study of rich spatiotemporal dynamics in one-dimensional PDEs, and thus the K-S equation has been well-studied numerically. In particular, Kevrekidis *et al.* [61], Demekhin *et al.* [30] and Hyman & Nicolaenko [55] reported a rich and diverse variety in the nature of the solutions to the K-S equation on periodic boundary conditions, as the control parameter L is varied. This ranges from reported 'chaos'—where no discernible regular spatiotemporal pattern is observed—to a simple time-independent steady state, with periodic, quasiperiodic and heteroclinic/homoclinic structures in between. Heteroclinic cycles have also been identified analytically in [3] in a centre-unstable manifold reduction. More recently, these heteroclinic cycles have been studied in [27, 84]. Christiansen *et al.* [24] argued that the unstable periodic/travelling wave solutions of the K-S equation are instrumental in 'ordering' the complex spatiotemporal features observed in numerical studies. There, the authors extended cycle expansion techniques utilised within a dynamical ζ-function formalism for low dimensional systems to the K-S equation. In particular, a cycle expansion technique was used to determine Liapunov exponents.

Equation (2.3) has the following translational symmetry:

$$\xi = x + x_0, \quad \tau = t, \quad \tilde{u} = u, \tag{2.4}$$

as well as the Galilean symmetry

$$\xi = x - \gamma t, \quad \tau = t, \quad \tilde{u} = u - \gamma, \tag{2.5}$$

where in both cases the equation for $\tilde{u}(\xi, \tau)$ is identical to (2.3).

It is now well known that unstable periodic orbits are an effective means of studying the properties of hyperbolic deterministic dynamical systems of low intrinsic dimension [6, 7, 24, 25, 117]. The recurrent spatiotemporal patterns observed in numerical simulations of the K-S equation have an interpretation in terms of special, unstable periodic solutions. The notion is not dissimilar to that used to describe observed dynamics in low-dimensional systems—such as the Lorenz equations—where an orbit will 'shadow' an unstable periodic orbit for a time before diverging from it. In this way it is useful to study the simple behaviours of (2.3), such as the travelling wave solutions of the form $u = u(x - vt)$, and the steady-state solutions.

We begin by substituting $\tilde{u} = u(\psi)$, where $\psi = x - vt$. Then equation (2.3) transforms to

$$-v\tilde{u}_\psi + \tilde{u}\tilde{u}_\psi + \tilde{u}_{\psi\psi} + \tilde{u}_{\psi\psi\psi\psi} = 0.$$

Thus we obtain an ODE from (2.3). This can be rewritten as a one-dimensional system by the change of variables $X = \tilde{u}$, $Y = \tilde{u}_\psi$, $Z = \tilde{u}_{\psi\psi}$ and $W = \tilde{u}_{\psi\psi\psi}$. Then

$$\begin{aligned} X_\psi &= Y, \\ Y_\psi &= Z, \\ Z_\psi &= W, \\ W_\psi &= vY - XY - Z. \end{aligned}$$

Integrating the last equation once gives

$$Z_\psi = vX - Y - \frac{1}{2}X^2 + \text{constant}.$$

We remove the constant by taking $X, Y, Z, W = 0$ to be a valid solution for all v. Now under the transformation $x = X - v$, $y = Y$, $z = Z$, $t = \psi$ we obtain the system

$$\dot{x} = y, \tag{2.6}$$

$$\dot{y} = z, \tag{2.7}$$

$$\dot{z} = \frac{v^2}{2} - \frac{1}{2}x^2 - y, \tag{2.8}$$

where the dot as before denotes differentiation with respect to time. Thus we have derived the Michelson system (2.2) with $v = c\sqrt{2}$.

We may also search for steady-state solutions; that is, solutions of the form $u(x,t) = u(x)$. Then $u_t = 0$ and we have

$$\frac{1}{2}(u^2)_x + u_{xx} + u_{xxxx} = 0$$

and by integrating once we obtain

$$\frac{1}{2}u^2 + u_x + u_{xxx} = c^2, \tag{2.9}$$

where c^2 is an integration constant. The above is identical to the Michelson ODE (2.1) with $t = x$ and $x = u$. We will see in section 2.2 why it is sensible to define the integration constant to be nonnegative: for negative values of the integration constant the corresponding ODE has no bounded solutions. Also it is clear from this simple derivation why the Michelson system is reversible (see section 2.2.1). The K-S equation has the following 'reversing' symmetry transformation

$$u \to -u, \qquad x \to -x, \qquad t \to t, \tag{2.10}$$

which leave equation (2.3) invariant. This symmetry trivially filters through to equation (2.9).

Clearly the reason that two different solution types lead to the same equation is the Galilean symmetry (2.5), which can bring any travelling wave solution trivially to rest, and so steady-state solutions and travelling wave solutions are symmetric images of each other.

It is interesting to note that in fact Michelson did not derive the system (2.2) from either of the previous two substitutions. His derivation is based on another common version of the K-S equation,

$$w_t + \frac{1}{2}w_x^2 + w_{xx} + w_{xxxx} = 0, \tag{2.11}$$

which is related to (2.3) by $u = w_x$ and integrating. Physically, the two forms of the K-S equation model different things; equation (2.3) models small disturbances in liquid films falling down an inclined or vertical plane [19, 20] and propagation of concentration waves in Belousov-Zhabotinskii chemical reactions [67], where equation (2.11) models instabilities in laminar flame fronts [81, 99]. Under the transformation

$$\xi = x - \gamma t, \quad \tau = t, \quad \tilde{w} = w - \beta t - \gamma\xi, \tag{2.12}$$

equation (2.11) becomes

$$\tilde{w}_\tau + \frac{1}{2}\tilde{w}_\xi^2 + \tilde{w}_{\xi\xi} + \tilde{w}_{\xi\xi\xi\xi} = \frac{1}{2}\gamma^2 - \beta.$$

If $\frac{1}{2}\gamma^2 = \beta$, then the above equation is identical to (2.11), and (2.12) is the Galilean symmetry to (2.11) corresponding to (2.5) with $\gamma = v$. Michelson's derivation is motivated by the observation in numerical studies that the K-S equation (2.11) exhibits an approximately constant drift [81]—on the assumed periodic boundary conditions $w(x,t) = w(x+L,t)$, the mean value of the solution $< w(x,t) >:= (1/L)\int_0^L w(x,t)dx$ satisfies the drift equation

$$\frac{\mathrm{d}}{\mathrm{d}t} < w(x,t) >= -\frac{1}{2L}\int_0^L (w_x)^2 dx \ \approx -c_0^2,$$

where $c_0^2 \approx 1.2$ is a constant independent of the initial condition. Hence we substitute a solution of the form

$$w(x,t) = -c^2 t + \varphi(x),$$

with $< \varphi(x,t) >$ close to zero, and c a parameter. Then we obtain the following ODE for $\varphi(x)$:

$$-c^2 + \varphi_{xxxx} + \varphi_{xx} + \frac{1}{2}(\varphi_x)^2 = 0$$

Now substituting $t = x$ and $x = \varphi_t$, $y = \varphi_{tt}$, $z = \varphi_{ttt}$, we arrive once more at the ODE (2.1). This is clear since solutions of the form $w(x,t) = -c^2 t + \varphi(x)$ correspond to steady states for $u(x,t)$.

We can extract the equations for the drifting solutions of the type $w(x,t) = -c^2 t + \varphi(x)$ from the general Galilean transformation (2.12) by setting $\tilde{w}_\tau = 0$ and $\beta = -c^2$, $\gamma = 0$. We may also substitute $\gamma = v$, $\beta = 0$ and $\tilde{w}_\tau = 0$ into (2.12) to search for travelling wave solutions, and derive equation (2.7).

2.2 Basic Properties

Here we summarise important properties of the Michelson system (2.2):

$$\begin{aligned}\dot{x} &= y \\ \dot{y} &= z \\ \dot{z} &= c^2 - \frac{1}{2}x^2 - y.\end{aligned}$$

2.2.1 Reversibility

The Michelson system is invariant under the following phase space transformation, together with a time reversal:

$$(x, y, z, t) \longrightarrow (-x, y, -z, -t).$$

Thus the Michelson system belongs to the class of reversible systems. We define the involution $R \in GL(3, \mathbb{R})$ as

$$R = \begin{bmatrix} -1 & 0 & 0 \\ 0 & 1 & 0 \\ 0 & 0 & -1 \end{bmatrix}. \tag{2.13}$$

Now if we write (2.2) in the form

$$\dot{\mathbf{x}} = f(\mathbf{x}, c), \qquad \mathbf{x}(\cdot) := (x(\cdot), y(\cdot), z(\cdot)) \in \mathbb{R}^3,$$
$$f(\mathbf{x}, c) = \begin{bmatrix} y \\ z \\ c^2 - \frac{1}{2}x^2 - y \end{bmatrix}, \tag{2.14}$$

then it is easily verified that

$$Rf(\mathbf{x}) = -f(R\mathbf{x}). \tag{2.15}$$

This is precisely the condition that guarantees that R is a reversing symmetry, see [71].

An important set in the phase space of reversible systems is the set of points that are left invariant under the symmetry action, in this case (2.13). These points are defined as Fix R:

$$\text{Fix } R := \{\mathbf{x} \in \mathbb{R}^3 \ : \ R\mathbf{x} = \mathbf{x}\}, \tag{2.16}$$

in the Michelson system this set is precisely the y-axis. Two basic properties of the class of such reversible systems regards the existence of symmetric fixed points and periodic orbits. These are points/orbits that are setwise invariant under the action of R. Reversible systems of this type (3 dimensional reversible vector fields where dim Fix $R = 1$) have the property that they do not generically possess symmetric fixed points. To see this, note that for each $\mathbf{x} \in \mathbb{R}^3$ we may write

$$\begin{aligned} \mathbf{x} &\equiv \frac{1}{2}(I + R)\mathbf{x} + \frac{1}{2}(I - R)\mathbf{x} \\ &:= \mathbf{x}_1 + \mathbf{x}_2, \end{aligned}$$

where $\mathbf{x}_1 \in$ Fix R and $\mathbf{x}_2 \in$ Fix $(-R)$. Thus Fix $(-R)$ is necessarily two dimensional. It is easily checked that

$$f : \text{Fix } R \to \text{Fix } (-R),$$

and now since Fix R is one dimensional and Fix $(-R)$ is two dimensional, f will not typically have zeros on Fix R. This may be formalised through Thom's Transversality Theorem. A general account of such properties for reversible-equivariant systems is the subject of current research.

However, isolated symmetric fixed points are generic in one parameter families of these reversible systems, as in the Michelson system, see also section 3.2. On the other hand, symmetric periodic orbits are generic (codimension zero) in this class of reversible systems, and moreover they appear generically isolated in phase space. We may intuitively expect that this is correct: symmetric periodic orbits intersect Fix R precisely twice, see Lemma 4.4.1. Now if we consider the return map F of a symmetric period orbit with section S, this will be a two dimensional map. Moreover, F is reversible: if R_S is R restricted to S, then $F \circ R = R \circ F^{-1}$, where in the section S, Fix R_S is one dimensional. Then we may expect $F(\text{Fix } R)$ and Fix R to intersect transversally. This result is proved formally in section 3.5, and means that a regular bifurcation analysis of the periodic orbits of the Michelson system is possible, similar to that carried out by Colin Sparrow for the Lorenz equations [101]. Such a bifurcation analysis for the Michelson system was studied by Kent [57] (and further developed in [47]), and revealed a rich and complicated solution structure. Aspects of this work are summarised in section 2.3.

There is by now a relatively large literature on reversible systems (e.g. [31, 68, 71, 83, 95, 96, 110]). Many of the early studies on reversible systems concentrated on the case of a $2m$-dimensional phase space with dim Fix $R = m$. It is interesting to note that although the Michelson system does not fit into this category, with the addition of the parameter c to the phase space it becomes 4 dimensional with dim Fix $R = 2$. Results in the following chapters at times appear to display characteristics of such a reversible system (Liapunov Centres, Blue Sky Catastrophe). However the Michelson system is a degenerate example of such a system, since it is really three dimensional.

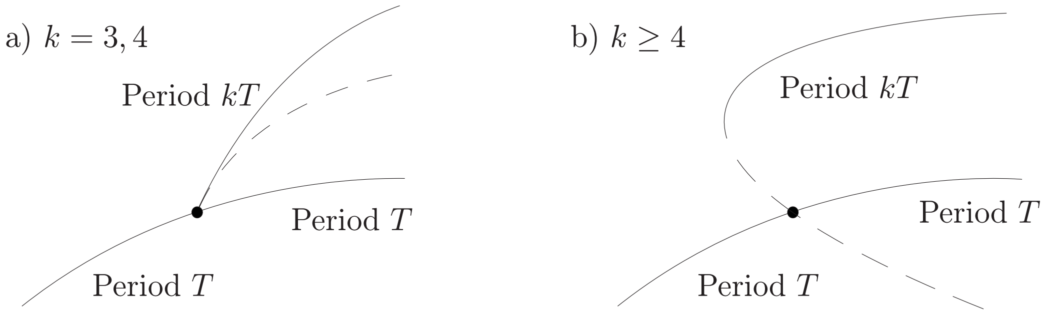

Figure 2.1: Bifurcation diagrams for period k-multiplying bifurcations given in [75]. When $k = 4$ there are two possibilities. Branches of elliptic periodic orbits are solid lines, hyperbolic periodic orbits are dashed.

This symmetry plays an important role in organising the dynamical behaviour seen in (2.2), and this thesis is largely motivated by the problem of studying systems which have such a symmetry.

2.2.2 Volume Preserving Flow

The flow of the Michelson system is divergence-free; that is,

$$\text{div } (\dot{x}, \dot{y}, \dot{z}) = 0. \tag{2.17}$$

Properties of divergence-free systems have been studied, for example, in [10, 11, 77, 91]. Although the work in this thesis does not focus on the aspects specifically due to the volume-preserving nature of the Michelson system, many of the results presented here in the context of reversible systems are equally valid in the case where additional volume-preserving structure is present.

Due to (2.17), we can use a result in [22] to show that the product of the Floquet multipliers of a periodic orbit of period T is equal to 1:

$$\Pi_i \mu_i = \mu_1 \mu_2 \mu_3 = \exp \left\{ \int_0^T \text{div } f(\mathbf{x}(t), c) dt \right\} = 1,$$

with μ_3 the trivial multiplier equal to one, so the nontrivial Floquet multipliers of an elliptic periodic orbit are complex conjugate pairs on the unit circle, which move as the parameter c is varied, passing through infinitely many roots of unity. We note that this condition on the eigenvalues is also enforced by the symmetry (2.15) for the symmetric periodic orbits, since the return map for a setwise R-invariant transverse section Σ to the periodic orbit will be a *reversible map* [71]—that is, if R_Σ is the restriction of R to Σ, and $\phi(\mathbf{y})$ ($\mathbf{y} \in \Sigma$) is the return map, then

$$R_\Sigma \circ \phi(\mathbf{y}) = \phi^{-1}(R_\Sigma \circ \mathbf{y}).$$

Moreover, according to Mackay [77], the return map of a volume-preserving vector field f to any transverse section S preserves the 'area' $f.dS$, and so is an area preserving map. Therefore we can expect many of the features of area-preserving maps (see e.g. [48, 75, 79]) to be present in the Michelson system, including period k-multiplying bifurcations of periodic orbits, see Figure 2.1. In [75] it is noted that in the case b) of Figure 2.1, the branch of hyperbolic orbits emanating from the bifurcating periodic orbit is often seen to undergo a tangent bifurcation. This is also true in numerical observations of the Michelson system, see section 2.3. This subharmonic branching behaviour is also typical due to the reversing symmetry, and the analysis in the reversible case [5, 95] is also valid for the study of symmetric periodic solutions, through the Takens normal form approach, see Theorem 2.3.2. We expect that this branching behaviour is also generic in reversible volume-preserving systems, as it appears in the Michelson system.

2.2.3 Equilibria and Liapunov functions

The Michelson system has the fixed points

$$A = (-c\sqrt{2}, 0, 0), \qquad B = (c\sqrt{2}, 0, 0). \tag{2.18}$$

The eigenvalues of the fixed point A, say, are given by the characteristic polynomial

$$\lambda^3 + \lambda - c\sqrt{2} = 0.$$

Using Cardan's formula [18], we can write the eigenvalues of A as $\lambda = \alpha$ and $\lambda = -\frac{1}{2}\alpha \pm \mathrm{i}\sqrt{1+\frac{3}{4}\alpha^2}$, where $\alpha \in \mathbb{R}^+$ is given by

$$\alpha = \sqrt[3]{\frac{c}{\sqrt{2}} + \sqrt{\frac{c^2}{2} + \frac{1}{27}}} + \sqrt[3]{\frac{c}{\sqrt{2}} - \sqrt{\frac{c^2}{2} + \frac{1}{27}}},$$

so the fixed point is hyperbolic for $c > 0$, and has a two dimensional stable focus manifold and a one dimensional unstable manifold. By the reversibility, the fixed point B has the same eigenvalues as A but with a change of sign (the characteristic polynomial for the fixed point B is $\lambda^3 + \lambda + c\sqrt{2} = 0$). Thus B is also a saddle focus fixed point for $c > 0$, with a two dimensional unstable focus manifold, and a one dimensional stable manifold.

At $c = 0$ there is just one fixed point at the origin, which has eigenvalues equal to $0, \pm\mathrm{i}$. This is a 'Hopf-zero' bifurcation, and the study of this bifurcation will be the subject of Chapter 3.

The Michelson system has the observed property that most orbits are unbounded and escape to infinity. Consideration of the Liapunov function

$$L = x + z, \qquad \dot{L} = c^2 - \frac{1}{2}x^2,$$

implies that at $c = 0$ the only bounded orbit is the fixed point at the origin. We can also easily see, using the same Liapunov function, that if we choose a constant in place of c^2 that is negative, then there are no bounded orbits at all. This is the reason in section 2.1 that the integration constant was taken to be nonnegative in the derivation of the steady-state equations.

The equations (2.2) can be rescaled by the following transformation:

$$(x, y, z, t) \to \left(\frac{x}{\sqrt{2}c}, \frac{y}{\sqrt[3]{2}c^{\frac{4}{3}}}, \frac{z}{\sqrt[6]{2}c^{\frac{5}{3}}}, \frac{tc^{\frac{1}{3}}}{\sqrt[6]{2}} \right),$$

to give in the limit of $c \to \infty$, the system

$$\begin{aligned} \dot{x} &= y \\ \dot{y} &= z \\ \dot{z} &= 1 - x^2. \end{aligned} \tag{2.19}$$

The above equations have the Liapunov function

$$L = \frac{1}{3}x^3 - x + yz, \quad \dot{L} = z^2 \geq 0.$$

Consideration of this function implies the non-existence of periodic solutions, and the restriction that the only possible bounded solutions are connecting heteroclinic orbits with ω-limit set (-1,0,0) and α-limit set (1,0,0); these are heteroclinic orbits lying in the intersection of the two 2-dimensional manifolds $W^s(A)$ and $W^u(B)$, where in the rescaled variables $A = (-1, 0, 0)$ and $B = (1, 0, 0)$. In fact, there are more results on the behaviour of the Michelson system for large c, which are summarised in the next section.

2.3 Previous Results

2.3.1 Unique heteroclinic connection

The system (2.19) has been studied by McCord [78], who proved that there exists a unique heteroclinic connection from B to A, lying in the intersection of the two 2-dimensional manifolds. This result has been generalised to a larger class of systems by Toland [106], who proved the following:

Theorem 2.3.1 (Toland). *Consider the equation*

$$-u''' = f(u), \qquad u = u(x), \tag{2.20}$$

and suppose that f is locally Lipschitz continuous on $[-\alpha, \alpha]$ with $f(\pm\alpha) = 0$ and $f > 0$ on $(-\alpha, \alpha)$. Then there exists (up to translation in x) a unique bounded solution of (2.20)*. This solution satisfies*

$$\lim_{x \to \pm\infty} u(x) = \pm\alpha.$$

Michelson proved that this heteroclinic orbit persists as c is decreased from infinity in (2.2), and is unique for all c greater than some finite c_0 [80]. It is conjectured in [60, 80] that this heteroclinic orbit exists for all $c \in (0, \infty)$. This agrees with numerical observations, and with the work carried out in Chapter 3 for c close to zero.

2.3.2 Small c

At $c = 0$ there is a unique fixed point at the origin in the Michelson system. This fixed point is nonhyperbolic, and has eigenvalues equal to $0, \pm \mathrm{i}$. We will call this type of bifurcation a 'Hopf-zero' bifurcation. Chang [20] has undertaken a normal form analysis up to second order for the Michelson system at $c = 0$, and found a degenerate one parameter family of heteroclinic cycles between the two fixed points for $c > 0$, and a one parameter family of invariant tori. However, this analysis does not comment on the effect of the addition of any higher order terms. This problem is dealt with in chapter 3, where we present a general study of the reversible Hopf-zero bifurcation, together with the derivation of an asymptotic analytic form of all bounded solutions in the formal normal form of the Michelson system in section 3.3. Also appearing in Chang's analysis is a single elliptic periodic orbit. In fact, this periodic orbit has been found previously by Michelson [80], where he proved it's existence by a series in sines for small c:

$$x(t) = 2c \sin \Omega t - (c^2/6) \sin 2\Omega t + (c^3/144) \sin 3\Omega t + \cdots , \tag{2.21}$$

where $\Omega = 1 - c^2/12 + \cdots$. This periodic orbit is also found by Liapunov-Schmidt reduction in section 3.1, and a truncated form is found in section 3.3. It is part of the 'noose bifurcation' [59], discussed in section 2.3.3.

2.3.3 Periodic Orbits

Kent & Elgin [57, 58, 59, 60] have carried out an extensive bifurcation analysis of the Michelson system. They used the periodic orbit (2.21) as a starting point for the continuation code AUTO, and studied the periodic solution structure emanating from many of the local bifurcations of (2.21).

We would first like to study what generic local bifurcations we may observe in a bifurcation analysis of the periodic orbits of the Michelson system. The properties of local bifurcations of symmetric periodic solutions can be studied by work carried out in [68], and using the Takens Normal Form [70, 104]. The Takens Normal Form is a very useful approach which enables the study of local bifurcations of maps to be reduced to the study of local bifurcations of vector fields. This may be applied to the return map of a bifurcating periodic orbit.

Theorem 2.3.2. *Consider a C^r R-reversible, area-preserving map $F : \mathbb{R}^2 \to \mathbb{R}^2$ (we assume that the reversing symmetry preserves the area) which has a fixed point at the origin, $F(0) = 0$. We may write $DF|_0 = Se^{B+N}$, such that*

1. *S, B are semi-simple (complex diagonalisable) and N is nilpotent,*
2. *S, B and N all commute with each other,*
3. *S, e^B, e^N are reversible and area-preserving,*
4. *$S^{2k} = I$,*
5. *B has no eigenvalues in $\pi i\mathbb{Q} - \{0\}$.*

Then there exists an R-equivariant, area preserving change of coordinates T such that for any m,

$$T^{-1} \circ F \circ T \quad \textit{and} \quad S \circ \phi_1$$

have the same Taylor expansion up to order m at the origin, where ϕ_1 is the time-one map of an S-equivariant, reversible, divergence free vector field X, where $X(0) = 0$ and $DX|_0 = B + N$. Without loss of generality, X can be chosen to be in normal form.

This Theorem is a reversible-volume preserving version of Takens' original Theorem [104]. In [70], the original result is generalised to the case that the map F possesses a reversible-equivariant symmetry group Σ and it has been shown that the coordinate change T can be chosen to be Σ equivariant, and that the vector field X is also symmetric with respect to Σ. To obtain Theorem 2.3.2 we may combine this work with results of Broer [11], where it was shown that the Takens Normal Form may also preserve a given Lie algebra structure. We may also use this Theorem in the case of unfoldings, by using the usual extended phase space with the inclusion of the parameter. In the general case the periodic orbit may possess spatiotemporal symmetry, and the reduction to the study of the vector field requires to take this into account, see [70]. In the case of the Michelson system the reversible-equivariant symmetry group is simply the reversing symmetry (2.13). We will use Theorem 2.3.2 to illustrate the expected behaviour of the simple local bifurcations of symmetric periodic solutions in the Michelson system—namely, the saddle-node, symmetry breaking and period doubling bifurcations. We note that in each case we consider, we have $B = 0$.

Recall the relation between the multipliers of symmetric periodic orbits, they must be of the form μ, $1/\mu$ and the trivial Floquet multiplier equal to 1. Let $P(y_0, z_0)$ be the return map about a symmetric periodic orbit, with respect to an R-invariant section plane, which is bisected by Fix R. Clearly we can choose local coordinates (y, z) on this section plane, and the reversing symmetry R acts on the section as $R(y, z) = (y, -z)$.

Consider first the case of both nontrivial multipliers equal to 1. Generically (codimension 1) [54] the Jordan normal form of the linear part of the return map for this periodic orbit will be either

$$L_1 = \begin{bmatrix} 1 & 1 \\ 0 & 1 \end{bmatrix} \qquad \text{or} \qquad L_2 = \begin{bmatrix} 1 & 0 \\ 1 & 1 \end{bmatrix}.$$

It is important to distinguish between these two cases, as they are not equivalent due to the presence of the reversing symmetry. In the case of L_1, we have

$$S_1 = \begin{bmatrix} 1 & 0 \\ 0 & 1 \end{bmatrix}, \qquad N_1 = \begin{bmatrix} 0 & 1 \\ 0 & 0 \end{bmatrix},$$

where S_1 is semi-simple and N_1 is nilpotent. Examining R-equivariant vector fields now with linear part equal to N_1, we refer to [68], where it is shown that the normal form is

$$\begin{aligned} \dot{y} &= z \\ \dot{z} &= g(y), \end{aligned}$$

where $g(0) = D_y g(0) = 0$. Note that this normal form is also volume-preserving. A generic unfolding of this bifurcation that preserves the symmetry may be written

$$\begin{aligned} \dot{y} &= z \\ \dot{z} &= \mu + y^2, \end{aligned} \tag{2.22}$$

where μ is the bifurcation parameter. This leads to a saddle-node bifurcation, as in Figure 2.2. As S_1 is equal to the identity we may now apply Theorem 2.3.2 to conclude that the return map for the periodic orbit will generically behave like the time-one map of the vector field (2.22), up to any finite order. However, there are degenerate structures in this vector field that we expect would break under addition of higher order terms in the return map. In particular, the homoclinic loop in Figure 2.2 will generically break and yield transverse intersections for the return map, leading to chaotic dynamics locally (see also section 3.5). This is also in agreement with the presence of k-bifurcations (subharmonic bifurcations) [5, 60, 75, 95], and with the analysis in section 2.4.

In the case of L_2, we have

$$S_2 = \begin{bmatrix} 1 & 0 \\ 0 & 1 \end{bmatrix}, \qquad N_2 = \begin{bmatrix} 0 & 0 \\ 1 & 0 \end{bmatrix},$$

where S_2 is semi-simple and N_2 is nilpotent. We use a volume-preserving

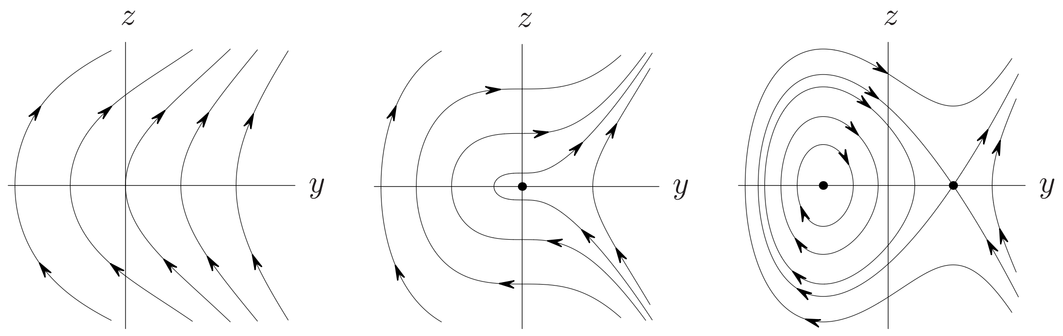

Figure 2.2: Saddle-node bifurcation of equations (2.22).

restriction to a symmetric normal form obtained in [68]:

$$\begin{aligned} \dot{y} &= zg(z^2) \\ \dot{z} &= y, \end{aligned}$$

with $g(0) = 0$. We find the unfolding may be written:

$$\begin{aligned} \dot{y} &= \mu z + az^3 \\ \dot{z} &= y, \end{aligned} \tag{2.23}$$

where again μ is the unfolding parameter and a is a constant which is generically nonzero. Note that this unfolding is also found in [68] in the case of the same linear part, but with a symmetry group consisting of the reversing mirror $(y, z) \to (y, -z)$ and the twofold rotation about the origin $(y, z) \to (-y, -z)$. This is a symmetry breaking bifurcation, see Figure 2.3. There are two types depending on the sign of a. For $a > 0$, a hyperbolic saddle bifurcates into a center and throws off an asymmetric pair of hyperbolic saddle points. For $a < 0$, a centre bifurcates into a hyperbolic saddle and throws off an asymmetric pair of fixed points of centre type. As before, $S_2 = I$ and we conclude that the return map for the periodic orbit with linear part L_2 in Jordan normal form will formally behave like the time-one map of one of the vector fields shown in Figure 2.3. This is the symmetry breaking bifurcation of periodic orbits. We would again expect the homoclinic/heteroclinic connections shown here to break under perturbation for the return map, and potentially lead to chaotic local dynamics.

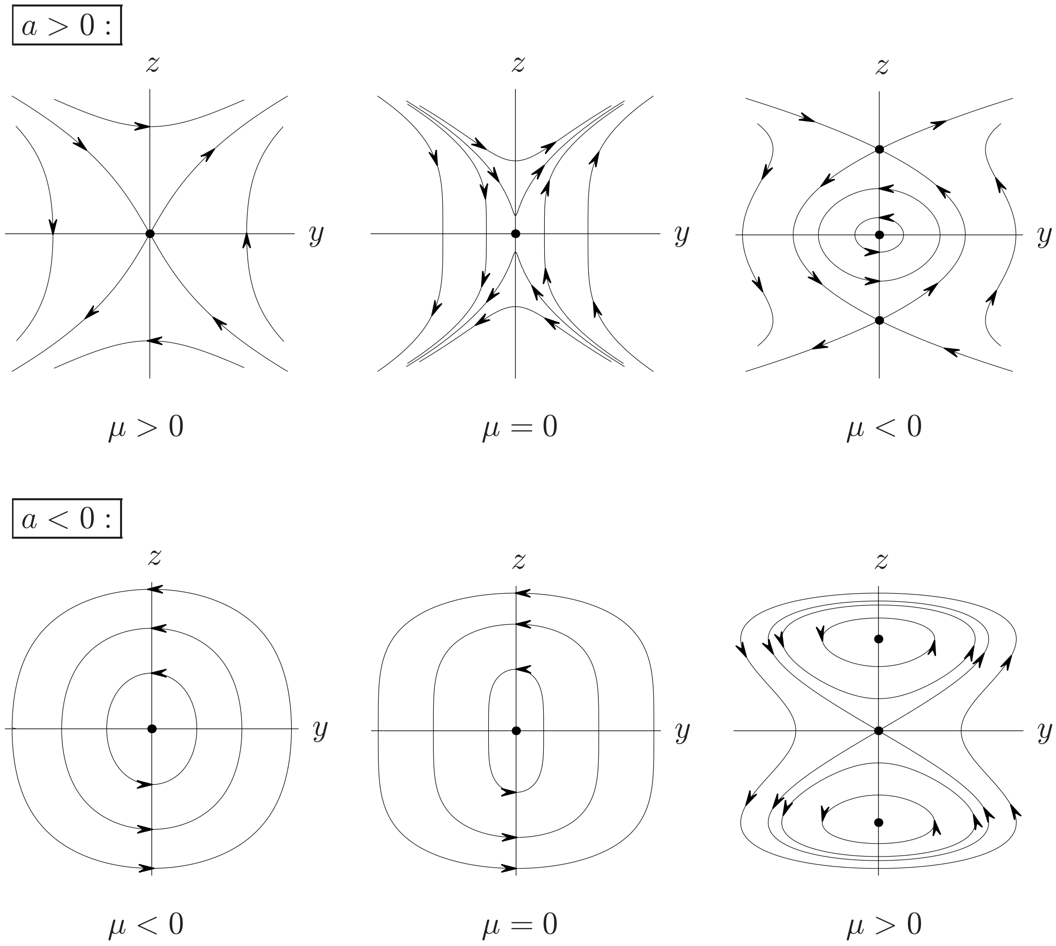

Figure 2.3: Symmetry breaking bifurcations of equations (2.23). These figures also arise in the period doubling bifurcation, where the return map is generated by $-I$ composed with the time-one map of the vector fields shown.

Finally we consider the case of both nontrivial multipliers equal to -1. Then we have the two following possibilities for the Jordan normal form of the linear part of the return map for this periodic orbit:

$$L_3 = \begin{bmatrix} -1 & 1 \\ 0 & -1 \end{bmatrix} \qquad \text{or} \qquad L_4 = \begin{bmatrix} -1 & 0 \\ 1 & -1 \end{bmatrix}.$$

In this case the nilpotent parts are the same up to a change of sign, but the semi-simple parts are equal to $-I$. Therefore the vector field will have an additional symmetry that is the twofold rotation about the origin $(y, z) \to (-y, -z)$. As previously mentioned, this case is also treated in [68] and we lead to the two possible normal forms

$$\begin{aligned} \dot{y} &= \mu z + a z^3 \\ \dot{z} &= y, \end{aligned} \tag{2.24}$$

$$\begin{aligned} \dot{y} &= z \\ \dot{z} &= \mu y + a y^3, \end{aligned} \tag{2.25}$$

Clearly these vector fields differ only by exchange of y and z, but recall that the reversing symmetry R strictly acts as a reflection in the y axis. This leads to four cases (also depending on the sign of the constant a). Equations (2.24) are illustrated in Figure 2.3, and see Figure 2.4 for the remaining cases. Since the semi-simple part in all cases is equal to $-I$, we find that the return map for the periodic orbit behaves like the composition of $-I$ with the time-one map of one of the cases in Figures 2.3, 2.4. Therefore the two bifurcating fixed points in (2.24), (2.25) are actually the two intersections of a periodic orbit of period approximately twice that of the original orbit, and we have the period doubling bifurcation. In each case, the period doubled orbit is symmetric in the full system—a systematic method of computing the symmetry properties of bifurcating orbits is given in [70]. The symmetry property is clear for (2.25), as the bifurcating fixed points lie in Fix R, see Figure 2.4. However, the fixed points in Figure 2.3 lie in Fix $(S \circ R)$, and this implies that the bifurcating orbit intersects Fix R at two points close to $x(T/2)$, where $x(t)$ is the original periodic orbit, and T is the period of this orbit. As before, under the addition of higher order terms we may obtain transverse homoclinic/heteroclinic connections appearing in the return map.

Having established the expected local bifurcation behaviour, we now return to the study of the bifurcation structure of the Michelson system. Kent & Elgin [57, 58, 60] call the branch of solutions emanating from the periodic orbit (2.21) the primary branch. One of the main features described is the

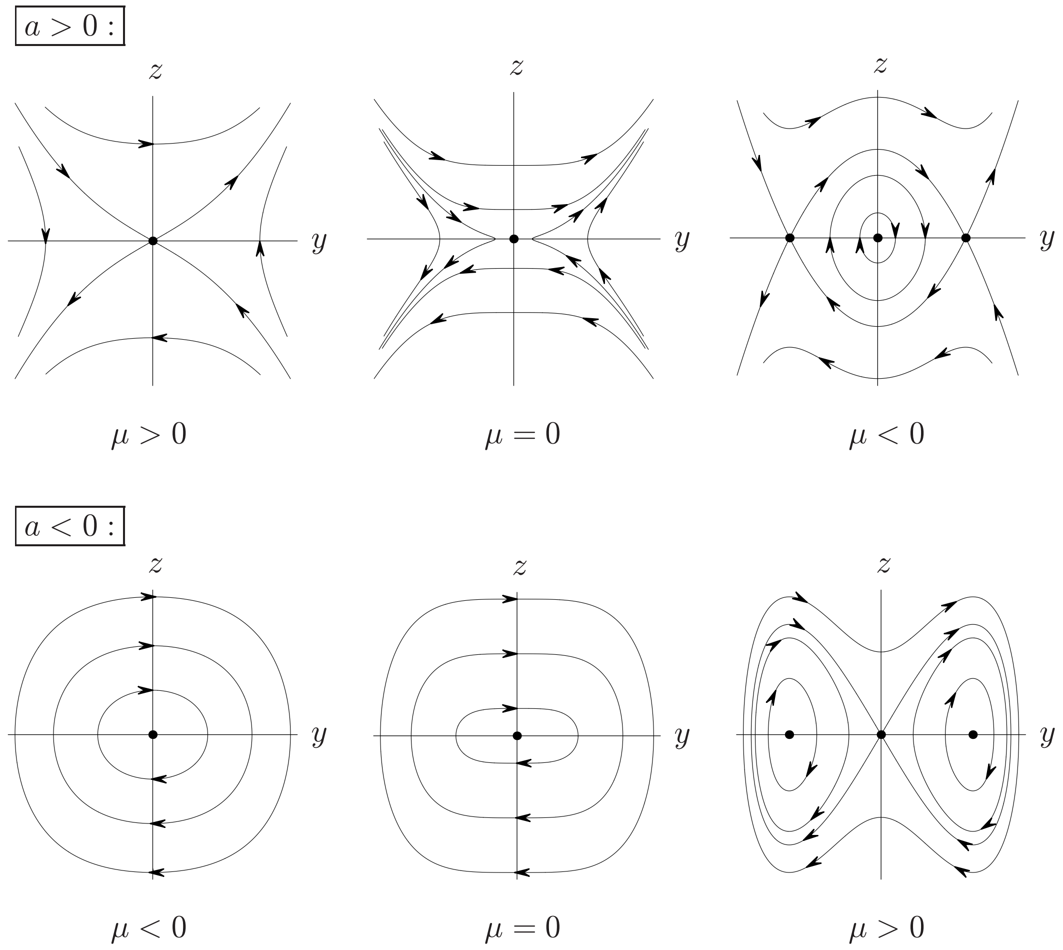

Figure 2.4: The remaining cases for the period doubling bifurcation, generated by (2.25). The return map acts as $-I$ composed with the time-one map of the vector fields shown.

'noose bifurcation', where this branch of periodic solutions undergoes a period doubling bifurcation, and these two branches meet each other in a saddle-node bifurcation as the parameter is increased, see Figure 2.5. Topological properties of the noose bifurcation were studied in [58], where they used interlinking of periodic orbits and 'self-linking' of stable/unstable manifolds of periodic orbits to show that the noose bifurcation requires the existence of a further local bifurcation to satisfy these topological invariants. In this case, this is a symmetry breaking bifurcation on the period-doubled branch at $c \approx 0.59779$.

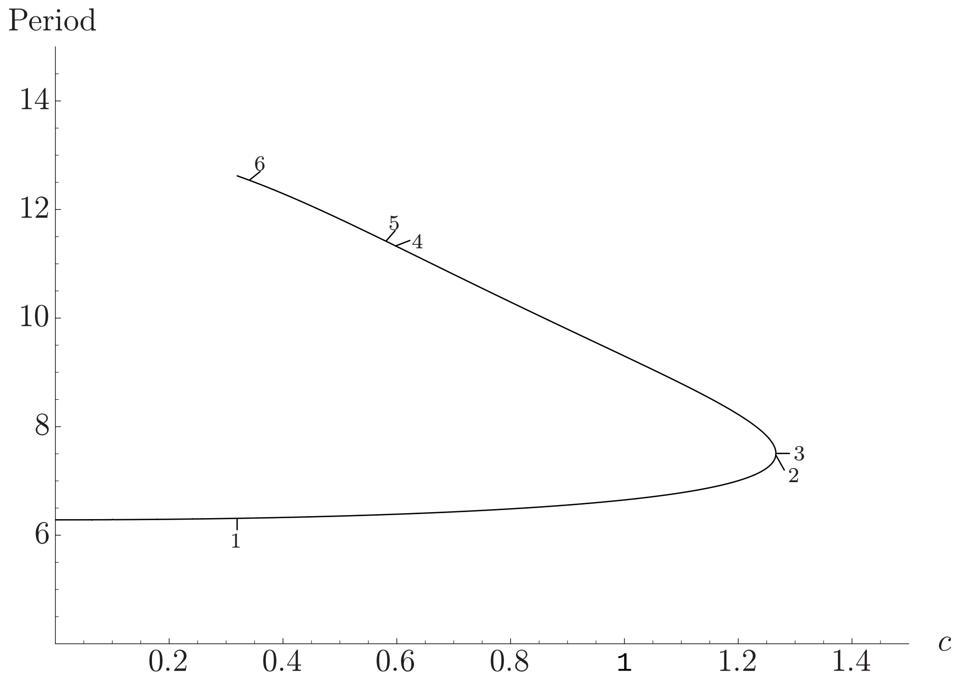

Figure 2.5: The primary periodic orbit branch (the "noose") and its local bifurcations.

Label	Bifurcation	Parameter Value
1	Period doubling bifurcation	0.31939
2	Period doubling bifurcation	1.26595
3	Saddle node bifurcation	1.26623
4	Symmetry breaking bifurcation	1.26623
5	Period doubling bifurcation	0.58086
6	Period doubling bifurcation	0.34010

The periodic orbit (2.21) born at $c = 0$ is initially elliptic, with multipliers lying on the unit circle, see section 3.2. There is the period doubling bifurcation at $c \approx 0.31939$, and the orbit is then hyperbolic until $c \approx 1.26595$, where there is another period doubling bifurcation. The orbit is then briefly elliptic until the saddle-node bifurcation of the primary branch at $c \approx 1.26623$. Continuing this branch around the fold bifurcation, we find that there the orbit is hyperbolic until $c \approx 0.59779$, which is the symmetry breaking bifurcation. There is another short elliptic region until $c \approx 0.58086$ where there is a period doubling bifurcation. The orbit is then again hyperbolic until another period doubling bifurcation at $c \approx 0.34010$. This orbit then has another elliptic region until $c \approx 0.31939$ where it has all Floquet multipliers equal to 1, and disappears in the period doubling bifurcation.

A more complete bifurcation diagram is shown in Figure 2.6, showing the primary branch, as well as many of the orbits that can be found by local bifurcations from the primary branch, including some k-bifurcations in the elliptic regions. This numerical data has been supplied by Sam Gratrix (as for Figure 2.8), and more detailed bifurcation diagrams still are included in [47]. The series of k-bifurcations of the primary branch occurring in the first elliptic region $c \in (0, 0.31939)$ is studied in [60]. An observed feature is the curious 'k-bifurcation branch', where orbits created in k-bifurcations appear to be joined up in phase space, as in Figure 2.6.

This numerical work agrees with the following theorem, which has been proved by Troy [107], and is concerned with the Michelson system at $c = 1$.

Theorem 2.3.3 (Troy). *There are at least two periodic solutions to the equation $x''' = 1 - \frac{1}{2}x^2 - x'$, $x = x(t)$ that are odd in t.*

Kent comments that these periodic solutions may be considered to be the two symmetric periodic solutions of the primary branch. In fact, there are infinitely many odd periodic solutions at $c = 1$, see section 2.4.

2.3.4 Connecting Orbits

As previously stated, in the limit $c \to \infty$, McCord [78] and Toland [106] have proved the existence of a unique heteroclinic connection lying in the intersection of the two dimensional manifolds $W^s(A)$ and $W^u(B)$, and Michelson [80] has proved that this connection exists for all c sufficiently large. We call this

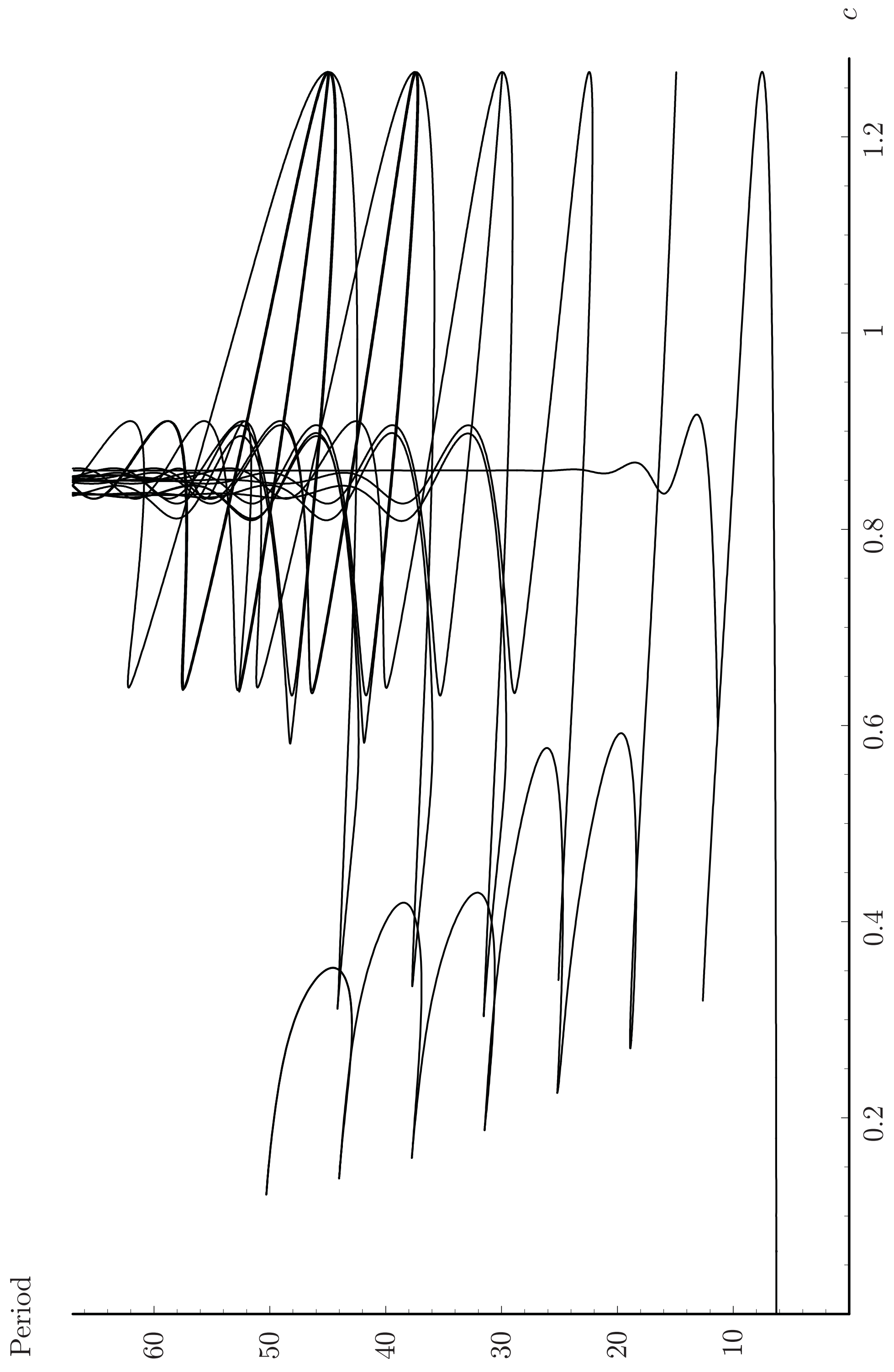

Figure 2.6: Numerical bifurcation diagram of the periodic orbits for the Michelson System, computed using AUTO [33, 46]. Period of the orbits is plotted against the parameter c.

connection $X_0(t)$, following [57]. Michelson also conjectures that this connection persists for all $c \in (0, \infty)$. This agrees with the analysis carried out in Chapter 3 which applies to the limit $c \to 0$. Numerically this orbit has been calculated by Hooper & Grimshaw [53] down to $c \approx 0.07$. This orbit plays a role in the analysis carried out in Chapters 3, 4, 5 and section 2.4.

Throughout this thesis, we will refer to heteroclinic orbits (such as $X_0(t)$), that lie in the intersection of two 2-dimensional manifolds as **2D heteroclinic orbits**. These connections typically persist over a range of c values. There are two more types of connecting orbits possible in the Michelson system—these are heteroclinic orbits formed by the coincidence of the two 1-dimensional manifolds (hereafter **1D heteroclinic orbits**), and homoclinic orbits. Hooper & Grimshaw call these connecting orbits oscillatory shocks, regular shocks and solitons/solitary waves respectively [53].

Homoclinic orbits clearly cannot be symmetric, and must occur in symmetric pairs. 1D heteroclinic orbits on the other hand *must* be symmetric. 2D heteroclinic orbits may or may not be symmetric. Heteroclinic orbits that are symmetric intersect Fix R precisely once.

Kent & Elgin [60] have studied further families of 2D heteroclinic connections lying in the manifolds $W^s(A)$ and $W^u(B)$. They found a sequence of symmetric connections. This sequence starts with a tangent bifurcation at $c \approx 1.283$ giving rise to two (odd) heteroclinic connections $X_1^{\pm}(t)$, both of which have three zeros (note that $X_0(t)$ has one zero). This is the first pair in a family of heteroclinics $X_n^{\pm}(t)$, $n \in \mathbb{N}$, each pair is a symmetric connection with n zeros for $t > 0$ and a zero at $t = 0$. Each member looks more and more like a periodic solution with the acquisition of each new zero, and this family accumulates to $c \approx 1.26623$, where there is the saddle-node of periodic orbits of the primary branch. Again, this work agrees with a Theorem by Troy [107], which is for the parameter value $c = 1$.

Theorem 2.3.4 (Troy). *There are at least two solutions to the equation* $x''' =$

$1 - \frac{1}{2}x^2 - x'$, $x = x(t)$ *that satisfy* $\lim_{t\to\infty} x(t) = -\sqrt{2}$ *and* $\lim_{t\to-\infty} = \sqrt{2}$. *The first has one zero in* x, *the second has exactly three zeros in* x.

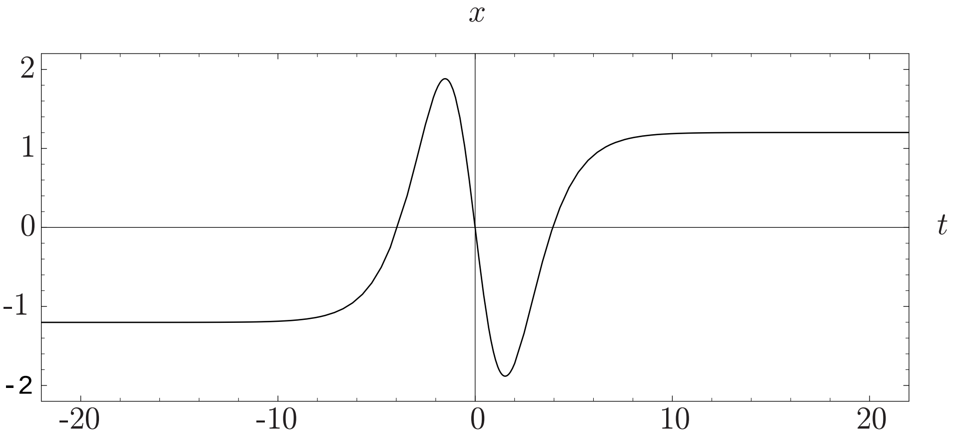

Figure 2.7: The Kuramoto-Tsuzuki exact 1D heteroclinic solution.

1D heteroclinic orbits are typically isolated in parameter space, and are therefore more difficult to find. Kuramoto & Tsuzuki [67] found an analytic solution for a 1D heteroclinic orbit at $c = \alpha\sqrt{2} \approx 0.84952$,

$$x(t) = \alpha(-9 \tanh \beta t + 11 \tanh^3 \beta t), \tag{2.26}$$

where $\alpha = 15\sqrt{\frac{11}{19^3}}$, $\beta = \frac{1}{2}\sqrt{\frac{11}{19}}$. This connection appears to be at the centre of a range of parameter values where there is a cluster of symmetric and asymmetric periodic solutions that have period tending to infinity in an 'oscillatory' manner, see Figure 2.8. This behaviour is typical of Shil'nikov saddle-focus homoclinic orbits under the well-known eigenvalue ratio condition [40, 97]. However, due to the 1D heteroclinic connection (2.26) the situation is much more complicated. Together with a (symmetric) 2D heteroclinic orbit (we conjecture there are infinitely many, see [73] and section 2.4), there is a heteroclinic cycle at $c \approx 0.84952$. The analysis for the consequences of such a heteroclinic cycle (including periodic orbit behaviour) is contained in Chapters 4 and 5. From this analysis, we see that there is a countable number of 1D heteroclinic connections (with an arbitrary number of zeros) converging to

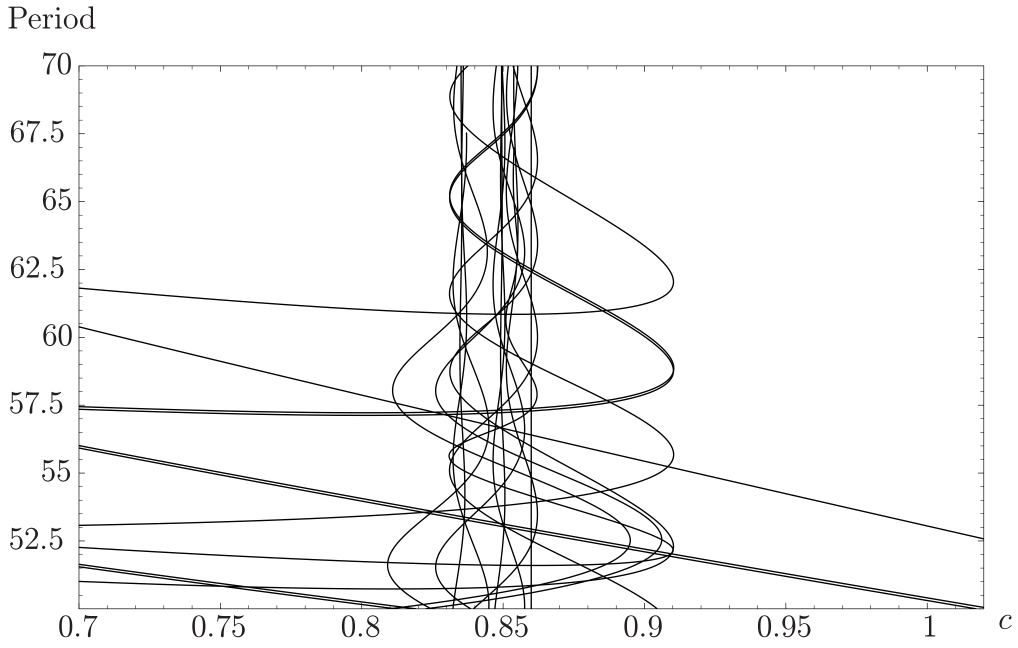

Figure 2.8: Numerical bifurcation diagram of periodic orbits about the parameter value $c \approx 0.84952$, where there exists a heteroclinic cycle. Period of the orbits is plotted against the parameter c.

(2.26) in parameter space. Numerical studies have revealed 1D heteroclinic connections at $c \approx 0.83520, 0.85416, 0.85422$ [53, 57]. Figure 2.9 shows corresponding heteroclinic cycles found numerically. Also, we will see in Chapter 3 that we expect countably many 1D heteroclinic connections to exist also for small c.

The analysis in Chapters 4 and 5 also reveal the existence of homoclinic solutions close to any one of the heteroclinic cycles. Homoclinic solutions have also been observed numerically, at $c \approx 0.83472, 0.84769, 0.85995$ and $c \approx 0.31554, 0.48661, 0.49821$, see Figure 2.10. The latter three parameter values for homoclinic solutions are observed to be connected with symmetry breaking bifurcations from the k-bifurcation branch—the asymmetric periodic solutions approach the homoclinic orbits in the infinite period limit, see [57]. The homoclinic at $c \approx 0.85995$ appears to be connected with the symmetry breaking bifurcation from the primary branch.

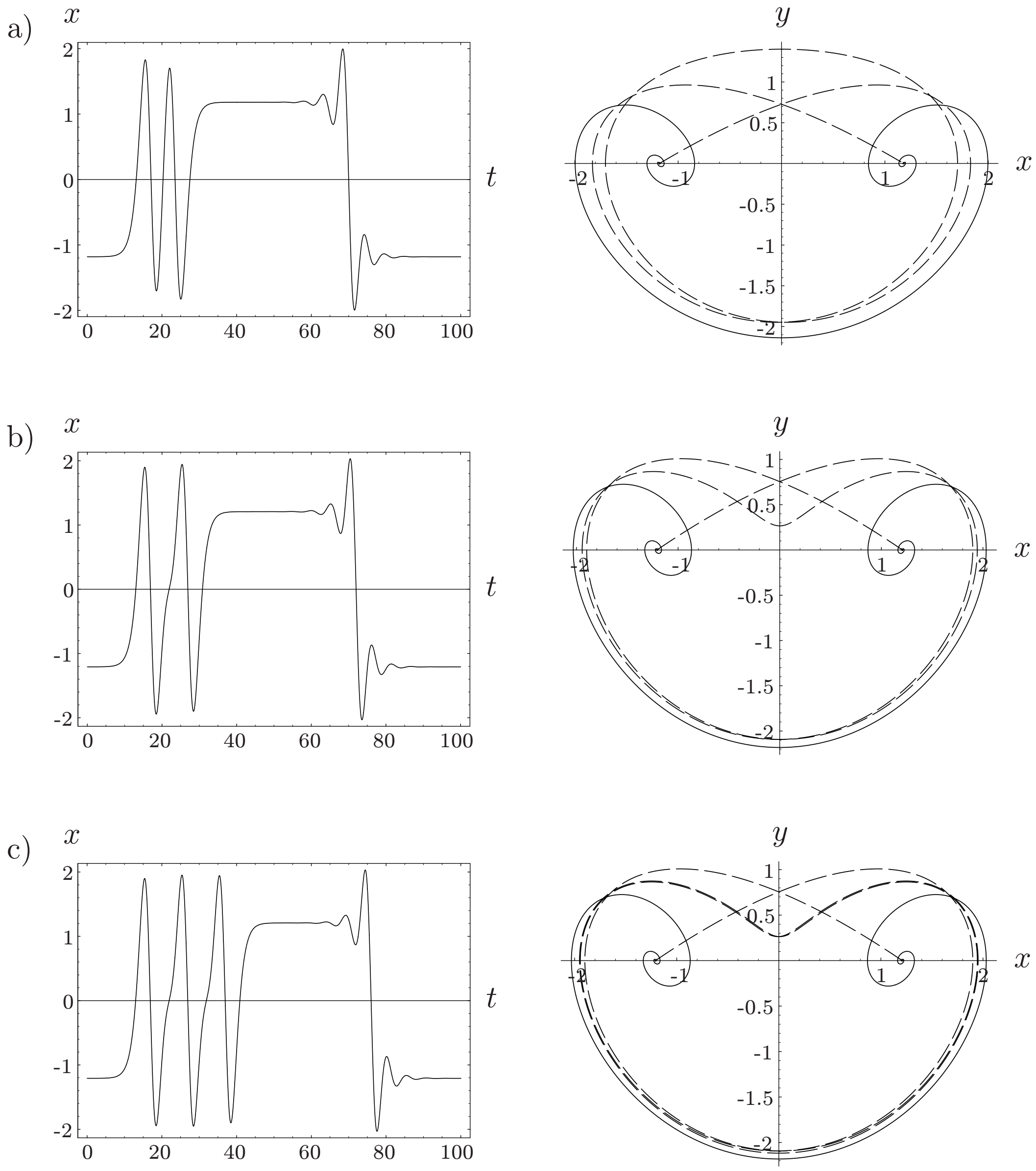

Figure 2.9: Heteroclinic cycles found numerically: each 1D connection is shown together with the simplest 2D heteroclinic $X_0(t)$. In the phase diagrams the 1D connection is shown dashed. Parameter values are a) $c = 0.83520$, b) $c = 0.85416$, c) $c = 0.85422$.

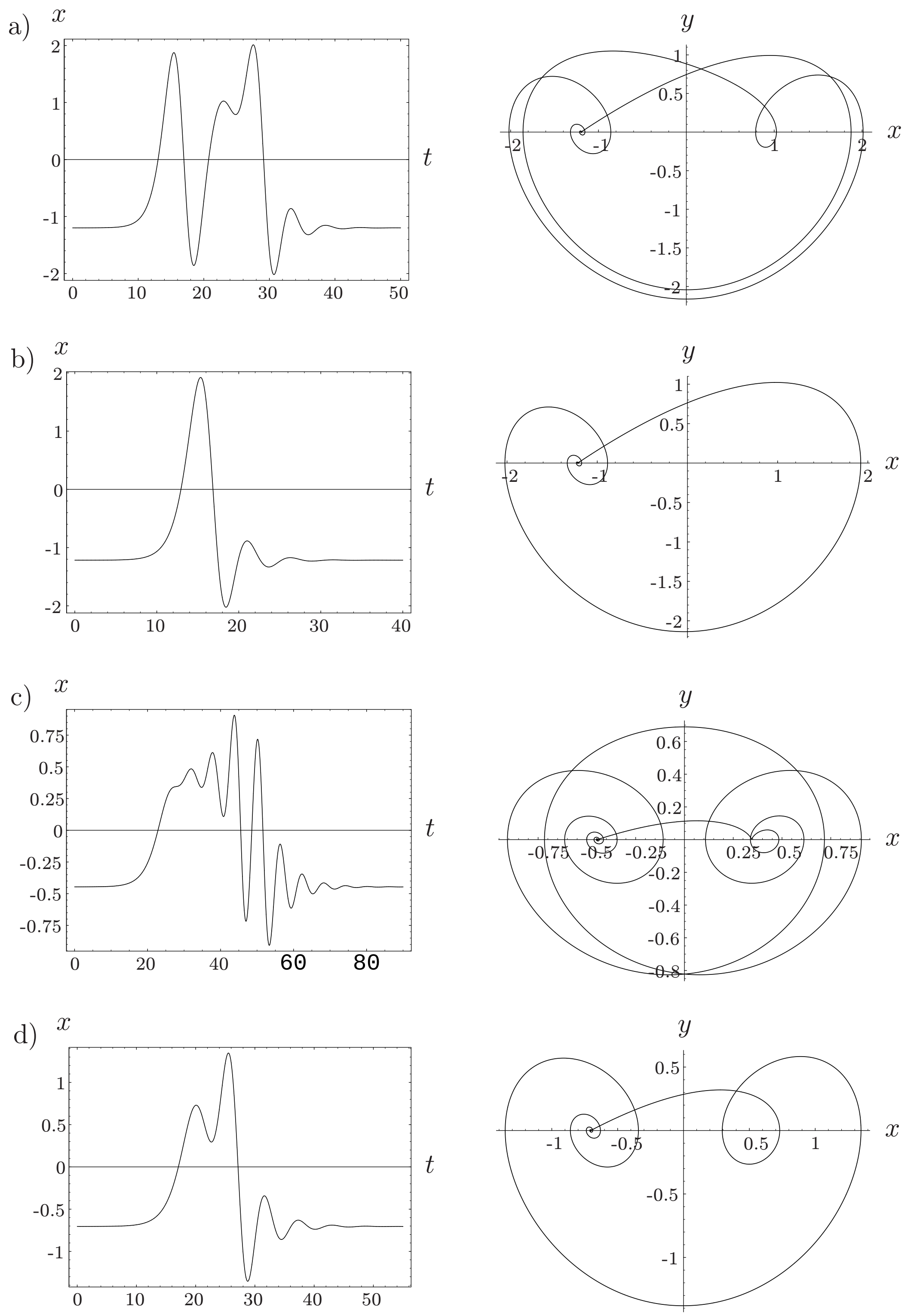

Figure 2.10: Homoclinic orbits for the fixed point A found numerically for the parameter values a) $c = 0.84769$, b) $c = 0.85995$, c) $c = 0.31554$, d) $c = 0.49821$.

2.4 Heteroclinic Solutions

Many of the features described in section 2.3 may be explained geometrically by a more detailed study of the heteroclinic solutions. Mackay describes the connecting orbits of a volume preserving flow as a *skeleton* for the flow, saying that they are a good starting point for understanding the behaviour of a divergence-free system [77]. In this section we briefly review work carried out by Lau [73], where the heteroclinic connections are used to describe the dynamics of the Michelson system for $c > 0.91839$. This work is numerical, and does not necessarily depend on the reversing symmetry or the volume preserving structure, although the reversibility does make the analysis easier. This work provides geometrical understanding of the many previous results on the Michelson system.

Symbolic dynamics is used to encode the 2-dimensional manifolds of the fixed points $F^{\pm}$ in order to identify heteroclinic bifurcations, and the formation of a horseshoe. Lau calls this process the "cocoon bifurcations", as the heteroclinic orbits trace out a cocoon-like tangle in phase space. The picture is different to that of Kent & Elgin, and it reveals a general geometric structure to system (2.2).

2.4.1 Invariant Manifolds and Time Delay Functions

We begin by introducing the Poincaré section plane $x = 0$, with corresponding Poincaré map φ. Note that this section is well defined (i.e. transverse to the flow) everywhere except on the z-axis. We track the movements of the respective 2-dimensional stable/unstable manifolds of the fixed points A and B under application of this map. From now on we will denote these 2-D manifolds by Σ_A and Σ_B. Also, the 1-dimensional invariant manifolds $W^u(A)$ and $W^s(B)$ are labelled γ_A and γ_B respectively. Most orbits are unbounded, and hence will escape from a given sphere centered on the origin, with radius r. The main tool for observing the manifolds Σ_A and Σ_B is the time delay function, defined by

$$T_{\pm}(\mathbf{x_0}) = |\int_{r_0}^{r} dt|, \qquad \|\mathbf{x}(0)\| = r_0, \tag{2.27}$$

where $T_{\pm}$ is for integrating along the trajectory $\mathbf{x}(t) = \mathbf{x}_0 + \int_0^{\pm t} f(\mathbf{x}(s), c)ds$, where $\mathbf{x} \in \mathbb{R}^3$ and $f(\mathbf{x}, c)$ is equal to the right hand side of (2.2), see (2.14). Thus the time delay function measures how long it takes for a given orbit to escape from the sphere of radius r. In the subsequent numerical work we have taken the radius $r = 20$. We observe numerically that for $c > 1.26624$ the only points starting in the section plane $x = 0$ whose trajectories remain bounded under evolution of the flow as $t \to \infty$ $(-\infty)$ are those points that belong to $\Sigma_A \cup \gamma_B$ $(\Sigma_B \cup \gamma_A)$. These points will show up as logarithmic singularities in $T_{\pm}$, and heteroclinic connections occur in the intersection of these manifolds. In this way, the time delay function acts as a numerical probe, searching along lines in the Poincaré plane for pieces of the invariant manifolds of the two fixed points A and B. As we further decrease c, we will continue to track these heteroclinic orbits as they form a skeleton for the structure of periodic and bounded aperiodic orbits.

First, we build a geometric picture in the parameter range for which there is the unique, monotone 2D heteroclinic connection $X_0(t)$ from B to A. This orbit lies in the transversal intersection of Σ_A and Σ_B. As a consequence of this orbit, and the complex eigenvalues at each fixed point, Σ_B wraps itself tightly around γ_A, and similarly for Σ_A and γ_B. It is the interacting roles of these manifolds that creates new heteroclinic orbits, and these heteroclinic orbits can be seen to act as the skeleton of the dynamics for this system.

To begin to see the structure of these manifolds, it is important first to observe the relative positions of the 1-D manifolds γ_A and γ_B. These manifolds are shown in Figure 2.11 for $c = 1.4$. The relative positions of these manifolds remains unchanged in the parameter interval we are concerned with.

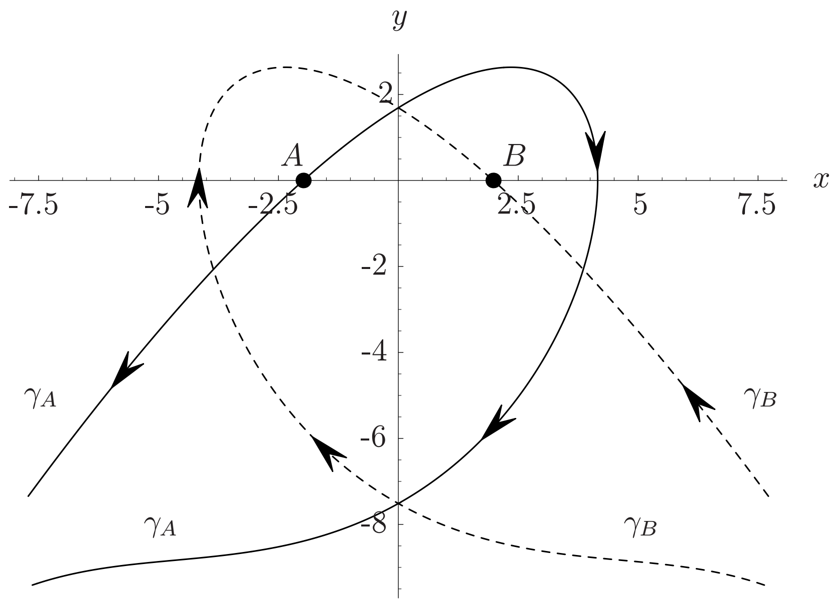

Figure 2.11: The one-dimensional manifolds γ_A and γ_B, and their intersections with the plane $x = 0$. The diagram here is shown for $c = 1.4$.

The fixed point A has one branch of γ_A that diverges to $-\infty$ (the non-interacting arm), and one branch that pierces the Poincaré section, comes close to B, returns to the section and again diverges to $-\infty$. The 1-D manifold γ_B behaves in a similar fashion due to the reversing symmetry.

Figure 2.12 gives a schematic diagram for the positions of the manifolds Σ_A and Σ_B at $c = 1.4$. This diagram may be constructed by evaluation of the time delay function along selected lines in the $y - z$ plane. The time delay functions shown have been evaluated along the line $z = 0.3$. The solid line indicates $T_+(y_0)$ and the dashed line indicates $T_-(y_0)$. Logarithmic singularities of these two functions detect points in Σ_A, Σ_B respectively. The plot for $T_+(y_0)$ has been magnified to show the logarithmic singularity with a local maxima that is not yet a logarithmic singularity. This maximum is detecting Σ_A^3 nearby, and as the Σ_3 manifolds will push through closer to the y-axis, this maximum will turn into a pair of logarithmic singularities.

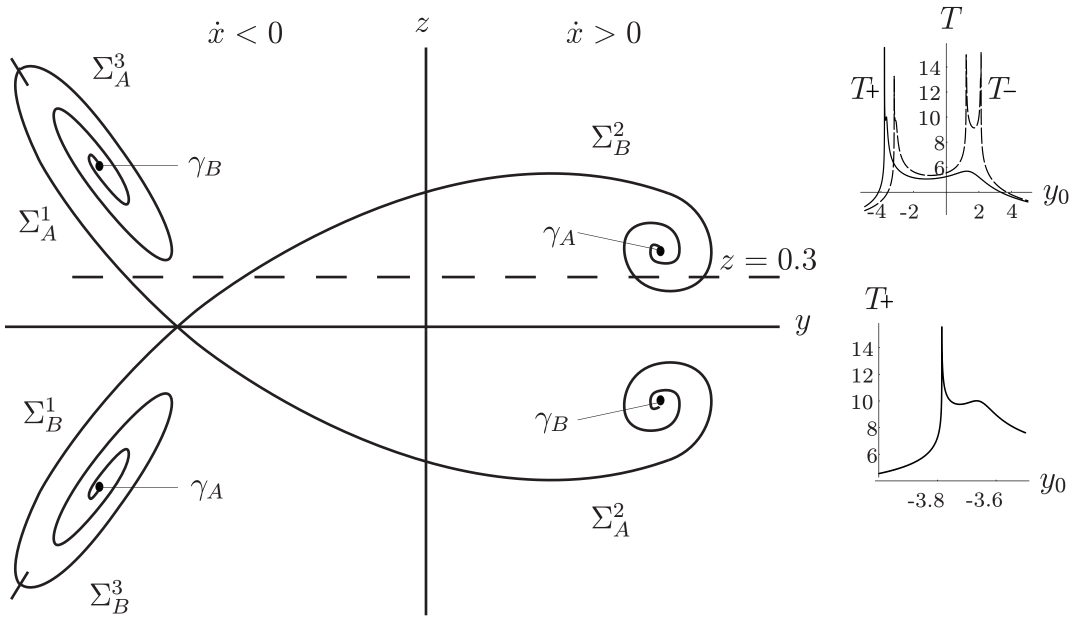

Figure 2.12: Sketch of the intersections of $\Sigma_{A,B}$ and $\gamma_{A,B}$ with the $y - z$ plane at $c = 1.4$, with time delay functions.

2.4.2 Heteroclinic Bifurcations

Recall that $dx/dt = y$ and so in Figure 2.12 orbits travel into the paper in the $y < 0$ half-plane, and out of the paper in the $y > 0$ half plane. We now explain the symbolic dynamics on the Σ manifolds. Different sections of $\Sigma_A \cap \{x = 0\}$ are labelled Σ_A^m, where m is the number of intersections with the plane $x = 0$ in positive time (including the point on that section itself), before converging to A. Similarly, points in Σ_B^n cross the plane $x = 0$ n times before converging to B in negative time. Thus the mapping rule is

$$\begin{array}{lllll} \Sigma_A^m \xrightarrow{into} \Sigma_A^{m-1} & \text{and} & \Sigma_B^n \xrightarrow{onto} \Sigma_B^{n+1} & \text{in positive time,} \\ \Sigma_A^m \xrightarrow{onto} \Sigma_A^{m+1} & \text{and} & \Sigma_B^n \xrightarrow{into} \Sigma_B^{n-1} & \text{in negative time.} \end{array} \tag{2.28}$$

The rules (2.28) are just applications of φ and φ^{-1} respectively. Clearly, due to the reversing symmetry, Σ_A (γ_A) is the image under reflection in the y-axis of Σ_B (γ_B). Another basic property of the Σ-manifolds is that Σ^m lies in the

$y < 0$ half plane if and only if m is odd. Figure 2.13 shows a numerically calculated plot of the Σ-manifolds, which uses the time delay function in a continuation-type algorithm to track the manifolds, and hence also the bifurcating heteroclinic orbits. This figure is also for $c = 1.4$, and is a numerical reproduction of Figure 2.12.

Due to the fact that γ_A has a non-interacting arm, each Σ_B^n can also have non-interacting parts. This is reflected in Figures 2.12 and 2.13; each piece of Σ_B^1 that lies to the left of Σ_A^1 is non-interacting, and does not return to the Poincaré plane in positive time. The remaining part of Σ_B^1 is interacting, and maps to Σ_B^2 (by (2.28), and then to Σ_B^3, which then again all lies in the non-interacting region.

At $c = c_1 = 1.2827$ the first heteroclinic bifurcation occurs—Σ_A^k touches Σ_B^{4-k} ($k = 1, 2, 3$), and unfolds immediately into a pair of symmetric heteroclinic orbits, see Figure 2.4.2. These orbits both have three zeros, and we shall call them (2,2) heteroclinic orbits—in general we label the heteroclinic point $\Sigma_A^m \cap \Sigma_B^n \cap \{x = 0\}$ by (m, n). Note that this labelling is not unique. Under the mapping rule (2.28), we have the following rule for the mapping of heteroclinic points under φ,

$$(m, n) \to (m - 1, n + 1). \tag{2.29}$$

The number of zeros of a (m, n) orbit is $m + n - 1$, the sum $m + n$ is even and is clearly invariant under (2.29). This (2,2) orbit is the first in the *principle sequence* of heteroclinic bifurcations, these have been identified by [60, 80]. Note however the consequences of these new orbits—a part of Σ_B^3 now becomes interacting, and so new pieces Σ_B^4 and Σ_B^5 appear (similarly for Σ_A). The principle sequence c_n continues to produce new (m, n) orbits by this mechanism as c is decreased. However, this is not the only heteroclinic family produced. After $c_2 = 1.2746$, there is what Lau calls a *degenerate* heteroclinic bifurcation,

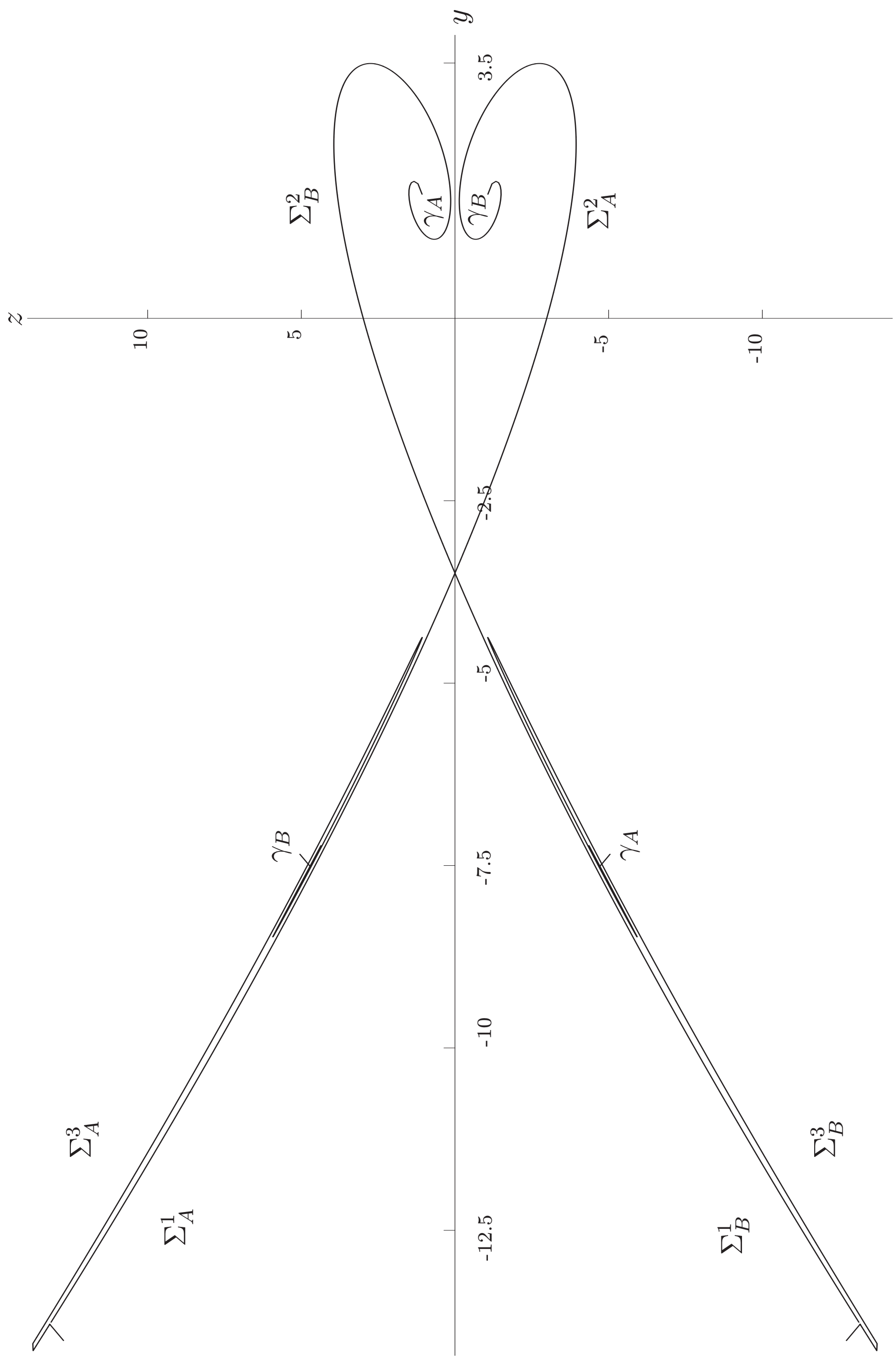

Figure 2.13: Numerical diagram of the intersections of $\Sigma_{A,B}$ and $\gamma_{A,B}$ with the $y-z$ plane at $c = 1.4$.

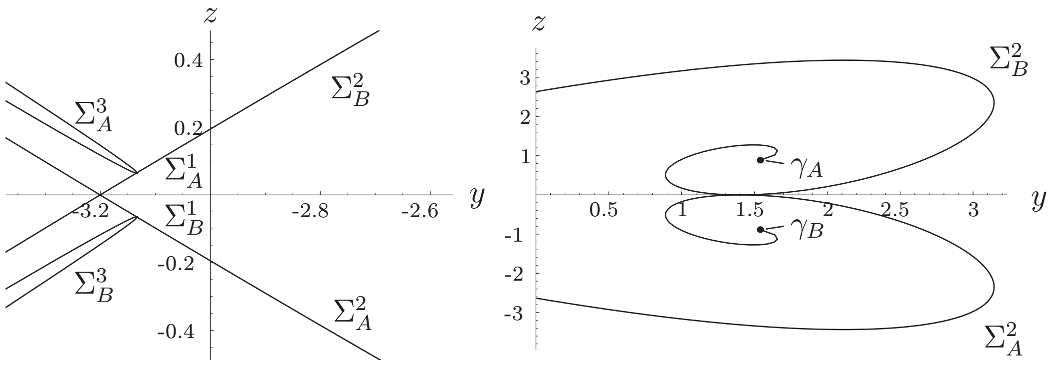

Figure 2.14: The first heteroclinic bifurcation at $c_1 = 1.2827$, which unfolds to give two (2,2) heteroclinic orbits.

at $\bar{c}_2 = 1.27442$. This is where the folding begins, the Σ_B begin to fold back onto Σ_A to create a new, symmetric pair of asymmetric heteroclinic orbits. These degenerate heteroclinic orbits appear to occur between each c_{2n} and c_{2n+1}.

There are many more heteroclinic bifurcations occurring as c decreases, the order of which is too complicated to analyse in detail. The principle sequence rapidly converges to $c_\infty = 1.26623$, at the limit of which is the saddle-node bifurcation of periodic orbits identified in section 2.3. These are the periodic orbits of the primary branch (the 'noose'). From the analysis in section 2.3.3, we know that immediately after the saddle-node bifurcation the stable and unstable manifolds of the hyperbolic orbit surround the elliptic orbit and will typically intersect transversally, and as a consequence for $c < c_\infty$ there is a chaotic 'explosion' of periodic orbits with arbitrarily high period. There is also a corresponding explosion of heteroclinic orbits at this point.

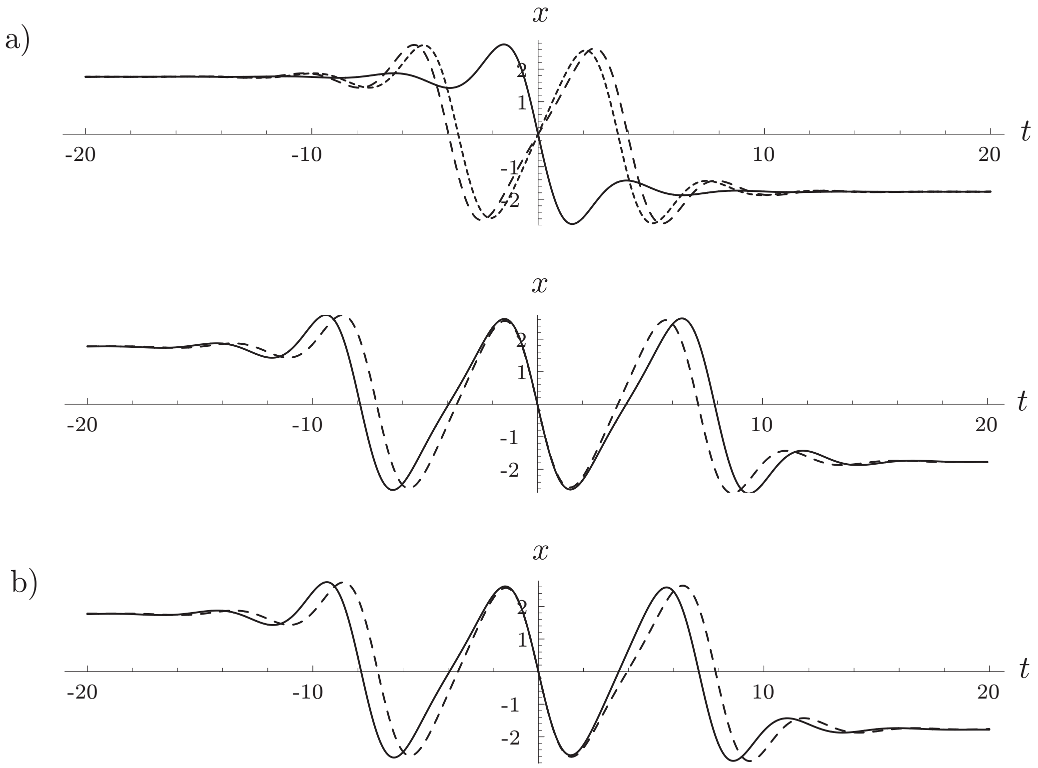

Figure 2.15: a) Odd heteroclinic orbits born in the principle sequence. b) Symmetric pair of asymmetric heteroclinic orbits, $c = 1.25$.

2.4.3 Formation of a Horseshoe

For $c < c_\infty$, more heteroclinic bifurcations continue to occur, until the 'last heteroclinic' at $c_L = 1.26390$. This produces two more (3,3) orbits, and marks the completion of the "cocoon" bifurcations and the formation of a Smale horseshoe for φ.

As can be seen from Figure 2.4.3, the cocoon bifurcations result in the remarkable situation where we can see a horseshoe being developed—we need only track the heteroclinic orbits that are born by the mechanisms described above. These heteroclinic orbits can be counted for $c < 1.26390$ from the following:

$$\mathcal{N}(\Sigma_A^m) = 2^{(m-1)/2} \quad (m \text{ odd}),$$

$$\mathcal{N}(\Sigma_B^n) = 2^{(n-1)/2} \quad (n \text{ odd})$$

where $\mathcal{N}$ denotes 'number of pieces'. This gives that the number of heteroclinic (m, n) orbits in is $\mathcal{N}(\Sigma_A^m \cap \Sigma_B^n) = 2^{(m-1)/2}2^{(n-1)/2}$. The symmetric orbits can be counted similarly. For heteroclinic orbits with a high number of zeros, we can see that most of them will be asymmetric connections [73], although only symmetric connections were identified in [57].

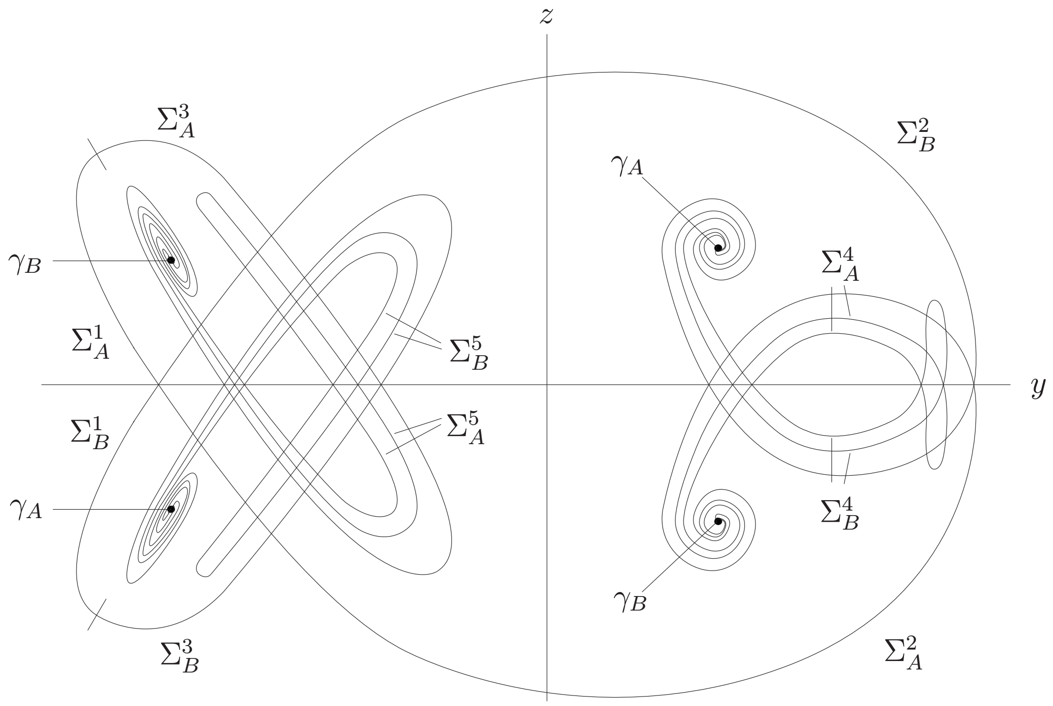

Figure 2.16: After the last heteroclinic bifurcation. The pieces of Σ^3 clearly trace out a Smale horseshoe [73].

Although this identifies only a topological horseshoe, it appears that the structure is hyperbolic. Standard analysis of hyperbolic horseshoes shows that the mapping is topologically conjugate to a full shift on two symbols [100], say $\mathbf{0}$ and $\mathbf{1}$. The symbols label the two 'vertical strips' of Σ_B^5, say. The periodic orbits found numerically all appear hyperbolic in the region for which the horseshoe exists, and match perfectly with the encoding for a full shift on two symbols. The primary branch comprises the two 'fixed points' for the horseshoe $\overline{\mathbf{0}}$ and $\overline{\mathbf{1}}$, where the bar denotes infinite repetition in both directions. It has been previously supposed that as we decrease c below 1.26624, the only periodic orbits created are those that are directly connected to k-bifurcations and subordinate period-doubling and symmetry breaking bifurcations of the primary branch [34, 57]. However, the presence of the horseshoe implies the existence of many more orbits, as may be easily seen, for example, by looking at the periodic orbits of prime period in the horseshoe.

Symmetry properties of the orbits in the horseshoe may also be deduced from the symbolic encoding, assuming hyperbolicity. Consider an orbit in terms of its bi-infinite sequence $\{\ldots, a_{-2}, a_{-1}, a_0, a_1, a_2, \ldots\}$, $a_i = \mathbf{0}$ or $\mathbf{1}$. This orbit intersects Fix R if and only if there exists $j \in \mathbf{Z}$ such that

$$a_{j-k} = a_{j+k}, \quad k \in \mathbf{Z} \qquad \text{or} \qquad a_{j-k+1} = a_{j+k}, \quad k \in \mathbf{Z}.$$

The number of distinct ways in which the sequence is symmetric in this way is the number of intersections the orbit has with Fix R. Note that an orbit is a symmetric periodic orbit if and only if it intersects Fix R twice, see Lemma 4.4.1.

The resulting topology found above remains unchanged in the parameter window $0.91839 < c < 1.26390$; the system is structurally stable. This also agrees with numerical observations, see Figure 2.6. Figure 2.17 shows a schematic diagram for sequence of heteroclinic and periodic orbit bifurcations leading up to the formation of the horseshoe.

Recently, Wilczak has produced a computer assisted proof for the existence of the horseshoe at the parameter value $c = 1$ [118]. The proof is based on the study of the return map of different regions in the plane $z = 0$ to find a topological horseshoe.

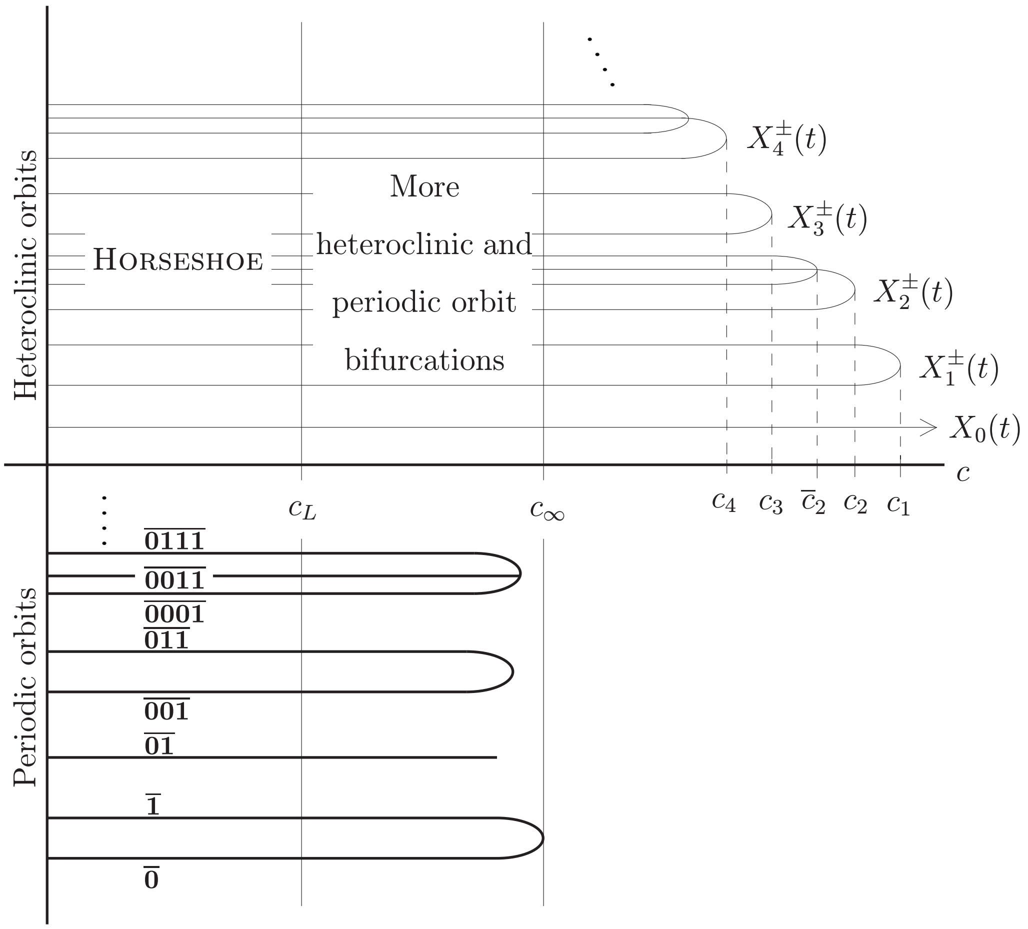

Figure 2.17: Schematic diagram showing heteroclinic bifurcations and periodic orbits bifurcations as c is decreased from 1.2827. Compare also with Figure 2.6.

Label	Bifurcation	Parameter Value
c_1	Heteroclinic bifurcation	1.2827
c_2	Heteroclinic bifurcation	1.2746
$\overline{c}_2$	Degenerate heteroclinic bifurcation	1.27442
c_3	Heteroclinic bifurcation	1.2677
c_4	Heteroclinic bifurcation	1.2669
c_∞	Saddle-node bifurcation	1.26623
c_L	Last heteroclinic bifurcation	1.26390

Chapter 3

Reversible Hopf-Zero Bifurcation

In this chapter we analyse the local 'Hopf-zero' bifurcation in the space of three dimensional purely R-reversible systems, where dim Fix $R = 1$,

$$\dot{\mathbf{x}} = F(\mathbf{x}, \lambda), \qquad \mathbf{x} := (x, y, z) \in \mathbb{R}^3, \ \lambda \in \mathbb{R},$$

where $F(R(\mathbf{x})) = -DR|_{\mathbf{x}} \cdot F(\mathbf{x})$. By Bochner's Theorem [9] (or see [82, Section 5.2, Theorem 1]), we may take the local action of R to be linear. Consistent with the Michelson system symmetry action (2.13), we take the action to be a twofold rotation about the y axis:

$$R(x, y, z) = (-x, y, -z). \tag{3.1}$$

R-reversibility then implies that

$$F \circ R = -R \circ F.$$

We assume that there is a symmetric equilibrium. A simple calculation shows that the eigenvalues about any symmetric equilibrium are either $0, \pm\alpha$ or $0, \pm\alpha i$. In the first case, without loss of generality we may assume that the linear part of the vector field is such that

$$D_{\mathbf{x}}F(0,0) = \begin{pmatrix} 0 & \alpha & 0 \\ \alpha & 0 & 0 \\ 0 & 0 & 0 \end{pmatrix},$$

and a standard centre manifold reduction will reduce the normal form to a one-dimensional system. This reduction may be chosen to respect the reversing symmetry. The normal form will then generically be given by

$$\dot{z} = \lambda + az^2 + \cdots$$

where $a \neq 0$, and the reversing symmetry acts as $R(z) = (-z)$. This bifurcation therefore generically (codimension one) gives rise to a saddle node of asymmetric equilibria, which meet at the singularity in a symmetric point, and the dynamics are trivial.

In this chapter we shall treat the case where the eigenvalues are $0, \pm\alpha\mathrm{i}$. This is a codimension one bifurcation in reversible (R), volume-preserving (VP), and reversible-volume-preserving (RVP) vector fields, it occurs in the Michelson system at $c = 0$, and has been studied in the dissipative and volume preserving cases in [10, 11, 12, 14, 29, 39, 49, 105]. We establish first the existence of simple solutions (fixed points and periodic orbits with period approximately equal to $2\pi/\alpha$) in section 3.1. Normal forms in the general (generic) case are given in section 3.2 for R, VP, and RVP vector fields, and the normal form for the Michelson system is computed in section 3.3, where the phase space is shown to have an asymptotically integrable form. The asymptotic solutions are computed analytically using the method of multiple time scales. In section 3.4 we prove the generic existence of complex codimension one phenomena in the R and RVP cases, in particular heteroclinic and homoclinic cycle bifurcations, see Theorems 3.4.1 and 3.4.2. However, the analysis shows that the presence of these heteroclinic/homoclinic bifurcations cannot be checked through any finite jet of the normal form, as is the case for homoclinic orbits in dissipative/divergence free systems, see [14].

3.1 Simple Solutions

Here we examine the simplest solutions emerging in unfoldings of the Hopf-zero bifurcation. These are stationary solutions, and periodic solutions with period approximately equal to $2\pi/\alpha$, due to the purely imaginary pair of eigenvalues. We find such solutions with Liapunov-Schmidt reduction.

In the x, y, z variables the system may be written

$$\begin{aligned} \dot{x} &= -\alpha y + xzg(x, y, z^2, \mu), \\ \dot{y} &= \alpha x + yzg(x, y, z^2\mu), \\ \dot{z} &= h(x, y, z^2, \mu). \end{aligned} \tag{3.2}$$

Denote the right hand side as $F : \mathbb{R}^3 \times \mathbb{R} \to \mathbb{R}^3$.

We search for periodic solutions with period approximately equal to $2\pi/\alpha$, since the fixed point solutions are trivially periodic with any period. Then let $\mathbf{x}(t)$ ($\mathbf{x} \in \mathbb{R}^3$) be periodic with period

$$\frac{2\pi}{\alpha(1+\tau)} \approx \frac{2\pi}{\alpha},$$

where $\tau \approx 0$. Now let $\mathbf{u}(t) = \mathbf{x}(\frac{t}{\alpha(1+\tau)})$, then $\mathbf{u}(t)$ is a solution of

$$\alpha(1+\tau)\frac{d\mathbf{u}}{dt} - F(\mathbf{u}, \mu) = 0, \tag{3.3}$$

with period equal to 2π. Let $C_{2\pi}$, $C^1_{2\pi}$ be the spaces of continuous (resp. C^1) functions from $\mathbb{R}$ into $\mathbb{R}^3$. These are Banach spaces with suitably defined norms. Now define the operator $\mathcal{N} : C^1([0, 2\pi], \mathbb{R}^3) \times \mathbb{R} \times \mathbb{R} \to C([0, 2\pi], \mathbb{R}^3)$ by

$$\mathcal{N}(\mathbf{u}, \mu, \tau) = \alpha(1+\tau)\frac{d\mathbf{u}}{dt} - F(\mathbf{u}, \mu). \tag{3.4}$$

Then zeros of $\mathcal{N}$ correspond to zeros of system (3.2) with period approximately equal to 2π. Note that in fact $\mathcal{N}$ is an $R \times S^1$ reversible-equivariant function, where S^1 acts like

$$\phi\mathbf{u}(t) = \mathbf{u}(t - \phi). \tag{3.5}$$

To use Liapunov-Schmidt reduction, we need to find the kernel of $D\mathcal{N}|_0$:

$$D\mathcal{N}|_0\mathbf{u} = \frac{d\mathbf{u}}{dt} - DF|_0\mathbf{u}.$$

We note that $D\mathcal{N}|_0$ is a Fredholm operator of index zero [28, 42]. Clearly $\mathbf{u}$ is in the kernel of $D\mathcal{N}|_0$ iff $\mathbf{u}(t) = e^{At}\mathbf{u}_0$, where $A = DF|_0$. We can then identify the kernel of $D\mathcal{N}|_0$ with $\mathbb{C} \times \mathbb{R}$ by letting $\mathbf{u}(t) = (\text{Re } \mathbf{v}(t), \text{Im } \mathbf{v}(t), \mathbf{z}_0) := (\text{Re } (e^{it}\mathbf{v}_0), \text{Im } (e^{it}\mathbf{v}_0), \mathbf{z}_0)$, where $\mathbf{v}_0 := x_0 + iy_0 \in \mathbb{C}$. Then we have proved part 1 of the following proposition.

Proposition 3.1.1. *1. $\dim\ \ker D\mathcal{N}|_0 = 3$.*

2. Solutions in the kernel of $D\mathcal{N}|_0$ in the reduced equation correspond to fixed points of the full system (3.2) if and only if $\mathbf{v}(t) = \mathbf{v}_0 = 0$.

We write $C^1_{2\pi} = \ker D\mathcal{N}|_0 \oplus M$ and $C_{2\pi} = \text{range } D\mathcal{N}|_0 \oplus N$, with M and N suitably chosen complements, defined in Lemma 3.1.2. Now $D\mathcal{N}|_0 : M \to \text{range } D\mathcal{N}|_0$ is invertible (this follows since $D\mathcal{N}|_0$ is Fredholm, see [42]) and hence we may apply the Implicit Function Theorem to reduce to a map $f : \ker D\mathcal{N}|_0 \times \mathbb{R} \times \mathbb{R} \to N$. Given that the $\ker D\mathcal{N}|_0$ and range $D\mathcal{N}|_0$ are invariant subspaces of the symmetry group $\mathbb{Z}_2(R) \times S^1$, the reduced equation will inherit all the symmetries of the original equation [41]; here the symmetries act on the kernel as:

$$\begin{aligned}
S^1 : \ \phi\big((\text{Re } (e^{it}\mathbf{v}_0), \text{Im } (e^{it}\mathbf{v}_0), \mathbf{z}_0)\big) &= (\text{Re } (e^{i(t-\phi)}\mathbf{v}_0), \text{Im } (e^{i(t-\phi)}\mathbf{v}_0), \mathbf{z}_0) \\
\mathbb{Z}_2(R) : \ R\big((\text{Re } (e^{it}\mathbf{v}_0), \text{Im } (e^{it}\mathbf{v}_0), \mathbf{z}_0)\big) &= (\text{Re } (e^{it}\overline{\mathbf{v}_0}), \text{Im } (e^{it}\overline{\mathbf{v}_0}), -\mathbf{z}_0)
\end{aligned}$$

The splittings as defined in Lemma 3.1.2 satisfy this condition. Now to prove part 2, we observe that fixed points and periodic orbits of (3.2) have different isotropies with respect to the S^1-symmetry, and isotropies are conserved by the Liapunov-Schmidt reduction [42].

Lemma 3.1.2. *There exists an $\mathbb{Z}_2(R) \times S^1$-invariant splitting of $C_{2\pi}$ given by*

$$C_{2\pi} = \textit{range } D\mathcal{N}|_0 \oplus \ker D\mathcal{N}|_0, .$$

and also an $\mathbb{Z}_2(R) \times S^1$-invariant splitting of $C^1_{2\pi}$ given by

$$C^1_{2\pi} = \ker D\mathcal{N}|_0 \oplus M,$$

where $M = range\ D\mathcal{N}|_0 \cap C^1_{2\pi}$.

Proof. Computations similar to those in [42] verify that the above are invariant splittings for $C_{2\pi}$ and $C^1_{2\pi}$.

Then we obtain a reduced equation

$$f : \ker D\mathcal{N}|_0 \times \mathbb{R} \times \mathbb{R} \to \ker D\mathcal{N}|_0$$

that is $\mathbb{Z}_2(R) \times S^1$ equivariant. As before we shall associate $\ker D\mathcal{N}|_0$ with $\mathbb{C} \times \mathbb{R}$. Let

$$f(\mathbf{v}, \mathbf{z}, \mu, \tau) = \begin{pmatrix} f^{\mathbf{v}}(\mathbf{v}, \mathbf{z}, \mu, \tau) \\ f^{\mathbf{z}}(\mathbf{v}, \mathbf{z}, \mu, \tau) \end{pmatrix}$$

Then the condition that f should be $\mathbb{Z}_2(R) \times S^1$ symmetric gives:

$$\mathbb{Z}_2(R) \quad \begin{cases} f^{\mathbf{v}}(\overline{\mathbf{v}}, -\mathbf{z}, \mu, \tau) &= -\overline{f^{\mathbf{v}}(\mathbf{v}, \mathbf{z}, \mu, \tau)} \\ f^{\mathbf{z}}(\overline{\mathbf{v}}, -\mathbf{z}, \mu, \tau) &= f^{\mathbf{z}}(\mathbf{v}, \mathbf{z}, \mu, \tau) \end{cases}$$

$$S^1 \quad \begin{cases} f^{\mathbf{v}}(e^{i\phi}\mathbf{v}, \mathbf{z}, \mu, \tau) &= e^{i\phi} f^{\mathbf{v}}(\mathbf{v}, \mathbf{z}, \mu, \tau) \\ f^{\mathbf{z}}(e^{i\phi}\mathbf{v}, \mathbf{z}, \mu, \tau) &= f^{\mathbf{z}}(\mathbf{v}, \mathbf{z}, \mu, \tau) \end{cases}$$

with $\mathbf{v} \in \mathbb{C}$, $\mathbf{z} \in \mathbb{R}$. Then f must have the form

$$f(\mathbf{v}, \mathbf{z}, \mu, \tau) = \begin{pmatrix} \mathbf{v}\mathbf{z}p(|\mathbf{v}|^2, \mathbf{z}^2, \mu, \tau) + i\mathbf{v}q(|\mathbf{v}|^2, \mathbf{z}^2, \mu, \tau) \\ \tilde{f}^{\mathbf{z}}(|\mathbf{v}|^2, \mathbf{z}^2, \mu, \tau) \end{pmatrix} \tag{3.6}$$

Again, standard computations as in the generic Hopf Theorem follow through here, to show that $q(0,0,0,0) = 0$ and $q_\tau(0,0,0,\tau) \neq 0$. Then we may apply the implicit function theorem to solve $q = 0$ with the implicit function $\tau = \tau(|\mathbf{v}|^2, \mathbf{z}, \mu)$.

Recall that fixed point solutions in the full system correspond to fixed point solutions in $\ker D\mathcal{N}|_0$ of $f(\mathbf{v}, \mathbf{z}, \mu, \tau) = 0$. Also these solutions have the extra symmetry of $\tau \to \tau + \epsilon$, for any ϵ. Thus we may remove τ from (3.6) and set $\mathbf{v} = 0$, and find solutions to the equation

$$\tilde{f}^{\mathbf{z}}(0, \mathbf{z}^2, \mu, 0) = 0.$$

It can be checked that with the generic conditions $\frac{\partial h}{\partial \mu}(0,0,0,0) \neq 0$, $\frac{\partial^2 h}{\partial \mathbf{z}^2}(0,0,0,0) \neq 0$ we obtain the following bifurcation equation for fixed points:

$$\tilde{f}^{\mathbf{z}}(0, \mathbf{z}^2, \mu, 0) = \mu + c\mathbf{z}^2 + \cdots, \quad c \neq 0.$$

Thus there is a saddle-node of fixed points. We also have that if $\operatorname{sgn}\left(\frac{\partial^2 h}{\partial \mathbf{z}^2}|_0\right) \neq \operatorname{sgn}\left(\frac{\partial h}{\partial \mu}|_0\right)$ then the fixed points appear for $\mu > 0$, otherwise they exist for $\mu < 0$.

Now we search for R-reversible periodic solutions. Since isotropies are conserved by Liapunov-Schmidt reduction, these solutions will exist in the plane $z = 0$ in $\ker D\mathcal{N}|_0$. Then we would like to solve the equation $\tilde{f}^{\mathbf{z}}(|\mathbf{v}|^2, 0, \mu, \tau(|\mathbf{v}|^2, 0, \mu)) = 0$. As before, the generic condition $\frac{\partial h}{\partial \mu}(0,0,0,0) \neq 0$ would imply that we can solve $\tilde{f}^{\mathbf{z}} = 0$ with the implicit function $\mu = \mu(|\mathbf{v}|^2)$ to find a one parameter family of periodic solutions with period approximately equal to 2π. As a final remark, we note that it can be shown that if $\operatorname{sgn}\left(\frac{\partial^2 h}{\partial r^2}|_0\right) \neq \operatorname{sgn}\left(\frac{\partial h}{\partial \mu}|_0\right)$ (where $r^2 = x^2 + y^2$) then the branch of periodic orbits appears for $\mu > 0$, otherwise it exists for $\mu < 0$.

3.2 Normal Forms

Here we present normal forms for unfoldings of the reversible (R), volume-preserving (VP), and reversible-volume-preserving (RVP) Hopf-zero singularity modulo flat terms, which as we shall see play an important role in the description of the unfolding of the singularity. As before, R again acts as (2.13).

A direct calculation shows that without loss of generality, in all cases R, VP, RVP, we may consider the linear part L (after Jordan Normal Form) of the singularity of the vector field on $\mathbb{R}^3$ to be

$$\begin{aligned}\dot{x} &= -\alpha y\\ \dot{y} &= \alpha x\\ \dot{z} &= 0.\end{aligned}$$

As previously mentioned, such a singularity is codimension 1 in the space of R, VP, and RVP vector fields. This follows as an indirect extension of the existing linear unfolding theory, see [11, 54].

The above linear part is invariant under rotations about the z-axis, and we can use a result by Elphick *et al.* [35] that at every order, the normal form of a vector field can be chosen such that it possesses the symmetry group

$$\overline{\{\exp(tS^T)|t \in \mathbb{R}\}}, \tag{3.7}$$

where $L = N + S$ is the decomposition of L into its nilpotent and semi-simple part. Thus each order of the Taylor series can systematically be made invariant under this same rotational symmetry. However, terms that are beyond all orders may break this S^1 symmetry, these are the 'flat' terms—every derivative evaluated at the singularity is equal to zero, see section 3.4.

In polar coordinates $x = r\cos\theta$, $y = r\sin\theta$ and rescaling time, we have that the S^1-symmetric part of the vector field may be written as

$$\begin{aligned}\dot{\theta} &= f(r^2, z)\\ \dot{r} &= rg'(r^2, z)\\ \dot{z} &= h'(r^2, z)\end{aligned} \tag{3.8}$$

where $g'(0,0) = h'(0,0) = \frac{\partial h'}{\partial z}(0,0) = 0$, $f(0,0) = \alpha$. In fact, we may take $f(r^2, z) \equiv \alpha$ which can be obtained by a reparametrisation of the vector field. The proof that this may be done respecting a volume preserving structure is contained in [10], and the same proof may also be used in the other cases here. We give the argument here for the case RVP, since the other cases then follow trivially.

In polar coordinates $x = r\cos\theta$, $y = r\sin\theta$ the volume $dx \wedge dy \wedge dz$ transforms to $rdr \wedge d\theta \wedge dz$, and the reversing symmetry (2.13) acts as $R(r,\theta,z) = (r, \pi - \theta, -z)$. We consider the vector field

$$\begin{aligned} \dot{\theta} &= \alpha, \\ \dot{r} &= r\frac{\alpha g'(r^2,z)}{f(r^2,z)}, \\ \dot{z} &= \frac{\alpha h'(r^2,z)}{f(r^2,z)}. \end{aligned} \tag{3.9}$$

Since our original vector field preserves the volume $rdr \wedge d\theta \wedge dz$, this vector field preserves the volume $frdr \wedge d\theta \wedge dz$. We note also that the normal form for this vector field will remain the same up to any arbitrarily high order, since $f(0,0) \neq 0$. We now would like to reparametrise the polar coordinate $\tilde{r} = \tilde{r}(r^2, z, \mu)$ such that in the new coordinates the volume transforms back to the form $\tilde{r}d\tilde{r} \wedge d\theta \wedge dz$, and the reversing symmetry is unaffected. We would then like to solve

$$f(r^2, z, \mu)rdr = \tilde{r}d\tilde{r},, \qquad \tilde{r}(0, z, \mu) = 0,$$

which has the solution

$$\tilde{r}^2(r^2, z, \mu) = \int_0^{r^2} f(s, z, \mu)ds.$$

We note also that $\tilde{r}^2(r^2, -z, \mu) = \tilde{r}^2(r^2, z, \mu)$, so the reversing symmetry is unaffected.

We shall denote such an S^1-symmetric vector field by $\tilde{X}(x,y,z) : \mathbb{R}^3 \to \mathbb{R}^3$. This is our original vector field X modulo flat terms, so we may write $X = \tilde{X} + p$, where $p(x,y,z) : \mathbb{R}^3 \to \mathbb{R}^3$ is flat in (x,y,z).

A result by Broer [11] shows that for volume preserving vector fields, the normal form may also be chosen to be volume preserving at every order. We can combine this result with that of Lamb [68], who showed that for reversible vector fields the normal form can be obtained directly from the general (non-symmetric) normal form, also respecting the symmetry group (3.7). So in the cases R, RVP, we may choose our form (3.9) so that it is also reversible, respectively reversible volume-preserving, giving

$$\begin{aligned} \dot{\theta} &= \alpha \\ \dot{r} &= rzg(r^2, z^2) \\ \dot{z} &= h(r^2, z^2), \end{aligned} \tag{3.10}$$

where $h(0,0) = 0$. We may then decouple the angle variable and write down the normal form for each case as:

$$\text{R}: \qquad \begin{aligned} \dot{r} &= a_1 rz + \qquad O(|r,z|^4) \\ \dot{z} &= b_1 r^2 + b_2 z^2 + O(|r,z|^4) \end{aligned} \tag{3.11}$$

$$\text{VP}: \qquad \begin{aligned} \dot{r} &= -a_1 rz + \qquad O(|r,z|^3) \\ \dot{z} &= b_1 r^2 + a_1 z^2 + O(|r,z|^3) \end{aligned} \tag{3.12}$$

$$\text{RVP}: \qquad \begin{aligned} \dot{r} &= -a_1 rz + \qquad O(|r,z|^4) \\ \dot{z} &= b_1 r^2 + a_1 z^2 + O(|r,z|^4) \end{aligned} \tag{3.13}$$

with a_1, b_1, b_2 constants. The above systems were shown by Takens to be 2-determined up to C^0 orbital equivalence [103]. Note that the S^1-symmetric 2-jets are the same for the generic (codimension 2) case and the reversible case. Phase portraits for these systems are given, for example, in [50]. We include them here for completeness. We are now interested in unfoldings of these planar vector fields. With the generic condition $\frac{\partial h}{\partial \mu}(0,0) \neq 0$ the according 1-parameter unfoldings of the reduced planar vector fields are versal (but *not* for the 3D vector fields):

$$\text{R}: \qquad \begin{aligned} \dot{r} &= a_1 rz + \qquad O(|r,z,\mu|^3) \\ \dot{z} &= b_1 r^2 + b_2 z^2 + \mu + O(|r,z,\mu|^3), \end{aligned} \tag{3.14}$$

$$\text{VP}: \qquad \begin{aligned} \dot{r} &= -a_1 rz + \qquad O(|r,z,\mu|^3) \\ \dot{z} &= b_1 r^2 + a_1 z^2 + \mu + O(|r,z,\mu|^3), \end{aligned} \tag{3.15}$$

$$\text{RVP}: \qquad \begin{aligned} \dot{r} &= -a_1 rz + \qquad O(|r,z,\mu|^3) \\ \dot{z} &= b_1 r^2 + a_1 z^2 + \mu + O(|r,z,\mu|^3). \end{aligned} \tag{3.16}$$

In the case VP this follows from a blow up of the vector field, see [11, 12]. The general normal form for the 2-jet in the case VP can be written

$$\begin{aligned}\dot{r} &= -a_1 r z + a_2 \mu r,\\ \dot{z} &= b_1 r^2 + a_1 z^2 + \mu - 2a_2\mu z + b_2\mu^2.\end{aligned}$$

We now rescale

$$\begin{aligned}\text{R}: &\qquad \overline{r} = \sqrt{|b_1 b_2|}\,r, \quad \overline{z} = -b_2 z, \quad \overline{\mu} = -b_2\mu\\ \text{VP, RVP}: &\qquad \overline{r} = \sqrt{|b_1 a_1|}\,r, \quad \overline{z} = -a_1 z, \quad \overline{\mu} = -a_1\mu\end{aligned}$$

and dropping bars, we obtain

$$\begin{aligned}\dot{r} &= arz + \qquad\qquad O(|r,z,\mu|^3)\\ \dot{z} &= br^2 - z^2 + \mu + O(|r,z,\mu|^3)\end{aligned} \tag{3.17}$$

with a, b constants, with

$$\text{R}: \qquad a = -a_1/b_2, \quad b = \begin{cases} +1 & \text{if } \operatorname{sgn}(b_1) \neq \operatorname{sgn}(b_2)\\ -1 & \text{else.}\end{cases}$$

$$\text{VP, RVP}: \qquad a = 1, \quad b = \begin{cases} +1 & \text{if } \operatorname{sgn}(b_1) \neq \operatorname{sgn}(a_1)\\ -1 & \text{else.}\end{cases}$$

The classification of such systems is known [50, 103], we include the phase portraits for each case in figure 3.1. For each case, the simplest solutions appearing in the normal form are two equilibria and a periodic solution, all which come out of the bifurcation point not necessarily together. Note that if we embed our system into a 4-dimensional system by extending the phase space with the inclusion of the parameter μ (now Fix R is two dimensional), then the branch of periodic solutions is reminiscent of a Liapunov centre for the fixed point, and this agrees with results obtained for reversible systems in [31].

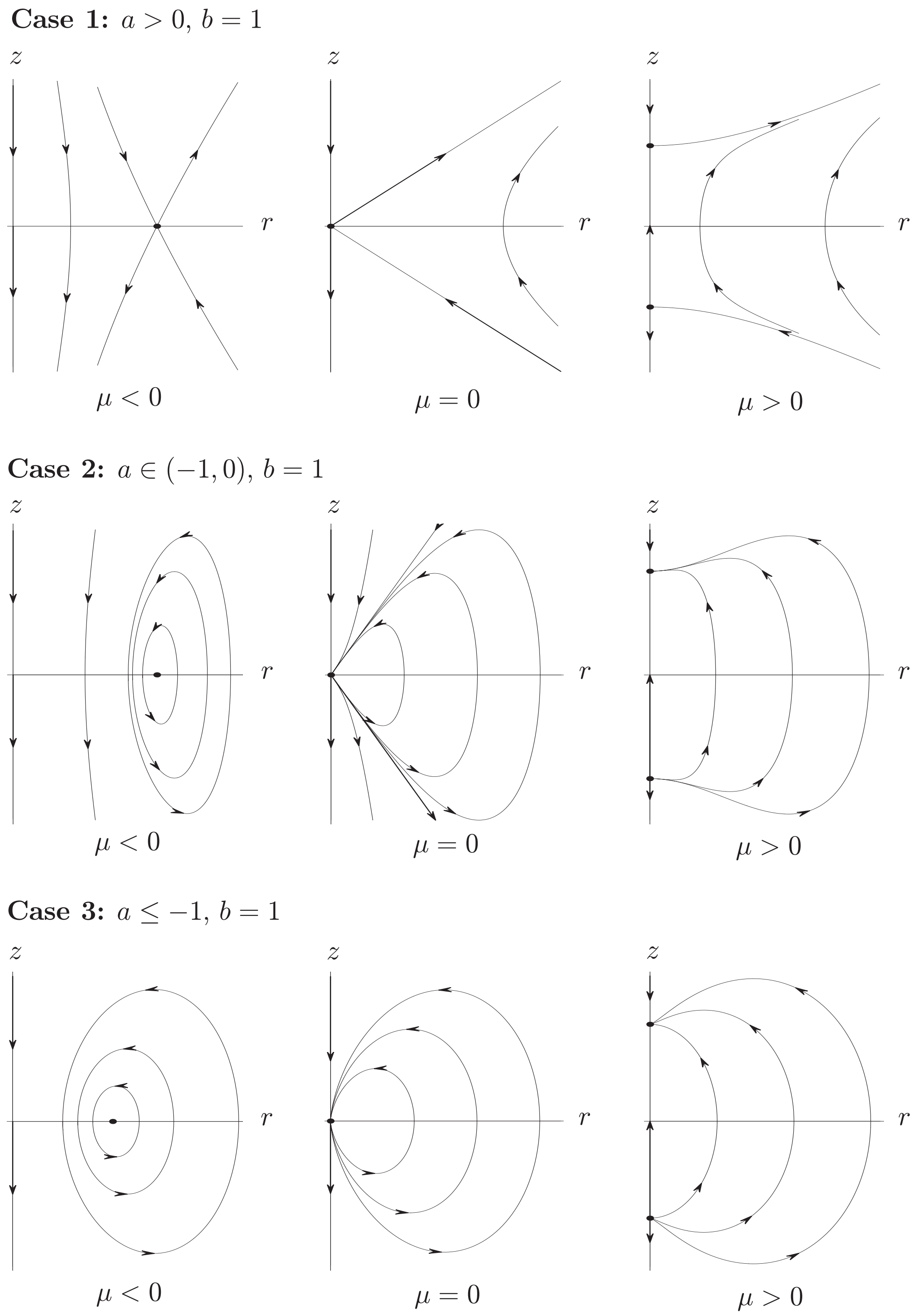

Figure 3.1: Unfoldings of the Hopf-zero bifurcation, cases 1–3.

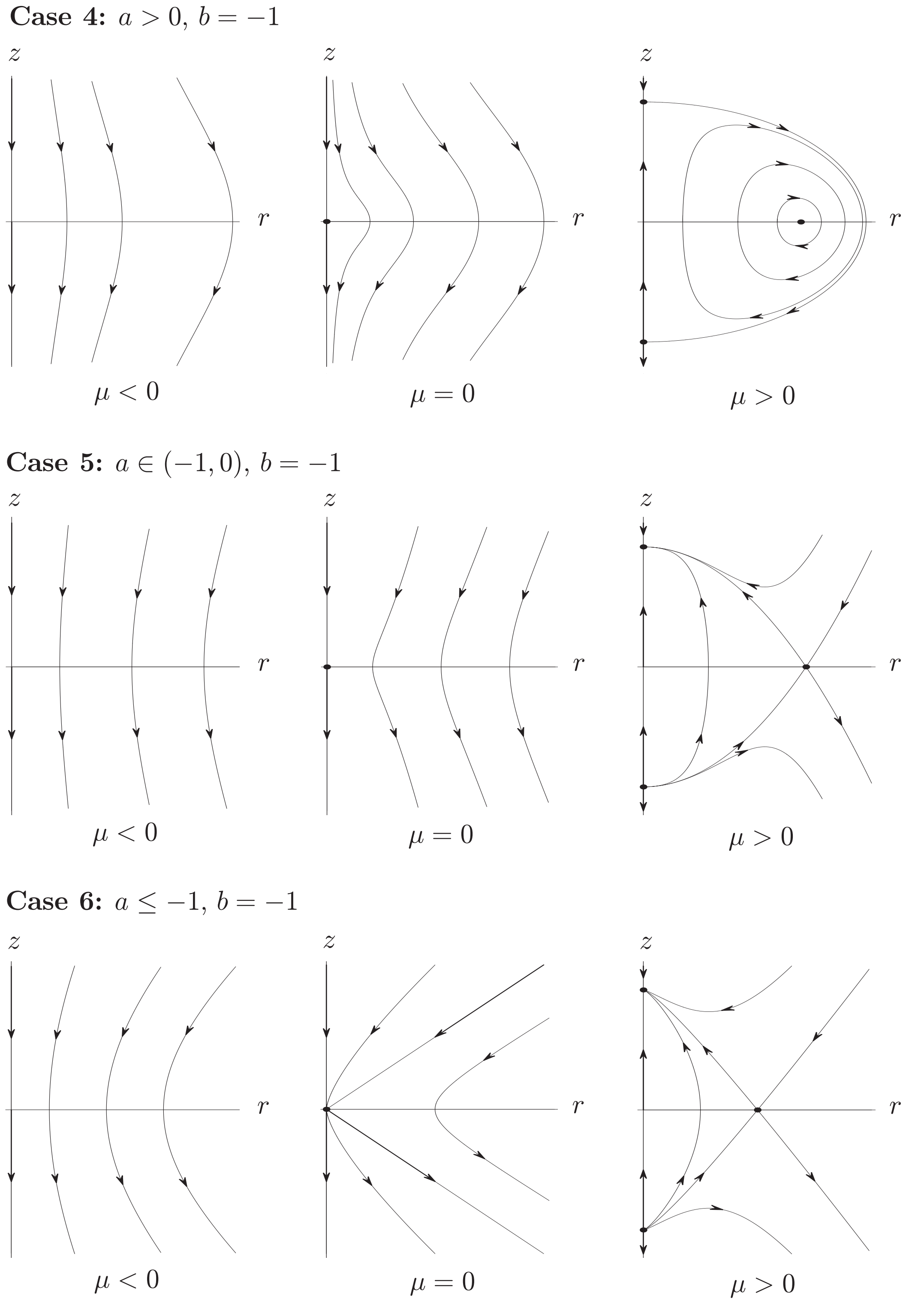

Figure 3.1: Unfoldings of the Hopf-zero bifurcation, cases 4–6.

Clearly only cases 1 and 4 are possible in the VP and RVP cases. Case 1 has been studied in [13], where it was shown that there exists infinitely many moduli of strong stability for generic unfoldings, depending on the saddle connection that appears for $\mu > 0$. All other features in this case are hyperbolic and therefore structurally stable. Case 2 is structurally stable for $\mu > 0$. For $\mu < 0$ the (reversible) KAM theory may be applied to show the existence of invariant tori close to the singularity. Similar properties hold for case 3. Cases 5 and 6 do not possess any centres, and since all fixed points and periodic orbits are hyperbolic, these unfoldings are structurally stable.

We will focus on case 4, and the effect of S^1-symmetry breaking terms. This unfolding displays degenerate features for $\mu > 0$—the two 2-dimensional invariant manifolds of each fixed point coincide, forming a continuous 'heteroclinic shell'. Also the two 1-dimensional manifolds coincide, forming a 1D connection for all $\mu > 0$, which is another degenerate feature. In section 3.2.1, we find that the Michelson system also falls into case 4 (in the RVP case), and we may expect many of the features discovered to occur generically in section 3.4 to appear in the Michelson system.

3.2.1 Normal Form for the Michelson System

We now compute the normal form for the Michelson system (2.2), so as to put it into the form (3.17). We begin with

$$\begin{aligned}\dot{x} &= y \\ \dot{y} &= z \\ \dot{z} &= c^2 - \frac{1}{2}x^2 - y.\end{aligned}$$

We first put the linear part of the extended 4-dimensional system (including the equation $\dot{(c^2)} = 0$) into Jordan Normal Form by the change of variables

$$\begin{bmatrix} \overline{x} \\ \overline{y} \\ \overline{z} \\ \overline{c}^2 \end{bmatrix} = \begin{bmatrix} 0 & 0 & 1 & 0 \\ 0 & 1 & 0 & 0 \\ 1 & 0 & 1 & 0 \\ 0 & -1 & 0 & 1 \end{bmatrix} \begin{bmatrix} x \\ y \\ z \\ c^2 \end{bmatrix}.$$

In the new coordinates the system becomes

$$\begin{aligned} \dot{\overline{x}} &= -\overline{y} - \frac{1}{2}(\overline{z} - \overline{x})^2 \\ \dot{\overline{y}} &= \overline{x} \\ \dot{\overline{z}} &= \overline{c}^2 - \frac{1}{2}(\overline{z} - \overline{x})^2 \\ \dot{(\overline{c}^2)} &= 0. \end{aligned}$$

We now introduce the nonlinear, locally invertible change of coordinates

$$\begin{bmatrix} \overline{x} \\ \overline{y} \\ \overline{z} \end{bmatrix} = \begin{bmatrix} \tilde{x} \\ \tilde{y} \\ \tilde{z} \end{bmatrix} + \begin{bmatrix} -\frac{1}{3}\tilde{x}\tilde{y} + \frac{1}{2}\tilde{y}\tilde{z} \\ -\frac{1}{6}\tilde{x}^2 - \frac{1}{3}\tilde{y}^2 - \frac{1}{2}\tilde{z}^2 \\ -\frac{1}{4}\tilde{x}\tilde{y} + \tilde{y}\tilde{z} \end{bmatrix}.$$

It may be checked that the system now takes the form

$$\begin{aligned} \dot{x} &= -y + \frac{1}{2}xz + O(|x, y, z|^3) \\ \dot{y} &= x + \frac{1}{2}yz + O(|x, y, z|^3) \\ \dot{z} &= c^2 - \frac{1}{2}z^2 - \frac{1}{4}(x^2 + y^2) + O(|x, y, z|^3), \end{aligned}$$

where we have dropped the tilde and relabelled $\overline{c} \to c$. Now, in polar coordinates $x = r\cos\theta$, $y = r\sin\theta$, we have:

$$\begin{aligned} \dot{\theta} &= 1 + O(|r, z|^2) \\ \dot{r} &= \frac{1}{2}rz + O(|r, z|)^3) \\ \dot{z} &= c^2 - \frac{1}{2}z^2 - \frac{1}{4}r^2 + O(|r, z|^3) \end{aligned}$$

In accordance with section 3.2, we drop the $\dot{\theta}$ equation and rescale

$$\begin{aligned} r &\to 2\sqrt{2}r \\ z &\to 2z \\ c^2 &\to 2c^2 \end{aligned}$$

to put the system into the form

$$\begin{aligned} \dot{r} = &\quad rz + O(|r,z|^3) \\ \dot{z} = &\quad c^2 - z^2 - r^2 + O(|r,z|^3). \end{aligned} \tag{3.18}$$

This system is now in the form (3.17), with $a = 1$ and $b = -1$. Therefore the Michelson system falls into case 4, as in figure 3.1. This is the case that we will analyse in section 3.4.

3.3 Asymptotic Solutions for the Michelson System

We now present an alternative approach for obtaining the asymptotic form of system (2.2) as $c \to 0$, where it is possible to derive analytic solutions for all bounded orbits. This analysis effectively recovers the formal normal form by searching for solutions which evolve on different time scales, but it does not depend on the introduction of normal form variables. The material in this section is to be published in *Nonlinearity* [115].

3.3.1 Perturbation Expansions

As previously mentioned, due to the pure imaginary pair of eigenvalues in the spectrum at $c = 0$, the normal form will exhibit an S^1 symmetry at each order of the expansion [35]. In order to reflect this symmetry, we introduce polar coordinates

$$y = \rho\cos\theta, \quad z = \rho\sin\theta,$$

into equations (2.2), giving

$$\begin{aligned} x_t &= \rho\cos\theta \\ \rho_t &= (c^2 - \frac{1}{2}x^2)\sin\theta \\ \theta_t &= -1 + (c^2 - \frac{1}{2}x^2)\frac{\cos\theta}{\rho}. \end{aligned} \tag{3.19}$$

We rescale

$$x \to 2\epsilon x, \quad \rho \to 2\epsilon\rho$$

and let $c^2 = 2\epsilon^2$. Then

$$\begin{aligned} x_t &= \rho\cos\theta \\ \rho_t &= \epsilon(1 - x^2)\sin\theta \\ \theta_t &= -1 + \epsilon(1 - x^2)\frac{\cos\theta}{\rho}. \end{aligned} \tag{3.20}$$

Now assume $\epsilon \ll 1$, and analyse equations (3.20) using a multiple time scale analysis. Let $x(t) = x(t, \tau_1, \tau_2, \cdots)$, where $\tau_1 \equiv \tau = \epsilon t$, $\tau_2 = \epsilon^2 t$. Expanding in the small parameter ϵ, we have

$$x \simeq x_0 + \epsilon x_1 + \cdots \tag{3.21}$$

with similar expressions for ρ and θ, together with

$$\frac{d}{dt} = \frac{\partial}{\partial t} + \epsilon\frac{\partial}{\partial \tau} + \cdots .$$

Then (3.20) may be formally written

$$(\tfrac{\partial}{\partial t} + \epsilon\tfrac{\partial}{\partial \tau} + \cdots)(x_0 + \epsilon x_1 + \cdots) \tag{3.22}$$

$$= (\rho_1 + \epsilon\rho_1 + \cdots).\cos(\theta_0 + \epsilon\theta_1 + \cdots), \tag{3.23}$$

$$(\tfrac{\partial}{\partial t} + \epsilon\tfrac{\partial}{\partial \tau} + \cdots)(\rho_0 + \epsilon\rho_1 + \cdots) \tag{3.24}$$

$$= \epsilon(1 - (x_0 + \epsilon x_1 + \cdots)^2).\sin(\theta_0 + \epsilon\theta_1 + \cdots), \tag{3.25}$$

$$(\tfrac{\partial}{\partial t} + \epsilon\tfrac{\partial}{\partial \tau} + \cdots)(\theta_0 + \epsilon\theta_1 + \cdots) \tag{3.26}$$

$$= -1 + \epsilon(1 - (x_0 + \epsilon x_1 + \cdots)^2).\tfrac{\cos(\theta_0 + \epsilon\theta_1 + \cdots)}{\rho_0 + \epsilon\rho_1 + \cdots}. \tag{3.27}$$

In the subsequent analysis we carry out the perturbation to order ϵ in x.

Equating successive powers of ϵ, we find

Order ϵ^0:
$$\begin{aligned}\frac{\partial x_0}{\partial t} &= \rho\cos\theta_0\\ \frac{\partial \rho_0}{\partial t} &= 0\\ \frac{\partial \theta_0}{\partial t} &= -1,\end{aligned}$$

with solutions

$$\begin{aligned}\theta_0 &= -t + A(\tau)\\ \rho_0 &= B(\tau)\\ x_0 &= B(\tau)\sin(t - A(\tau)) + C(\tau).\end{aligned}\tag{3.28}$$

Order ϵ^1:
$$\begin{aligned}\frac{\partial x_0}{\partial \tau} + \frac{\partial x_1}{\partial t} &= \rho_1\cos\theta_1 - \rho_0\theta_1\sin\theta_0\\ \frac{\partial \rho_0}{\partial \tau} + \frac{\partial \rho_1}{\partial t} &= (1 - x_0^2)\sin\theta_0\\ \frac{\partial \theta_0}{\partial \tau} + \frac{\partial \theta_1}{\partial t} &= (1 - x_0^2)\frac{\cos\theta_0}{\rho_0},\end{aligned}$$

which become

$$\frac{\partial x_1}{\partial t} = \rho_1\cos\theta_0 - \rho_0\theta_1\sin\theta_0 + \frac{\partial B}{\partial \tau}\sin\theta_0 + B\frac{\partial A}{\partial \tau}\cos\theta_0 - \frac{\partial C}{\partial \tau}\tag{3.29}$$

$$\frac{\partial \rho_1}{\partial t} = (1 - (B\sin\theta_0 - C)^2)\sin\theta_0 - \frac{\partial B}{\partial \tau}\tag{3.30}$$

$$\frac{\partial \theta_1}{\partial t} = (1 - (B\sin\theta_0 - C)^2)\frac{\cos\theta_0}{B} - \frac{\partial A}{\partial \tau}.\tag{3.31}$$

The idea now is to remove secular terms from this system. In the equations (3.30), (3.31), the right hand sides contain terms (similar to)

$$\begin{aligned}&(1 - (B\sin\theta_0 - C)^2)\sin\theta_0\\ &\qquad = (1 - B^2\sin^2\theta_0 + 2BC\sin\theta_0 - C^2)\sin\theta_0\\ &\qquad = (1 - C^2 - \frac{3B^2}{4})\sin\theta_0 - BC\cos 2\theta_0 + \frac{B^2}{4}\sin 3\theta_0 + BC.\end{aligned}$$

Thus we can write $\frac{\partial\rho_1}{\partial t} = \frac{\partial\rho_1}{\partial t}\Big|_{\mathrm{s}} + \frac{\partial\rho_1}{\partial t}\Big|_{\mathrm{n}}$, where the suffixes s and n indicate secular and nonsecular terms respectively. Separating the parts, we have

$$\begin{aligned}\frac{\partial\rho_1}{\partial t}\bigg|_{\mathrm{n}} &= (1 - C^2 - \frac{3B^2}{4})\sin\theta_0 - BC\cos 2\theta_0 + \frac{B^2}{4}\sin 3\theta_0\\ \frac{\partial\rho_1}{\partial t}\bigg|_{\mathrm{s}} &= BC - \frac{\partial B}{\partial \tau}.\end{aligned}$$

To avoid secular growth in equation (3.30), we require

$$\frac{\partial B}{\partial \tau} = BC. \tag{3.32}$$

Similarly for equation (3.31),

$$\begin{aligned}(1-(B\sin\theta_0 - C)^2)\frac{\cos\theta_0}{B} &= \frac{1}{B}(1-C^2)\cos\theta_0 + C\sin 2\theta_0 \\ &\quad -\frac{B}{4}(-\cos 2\theta_0 + \cos\theta_0),\end{aligned}$$

giving

$$\frac{\partial \theta_1}{\partial t} = \frac{(1-c^2)}{B}\cos\theta_0 + C\sin 2\theta_0 - \frac{B}{4}(-\cos 3\theta_0 + \cos\theta_0) - \frac{\partial A}{\partial \tau}.$$

To avoid secular growth in equation (3.31), we require

$$\frac{\partial A}{\partial \tau} = 0, \tag{3.33}$$

so $A(\tau)$ is constant, equal to A, say. In equation (3.29), we ignore the non-secular terms $\frac{\partial B}{\partial \tau}\sin\theta_0$ and $B\frac{\partial A}{\partial \tau}\cos\theta_0$. Consider $\rho_1\cos\theta_0$: from equations (3.30), (3.32) the solution for ρ_1 is

$$\rho_1 = (1 - C^2 - \frac{3B^2}{4})\cos\theta_0 + \text{terms with } \sin 2\theta_0,\ \cos 3\theta_0.$$

Hence,

$$\begin{aligned}\rho_1\cos\theta_0 &= (1-C^2-\frac{3B^2}{4})\frac{(1+\cos 2\theta_0)}{2} + \cdots \\ &= \frac{1}{2}(1-C^2-\frac{3B^2}{4}) + \text{oscillatory terms.}\end{aligned}$$

Similarly, consider $\rho_0\theta_1\sin\theta_0$. By (3.31), (3.33), the solution for θ_1 is

$$\theta_1 = -\left(\frac{1-C^2}{B}\right)\sin\theta_0 + \frac{B}{4}\sin\theta_0 + \text{terms with } \cos 2\theta_0,\ \cos 3\theta_0,$$

and so

$$\begin{aligned}\rho_0\theta_1\sin\theta_0 = -B\left(\frac{1-C^2}{2B}\right) + \frac{B^2}{8} + \cdots - \left(\frac{1-C^2}{2}\right) + \frac{B^2}{8} \\ + \text{oscillatory terms.}\end{aligned}$$

To avoid secular growth in equation (3.29), we require

$$\frac{1}{2}\left(1 - C^2 - \frac{3B^2}{4}\right) - \left(-\frac{(1-C^2)}{2} + \frac{B^2}{8}\right) - \frac{\partial C}{\partial \tau} = 0$$

or

$$\frac{\partial C}{\partial \tau} = 1 - C^2 - \frac{B^2}{2}. \tag{3.34}$$

We now analyse equations (3.32) and (3.34), which describe evolutions of the amplitudes B and C on the slow time scale τ. In particular, a full analytic solution to this coupled system is obtained. Moreover, the connection between (x, ρ) and (B, C) is given in equations (3.18), and we see that the latter variables are obtained by averaging the former over one period in the fast time scale: i.e.

$$\overline{\rho}_0 \;:=\; \frac{1}{2\pi}\int_0^{2\pi} \rho_0(\tau)dt = \rho_0(\tau) = B(\tau), \tag{3.35}$$

$$\overline{x}_0 \;:=\; \frac{1}{2\pi}\int_0^{2\pi} x_0(t,\tau)dt \simeq C(\tau). \tag{3.36}$$

3.3.2 Explicit Solutions

Hamiltonian Structure

Equations (3.32) and (3.34) can be written in Hamiltonian form with canonical variables (B^2, C), and Hamiltonian function

$$H = B^2(1 - C^2 - \frac{B^2}{4}) \tag{3.37}$$

Level surfaces then correspond to $H =$ const, which are shown in figure 3.2, and which we now examine in detail. Evolution of $(B(\tau), C(\tau))$ on the slow time scale occurs on the level surfaces shown in figure 3.2. This is consistent with the normal form procedure, which produces the same figure (see section 3.2): as noted earlier, the normal form can be made S^1-symmetric at every order; that is, the angular coordinate equation will decouple and will be equal to $\dot{\theta} = 1$ at every order. This is equivalent to averaging over the period of θ in the fast time scale.

It is apparent from (3.28) that the variable x_0 undergoes one complete fast time oscillation, with period 2π. The nature of the oscillation is understood by converting (3.28) back to Cartesian coordinates:

$$\begin{aligned} x_0 &= B(\tau)\sin(t-A) + C(\tau) \\ y_0 &= B(\tau)\cos(A-t) \\ z_0 &= B(\tau)\sin(A-t) \end{aligned} \tag{3.38}$$

Thus $x_0 = -z_0 + C(\tau)$, and on the fast time scale the motion in the phase space is contained in this level set of planes, forcing the fast time oscillation present in (3.28). This will become more apparent in the numerical studies.

Analytic Solutions

The level surfaces $H = \text{const}$ are shown schematically in figure 3.2, modulo S^1-symmetry about the C-axis.

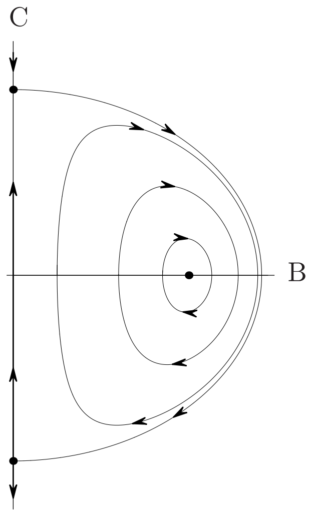

Figure 3.2: Phase portrait for Hamiltonian System defined by equations (3.32) and (3.34).

The level surface $H = 0$ consists of two parts, namely the 1D heteroclinic and the 2D heteroclinic orbits joining the fixed points $(B, C) = (0, \pm 1)$. An analytic expression for the latter is

$$B(\tau) = 2\,\mathrm{sech}\,\tau \tag{3.39}$$

$$C(\tau) = -\tanh\tau \tag{3.40}$$

while the analytic expression for the former is

$$B(\tau) = 0 \tag{3.41}$$

$$C(\tau) = \tanh\tau \tag{3.42}$$

The level surface $H = 1$ corresponds to the fixed points $(B^2, C) = (\sqrt{2}, 0)$, which in affect is the periodic orbit of equation (2.21). The invariant tori indicated in figure 3.2, lying between the fixed point and the outer shell are level surfaces $H =$ const $= E$, say, with $0 < E < 1$. Explicit solutions for $B(\tau)$ and $C(\tau)$ are obtained as

$$B(\tau) = \frac{2}{\sqrt{2-m}}\,\mathrm{dn}\,(\frac{1}{\sqrt{2-m}}\tau) \tag{3.43}$$

$$C(\tau) = \frac{-m}{\sqrt{2-m}}\,\mathrm{cn}\,(\frac{1}{\sqrt{2-m}}\tau)\,\mathrm{sd}\,(\frac{1}{\sqrt{2-m}}\tau) \tag{3.44}$$

where dn, cn and sd = sn/dn are Jacobi elliptic functions, and m is the elliptic parameter. Substituting these into the expression for H produces

$$H = -\frac{4(1-m)}{(2-m)^2} = E \tag{3.45}$$

which increases monotonically from -1 to 0 as m increases from 0 to 1. The period of the solutions (3.43) and (3.44) is obtained as

$$T(m) = 4K(m) \tag{3.46}$$

where $K(m)$ is the complete elliptic integral of the first kind. As $m \to 1$, $T(m) \to 2\ln\left(\frac{16}{1-m}\right)$ in the usual way.

This concludes an exhaustive study of the equations (3.32) and (3.34). Before leaving this section, we note that as $m \to 1$, the solutions (3.43) and (3.44) asymptote to (3.39) and (3.40) on using standard asymptotic expressions for the elliptic functions, while letting $m \to 0$ produces $(B, C) = (\sqrt{2}, 0)$ as expected.

Approximate solutions to the Michelson system

Consider now equations (3.28) for leading order solutions for $x_0(t,\tau)$, $\rho_0(t,\tau)$ and $\theta_0(t,\tau)$. Consider first the case when $B(\tau)$ and $C(\tau)$ are given by equations (3.39) and (3.40). Then, at $\mathcal{O}(\epsilon)$, we have a family of heteroclinic connections lying in the 2 dimensional manifolds $W^u(F^+)$ and $W^s(F^-)$:

$$x_0 = 2 \text{ sech } \tau \sin(t - A) - \tanh \tau \tag{3.47}$$

$$\rho_0 = 2 \text{ sech } \tau \tag{3.48}$$

$$\theta_0 = -t + A \tag{3.49}$$

The constant A parametrises this continuous family of heteroclinic connections. This coincidence at low order was observed by [19, 60]. Typically with consideration of higher order terms we would expect such a structure to break and yield transverse heteroclinic connections, but for small ϵ we would expect to see a structure which remains close to that resulting from equations (3.47), (3.48), (3.49). This is indeed backed up by numerical results. Figure 3.3 shows a trajectory illustrating the structure of the phase space for the parameter value $c = 0.074$, along with the time delay function evaluated for a set of initial points in the plane $x = 0$ along the y-axis; the plateau indicates that the orbit is trapped for times greater than the maximum shown. We observe numerically that orbits with initial points within the heteroclinic shell shown in figure 3.2 remain bounded for very long times (possibly infinite), emphasising the near integrable state of the system.

Closer inspection of the time delay function reveals logarithmic singularities in a narrow region on the edge of this structure, implying transverse intersections and chaotic motion, i.e., a departure from the integrable Hamiltonian model, see figure 3.4. However, these chaotic regions become smaller as $c \to 0$ and evidence for transverse intersections become harder to detect.

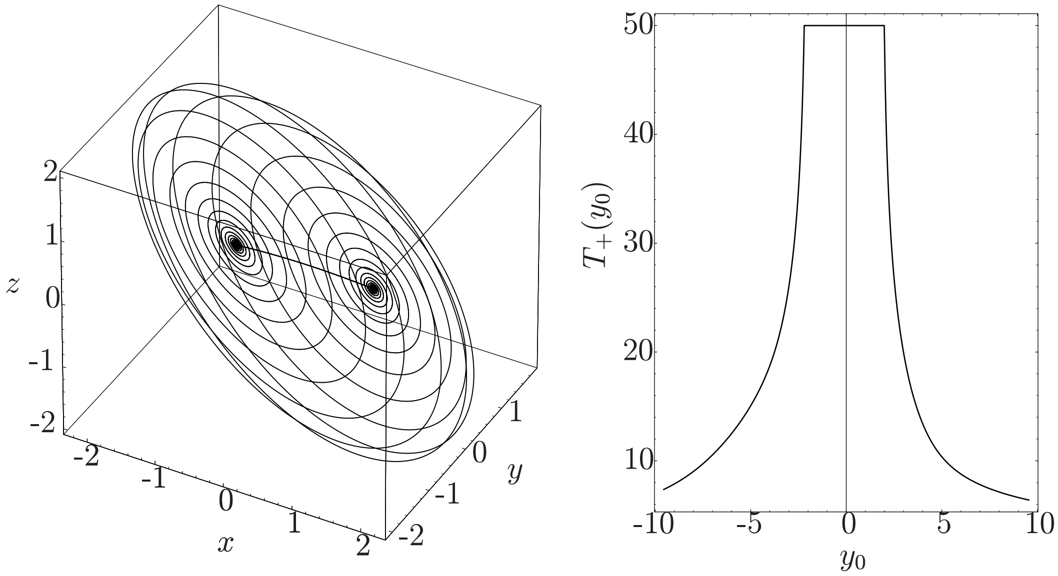

Figure 3.3: $c = 0.074$ ($\epsilon = 0.0523\ldots$); single trajectory illustrating near integrability of the system, together with a time delay function for points selected on the section $x = 0$; see text for details.

Next, with (B, C) given by solutions (3.43), (3.44), we find

$$\begin{aligned} x_0 &= \frac{2}{\sqrt{2-m}} \,\mathrm{dn}\left(\frac{\tau}{\sqrt{2-m}}\right) \sin(t-A) \\ &\quad - \frac{m}{\sqrt{2-m}} \frac{\mathrm{cn}\left(\frac{\tau}{\sqrt{2-m}}\right) \mathrm{sn}\left(\frac{\tau}{\sqrt{2-m}}\right)}{\mathrm{dn}\left(\frac{\tau}{\sqrt{2-m}}\right)} \end{aligned} \tag{3.50}$$

$$\rho_0 = \frac{2}{\sqrt{2-m}} \,\mathrm{dn}\left(\frac{\tau}{\sqrt{2-m}}\right) \tag{3.51}$$

$$\theta_0 = -t + A, \tag{3.52}$$

where A is a constant. As $m \to 1$, and using asymptotic forms for the elliptic functions, the solutions (3.50)-(3.52) asymptote to (3.47)-(3.49), as expected. Conversely, in the limit $m \to 0$, we find

$$\begin{aligned} x_0 &= \sqrt{2}\sin(t-A) \\ \rho_0 &= \sqrt{2} \\ \theta_0 &= -t + A \end{aligned} \tag{3.53}$$

which, with constant $A = 0$ is the periodic orbit (2.21) discussed by Kent and

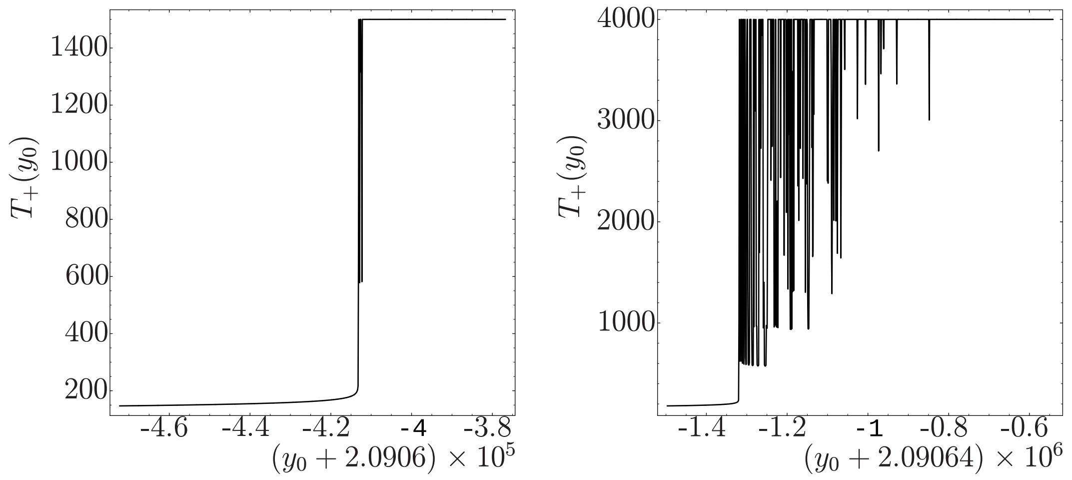

Figure 3.4: Magnification of the Time Delay function of figure 3.3, marginal chaotic regions are present.

Elgin [60], taken to $\mathcal{O}(c^2)$. This is a fixed point of the equations (3.32), (3.34). The other fixed points are $(B, C) = (0, \pm 1)$. These are simply the fixed points of (2.2) in the scaled variables. Linearising about the fixed points of (3.32), (3.34) reveals that the periodic orbit (3.53) has eigenvalues $\lambda = \pm\sqrt{2}\mathrm{i}$. It is elliptic, and this is consistent with [19, 72]. It is also consistent with (3.43), (3.44), since close to the periodic orbit where $m \to 0$, we have

$$\begin{aligned} B(\tau) &= \alpha \,\mathrm{dn}\,(\lambda\tau) \\ &\sim \sqrt{2}(1 - m\sin^2\lambda\tau)^{1/2} \\ &= \sqrt{2}(1 - \frac{m}{4}) + \frac{m}{2\sqrt{2}}\cos(\sqrt{2}\tau) \end{aligned} \tag{3.54}$$

Similarly,

$$C(\tau) \sim -\frac{m}{2\sqrt{2}}\sin(\sqrt{2}\tau) \tag{3.55}$$

For small $m > 0$ these are the toroidal solutions close to the elliptic periodic orbit of equation (3.53). They exist in the region bounded by (3.47), (3.48), (3.49), parametrised by $0 < m < 1$.

To conclude, consider the solution

$$B(\tau) = 0 \tag{3.56}$$

$$C(\tau) = \tanh \tau \tag{3.57}$$

This is the heteroclinic connection between the two fixed points of (2.2) to $\mathcal{O}(\epsilon)$, lying in the coincidence of the 1 dimensional manifolds $W^s(F^+)$ and $W^u(F^-)$:

$$x_0 = \tanh \tau \tag{3.58}$$

$$\rho_0 = 0 \tag{3.59}$$

As before, this is a degenerate situation and we would expect this structure to break under perturbation of the higher order terms, as studied in the generic case in section 3.4. We have studied system (2.2) for evidence of 1D heteroclinic connections by taking the $x = 0$ plane as a section plane and following a trajectory close to F^- in $E^u(F^-)$, and searching for parameter values c_0 where orbits strike the section plane with $z \lesseqgtr 0$ for $c > c_0$ and $z \gtreqless 0$ for $c < c_0$. Then the orbit should pass through the y-axis, where by the symmetry R it is a symmetric 1D heteroclinic orbit. However, this numerical process was found to be very sensitive to such variables as step size and initial condition so that to detect such connections in this manner is computationally difficult, if not intractable. An approximate 1D heteroclinic connection is shown in figure 3.5 for the parameter value $\epsilon = 0.0282$.

3.3.3 Numerical Studies and Validity of the Results

1D Heteroclinic Orbits

The solutions found in section 3.3.1 (to $\mathcal{O}(\epsilon)$) in the expansion (3.21) turn out to be a very good approximation in the numerical simulations. The approximate analytic solution found for the 1D heteroclinic connection (in the rescaled variables) was $x(t) = \tanh \epsilon t$, which is plotted in figure 3.5 for parameter value $\epsilon = 0.0282$, overlayed with the numerical solution.

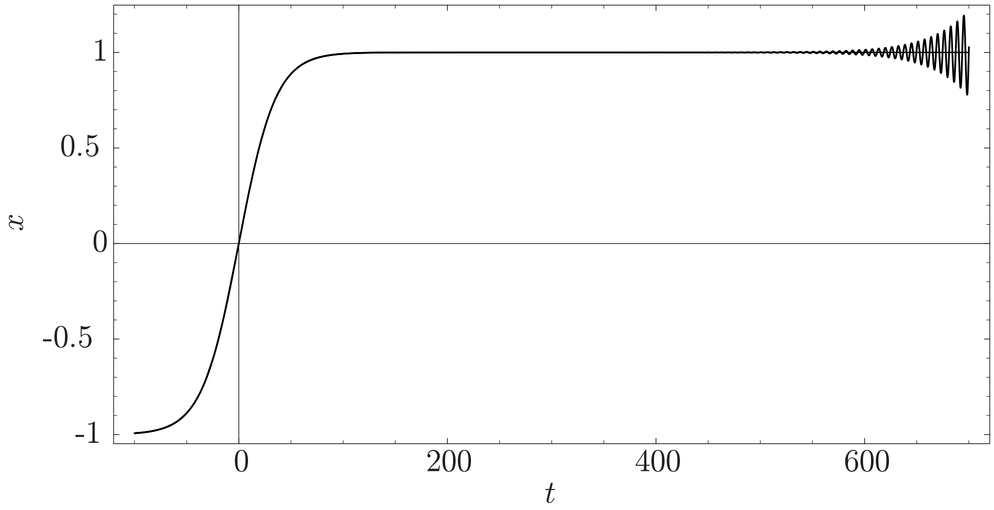

Figure 3.5: Analytic 1D heteroclinic orbit, shown overlayed with numerically calculated orbit, $\epsilon = 0.0282$. The figures are identical to within the resolution used in the plotting routine, until $t \simeq 450$.

2D Heteroclinic Orbits

Figure 3.6 shows the analytic solution for a symmetric heteroclinic orbit lying in the 2 dimensional manifolds $W^u(F^+)$ and $W^s(F^-)$ for $t > 0$. It is part of the heteroclinic shell found in section 3.3.2 and has the analytic form $x(t) = 2 \operatorname{sech} \epsilon t \sin t$. Note that this is one of two symmetric 2D heteroclinic connections in the heteroclinic shell, the other one is obtained by setting the constant $A = \pi$ in (3.47). This is again overlayed by a numerically calculated solution. The two are again in agreement to within the resolution of the figure.

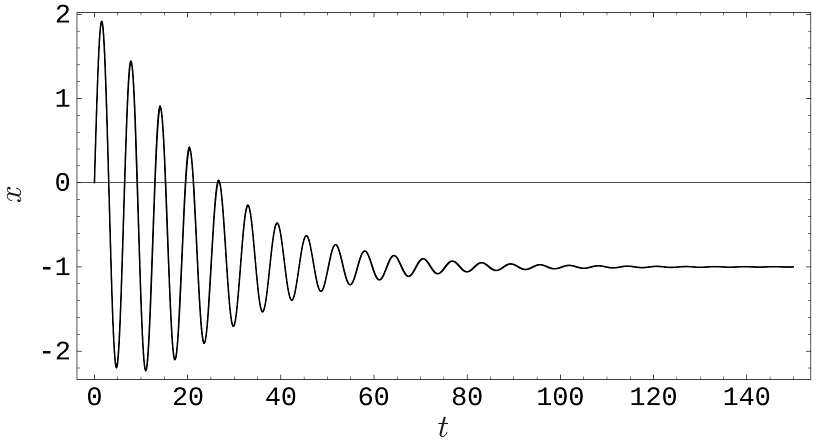

Figure 3.6: Analytic symmetric 2D heteroclinic orbit, shown overlayed with numerically calculated orbit, $\epsilon = 0.05294$.

Toroidal Solutions

Consider finally the toroidal solutions (3.50)–(3.52), $0 < m < 1$. We now examine whether the behaviour of the system as determined numerically is well approximated by the 'simple' phase space structure the analytic toroidal solutions suggest. Results are shown in figures 3.7 and 3.8 for the parameter value $\epsilon \simeq 0.02121$ (i.e. $c = 0.03$). Here a Poincaré map, defined with section plane $x = 0$ has been introduced, and the figure indicates intersections of the orbit with this plane. The parameter A is set to zero in the analytic solutions. A small discrepancy between analytic and numerical predictions is clearly discernable, but this appears only as a slight change in shape of the torus. Qualitatively, agreement is excellent, more so in view of the fact that the numerical results imply a near-integrable system. Discrepancies result from the time-duration required to compute the figures, which is long past the point where the multiple scale expansion might be expected to fail, as slower time scales $\tau_2, \tau_3, \ldots$ come into play.

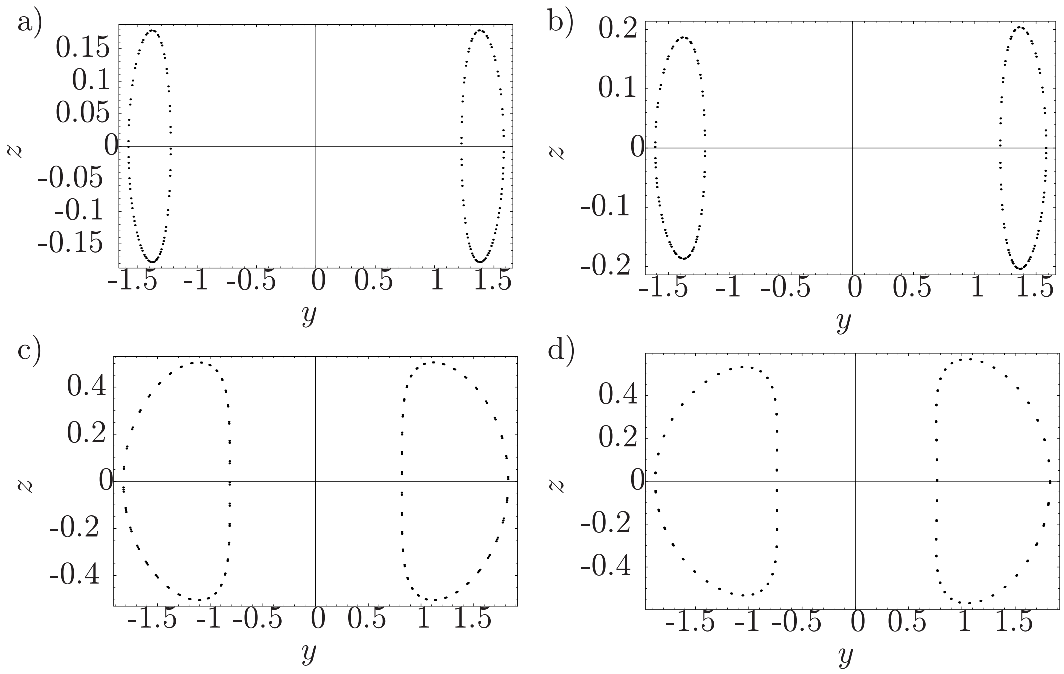

Figure 3.7: a) Analytic Poincaré map, $m = 0.4$, b) Numerical Poincaré map, $m = 0.4$, c) Analytic Poincaré map, $m = 0.8$, d) Numerical Poincaré map, $m = 0.8$; $\epsilon \simeq 0.02121$ in each case.

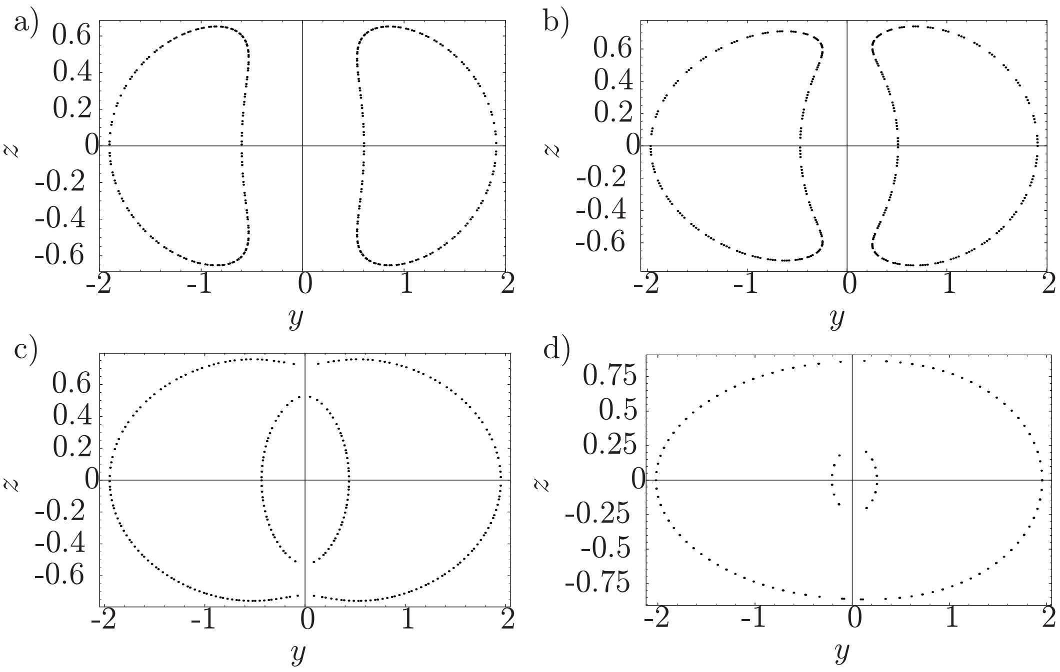

Figure 3.8: a) Analytic Poincaré map, $m = 0.9$, b) Numerical Poincaré map, $m = 0.9$, c) Analytic Poincaré map, $m = 0.95$, d) Numerical Poincaré map, $m = 0.95$; $\epsilon \simeq 0.02121$ in each case.

3.4 Breaking the Formal Symmetry

Here we consider the normal form unfoldings of the Hopf-zero bifurcation presented in section 3.2 and the effect of the additional higher order terms that break the formal S^1 symmetry that appears in the normal form. We will present our theorems for the R-reversible case, but remark that the results are equally valid in the reversible volume-preserving case, by the same proofs. The analogous results for the volume preserving case is contained in [14].

In this section we prove the generic existence of heteroclinic and homoclinic cycles in unfoldings of the Hopf-zero bifurcation that break the formal S^1 symmetry. We will work in the C^∞ topology. In this topology, two vector fields

X, Y are close if the vector fields and all their derivatives are close everywhere on the manifold on which they are defined (in the C^r topology, only the vector fields and their derivatives up to order r are counted). The results are summarised in the following theorems:

Theorem 3.4.1. *Denote by $\mathfrak{X}_R^\mu$ the space of unfoldings of R-reversible vector fields exhibiting the Hopf-zero bifurcation as above, endowed with the C^∞ topology. There is a C^2-open set $D \subset \mathfrak{X}_R^\mu$ of unfoldings, dictated by the conditions of case 4 in section 3.2. The set of vector fields for which in a neighbourhood of the origin in $\mathbb{R}^3 \times \mathbb{R}$ there exists a countable infinity of 1-homoclinic orbits and 1-heteroclinic cycles between the two saddle-focus fixed points, is residual in $D \subset \mathfrak{X}_R^\mu$.*

An analysis of the symmetric heteroclinic bifurcation is contained in Chapters 4 and 5, and many additional heteroclinic and homoclinic cycles are shown to be present. The analysis contained in these chapters allows us also to state the following theorem.

Theorem 3.4.2. *Let D, $\mathfrak{X}_R^\mu$ be defined as above. Then in an open and dense subset of D (in the C^k topology) of vector fields exhibiting the Hopf-zero bifurcation, there exists a countable infinity of n-heteroclinic orbits for each $n = 2, 3, \ldots$, and a countable infinity of n-homoclinic orbits for each $n \in \mathbb{N}$.*

The residual property in Theorem 3.4.1 has been replaced by open and dense in Theorem 3.4.2 because the existence of a countable number of n-heteroclinic/homoclinic orbits may be shown by analysis of just one 1-heteroclinic cycle from Theorem 3.4.1. The case we are interested in is labelled as case 4 in the preceding section, and this determines part of the open conditions as described in Theorems 3.4.1 and 3.4.2. We shall denote a typical S^1-symmetric vector field as $\tilde{X}^\mu$. It is easy to see that our S^1-symmetric vector fields are qualitatively those of case 4. Clearly the structure of the phase space for $\mu > 0$ is degenerate for the 3 dimensional vector field; we would not expect the 2-dimensional manifolds of both fixed points to coincide in such an invariant 2-sphere. Also, it is clear that in the break up of such a 2-sphere there would be at least 2 heteroclinic orbits persisting, due to the fact that Fix R intersects the sphere transversely in exactly two points. Thus the break up will be to a 'perturbed globe' as portrayed in [14]. We will consider the effect of perturbing the vector field $\tilde{X}^\mu$ with a flat perturbation—this is a perturbation which is beyond all orders in the normal form, it is equal to zero at the origin together with every derivative. An example of a C^∞ function $\alpha : \mathbb{R} \to \mathbb{R}$ which is flat at the origin is given by

$$\alpha(x) \;=\; \begin{cases} 0 & x \leq 0, \\ e^{-1/x} & x > 0. \end{cases}$$

This function may in fact be used to derive the bump functions used later, see [51]. We shall see that the break up of the invariant 2-sphere is extremely sensitive on the nature of the S^1-symmetry breaking flat perturbation, which we will denote as p^μ.

Lemma 3.4.3. *Let $\tilde{X}^\mu$ be an S^1-symmetric vector field in the open set D, as described in Theorem 3.4.1. There exists a flat perturbation p^μ such that the perturbed vector field $\tilde{X}^\mu + p^\mu$ has a sequence of Shil'nikov homoclinic bifurcations at a discrete set of parameter points μ_i which accumulate at $\mu = 0$, as well as a sequence of parameter points μ_j for which there exists a heteroclinic cycle.*

We postpone the proof of this Lemma until later in this section. We will now describe specific flat perturbations p^μ for an S^1-symmetric unfolding of the singularity $\tilde{X}^\mu$ as above. We will then discuss genericity of the phenomena in the space of reversible vector fields. In fact, it is no extra effort to extend the result to the class of reversible volume-preserving vector fields, due to the type of perturbation used here.

The techniques used in this section were employed by Broer and Vegter [14], where they proved the existence of an infinite sequence of Shil'nikov homoclinic bifurcations for certain flat perturbations of a class of volume-preserving vector fields.

The flat perturbation to be constructed will consist of two separate flat perturbations. We write $p^\mu = p_1^\mu + p_2^\mu$, where each $p_1^\mu + p_2^\mu$ is flat in μ at $\mu = 0$. Now we will describe these perturbations. The perturbation p_1^μ is of the type

$$p_1^\mu(x,y,z) = \delta_1(\mu) P_1^\mu(x,y,z),$$

where $P_1^\mu : \mathbb{R}^3 \to \mathbb{R}^3$ is of the form:

$$\begin{aligned} \dot{x} &= -\frac{\partial}{\partial y}(x\beta_\mu(\xi)) \\ \dot{y} &= \frac{\partial}{\partial x}(x\beta_\mu(\xi)) \\ \dot{z} &= 0, \end{aligned} \tag{3.60}$$

where $\xi = (x,y,z) \in \mathbb{R}^3$ and $\delta_1(\mu)$ is an appropriate flat function in μ at $\mu = 0$, appropriate in a sense to be defined later. $\beta^\mu : \mathbb{R}^3 \to \mathbb{R}$ is a bump function such that $\beta^\mu(R(x,y,z)) = \beta^\mu(x,y,z)$, recall that $R(x,y,z) = (x,-y,-z)$. This bump function is given by

$$\begin{aligned} \beta^\mu(x,y,z) &= \gamma(\frac{1}{\mu}(\sqrt{x^2+y^2})).\gamma(\frac{1}{\mu^2}z) \\ &= \gamma(\frac{1}{\mu}r).\gamma(\frac{1}{\mu^2}z), \quad \mu > 0 \text{ small.} \end{aligned} \tag{3.61}$$

where as before $x = r\cos\theta$, $y = r\sin\theta$, $\gamma : \mathbb{R} \to \mathbb{R}$ is a bump function with $\mathrm{supp}(\gamma) = [-2,2]$, $\gamma(-s) = \gamma(s)$ and $\gamma(s) \equiv 1$ for $s \in [-1,1]$, see [14, 51]. The support box in 3 dimensions then is a cylinder, denote it by η^μ, and define $\nu_\mu^1, \nu_\mu^2 \subset \eta^\mu$ by

$$\nu_\mu^1 := \{(x,y,z) \in \mathbb{R}^3 : \sqrt{x^2+y^2} = r \leq \mu\}, \qquad \text{and}$$

$$\nu_\mu^2 := \{(x,y,z) \in \mathbb{R}^3 : |z| \leq \mu^2\}.$$

Then it is clear from (3.60), (3.61) that for $(x,y,z) \in \nu_\mu^1$, $p_1^\mu(x,y,z) = \delta_1(\mu).\gamma(\frac{1}{\mu^2}z)\frac{\partial}{\partial y}$ and for $(x,y,z) \in \nu_\mu^2$, $p_1^\mu(x,y,z) = \delta_1(\mu)\frac{\partial}{\partial y}$. The support for this perturbation is sketched in figure 3.9. Note that p_1^μ is a C^∞, reversible, divergence free perturbation [91].

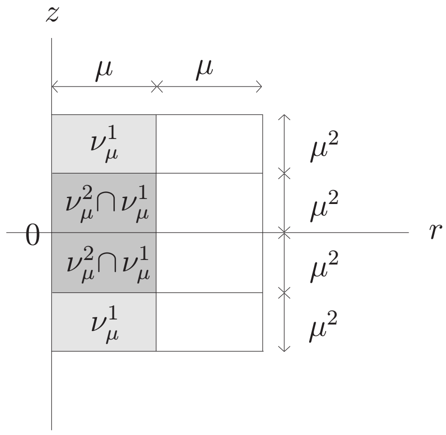

Figure 3.9: Sketch of the support cylinder η^μ.

The perturbation as described above was studied by [13, 14]. Here we review the relevant effects of p_1^μ for our system.

Lemma 3.4.4. *Let r_μ^* be the r-coordinate of the 1-dimensional unstable manifold $W^u(F^-)$ when it enters η^μ for all $\mu > 0$ sufficiently small. Then we have*

$$r_\mu^* \sim \mu\delta_1(\mu)^1 \tag{3.62}$$

Proof. Recall from section 3.2 that we have

$$\begin{aligned}
\text{R}: \quad & \dot{r} = a_1 rz + a_2\mu rz + O(|r,z,\mu|^4) \\
\text{VP}: \quad & \dot{r} = -a_1 rz + a_2\mu r + O(|r,z,\mu|^3) \\
\text{RVP}: \quad & \dot{r} = -a_1 rz + a_2\mu rz + O(|r,z,\mu|^4).
\end{aligned}$$

So for $\xi \in \eta^\mu$,

$$\begin{aligned}
\text{R,RVP}: \quad & \dot{r} \leq C_1\mu^2 r + \omega(\mu) \\
\text{VP}: \quad & \dot{r} \leq C_2\mu r + \omega(\mu),
\end{aligned}$$

[1] Here the relation $\sim$ means there exist constants C^1, C^2 such that $r_\mu^* \leq C^1\mu\delta(\mu)$ and $\mu\delta(\mu) \leq C^2 r_\mu^*$.

where the $C_i > 0$ are constants and $\omega(\mu)$ is a flat function depending on p_1^μ. For all cases $\dot{z} \sim \mu$. We shall now only consider the case of R, RVP, since the proof is similar for the case VP. Then let $C = C_1$. Then

$$r(t) \leq \frac{\omega(\mu)}{C\mu^2}(e^{C\mu^2 t} - 1)$$

Let $T_1(\mu)$ be the time that the 1D unstable manifold $W^u(F^-)$ spends in the support box η^μ. Since the height of η^μ is $4\mu^2$, we have

$$\begin{aligned} T_1(\mu) &\sim \mu \\ r(t) &\leq \mu\omega(\mu), \qquad 0 \leq t \leq T_1(\mu). \end{aligned}$$

Since $\omega(\mu)$ is a flat function, we can control $W^u(F^-)$ so that it remains in ν_μ^1. We will show that the perturbation in ν_μ^2 is dominant in controlling the coordinate r_μ^*.

Since in ν_μ^1, we have $p_1^\mu = \delta_1(\mu)\gamma\left(\frac{z}{\mu^2}\right)\frac{\partial}{\partial y}$, we can write

$$r(t) \leq \mu\delta_1(\mu), \qquad 0 \leq t \leq T_1(\mu). \tag{3.63}$$

Conversely, we have

$$\begin{aligned} \dot{x} &= -\alpha y + xzg(r^2, z^2, \mu) \\ \dot{y} &= \alpha x + yzg(r^2, z^2, \mu) \\ \dot{z} &= h(r^2, z^2, \mu). \end{aligned}$$

Thus in ν_μ^1, under the perturbation p_1^μ the $\frac{\partial}{\partial y}$ component of the vector field becomes

$$\dot{y} = \alpha x + yzg(r^2, z^2, \mu) + \delta_1(\mu)\gamma\left(\frac{z}{\mu^2}\right)$$

Then it follows, using (3.63), that

$$\dot{y} \geq \frac{1}{2}\delta_1(\mu) \quad \text{in } \nu_\mu^2$$

for $\mu > 0$ sufficiently small.

Similarly we have

$$\dot{y} \geq -C_1\mu\delta_1(\mu) \quad \text{in } \nu_\mu^1,$$

where C_1 is a constant, and μ is sufficiently small. Now define $T_2(\mu)$ to be the time that $W^u(F^-)$ spends in ν_μ^2. Then as before $T_2(\mu) \sim \mu$. Thus we have

$$\begin{aligned} y(T_1(\mu)) &\geq \frac{1}{2}\delta_1(\mu)T_2(\mu) - C_1\mu\delta_1(\mu)(T_1(\mu) - T_2(\mu)) \\ &\sim \mu\delta(\mu), \end{aligned}$$

and so $r_\mu^* \sim \mu\delta_1(\mu)$. □

In this way we can control the order of magnitude of the r-coordinate of the 1-dimensional manifold of F^-, relative to the flat function $\delta(\mu)$. Note that for the according angle coordinate we have $\theta_\mu^* = o(1)$ as $\mu \to 0^+$.

The perturbation p_2^μ is designed to make the two dimensional manifolds $W^s(F^-)$ and $W^u(F^+)$ intersect transversally. We would like this to be a flat perturbation, so let $p_2^\mu = \delta_2(\mu)P_2^\mu$. First note that the invariant 2-sphere formed by $W^s(F^-)$ and $W^u(F^+)$ has the form (as $\mu \to 0^+$):

$$\frac{r}{1+a} + z^2 = \mu.$$

Thus we choose the support of P_2^μ to be a torus centred on the circle $x^2 + y^2 = (1+a)\mu$, $z = 0$ in the full 3 dimensional system. The following Lemma implies that we can construct $p_2^\mu = \delta_2(\mu)P_2^\mu$ so that $\tilde{X}^\mu + p_2^\mu$ has transverse heteroclinic connections lying in $W^s(F^-) \cap W^u(F^+)$. It is proved in section 3.5.

Lemma 3.4.5. *Let $\mathfrak{X}_R$ be the space of reversible vector fields with the C^∞ topology, with the reversing symmetry acting as diag(1,-1,-1), and $\mathcal{S}_R \subset \mathfrak{X}_R$ be the subset for which all fixed points have transversally intersecting invariant manifolds. Then $\mathcal{S}_R$ is residual in $\mathfrak{X}_R$.*

Remark 3.4.6. *This theorem is also valid for volume-preserving vector fields [91], and reversible volume-preserving vector fields, again due to the type of perturbation used.*

Proof of Lemma 3.4.3. Our perturbed vector field $\tilde{X}^\mu + p_1^\mu + p_2^\mu$ now has transverse heteroclinic connections. We would now like to know the behaviour of $W^s(F^-)$ close to $W^s(F^+)$. By the λ-lemma, $W^s(F^-)$ will wrap itself tightly around $W^s(F^+)$ in a logarithmic spiral. Suppose we look on the top of the support box η^μ, that is $\eta^\mu \cap \{z = 2\mu^2\}$. We assume here that the angle θ is lifted to $\mathbb{R}$. Then $W^s(F^+)$ intersects $\eta^\mu \cap \{z = 2\mu^2\}$ along the z-axis (the perturbations p_1^μ and p_2^μ) do not affect the relevant part of $W^s(F^+)$), and $W^s(F^-)$ will trace out a 1-dimensional curve in this section, with equation $r(\theta, \mu) \sim \delta_3(\mu) e^{a\theta\sqrt{\mu}}$, where $\delta_3(\mu)$ is a flat function depending on p_1^μ. Note that the perturbation p_1^μ does not affect this logarithmic spiral. Since $\theta_\mu^* = o(1)$ and from (3.62), if we set, for example $\mu\delta_1(\mu) = \delta_3(\mu) e^{-1/\mu}$ we will obtain a sequence of Shil'nikov homoclinic bifurcations. Finally, choosing $p^\mu = \sin(\frac{1}{\mu})\delta_1(\mu) P^\mu$ will create a sequence of 1D heteroclinic connections (these will be the same connections that appear in the S^1-symmetric normal form) whenever $\sin(\frac{1}{\mu}) = 0$. When $\sin(\frac{1}{\mu}) = 1$ we have $r_\mu^* \sim \mu\delta_1(\mu)$ as before. We perturb the heteroclinic and homoclinic connections in the 1-parameter family in order to make them generic. In the vicinity of a 'generic' heteroclinic bifurcation there exist countably many homoclinic bifurcations, accumulating on the heteroclinic bifurcation. This is studied in the next section. This completes the proof of Lemma 3.4.3. □

Proof of Theorem 3.4.1. We now need to study the generic properties of such sequences of global bifurcations. From Section 3.2 we have that $\{\tilde{X}^\mu\}$—the set of S^1-symmetric vector fields—is dense in $\mathfrak{X}_R$ in the C^∞ topology. Since the perturbations we have used to prove existence are flat, this proves that our bifurcation sequences are dense in $\mathfrak{X}_R$. Let $\mathcal{B}^k_{\mathrm{hom/het}}$ be the set of vector fields with k homoclinic (resp. heteroclinic) bifurcations close to the bifurcation point. Given any element $\tilde{X}^\mu + p^\mu$ in the dense set which has an infinite sequence of homoclinic and heteroclinic bifurcations accumulating at the bifurcation point, this family will have k such bifurcations all for $\mu > 0$ sufficiently small. Each such bifurcation in persistent in the C^1 topology, thus

$\mathcal{B}^k_{\mathrm{hom/het}}$ is open in the C^1 topology. Note that this set says nothing about what happens in a neighbourhood of the bifurcation point itself; any finite number of bifurcations will be bounded away from zero. This is the weak C^1 topology. A different point of view is that the infinite sequences of bifurcations is open in the strong C^1 topology, see [14]. The property of an infinite set of homoclinic and heteroclinic bifurcations is the set $\bigcap_k \mathcal{B}^k_{\mathrm{hom/het}}$, and this is residual in the C^1 topology. This completes the proof of Theorem 3.4.1. □

3.5 A Reversible Kupka-Smale Theorem

In this section we prove a result which was used in the proof of Theorem 3.4.1—that is, the invariant manifolds of fixed points generically intersect transversally, in the space of three dimensional volume preserving, R-reversible vector fields where dim Fix $R = 1$. Moreover, we shall prove the analogous statements that appear in the standard Kupka-Smale Theorem for purely R-reversible vector fields with $R^2 = I$ and dim Fix R=1 (R), and reversible volume preserving vector fields (RVP). Throughout this section, we shall assume that the reversing symmetry preserves the volume. The standard Kupka-Smale theorem says that for a residual set in the space of all vector fields, all fixed points and periodic orbits of the vector field are hyperbolic, and that for a residual subset of all vector fields, the stable and unstable manifolds of closed orbits meet transversally. For subsets of vector fields (or diffeomorphisms) this theorem may or may not be true, depending on the structure of the systems. The case for volume preserving vector fields (VP) has been proved by Robinson [91]. We shall use theorems from [91], and also results from the standard Kupka-Smale Theorem to prove the case for reversible and reversible volume preserving vector fields. These results follow the approach by Robinson [91], adapted to the cases R, RVP. In particular, we show the following for such vector fields on a compact manifold M:

- All fixed points are generically hyperbolic.
- All periodic orbits are generically isolated, and are persistently hyperbolic.
- All invariant manifolds of fixed points and periodic orbits generically intersect each other transversally.

The precise sense of 'generic' in each case is formalised in Theorems 3.5.4 and 3.5.5. These Theorems are valid in all cases R, VP, RVP. We note that Theorems presented in [31] are not valid in our case. For an account of the Kupka-Smale Theorem for general systems, see [1, 88, 102].

3.5.1 Definitions and Main Theorems

Throughout the remainder of this section we will use the following function spaces.

Definition 3.5.1.
$\mathfrak{X}^r = \{C^r$ *vector fields on a 3-manifold* $M\}$
$\mathfrak{X}^r_V = \{X \in \mathfrak{X}^r : X$ *is volume preserving*$\}$
$\mathfrak{X}^r_R = \{X \in \mathfrak{X}^r : X$ *is R-reversible*$\}$
$\mathfrak{X}^r_{R,V} = \{X \in \mathfrak{X}^r : X$ *is R-reversible and volume preserving*$\}$
$\mathcal{I}^r_V(p) = \{X \in \mathfrak{X}^r_V :$ *All fixed points and periodic orbits of* X *are isolated in phase space*$\}$
$\mathcal{H}^r_V(p) = \{X \in \mathfrak{X}^r_V :$ *All fixed points and periodic orbits of period* $\leq p$ *are hyperbolic (fixed points are* $p = 0$*)*$\}$
$\overline{\mathcal{H}}^r_V(p) = \{X \in \mathfrak{X}^r_V :$ *All fixed points and periodic orbits of period* $\leq p$ *have transversally intersecting manifolds*$\}$
We similarly define $\mathcal{I}^r_R(p), \mathcal{I}^r_{R,V}(p), \mathcal{H}^r_R(p), \mathcal{H}^r_{R,V}(p), \overline{\mathcal{H}}^r_R(p), \overline{\mathcal{H}}^r_{R,V}(p)$.

We will work in the C^r Whitney topology, where a property is said to be *generic* if it holds on a residual subset. Recall a residual set is a set that is a countable intersection of open and dense sets. By the following Lemma, the spaces $\mathfrak{X}^r_R$, $\mathfrak{X}^r_V$, $\mathfrak{X}^r_{R,V}$ have the Baire property, that residual subsets are dense.

Lemma 3.5.2. *Any closed subspace $\mathcal{K}$ of $\mathfrak{X}^r$ has the Baire property.*

Proof. The proof that $\mathfrak{X}^r$ $(1 \leq r \leq \infty)$ has the Baire property is contained in [90]. Given U_i, $i \in \mathbb{N}$ dense and open sets in $\mathfrak{X}^r$, for any neighbourhood A in $\mathfrak{X}^r$ it is shown that there exists a Cauchy sequence $X_j \in A \cap \bigcap_{i=1}^{j} U_i$ converging to a vector field $Y \in A \cap \bigcap_{i=1}^{\infty} U_i$. Thus $\bigcap_{i=1}^{\infty} U_i$ is dense.

Now, let U_i be open and dense in $\mathcal{K}$. Let $U_i = V_i \cap \mathcal{K}$ where V_i is open in $\mathfrak{X}^r$. Then given A as above, choose $X_j \in A \cap \bigcap_{i=1}^{j} U_i$, a Cauchy sequence converging to $Y \in \mathfrak{X}^r$. Since $\mathcal{K}$ is closed, $Y \in \mathcal{K}$. □

Corollary 3.5.3. *$\mathfrak{X}^r_R$, $\mathfrak{X}^r_V$, $\mathfrak{X}^r_{R,V}$ are Baire spaces. That is, residual sets are dense.*

Proof. The divergence of the vector fields and the function

$$f(R(x)) + R'(x) \cdot f(x)$$

are continuous on $\mathfrak{X}^r$ and so $\mathfrak{X}^r_R$, $\mathfrak{X}^r_V$, $\mathfrak{X}^r_{R,V}$ are closed in $\mathfrak{X}^r$. Then $\mathfrak{X}^r_R$, $\mathfrak{X}^r_V$, $\mathfrak{X}^r_{R,V}$ are also Baire spaces. □

A useful property to be used in the proof of Theorem 3.5.5 are subsets $S \subset A$ that are *locally residual*. $S \subset A$ is locally residual if there exists a dense subset $D \subset A$ such that for each $d \in D$ there exists a neighborhood P_d of d such that $P_d \cap S$ is residual in P_d. A result of topology is that if S is locally residual then it is residual [56].

We are now in a position to make explicit the statements of the results. These are summarised in the following theorems.

Theorem 3.5.4. *Let Ω be a smooth volume on M and $1 \leq r \leq \infty$.*

i) $\mathcal{H}^r_R(0)$ *and* $\mathcal{H}^r_{R,V}(0)$ *are open and dense in* $\mathfrak{X}^r_R$, $\mathfrak{X}^r_{R,V}$ *respectively.*

ii) $\mathcal{H}^r_R(p)$, $\mathcal{H}^r_{R,V}(p)$ *are open but not dense in* $\mathfrak{X}^r_R$, $\mathfrak{X}^r_{R,V}$ *respectively.*

iii) $\mathcal{I}^r_R(p)$, $\mathcal{I}^r_{R,V}(p)$ *are open and dense in* $\mathfrak{X}^r_R$, $\mathfrak{X}^r_{R,V}$ *respectively.*

An immediate consequence of part *iii)* is that $\mathcal{I}^r_R := \cap_{p\geq 0}\mathcal{I}^r_R(p)$ is residual, similarly for $\mathcal{I}^r_{R,V}$.

Theorem 3.5.5. *Let* Ω *be a smooth volume on* M *and* $1 \leq r \leq \infty$. $\overline{\mathcal{H}}^r_R(p)$, $\overline{\mathcal{H}}^r_{R,V}(p)$ *are residual in* $\mathcal{H}^r_R(p)$, $\mathcal{H}^r_{R,V}(p)$ *respectively.*

Again, this theorem also implies that $\overline{\mathcal{H}}^r_R := \cap_{p\geq 0}\overline{\mathcal{H}}^r_R(p)$ is residual in $\mathcal{H}^r_R(p)$, similarly for $\overline{\mathcal{H}}^r_{R,V}$.

The above theorems are also true for the sets $\mathcal{H}^r_V(0)$, $\mathcal{H}^r_V(p)$, $\mathcal{I}^r_V(p)$ and $\overline{\mathcal{H}}^r_V(p)$ in the space $\mathfrak{X}^r_V$ [91]. Clearly $\mathcal{H}^r_V(p)$, $\mathcal{H}^r_R(p)$, $\mathcal{H}^r_{R,V}(p)$ are not dense since there exist stably elliptic periodic orbits in $\mathfrak{X}^r_R$, $\mathfrak{X}^r_V$, $\mathfrak{X}^r_{R,V}$.

In the rest of the section we will prove Theorems 3.5.4 and 3.5.5.

3.5.2 $\mathcal{H}^r_R(0)$ and $\mathcal{H}^r_{R,V}(0)$ are open and dense

Note that whenever the fixed points or periodic orbits are not symmetric, the result for a compact manifold M follows from the standard Kupka-Smale theorem (see e.g. [88], or [91]). Since $f : \mathrm{Fix}(R) \to \mathrm{Fix}(-R) \simeq \mathbb{R} \to \mathbb{R}^2$, f will generically not have any zeros on Fix R. Therefore the fixed points are generically asymmetric, and Theorem 1 *i)* follows from [88, 91] for a compact manifold M. (Formally, we may use Thom's transversality theorem to show that it is an open and dense property that there are no fixed points on any compact subset of Fix R.)

In the case where M is noncompact, we cover M with a countable number of compact sets M_i. Then $\mathcal{H}^r_R(0) = \bigcap_i \mathcal{H}^r_R(0)|_{M_i}$ and $\mathcal{H}^r_{R,V}(0) = \bigcap_i \mathcal{H}^r_{R,V}(0)|_{M_i}$

are residual. The proof that $\mathcal{H}_R^r(0)$, $\mathcal{H}_{R,V}^r(0)$ are open is a special case of $\mathcal{H}_R^r(p)$, $\mathcal{H}_{R,V}^r(p)$ being open on a noncompact manifold. We defer the proof to section 3.5.4. The proof is also contained in [91, Lemma 15]. We note here that the proof works in the case $r = \infty$. □

In the proof of the other results, we shall prove the case for $\mathfrak{X}_{R,V}^r$, since this is the most restrictive case. Note however that the proofs for $\mathfrak{X}_{R,V}^r$ also work without modification as proofs for the other case $\mathfrak{X}_R^r$. We shall also begin by proving all theorems on a compact manifold M, these results then can be generalised to noncompact manifolds similar to [91].

3.5.3 Transversality and Perturbation Theorems

To prove Theorem 3.5.4 *ii), iii)* and Theorem 3.5.5, we need theorems to study the transversality of manifolds and effect of certain perturbations that we will apply. For a detailed account see [1].

Definition 3.5.6. *Let K and W be two C^1 submanifolds of a C^1-Banach manifold M. K and W are transversal at a point $x \in K \cap W$ if*

$$T_x(K) + T_x(W) = T_x(M).$$

We write $K \top_x W$. If K and W are transversal at every $x \in K \cap W$ then we say they are transversal.

The following definition defines transversality for functions.

Definition 3.5.7. *Let M, N be C^1-Banach manifolds, W a C^1-submanifold of N, $f : M \to N$ a C^1 map. f is transversal to W at a point $x \in M$, if either*

1. *$f(x) \notin W$,*

2. *$df(x)(T_x(M)) + T_{f(x)}W = T_{f(x)}N$.*

We write $f \top_x W$. If f is transversal to W at every point $x \in M$, then f is transversal to W, we write $f \top W$.

Having defined the concept of transversality, we now state without proof transversality theorems that we will use.

Definition 3.5.8. *Let $\mathcal{A}$, M, N be C^r-Banach manifolds. Consider a mapping $\rho : \mathcal{A} \to C^r(M, N)$. We define the evaluation map $ev^0_\rho : \mathcal{A} \times M \to N$ by*

$$ev^0_\rho(a, m) = \rho(a)(m) \tag{3.64}$$

The map ρ is a C^r-representation if the evaluation map is C^r.

This definition is of use in the following 'openness of non-intersection' theorem.

Theorem 3.5.9. *Let $\mathcal{A}$, M, N be C^0 manifolds. Let $K \subset M$ be a compact subset, $W \subset N$ a closed subset, and $\rho : \mathcal{A} \to C^0(M, N)$ a C^0-representation. Then the set*

$$\{a \in \mathcal{A} : \rho(a)(K) \cap W = \varnothing\} \tag{3.65}$$

is an open subset of $\mathcal{A}$.

For a proof of this theorem, see [88, 102]. The following definitions are of use in Theorem 3.5.12, which we will use to study perturbations within the class of vector fields $\mathfrak{X}^r_{R,V}$.

Definition 3.5.10. *Let A be a topological Baire space, and let M, N be manifolds, $K \subset M$ a subset, $V \subset N$ a submanifold and $F : A \to C^1(M, N)$. F is a C^1 pseudorepresentation if the evaluation map $ev(F^{(1)}) : A \times TM \to TN$ defined by $ev(F^{(1)})(a, q) = T(Fa)q$ is continuous.*

Definition 3.5.11. *Let A, M, N, K, V, F be as above. F is said to be C^r pseudotransverse to V on K if*

a) F is a C^1 pseudorepresentation.

b) There exists a dense subset $D \subset A$ such that for each $a \in D$ there exist an open subset B_a in a separable Banach space, a continuous function $\psi_a : B_a \to A$ and $a' \in B_a$ such that

i) $\psi_a(a') = a$, and

ii) the evaluation map $ev(F\psi_a) : B_a \times M \to N$ is C^r and transverse to V on $a' \times K$.

The Baire space A can be considered to be $\mathfrak{X}^r_R$, $\mathfrak{X}^r_V$, $\mathfrak{X}^r_{R,V}$, and we will use the separable Banach space to be the space of perturbations of particular vector fields $X \in \mathfrak{X}^r_{R,V}$. The following theorem is used in [91], and is proved in [92].

Theorem 3.5.12. *With the above spaces and maps defined, let $F : A \to C^1(M, N)$ be C^r pseudotransverse to V on K with*

$$r \geq Max\{1, 1 + dimM - codimV\}.$$

Let $R = \{a \in A : F(a) \top_K V\} = \{a \in A : F(a)$ is transverse to V at points of $K\}$. If $K = M$ then R is residual in A. If V is a closed submanifold and $K \subset M$ is compact then R is dense and open in A.

The effect of the Banach space space of perturbations will be studied using the following theorem.

Theorem 3.5.13. *Let M be a compact C^{r+1} manifold, $r \geq 2$, $X_0, Y \in \mathfrak{X}^r$, $\varphi^0 : \mathbb{R} \times M \to M$ be the flow of X_0, and $\varphi^\lambda : \mathbb{R} \times M \to M$ ($\lambda \in \mathbb{R}$) be the flow of the vector field $X_\lambda = X_0 + \lambda Y$. Then for $m \in M$ and $t \in \mathbb{R}$,*

$$\frac{d}{d\lambda}\{\varphi^\lambda(t, m)\}_{\lambda=0} = \int_0^t T\varphi^0(s, Y(\varphi^0(t - s, m)))ds. \tag{3.66}$$

For a proof, see [1]. The geometrical interpretation of this theorem, is that for fixed t, the curve $D : \mathbb{R} \to M$ given by $D(\lambda) = \varphi^\lambda(t, m)$ passes through the point $\varphi^0(t, m)$ at $\lambda = 0$, and the left hand side of the equation above is the tangent direction of this curve at $\lambda = 0$, that is the infinitesimal displacement of the orbit through m at time t, due to Y. The integrand of the right hand side is simply the sum of the instantaneous displacements (or slope vectors) of the points along the curve $\varphi^0(s,m)$, $0 \leq s \leq t$.

3.5.4 $\mathcal{H}^r_{R,V}(p)$ is open

We begin with the following Lemma.

Lemma 3.5.14. *Let M be compact, and $X \in \mathfrak{X}^r_{R,V}$ be such that all fixed points are nondegenerate; that is, the linearisation about each fixed point does not have a zero eigenvalue. Then there exists a neighbourhood V of X in $\mathfrak{X}^r_{R,V}$ and a number $b > 0$ such that for each vector field in V, every periodic orbit has period $T \geq b$.*

Proof. See [102, Theorem 3.4.4]. □

Let M be compact. Define $G : \mathfrak{X}^r_{R,V} \to C^r(M \times \mathbb{R}, M \times M \times \mathcal{L}(T(M), T(M)))$ by

$$G(X)(x,t) = (x, \varphi(X,t,x), D\varphi(X,t,x)),$$

where $\varphi(X,t,x)$ denotes the flow of X. We define the subset $W \subset M \times M \times \mathcal{L}(T(M), T(M))$ by

$$W = (x, x, A), \qquad x \in M,\ A \in \mathcal{L}(T(M), T(M)),$$

where A has at least two eigenvalues of modulus 1 (counting multiplicities). It is easy to see that W is closed. By definition, a vector field $X \in \mathfrak{X}^r_{R,V}$ is in $\mathcal{H}^r_{R,V}(p)$ if and only if $X \in \mathcal{H}^r_{R,V}(0)$ and $G(X)(x,t) \notin W$ for all $(x,t) \in M \times (0,p]$. Assume that $X_0 \in \mathcal{H}^r_{R,V}(p)$. Then, from Lemma 3.5.14, there exists a neighbourhood V_1 of X_0 in $\mathfrak{X}^r_{R,V}$, and a number b, $0 < b < p$, such that for every $Y \in V_1$ all closed orbits have (prime) period not less than b. Now $M \times [b,p]$ is compact, W is closed, and

$$G(X_0)(x,[b,p]) \cap W = \varnothing, \qquad \forall x \in M.$$

Then we may apply Theorem 3.5.9 to conclude that there is an open neighbourhood V_2 of X_0 such that $G(Y)(x,[b,p]) \cap W = \varnothing$ for all $x \in M$ and $Y \in V_2$. Also by Theorem 3.5.4 *i)*, there is a neighbourhood V_3 of X_0 such that $Y \in \mathcal{H}^r_{R,V}(0)$ for all $Y \in V_3$. Then $Y \in \mathcal{H}^r_{R,V}(p)$ for all $Y \in V_1 \cap V_2 \cap V_3$, and so $\mathcal{H}^r_{R,V}(p)$ is open. □

It remains to prove the following Lemma for a noncompact manifold M.

Lemma 3.5.15. *Let M be noncompact. Then $\mathcal{H}^r_{R,V}(p)$ is open.*

Proof. Let $M = \cup_{i\in\mathbb{N}} M_i$, where each M_i is a compact submanifold with $M_i \subset$ interior M_{i+1}. Let $X \in \mathcal{H}^r_{R,V}(p)$, and $\varphi(X,t,x)$ denote the flow of X, where $t \in \mathbb{R}$ and $x \in M$. For each $i \in \mathbb{N}$ there is an $N(i) \in \mathbb{N}$ such that

$$\varphi(X,t,m) \in M_{N(i)}, \qquad \forall 0 \le t \le p, \quad x \in M_i.$$

We choose $N(i) \ge i$ to be an increasing function of i. Now, for each i there is an $\varepsilon_i > 0$ such that $d(X,Y)_{C^r,m} < \varepsilon_i$ $(m \in M_{N(i)})$ implies that

$$\begin{aligned} \varphi(Y,t,m) &\in M_{N(i)}, \qquad \forall 0 \le t \le p, \quad x \in M_i \\ \text{and} \qquad Y &\in \mathcal{H}^r_{R,V}(p)(M_i), \end{aligned}$$

where $d(\cdot,\cdot)_{C_r,m}$ is the distance in the C^r topology at a point m, and $\mathcal{H}^r_{R,V}(p)(M_i)$ is $\mathcal{H}^r_{R,V}(p)$ restricted to the manifold M_i. This is true since $\mathcal{H}^r_{R,V}(p)(M_i)$, $\mathcal{H}^r_{R,V}(p)(M_{N(i)})$ are open. Now we introduce a continuous function $\varepsilon : M \to \mathbb{R}$ such that for each $i \in \mathbb{N}$, $m \in M_{N(i)}$, $\varepsilon(m) < \varepsilon_i$. Then the neighbourhood

$$\{Y \in \mathfrak{X}^r_{R,V} : d(X,Y)_{C^r,m} < \varepsilon(m)\} \subset \mathcal{H}^r_{R,V}(p),$$

and so $\mathcal{H}^r_{R,V}(p)$ is open. This proof also applies in the $r = \infty$ case. □

3.5.5 Coordinate system

To prove the remaining statements, we will need to perturb vector fields in $\mathfrak{X}^r_{R,V}$, for which we will need to construct reversible, volume-preserving perturbations.

For this we will use the following Lemma, which is the reversible volume preserving version of Lemma 12 in [91]. By Bochner's Theorem [9, 82], any involutory reversing symmetry is locally smoothly conjugated to $R(x, y, z) = (-x, y, -z)$. We construct a local coordinate system in which the reversing symmetry action is unchanged and the volume $\Omega(m)$ becomes the standard volume $\mathrm{d}x \wedge \mathrm{d}y \wedge \mathrm{d}z$. It is important to make the hypothesis that the reversing symmetry action also preserves the volume form.

Lemma 3.5.16. *Given a frame $Y_i(m) \in T_m M$ with $\Omega(Y_1(m), Y_2(m), Y_3(m)) = 1$, and coordinates (y_1, y_2, y_3) with $Y_i(m) = \frac{\partial}{\partial y_i}(m)$, and $R(y_1, y_2, y_3) = (-y_1, y_2, -y_3)$, where R preserves the volume Ω, there exists local coordinates (x_1, x_2, x_3) about m such that $\Omega = \mathrm{d}x_1 \wedge \mathrm{d}x_2 \wedge \mathrm{d}x_3$, $Y_i(m) = \frac{\partial}{\partial x_i}$ and $R(x_1, x_2, x_3) = (-x_1, x_2, -x_3)$.*

Proof. In the coordinates (y_1, y_2, y_3), $\Omega(y_1, y_2, y_3) = v(y_1, y_2, y_3)\mathrm{d}y_1 \wedge \mathrm{d}y_2 \wedge \mathrm{d}y_3$, with $v(y_1, y_2, y_3) \neq 0$. The reversing symmetry preserves the orientation of the volume, and implies that $v(-y_1, y_2, -y_3) = v(y_1, y_2, y_3)$. Now choose new coordinates

$$\begin{aligned} x_1 &= y_1, \\ x_2 &= \int_0^{y_2} v(y_1, s, y_3) ds, \\ x_3 &= y_3. \end{aligned}$$

Then in these coordinates the reversing symmetry acts in the same way. Also $\mathrm{d}x_1 = \mathrm{d}y_1$, $\mathrm{d}x_3 = \mathrm{d}y_3$ and $\mathrm{d}x_2 = v(y_1, y_2, y_3)\mathrm{d}y_2 + \cdots$, where the dots denote terms in $\mathrm{d}y_1$ and $\mathrm{d}y_3$. Then

$$\Omega(y_1, y_2, y_3) = v(y_1, y_2, y_3)\mathrm{d}y_1 \wedge \mathrm{d}y_2 \wedge \mathrm{d}y_3 = \mathrm{d}x_1 \wedge \mathrm{d}x_2 \wedge \mathrm{d}x_3.$$

From now on we shall use these local coordinates in which Ω is the volume $\mathrm{d}x_1 \wedge \mathrm{d}x_2 \wedge \mathrm{d}x_3$ and $R(x_1, x_2, x_3) = (-x_1, x_2, -x_3)$. $\square$

3.5.6 $\mathcal{I}^r_{R,V}(p)$ open and dense

In the proof of Theorem 3.5.4 *iii)* we will use the following Lemma, which gives a characterization of symmetric periodic orbits.

Lemma 3.5.17. *An orbit γ is a symmetric periodic orbit if and only if γ intersects Fix R exactly twice.*

Proof. We postpone the proof until section 4.4, where the result is part of Lemma 4.4.1. $\square$

We suppose first that $r < \infty$ and M is compact. Let γ be a periodic orbit of $X \in \mathfrak{X}^r_{R,V}$, let $m \in \gamma$, and Σ be a local section plane transverse to γ at m, and $k \in \mathbb{N}$. For a neighbourhood $S \subset \mathbb{R}^3$ of m, let $\Sigma_S = \Sigma \cap S$. As usual, we shall denote the flow of X as $\varphi(X, t, x)$, where $\varphi : \mathfrak{X}^r_{R,V} \times \mathbb{R} \times M \to M$ is C^r. Assume $\varphi(X, T, m) = m$. We construct the Poincaré return map for X. As the flow is transverse to Σ at m, by the Implicit Function Theorem there exist neighbourhoods U_1 of m and V of X in $\mathfrak{X}^r_{R,V}$, and a C^r function $\tau : V \times \Sigma_{U_1} \to \Sigma$ such that $\varphi(Y, \tau(Y, p), p) \in \Sigma$. Then $\theta(Y, q) = \varphi(Y, \tau(Y, p), p)$ is the C^r Poincaré map. Then we have the following:

Lemma 3.5.18. *There exists a neighbourhood U_2 of m in M such that*

$$\begin{aligned} \mathcal{I}^r_{R,V}(k, \Sigma_{\overline{U}_2}) \quad := \quad & \{Y \in V : \textit{all periodic orbits of } Y \textit{ corresponding to} \\ & \textit{periodic points of period} \leq k \textit{ for the Poincaré map} \\ & \textit{on } \Sigma_{\overline{U}_2} \textit{ are isolated}\} \end{aligned}$$

is open and dense in V.

Proof. For asymmetric periodic orbits, the results follows from [91]. Then by Lemma 3.5.17 it is enough to show that the symmetric periodic orbits are isolated in Fix R. Then suppose the periodic orbit γ is symmetric, and let $m \in$ Fix R.

Let $\rho_i : \mathcal{X} \to C^r(\Sigma_{U_1} \cap \mathrm{Fix}\ R, \Sigma_{U_1} \cap \mathrm{Fix}\ R \times \Sigma)$ $(i = 0, 1, 2, \ldots)$ be defined by

$$\rho_i(X)(m) = (m, \theta^i(X, m)).$$

From Lemma 3.5.17, an orbit is a symmetric periodic orbit if and only if it intersects Fix R exactly twice. It is then sufficient to show that the symmetric periodic orbits are generically isolated in Fix R.

Let $m \in \mathrm{Fix}\ R$, and let $W = \{(p, q) : p, q \in \Sigma \cap \mathrm{Fix}\ R\}$. Then $W \subset \Sigma_{U_1} \cap \mathrm{Fix}\ R \times \Sigma$. Then $\rho_i(Y)(q) \in W$ $(Y \in V)$ if q is a symmetric periodic orbit of period i for the Poincaré map θ. Let $U_2 \subset \overline{U}_2 \subset U_1$ be a neighbourhood of γ with $\overline{U}_2$ compact. Now assume that

$$\begin{aligned} \mathcal{I}^r_{R,V}(k-1, \Sigma_{\overline{U}_2}) &= \{Y \in V : \text{All periodic points in } \Sigma_{\overline{U}_2} \text{ of period} \\ &\qquad \leq k-1 \text{ for the Poincaré map are isolated}\} \end{aligned}$$

is open and dense in V and use induction.

The fact that ρ_i is a C^1 pseudorepresentation is implicit in our assumption that $1 \leq r < \infty$. We would like to apply Theorem 3.5.12 to the function ρ_i. The space A in the statement of the theorem will be V, and the dense set in the definition of pseudotransverse will be $\mathcal{I}^r_{R,V}(k-1, \Sigma_{\overline{U}_2}) \cap \mathfrak{X}^{r+1}_{R,V}$. We claim that if $\mathcal{I}^r_{R,V}(k-1, \Sigma_{\overline{U}_2})$ is open and dense in $\mathfrak{X}^r_{R,V}$, then ρ_i is C^r pseudotransverse to W on $\Sigma_{\overline{U}_2} \times \mathrm{Fix}\ R$. The Banach space of perturbations will be $\mathfrak{X}^r_{R,V}$. We need to prove that for $X \in \mathcal{I}^r_{R,V}(k-1, \Sigma_{\overline{U}_2}) \cap \mathfrak{X}^{r+1}_{R,V}$, ρ_j is transverse to W on $X \times \Sigma_{U_2}$.

Note that for $\theta^j(X, q) = q$, $0 < j < k$, then $\rho_j(X)q \in W$ and we have $\rho_j(X) \top_q W$ by assumption and so $\rho_j \top_{(X,q)} W$. So let γ be k-periodic (minimal period) under θ, and then we want to prove $\rho_k(X) \top_{(X,m)} W$. We require the dense set to be $\mathcal{I}^r_{R,V}(k-1, \Sigma_{\overline{V}}) \cap \mathfrak{X}^{r+1}_{R,V}$ since we want to take flow box coordinates (t, y, z) about the periodic orbit γ, the coordinate t parametrising the orbit γ, $(0, y, 0) = \mathrm{Fix}\ R$ and $(0, 0, z) \in \mathrm{Fix}(-R)$. Then according to [91], if these coordinates are C^{r+1}, then vector fields that are C^r in these coordinates will be C^r on M. We use coordinates as in section 3.5.5, such that $\{(t,0)\}$ is on the periodic orbit, $t=0$ at $m \in \mathrm{Fix}\ R$. Let T be the period of γ. Then also the point $\varphi(X, T/2, m) \in \mathrm{Fix}\ R$. Let the range of coordinates be $\overline{Y} = [0,T] \times [-b,b] \times [-b,b]$. Choose $L : [-b,b] \times [-b,b] \to \mathbb{R}$ to be a C^{r+1} function with $\mathrm{supp}(L) \subset (-b,b) \times (-b,b)$, $L(0)=0$. The perturbation needs to be chosen to be reversible, and to this end, let $L(y,-z) = L(y,z)$. Then $\frac{\partial}{\partial z} L(y,0) = 0$, but we also choose L such that $\frac{\partial}{\partial y} L(0,0) \neq 0$.

Next let $g : S^1 \to \mathbb{R}$ be a C^{r+1} function with $\mathrm{supp}(g) \subset (0,T)$. Choose g to be $T/2$-periodic such that $\int_0^T g(t)dt = 1$ and $g(-t) = g(t)$. Let c be the parameter of the perturbation, $0 < c \ll 1$. Then the perturbed vector field shall be denoted by $X^c = X + c\mathcal{L}$, where $\mathcal{L} : \overline{y} \to T_{\overline{y}}M$ ($\overline{y} \in \overline{Y}$) is given by

$$\mathcal{L}(t,y,z) = \begin{pmatrix} 0 \\ -g(t)\frac{\partial}{\partial z}(L(y,z)) \\ g(t)\frac{\partial}{\partial y}(L(y,z)) \end{pmatrix}$$

Then clearly $\mathcal{L}$ is a reversible-volume-preserving perturbation. As before, $\varphi(X^c, T, q)$ represents the time-T map from q under the flow of X^c. Then by Theorem 3.5.13,

$$\begin{aligned} \frac{d}{dc}\varphi(X^c,T,0)|_{c=0} &= \int_0^T \mathcal{L}(T-t,0,0)dt \\ &= \begin{pmatrix} 0 \\ -\int_0^T g(T-t)\frac{\partial}{\partial z}(L(0,0))dt \\ \int_0^T g(T-t)\frac{\partial}{\partial y}(L(0,0))dt \end{pmatrix} \\ &= \begin{pmatrix} 0 \\ -\frac{\partial}{\partial z}(L(0,0)) \\ \frac{\partial}{\partial y}(L(0,0)) \end{pmatrix} \\ &= \begin{pmatrix} 0 \\ 0 \\ \frac{\partial}{\partial y}(L(0,0)) \end{pmatrix}, \end{aligned} \tag{3.67}$$

where $-\frac{\partial}{\partial y}(L(0,0)) \neq 0$. Then $D_X\theta^k(X,m) \cdot T_X V \oplus T_m(\mathrm{Fix}\ R)$ spans $T_m\Sigma$, and we have that $\rho_k \top_{(X,m)} W$ at all points m such that $\theta^k(X,m) = m$. Thus $\mathcal{I}^r_{R,V}(p, \Sigma_{\overline{U}_2})$ is dense and open in V. $\square$

The modifications for the proof of Lemma 3.5.18 in the case $r = \infty$ or M noncompact are the same as in [91].

Now we prove Theorem 3.5.4 *iii)*. If M is noncompact let $M = \cup_{i\in\mathbb{N}} M_i$, where each M_i is compact and $M_i \subset$ interior M_{i+1}. Let $X \in \mathcal{H}^r_{R,V}(0)$. By Lemma 3.5.14 there is a neighbourhood V_1 of X contained in $\mathcal{H}^r_{R,V}(0)$ such that all periodic orbits of $Y \in V_1$ meeting M_j have period greater than some $b > 0$. For each periodic orbit γ_n of X of period $d \le p$ that meets M_j, choose a $k_n \in \mathbb{N}$ such that $k_n d > p$. Choose $\overline{U}_2(n)$ as in Lemma 3.5.18 small enough so that all periodic orbits through $\Sigma_{\overline{U}_2(n)}$ of period $\le p$ are closed by some θ^i, $1 \le i \le k_n$. Choose a neighbourhood G of γ_n such that all periodic orbits for $Y \in V$ (V as in Lemma 3.5.18) meeting G intersect $\Sigma_{\overline{U}_2}$. The set of periodic points of period $\le p$ intersecting M_j is compact, so we require finitely many such $G_1, \dots, G_q$. Finally, take a neighbourhood V_2 of X such that $Y \in V_2$ has no periodic orbits of period $\le p$ meeting $M_j - \cup_{i=1}^q G_i$. Then

$$V_1 \cap V_2 \cap \mathcal{I}^r_{R,V}(p, \Sigma_{\overline{U}_2(1)}) \cap \cdots \cap \mathcal{I}^r_{R,V}(p, \Sigma_{\overline{U}_2(q)})$$

is open and dense at X. Hence $\mathcal{I}^r_{R,V}(p)(M_j)$ is open and dense at X, and by Theorem 3.5.4 *i)*, it is open and dense in $\mathfrak{X}^r_{R,V}$. So $\mathcal{I}^r_{R,V}(p)$ is residual. Openness follows the same as in Lemma 3.5.15.

3.5.7 $\overline{\mathcal{H}}^r_{R,V}(p)$ is residual

To prove Theorem 3.5.5 we prove that for each $X \in \mathcal{H}^r_{R,V}(p)$, there is a neighbourhood N in $\mathfrak{X}^r_{R,V}$ such that $\overline{\mathcal{H}}^r_{R,V}(p) \cap N$ is residual in N. This proves that $\overline{\mathcal{H}}^r_{R,V}(p)$ is locally residual in $\mathcal{H}^r_{R,V}(p)$ and so residual. The proof is much the same as for the generic case [1, 88, 102], so we will sketch the proof here with the changes necessary for the space $\mathfrak{X}^r_{R,V}$.

Let $X \in \mathcal{H}^r_{R,V}(p)$ suppose that M is compact, and let $\gamma_1, \ldots \gamma_k$ be critical elements (fixed points or periodic orbits) of X. Then there is a neighbourhood N of X and a C^1 pseudorepresentation $\sigma_i^{\pm} : N \to C^r(P^i, M)$ that parametrises the stable(-)/unstable(+) manifold of each fixed point, where P^i is either $\mathbb{R}^{s(i)}$ $(s(i) = 0, 1, 2, 3)$, $\mathbb{R}^{s(i)} \times S^1$ or $\mathbb{R}^{s(i)} \dot{\times} S^1$ $(s(i) = 0, 1, 2)$. This is because the local stable/unstable manifolds depend continuously in the C^1 topology on the vector field in the C^r topology. From Theorem 3.5.4 *i)* we may assume that all fixed points remain hyperbolic in N.

Lemma 3.5.19. *The map $F : N \times P^1 \times P^2 \to M \times M$ defined by*

$$F(Y)(p_i, p_j) = (\sigma_i(Y)(p_i), \sigma_j(Y)(p_j)), \qquad p_{i,j} \in P^{i,j}$$

is transversal to the diagonal $\Delta = (m, m) \subset M \times M$.

Proof. We first consider fixed points. In the case of a general pair of asymmetric fixed points, the results follows from [91]. As noted in section 3.5.2, fixed points are generically non-symmetric in our case, and so to prove the Lemma, we need only consider stable/unstable manifolds of an symmetric pair of asymmetric fixed points. So let F^+ be a fixed point of X with a 2 dimensional unstable manifold, and let F^- be a fixed point with a 2 dimensional stable manifold, such that $R(F^+) = F^-$. (The case for 1 dimensional stable/unstable manifolds will follow trivially from this case.) Finally suppose that $W^u(F^+)$ and $W^s(F^-)$ intersect tangentially at Fix R. For intersections that do not intersect Fix R, the result again follows from [91]. Since transversality is preserved along trajectories, we let $m \in W^s(F^-) \cap W^u(F^+) \cap \text{Fix } R$. Then $T_m(W^s(F^-)) = R(T_m(W^u(F^+)))$ and so it follows that $T_m(W^s(F^-)) = (T_m(W^u(F^+))) \in \text{Fix}(-R)$, and m is a heteroclinic point between F^+ and F^-. Since the stable/unstable manifolds are transverse to Fix R, a small perturbation cannot destroy this intersection, and the orbit through m is a stable heteroclinic connection.

Now let U_1 be a C^∞ coordinate neighbourhood of m. Let $U_2 \subset \overline{U}_2 \subset U_1$, and again take flow box coordinates (t, y, z) in $\overline{U}_2$. Use coordinates as in section 3.5.5, $\Omega = dx \wedge dy \wedge dz$. The range of coordinates valid in $\overline{U}_2$ is $\overline{Y} = [-T, T] \times [-b, b] \times [-b, b]$, and $\{(t, 0, 0)\}$ is the orbit through m, and $(0, y, 0) = \text{Fix } R$, $(0, 0, z) \in \text{Fix}(-R)$.

Suppose the dense set we are using for the transversality theorem is $\mathcal{H}^r_{R,V}(0)$, then both fixed points are hyperbolic. N is such that the fixed points F^+ and F^- persist and remain hyperbolic, the N-dependence of F^+, F^- will be omitted in the notation.

Let $L : [-b, b] \times [-b, b] \to \mathbb{R}$ be a C^{r+1} function such that support $L \subset (-b, b) \times (-b, b)$. For reversibility we require $L(y, -z) = L(y, z)$. Then $\frac{\partial}{\partial z} L(0, 0) = 0$, and let $\frac{\partial}{\partial y} L(0, 0) = 0$, $\frac{\partial^2}{\partial z^2} L(0, 0) \neq 0$. Also let $g : [-T, T] \to \mathbb{R}$ be a C^{r+1} function with support$(g) \subset [-T, T]$ such that $g(-t) = g(t)$ and $\int_0^T g(t)dt = 1$. Again, $X^c = X + c\mathcal{L}$ is the perturbed vector field, with $\mathcal{L} : \overline{y} \to T_{\overline{y}}M$ $(\overline{y} \in \overline{Y})$ given by

$$\mathcal{L}(t, y, z) = \begin{pmatrix} 0 \\ g(t)\frac{\partial}{\partial z} L(y, z) \\ -g(t)\frac{\partial}{\partial y} L(y, z) \end{pmatrix}$$

Note $\mathcal{L} \in \mathfrak{X}^r_{R,V}$. Then the orbit through $m = (0, 0, 0)$ is unaffected by the perturbation for all c. We would like to see the effect of the perturbation on orbits in the manifold close to $\{(t, 0, 0)\}$, so let $\vec{v}$ be the unit tangent direction of the unstable manifold $W^u(F^+)$ at $t = -T$, in the direction of $\text{Fix}(-R)$. Then the directional derivative is given by

$$\begin{aligned} \nabla_{\vec{v}} \left(\frac{d}{dc} \varphi(X^c, T, (-T, y, z)) \right) \Bigg|_{y,z=0} &= \nabla_{\vec{v}} \begin{pmatrix} 0 \\ \frac{\partial}{\partial z} L(y, z) \\ -\frac{\partial}{\partial y} L(y, z) \end{pmatrix}_{y,z=0} \\ &= \begin{pmatrix} 0 \\ \frac{\partial^2}{\partial z^2}(L(0, 0)) \\ 0 \end{pmatrix}, \end{aligned} \tag{3.68}$$

where $\frac{\partial^2}{\partial z^2}(L(0,0)) \neq 0$, so the effect of the perturbation of $W^u(F^+)$ is to make it transversal to $\mathrm{Fix}(-R)$ at $t = 0$. The effect on $W^s(F^-)$ is the R-image, and so the manifolds can be made transversal with an arbitrarily small perturbation.

The case for periodic orbits may be treated in the same way. We need only consider saddle symmetric periodic orbits whose stable and unstable manifolds coincide in a homoclinic loop. Then we set up the perturbation about a symmetric homoclinic orbit at a point $m \in \mathrm{Fix}\, R$ exactly as for the fixed points. Such a homoclinic orbit cannot be perturbed away, but may be perturbed to become a transversal homoclinic intersection. This completes the proof of the Lemma. $\square$

The proof of Theorem 3.5.5 is now the same as in the general case [88, 102]. These arguments can now be applied with these special perturbations in the stable/unstable manifolds to show that for each $X \in \mathcal{H}^r_{R,V}(p)$ there is a neighbourhood N in $\mathfrak{X}^r_{R,V}$ such that $\overline{\mathcal{H}}^r_{R,V}(p) \cap N$ is residual in N for $p > 0$. This proves $\overline{\mathcal{H}}^r_{R,V}(p)$ is locally residual and so residual. The case $r = \infty$ or M noncompact is the same as in [91]. $\square$

Chapter 4

Heteroclinic Cycle Bifurcation: Geometrical Analysis

We have seen in Chapter 3 that heteroclinic cycles are generic in the unfolding of the codimension one reversible Hopf-zero bifurcation. This heteroclinic cycle bifurcation is also known to exist for the Michelson system at $c \approx 0.84952$, see equation (2.26). In this chapter we study the dynamics near a heteroclinic cycle bifurcation in reversible systems. The analysis contained in this chapter is original for the reversible case—see [72], which also includes parts of chapter 3. An analysis for the general (nonsymmetric) codimension 2 case appears in [16, 17], which contain some of the same results obtained here, including existence of certain periodic, heteroclinic and homoclinic solutions in a neighbourhood of the unfolding of the heteroclinic cycle bifurcation.

4.1 Hypotheses and Main Theorems

We consider a one-parameter family of R-reversible vector fields $F : \mathbb{R}^3 \times \mathbb{R} \to \mathbb{R}^3$, with R acting as (3.1), satisfying the following properties:

H1 F has two fixed points p_1 and p_2, such that $R(p_1) = p_2$.

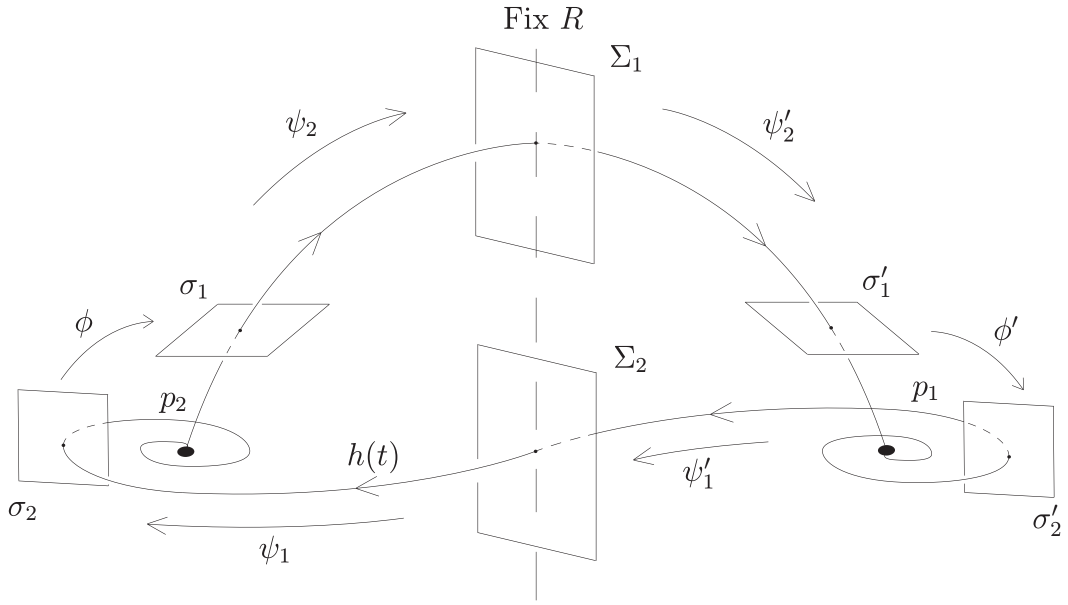

Figure 4.1: The heteroclinic cycle at $\lambda = 0$ with section planes and return maps indicated.

H2 $Df(p_1)$ has one real eigenvalue $\mu < 0$ and a complex pair of eigenvalues $\rho \pm i\omega$ with $\rho, \omega > 0$. By the reversing symmetry, the spectrum of $Df(p_2)$ is $-\mu$, $-\rho \pm i\omega$.

H3 There exists a symmetric heteroclinic solution $q_2(t)$ contained in the (transversal) intersection the two dimensional stable manifold of p_2 and the two dimensional unstable manifold of p_1, ie $q_2(t) \in W^s(p_0) \cap W^u(p_1)$ for all $\lambda \in [-\bar{\varepsilon}, \bar{\varepsilon}]$ for $\bar{\varepsilon}$ sufficiently small.

H4 At $\lambda = 0$ the unstable manifold of p_2 coincides with the stable manifold of p_1 to form a symmetric heteroclinic connection $q_1(t)$, ie $W^u(p_2) = W^s(p_1)$. This connection is necessarily symmetric, so $F(\cdot, 0)$ has a symmetric heteroclinic loop. Additionally $W^u(p_2)$ passes with positive speed with respect to the parameter λ through Fix R at $\lambda = 0$.

Hypothesis [H1-H4] are persistent in one-parameter families of smooth R-reversible vector fields in $\mathbb{R}^3$. See Figure 4.1 for a sketch of the situation.

Our results include the existence of certain symmetric heteroclinic and periodic solutions close to our original heteroclinic cycle. We shall recall some terminology in order to distinguish different types of these orbits. A heteroclinic orbit connecting p_2 to p_1 is called a 1D heteroclinic orbit, and this must be a symmetric connection by uniqueness. By Lemma 4.4.1, a symmetric heteroclinic orbit must intersect Fix R precisely once. 1D heteroclinic orbits may intersect Fix R in Σ_1 (see section 4.2 for definitions of the sections), or in Σ_2. We call these 'upper' and 'lower' symmetric heteroclinic connections respectively. 1D heteroclinic orbits that intersect Σ_1 n times are called n-heteroclinic connections. Heteroclinic orbits connecting p_1 to p_2 are called 2D heteroclinic orbits. These orbits may be symmetric, or may occur in asymmetric pairs. Symmetric 2D heteroclinic orbits may similarly intersect Fix R in Σ_1 or Σ_2; these are 'upper' and 'lower' connections respectively. 2D heteroclinic connections which intersect Σ_2 n times are called n-heteroclinics. Our original heteroclinic cycle is a 1-heteroclinic cycle.

It can be shown that an orbit in such an R-reversible system is a symmetric periodic solution if and only if it intersects Fix R exactly twice, see Lemma 4.4.1. An n-periodic solution is one that intersects Σ_2 (or Σ_1) n times. Note that homoclinic solutions to either fixed point p_1, p_2 cannot be symmetric in our situation. We define n-homoclinic solutions in the same way as for n-periodic solutions.

Our main results are summarized in the following theorems:

Theorem 4.1.1. *At $\lambda = 0$, when there is a 1-heteroclinic cycle, for all $n \in \mathbb{N}$ there is a countably infinite number of (upper and lower) symmetric, and asymmetric, transverse n-2D heteroclinic orbits accumulating to the 1-heteroclinic cycle. Each n-2D heteroclinic solution constitutes – in combination with the 1D heteroclinic – a symmetric heteroclinic cycle.*

Theorem 4.1.2. *For each of these heteroclinic cycles there exists a countably infinite family of symmetric periodic solutions with growing period, converging* *to the heteroclinic cycle as the period goes to infinity. For small λ, these symmetric periodic solutions form a one parameter family, parametrised by period.*

Theorem 4.1.3. *For sufficiently small $|\lambda|$ there exists a countably infinite set of parameter values $\{\lambda_k\}$, converging exponentially to zero such that at $\lambda = \lambda_k$, there exists an upper (or lower) n-1D heteroclinic orbit. Such a heteroclinic connection is symmetric.*

Theorem 4.1.4. *For sufficiently small $|\lambda|$ there exists a countably infinite set of parameter values $\{\lambda_j\}$, converging exponentially to zero such that at $\lambda = \lambda_j$, p_0 and p_1 have n-homoclinic solutions. These homoclinic connections are asymmetric.*

Theorem 4.1.5. *At $\lambda = 0$ there exists a 'symmetric horseshoe' - that is, for any $n \in \mathbb{N}$, there exists a uniformly hyperbolic invariant set which is R-invariant and indecomposable, whose dynamics is topologically conjugate to a full shift on n symbols. Each of these sets is structurally stable, and so persists for $|\lambda|$ sufficiently small. However, the union of all of these sets is not structurally stable and is destroyed with any small perturbation of λ.*

This chapter is organized as follows. In Section 4.2 we discuss the surface of sections we use in our study of the heteroclinic bifurcation. In Section 4.2.1 we present the return maps that represent the dynamics around the heteroclinic loop. In section 4.3 we study the important properties of these return maps. We will use these return maps together with their geometric properties to prove our results in sections 4.4 and 4.5.

4.2 Sections and return maps

In this section we lay out the surfaces of sections that we will employ to define our return maps.

We define two main local sections, Σ_1 and Σ_2, satisfying the following properties.

- The sections are setwise invariant under R: $R(\Sigma_1) = \Sigma_1$ and $R(\Sigma_2) = \Sigma_2$. Consequently, Fix (R) bisects Σ_1 and Σ_2. We distinguish between the local actions of the time-reversal symmetry R: $R_1 = R|_{\Sigma_1}$ and $R_2 = R|_{\Sigma_2}$.
- The sections are locally transverse to the the flow of F at $\lambda = 0$ (and hence also at sufficiently small values of λ).
- The section Σ_1 is locally transverse to $W^s(p_1)$ and $W^u(p_2)$. Similarly the section Σ_2 is locally transverse to $W^s(p_2)$ and $W^u(p_1)$;

We now define more sections close to the saddle-foci p_1 and p_2. σ_2 is a local section transversal to $W^s(p_2)$. σ_1 is a local section transversal to $W^u(p_2)$.

We define $\sigma_1' = R(\sigma_1)$ and $\sigma_2' = R(\sigma_2)$. Next we define first hit maps between the surfaces of section. Note that these maps are locally well defined since at $\lambda = 0$ the surfaces of section intersect the heteroclinic loop between p_1 and p_2 transversally.

We first define the Poincaré return map $F_2 : \Sigma_2 \to \Sigma_2$:

$$F_2 = \psi_1' \circ \phi' \circ \psi_2' \circ \psi_2 \circ \phi \circ \psi_1, \tag{4.1}$$

where the maps $\psi_1 : \Sigma_2 \to \sigma_2$, $\phi : \sigma_2 \to \sigma_1$, $\psi_2 : \sigma_1 \to \Sigma_1$, $\psi_2' : \Sigma_1 \to \sigma_1'$, $\phi' : \sigma_1' \to \sigma_2'$, and $\psi_1' : \sigma_2' \to \Sigma_2$ are first hit maps, see Figure 4.1.

We may use the reversibility of the vector field to express the maps ψ_1', ψ_2' and ϕ' in terms of ψ_1, ψ_2, ϕ, R, R_1 and R_2. Namely:

$$\psi_1' = R_2 \circ \psi_1^{-1} \circ R, \psi_2' = R \circ \psi_2^{-1} \circ R_1, \phi' = R\phi^{-1}R.$$

Consequently, we have:

$$F_2 = R_2 \circ \psi_1^{-1} \circ \phi^{-1} \circ \psi_2^{-1} \circ R_1 \circ \psi_2 \circ \phi \circ \psi_1. \tag{4.2}$$

and it is readily verified that F_2 is a R_2-reversible map, ie

$$F_0^{-1} = R_0 \circ F_0 \circ R_0^{-1}. \tag{4.3}$$

Similarly it is easy to show that the Poincaré return map $F_1 : \Sigma_1 \to \Sigma_1$ satisfies

$$F_1 = \psi_2 \circ \phi \circ \psi_1 \circ R_0 \circ \psi_1^{-1} \circ \phi^{-1} \circ \psi_2^{-1} \circ R_1. \tag{4.4}$$

and that hence F_1 is a R_1-reversible map, ie

$$F_1^{-1} = R_1 \circ F_1 \circ R_1^{-1}. \tag{4.5}$$

4.2.1 Return map for local flow

We now will find expressions for the local return maps. We will consider the local map ϕ about the saddle point p_2, the corresponding properties for the map ϕ' can be deduced from the form of ϕ and the fact that $\phi' = R\phi^{-1}R$. This local map will provide an important basis for understanding the features of the dynamics we are interested in.

Since the saddle fixed point p_2 is hyperbolic, there will be a unique hyperbolic saddle point p_2^λ for each $|\lambda|$ sufficiently small. We can make smooth (C^∞) bump function transformations such that $p_2^\lambda = p_2$ for all sufficiently small $|\lambda|$. We will assume we have carried out such a change of coordinates. The effect of this change coordinates in some neighbourhood of p_2^λ is to just translate the neighbourhood to around p_2. We may assume that the fixed point p_2 is at the point $(-p, 0, 0)$ in global coordinates. Fix R is spanned by $(0, 1, 0)$.

We now choose local coordinates around p_2 such that p_2 is at the origin. Recall the eigenvalues of the fixed point p_2 are $-\rho(\lambda) \pm i\omega(\lambda)$, $\mu(\lambda)$, with $\rho(\lambda), \mu(\lambda) > 0$. From now on we shall drop the argument λ. It can be shown [8] that there exists a local C^1 change of coordinates (and a reparametrisation of time), such that in these coordinates the flow in an ϵ-neighbourhood near the saddle point p_2 is linear:

$$\begin{aligned}
\dot{x_L} &= -(\rho/\mu)x_L + (\omega/\mu)y_L \\
\dot{y_L} &= -(\omega/\mu)x_L - (\rho/\mu)y_L \\
\dot{z_L} &= z_L
\end{aligned} \tag{4.6}$$

In these coordinates the local stable and unstable manifolds are flattened. We will define the local section σ_2 as follows:

$$\sigma_2 = \{(x_L, y_L, z_L) \in \mathbb{R}^3 \mid x_L = 0, y_L = y^* \pm \overline{\delta}\},$$

where the point of first intersection of $q_2(t)$ and σ_2 is $(0, y^*, 0)$, and $\overline{\delta}$ is sufficiently small such that $(0, y^*, 0)$ is the only intersection of $q_2(t)$ with σ_2. Note that $\{(0, y, 0)\} \subset \sigma_2$ is the trace of the two dimensional stable manifold $W^s(p_2)$ in σ_2. We also have

$$\sigma_1 = \{(x, y, z) \in \mathbb{R}^3 \mid z = d\}.$$

Note also that $\{(0, 0, d)\} \in \sigma_1$ is the trace of the one dimensional unstable manifold $W^u(p_2)$.

Clearly the flow in these local coordinates is given by:

$$\begin{aligned}
x_L(t) &= x_L(0)\exp(-\frac{\rho t}{\mu})\cos(\frac{\omega}{\mu}t) + y_L(0)\exp(\frac{-\rho t}{\mu})\sin(\frac{\omega}{\mu}t) \\
y_L(t) &= y_L(0)\exp(-\frac{\rho t}{\mu})\cos(\frac{\omega}{\mu}t) - x_L(0)\exp(\frac{-\rho t}{\mu})\sin(\frac{\omega}{\mu}t) \\
z_L(t) &= z_L(0)\exp(t),
\end{aligned} \tag{4.7}$$

We can calculate the time of flight from σ_2 to σ_1 from the third equation of (4.7) as $t^* = -\ln(z_L(0)/d)$. Then we can write down the local map $\phi : \sigma_2 \to \sigma_1$ as:

$$\begin{aligned}
x_L &= \phi_1(y_L, z_L) &= y_L \left(\tfrac{z_L}{d}\right)^{\rho/\mu} \sin\left(\tfrac{\omega}{\mu}\ln\left(\tfrac{z_L}{d}\right)\right) \\
y_L &= \phi_2(y_L, z_L) &= y_L \left(\tfrac{z_L}{d}\right)^{\rho/\mu} \cos\left(\tfrac{\omega}{\mu}\ln\left(\tfrac{z_L}{d}\right)\right)
\end{aligned} \tag{4.8}$$

We carry out analogous changes of coordinates for the fixed point p_1, and denote the corresponding coordinates as (x'_L, y'_L, z'_L).

We also choose the following surfaces of section:

$$\Sigma_{1,2} = \{(x, y, z) \in \mathbb{R}^3 \mid x = 0\}, \tag{4.9}$$

We will use local coordinates (y_i, z_i) on these sections, such that $(0, 0)$ is the point of intersection of the heteroclinic orbits that exist at $\lambda = 0$, and the sections Σ_i. Fix R_i is spanned by $(1, 0)$.

For the construction of the global maps, we may write, for example $\psi_1 : \Sigma_2 \to \sigma_2$ as

$$\psi_1 \begin{pmatrix} y_0 \\ z_0 \end{pmatrix} = \begin{pmatrix} y_L \\ z_L \end{pmatrix} = \begin{pmatrix} y^* \\ 0 \end{pmatrix} + A \begin{pmatrix} y_0 \\ z_0 \end{pmatrix} + \cdots \tag{4.10}$$

where the dots denote terms of higher order. Since the map ψ_1 is a diffeomorphism, A is a nonsingular matrix. We can similarly write

$$\psi_2 \begin{pmatrix} x_L \\ y_L \end{pmatrix} = \begin{pmatrix} y_1 \\ z_1 \end{pmatrix} = B \begin{pmatrix} x_L \\ y_L \end{pmatrix} + \cdots \tag{4.11}$$

$$\psi'_2 \begin{pmatrix} y_1 \\ z_1 \end{pmatrix} = \begin{pmatrix} x'_L \\ y'_L \end{pmatrix} = RB^{-1}R_1 \begin{pmatrix} y_1 \\ z_1 \end{pmatrix} + \cdots \tag{4.12}$$

$$\psi'_1 \begin{pmatrix} y'_L \\ z'_L \end{pmatrix} = \begin{pmatrix} y_0 \\ z_0 \end{pmatrix} = R_0 A^{-1} R \begin{pmatrix} y'_L - y^* \\ z'_L \end{pmatrix} + \cdots \tag{4.13}$$

We may assume by fixing a choice of coordinates that A is an orientation preserving matrix, where B is an orientation reversing matrix. Note then that the compositions $\psi'_2 \circ \psi_2$ and $\psi'_2 \circ \psi_2$ appear to be orientation reversing if we identify (x_L, y_L, z_L) with (x'_L, y'_L, z'_L), but this is just due to the choice of local coordinates about the points p_1, p_2. Finally, $R_{1,2}$ act on the sections $\Sigma_{1,2}$ as:

$$R_{1,2} : \begin{pmatrix} 0 \\ y \\ z \end{pmatrix} \to \begin{pmatrix} 0 \\ y \\ -z \end{pmatrix}. \tag{4.14}$$

4.3 Dynamics of the return maps

In this section we establish three Lemmas that are central to the proofs of the existence theorems 4.1.1–4.1.5.

Lemma 4.3.1. *Let $(y_L(s), z_L(s))$ be a line segment in σ_2, parameterised by s, such that $y_L(0)$ is close to y^*, $z_L(0) = 0$, $\frac{\partial z(s)}{\partial s}|_{s=0} \neq 0$, and $(y_L(s), z_L(s))$ is transverse to the local stable manifold $W^s(p_2)$. Then the image of $(y_L(s), z_L(s))$ under the local map ϕ is a logarithmic spiral in σ_1. That is, in polar coordinates $x_L = r\sin\theta$, $y_L = r\cos\theta$, the image of $(y_L(s), z_L(s))$ takes the form*

$$\begin{aligned} r &= y_L(s)\left(\tfrac{z_L(s)}{d}\right)^{\rho/\mu} \\ \theta &= \tfrac{\omega}{\mu}\ln\left(\tfrac{z_L(s)}{d}\right). \end{aligned} \tag{4.15}$$

Proof. From (4.8), we may write the image of $(y_L(s), z_L(s))$ in σ_1 as

$$\begin{aligned} x_L &= \phi_1(y_L(s), z_L(s)) &= y_L(s)\left(\tfrac{z_L(s)}{d}\right)^{\rho/\mu}\sin\left(\tfrac{\omega}{\mu}\ln\left(\tfrac{z_L(s)}{d}\right)\right) \\ y_L &= \phi_2(y_L(s), z_L(s)) &= y_L(s)\left(\tfrac{z_L(s)}{d}\right)^{\rho/\mu}\cos\left(\tfrac{\omega}{\mu}\ln\left(\tfrac{z_L(s)}{d}\right)\right), \end{aligned} \tag{4.16}$$

from which the statement of the Lemma is immediate. □

The following theorem gives the image in σ_2' of a logarithmic spiral in σ_1' under the map ϕ'.

Lemma 4.3.2. *Consider a logarithmic spiral Γ in σ_1' which has the form*

$$\begin{aligned} x_L'(s) &= a y_L(s)\left(\frac{z_L(s)}{d}\right)^{\rho/\mu}\sin\left(\frac{\omega}{\mu}\ln\left(\frac{z_L(s)}{d}\right)\right) \\ &\quad + b y_L(s)\left(\frac{z_L(s)}{d}\right)^{\rho/\mu}\cos\left(\frac{\omega}{\mu}\ln\left(\frac{z_L(s)}{d}\right)\right) + \cdots \end{aligned} \tag{4.17}$$

$$\begin{aligned} y_L'(s) &= c y_L(s)\left(\frac{z_L(s)}{d}\right)^{\rho/\mu}\sin\left(\frac{\omega}{\mu}\ln\left(\frac{z_L(s)}{d}\right)\right) \\ &\quad + d y_L(s)\left(\frac{z_L(s)}{d}\right)^{\rho/\mu}\cos\left(\frac{\omega}{\mu}\ln\left(\frac{z_L(s)}{d}\right)\right) + \cdots \end{aligned} \tag{4.18}$$

where a, b, c, d are constants, $ad - bc = -1$, and the ellipsis denotes terms of higher order in $z_L(s)$ (as $z_L(s) \to 0$). Here $(y_L(s), z_L(s))$ satisfies the same *properties as in Lemma 4.3.1. Generically, the image of* Γ *under* ϕ' *in* σ_2' *will be a countably infinite set of lines which accumulate exponentially* C^1 *close to* $W^u(p_1)$ *with the order of* $z_L' \sim \exp\left(-\frac{\mu}{\omega}n\pi\right)$ *for* $n \in \mathbb{N}$.

Proof. Recall that $\phi'^{-1} = R\phi R$, so the pre-image of a point $(y_L', z_L') \in \sigma_2'$ will be, in polar coordinates $x_L' = r'\sin\theta'$, $y_L' = r'\cos\theta'$:

$$\begin{aligned} r' &= y_L'\left(\tfrac{z_L'}{d}\right)^{\rho/\mu} \\ \theta' &= \tfrac{\omega}{\mu}\ln\left(\tfrac{z_L'}{d}\right). \end{aligned} \tag{4.19}$$

We will first consider the case where the matrix $A_1 = \begin{bmatrix} a & b \\ c & d \end{bmatrix} = \begin{bmatrix} -1 & 0 \\ 0 & 1 \end{bmatrix}$ and neglect the higher order terms. Then, in (r', θ') coordinates Γ will have the form

$$\begin{aligned} r' &= y_L(s)\left(\tfrac{z_L(s)}{d}\right)^{\rho/\mu} \\ \theta' &= -\tfrac{\omega}{\mu}\ln\left(\tfrac{z_L(s)}{d}\right). \end{aligned} \tag{4.20}$$

We note that the equations for θ' are modulo 2π, and that the θ' equation in (4.19) is valid for $-\theta'$ sufficiently large, and the equation for θ' in (4.20) is valid for θ' sufficiently large. We will consider first fixing $y_L \in \sigma_2'$, and search for values of $z_L \in \sigma_2'$ that are in the image of Γ under ϕ'.

By equating the radius coordinates of (4.19), (4.20), we obtain

$$z_L' = \left(\frac{y_L(s)}{y_L'}\right)^{\mu/\rho} z_L(s). \tag{4.21}$$

Note that (4.21) gives z_L' as a function of s, we write $z_L' = z_L'(s)$. $y_L(s)$ is $\mathcal{O}(1)$ in s as $s \to 0$, so $z_L'(s)$ and $z_L(s)$ are of the same order as $s \to 0$.

Now recall that the equations for the arguments in (4.19), (4.20) are modulo 2π, and so for $z_L'(s)$, $z_L(s)$ sufficiently small, equating the angle equations in (4.19), (4.20) gives

$$z_L'(s) = d\left(\frac{y_L(s)}{y_L'}\right)^{\mu/2\rho} . \exp\left(-\frac{\mu}{\omega}n\pi\right), \tag{4.22}$$

for $n \in \mathbb{N}$. As $s \to 0$, $y_L(s)$ tends to a constant and $z'_L(s) \to 0$. Then for a fixed large $n \in \mathbb{N}$, (4.22) has a solution for s close to zero. This is a point at which the curves Γ and the pre-image of (y'_L, z'_L) (for fixed y'_L) in σ'_1 intersect. Moreover since $\frac{dz_L(s)}{ds}$ (and hence $\frac{dz'_L(s)}{ds}$) is bounded away from zero for s sufficiently close to zero, and $\frac{dy_L(s)}{ds}$ is approximately constant for s sufficiently close to zero, for n large enough this intersection is transverse. Substituting (4.22) into (4.19), we see that these intersections (for each $n \in \mathbb{N}$) occur every π in the angle argument, asymptotically as $s \to 0$. We may use the Implicit Function Theorem to show that as y_L is varied, we can still find a unique value for s such that the two curves intersect transversally. Then the image of Γ under the map ϕ' is a countable set of lines that exponentially accumulate to $z' = 0$ (the unstable manifold of p_1). They accumulate with the order of $\exp\left(-\frac{\mu}{\omega} n\pi\right)$ for $n \in \mathbb{N}$.

We now consider the matrix $A_1 \neq \begin{bmatrix} -1 & 0 \\ 0 & 1 \end{bmatrix}$. Let $B_1 \neq I$ be a matrix such that $A_1 = B_1 \begin{bmatrix} -1 & 0 \\ 0 & 1 \end{bmatrix}$, so B_1 has determinant 1. Then B_1 has the effect of a linear transformation of the curve Γ previously studied. Assume B_1 is a hyperbolic matrix, since if it acts as a rotation the effect is trivial. As before first fix y'_L and consider the intersections of Γ with the pre-image of (y'_L, z'_L). These intersections are approximately π apart in the angle θ'. Now consider the line $\mathcal{L}$ in σ'_1 that is spanned by an eigenvector of B_1, such that this line bisects these intersections, see Fig 4.2. We use $\mathcal{L}$ to divide Γ into disjoint, countably many arcs, each of length 2π in the angle variable, such that each endpoint of each arc is in $\mathcal{L}$. The effect of B_1 on each of these arcs is similar, so we just consider one of these arcs. In fact, by rotational symmetry of Γ and of B_1, the effect of the transformation is similar on each half of these arcs, each of length π. It is clear that the transformed curve $B_1\{\Gamma\}$ cannot have fewer intersections with the pre-image of (y'_L, z'_L) than Γ. (Each intersection can be 'continued' as we linearly continuously deform the curve Γ to $B_1\{\Gamma\}$.

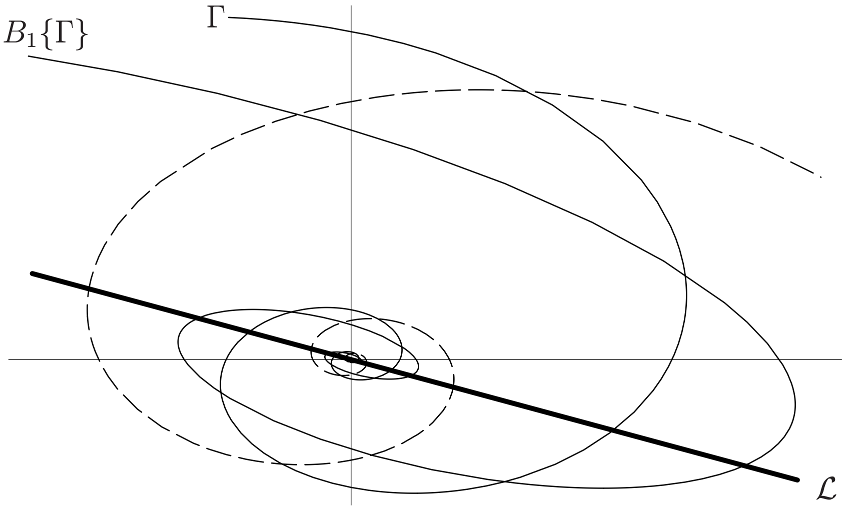

Figure 4.2: The spirals Γ and $B_1\{\Gamma\}$ in the section σ_1'. The line $\mathcal{L}$ shown is spanned by the expanding eigenvector of B_1. The dashed spiral is the preimage of $(y_L', z_L') \in \sigma_2'$ under ϕ', for fixed y_L'.

Moreover, for the reasons of symmetry just mentioned, the intersections will still be π apart in the angle variable.) The only possible problem is that these intersections will be nontransverse. Again it is clear that these intersection could not be quadratic (or any tangency of 'even' type). However we cannot necessarily avoid a tangency in general, and so must make a condition to avoid tangencies. This condition is satisfied on an open and dense set, see section 4.5.

We conclude that the curve Γ in the statement of the Lemma generically intersects transversally with the pre-image of (y_L', z_L') at least in countably many points, all of which are asymptotically π apart in the angle variable. As before we may use transversality arguments to conclude that the image of Γ in σ_2' is a set of lines exponentially accumulating to $z' = 0$ (the unstable manifold of p_1). They accumulate with the order of $\exp\left(-\frac{\mu}{\omega} n\pi\right)$ for $n \in \mathbb{N}$. As all intersections are transversal, the addition of the (arbitrarily small) higher order terms in the expression of Γ do not affect this result for (x_L', y_L') sufficiently small in σ_1'. $\square$

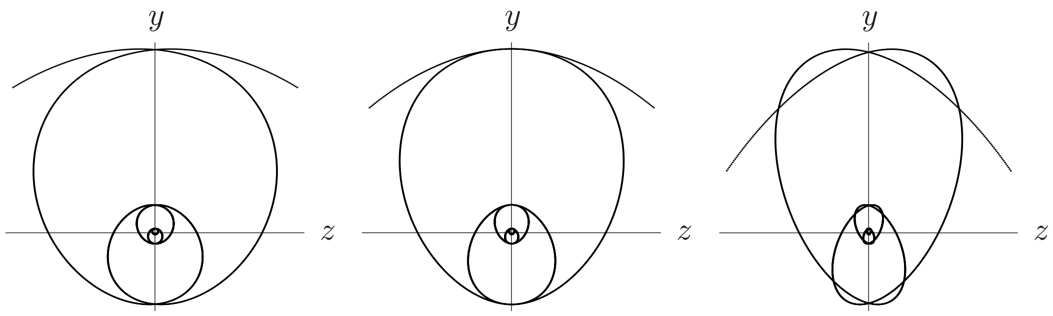

Figure 4.3: Unfolding of a tangency of two spirals. The above case may occur for 2-2D heteroclinic orbits, for example. The spirals shown here are a symmetric pair, but in general this need not be the case for orbit bifurcation.

Remark 4.3.3. *Even without the generic condition, the image would still be that of an exponentially accumulating set of lines, and the existence theorems for heteroclinic and homoclinic orbits would remain unaffected. However, in the case of a tangency, nearby orbits (found in section 4.4) may bifurcate, see Figure 4.3, and also Figures 5.4 and 5.5 in section 5.5.*

The following gives the same result as Lemma 4.3.2 for a line segment in σ_1'.

Lemma 4.3.4. *Consider a line segment γ in σ_1' which has the form*

$$\begin{aligned} x_L'(s) &= as + \cdots \\ y_L'(s) &= bs + \cdots \end{aligned} \tag{4.23}$$

where a, b are constants, with at least one of them not equal to zero, and the ellipsis denotes terms of higher order in s (as $s \to 0$). The image of γ under ϕ' in σ_2' will be a countably infinite set of lines which accumulate exponentially C^1 close to $W^u(p_1)$ with the order of $z_L' \sim \exp\left(-\frac{\mu}{\omega}n\pi\right)$ for $n \in \mathbb{N}$.

Proof. The proof is similar to Lemma 4.3.2. The line γ and the preimage of (y_L', z_L') in σ_1' for constant y_L' intersect transversally in countably many points, and we may use the Implicit Function Theorem to show that as we vary y_L', we see that the image of γ in σ_2' is a countable set of lines accumulating exponentially to $z_L' = 0$ at the rate $z_L' \sim \exp\left(-\frac{\mu}{\omega}n\pi\right)$ for $n \in \mathbb{N}$. $\square$

Now we have the appropriate results to enable us to prove Theorems 4.1.1–4.1.4.

4.4 Analysis of the Return Maps

The following Lemma characterizes symmetric orbits in R-reversible vector fields. We will use this result when searching for symmetric orbits in this section. For a proof, see [112].

Lemma 4.4.1. *A maximal orbit γ (i.e. the orbit does not retrace itself) of an R-reversible vector field is symmetric if and only if*

$$\gamma \cap \mathit{Fix}\ R \neq \emptyset.$$

If γ is a symmetric orbit then precisely one of the following holds:

1. *$\gamma \subset \mathit{Fix}\ R$: then γ is a symmetric fixed point,*
2. *$\gamma \not\subset \mathit{Fix}\ R$, $\gamma \cap \mathit{Fix}\ R$ consists of exactly one point: then γ is not a closed orbit.*
3. *$\gamma \not\subset \mathit{Fix}\ R$, $\gamma \cap \mathit{Fix}\ R$ consists of exactly two distinct points: then γ is a closed orbit.*

From this Lemma we see that heteroclinic orbits fall into case 2. Periodic orbits fall into case 3, but note that in general a closed orbit that intersects Fix R twice may be considered to be a symmetric homoclinic orbit. In our situation this case does not arise.

4.4.1 Symmetric and asymmetric 2D heteroclinic orbits

From Lemma 4.4.1 we have a simple characterization of symmetric heteroclinics (from p_1 or p_2). A solution starting at p_1 or p_2 is a symmetric heteroclinic solution if and only if it intersects Fix R. This solution intersects Fix R precisely once.

Throughout, we will have a shortest symmetric 2D heteroclinic connection $q_2(t)$ formed by the transversal intersection of $W^s(p_2)$ and $W^u(p_1)$. The characterization of this heteroclinic orbit is that it does not pass through Σ_1. This heteroclinic orbit is the unique 1-2D heteroclinic.

Note that for an n-2D heteroclinic, it is a 'lower' heteroclinic if and only if n is odd.

Proof of Theorem 4.1.1. We first follow the unstable manifolds of p_1 to track down 2D heteroclinics at $\lambda = 0$. The local unstable manifold of p_1 in σ_2' is given by the set $z_L' = 0$. Consider first the map ψ_1' acting on $W^u(p_1)$. By (4.13) and the symmetry (4.14), the image of $W^u(p_1)$ under ψ_1' will be a C^1 line segment in Σ_2, which lies transverse to Fix R and the image of $W^s(p_2)$ under ψ_1^{-1}. By (4.10), the image of this line segment under ψ_1 will be another line segment in σ_2, which satisfies the hypotheses of Lemma 4.3.1. So by Lemma 4.3.1, the image of this line segment is a logarithmic spiral in σ_1. We may then diffeomorphically transport this spiral to Σ_1 under ψ_2. Call this spiral Υ. Now, arguments similar to those used before show that this spiral will intersect Fix R in countable many points, that exponentially accumulate to the centre of the spiral. By Lemma 4.4.1, each of these points indicate a symmetric 2-2D heteroclinic orbit. In fact, all 2-2D heteroclinic orbits must be symmetric for $\lambda = 0$, since the image of $W^s(p_0)$ under $(\psi_2')^{-1} \circ (\phi')^{-1} \circ (\psi_1')^{-1} \circ \psi_1^{-1}$ in Σ_1 is the R_1-image of Υ, and it is easy to see that for (y, z) sufficiently small in Σ_1, these two spirals only intersect along Fix R. These intersections are transverse.

Now take the pre-image of Υ in σ_1, and consider mapping it to σ_1' by $\psi_2' \circ \psi_2$. By (4.11), (4.12), the linear part of this map does have determinant -1, and so the spiral satisfies the hypotheses of Lemma 4.3.2. Applying Lemma 4.3.2 shows now that the image of the unstable manifold of p_1 exponentially accumulates on itself as a set of lines in σ_2'. By (4.13), any one of these lines (sufficiently close to $z_L' = 0$ in σ_2') maps to Σ_2 by ψ_1' as a line segment which is transversal to Fix R and $W^s(p_2)$. Where it intersects Fix R we have a symmetric 3-2D heteroclinic orbit, and where it intersects $W^s(p_2)$ we have a 2-2D heteroclinic orbit. By the previous arguments, this connection must in fact be symmetric. We can repeat this procedure *ad infinitum* to reveal the existence of n-2D heteroclinic orbits, for any n. For $n \geq 3$ the connections may be symmetric or asymmetric, and there are countable many of each. We note that for $n \geq 3$, most of the connections are asymmetric.

This completes the proof of Theorem 4.1.1. □

As λ is varied from 0, many of these heteroclinic orbits will be removed in saddle-node-type bifurcations. For any $\lambda \neq 0$, there will be only finitely many n-2D heteroclinic orbits for each n. This is because the centres of the spirals above no longer lie on Fix (R_1). Also, many more asymmetric 2D heteroclinic orbits will be created, but the nature of how these are created is complicated, and will depend sensitively on the precise unfolding.

4.4.2 Symmetric periodic solutions

We use the return maps F_1 and F_2 to study the occurrence of R-symmetric periodic solutions. To that effect, we recall some simple characterization of symmetric periodic orbits for reversible maps. It is readily verified that symmetric periodic solutions of the reversible vector field near the heteroclinic cycle give rise to R-symmetric periodic orbits of the return maps F_1 and F_2.

Proposition 4.4.2. *Let F be an R-reversible map, then an orbit of F is periodic and R-symmetric if and only if it intersects Fix $(R) \cup$ Fix $(R^{-1} \circ F)$ precisely twice.*

It is important to note that due to the reversibility, $F_2 = R_2 \circ P_1$ where $P_1 : \Sigma_2 \to \Sigma_2$ is an involution, ie $P_1^2 = Id$. In fact, Fix (P_1) is precisely the pull-back by the flow of Fix (R_1) inside Σ_1 to Σ_2, so that dim Fix $(P_1) =$ dim Fix $(R_1) = 1$. Similarly we may define the involution $P_2 : \Sigma_1 \to \Sigma_1$ so that $F_1 = P_2 \circ R_1$. Note that with our one-parameter family of vector fields $F(\cdot, \lambda)$ it is natural to think of P_2 and P_1 being nonlinear involutions depending on a parameter λ.

Given the interpretation of P_1 and P_2, we may reformulate the result on periodic solutions as follows:

Proposition 4.4.3. *A periodic solution of $F(\cdot, \lambda)$ near the heteroclinic cycle is R-symmetric if and only if it intersects Fix $(R_1) \cup$ Fix (R_2) precisely twice.*

Proof. Consider F_2. Then $P_1 = R_2 \circ F_2$ and $x \in$ Fix (P_1) if and only if the solution of the vector field through $x \in \Sigma_2$ intersects Fix (R_1). Similarly for F_1. □

Of course, this property coincides exactly with the observation that for an R-reversible vector field a solution is periodic and R-symmetric if and only if it intersects Fix (R) precisely twice, see Lemma 4.4.1.

We now distinguish between lower periodic solutions which have two intersections with Fix (R_2), upper periodic solutions which have two intersections with Fix (R_1), and mixed periodic solutions which have one intersection with Fix (R_2) and one with Fix (R_1). The latter type of symmetric periodic solution is the simplest since these may occur as 1-periodic solutions, although all types will occur in our unfolding, see section 4.5.

Proof of Theorem 4.1.2. We will consider first symmetric 1-periodic solutions that are close to the 1-heteroclinic cycle consisting of the unique 1-2D heteroclinic connection $q_2(t)$ and the 1D heteroclinic connection $q_1(t)$ that exists only for $\lambda = 0$. To find these symmetric periodic solutions then, we evolve

Fix R_2 itself under the composition $\psi_2\circ\phi\circ\psi_1$. Where this set intersects Fix R_1 we will find symmetric 1-periodic solutions, by Lemma 4.4.1. By Lemma 4.3.1 we find

$$\psi_2 \circ \phi \circ \psi_1 \begin{bmatrix} y \\ 0 \end{bmatrix} = B \begin{bmatrix} \hat{y}_L \left(\frac{\hat{z}_L}{d}\right)^{\rho/\mu} \sin\left(\frac{\omega}{\mu}\ln\left(\frac{\hat{z}_L}{d}\right)\right) \\ \hat{y}_L \left(\frac{\hat{z}_L}{d}\right)^{\rho/\mu} \cos\left(\frac{\omega}{\mu}\ln\left(\frac{\hat{z}_L}{d}\right)\right) \end{bmatrix} + O(\hat{z}_L^{2\rho/\mu}),$$

where $\hat{y}_L = y^* + a_1 y + O(y^2)$, $\hat{z}_L = a_3 y + O(y^2)$. Then we may write

$$\begin{aligned} \psi_2 \circ \phi \circ \psi_1 \begin{bmatrix} y \\ 0 \end{bmatrix} &= \begin{bmatrix} y^* \left(\frac{a_3 y}{d}\right)^{\rho/\mu} (b_1^2+b_2^2)^{1/2} \sin\left(\frac{\omega}{\mu}\ln\left(\frac{\hat{z}_L}{d}\right) + \Phi_1\right) \\ y^* \left(\frac{a_3 y}{d}\right)^{\rho/\mu} (b_3^2+b_4^2)^{1/2} \sin\left(\frac{\omega}{\mu}\ln\left(\frac{\hat{z}_L}{d}\right) + \Phi_2\right) \end{bmatrix} \\ &\quad + O(y^{(\min\{1+(\rho/\mu), 2\rho/\mu\})}), \end{aligned} \tag{4.24}$$

where $\Phi_1 = \tan^{-1}\left(\frac{b_1}{b_2}\right)$ and $\Phi_2 = \tan^{-1}\left(\frac{b_3}{b_4}\right)$. Hence symmetric periodic solutions are given by the solutions to the equation

$$y^{\rho/\mu} \sin\left(\frac{\omega}{\mu}\ln\left(\frac{\hat{z}_L}{d}\right) + \Phi_2\right) + O(y^{(\min\{1+(\rho/\mu), 2\rho/\mu\})}) = 0. \tag{4.25}$$

Note that the fact that B is nonsingular implies that b_3, b_4 are not both zero, and $\Phi_1 \neq \Phi_2$. From (4.25) it is clear that at $\lambda = 0$ there are countably many intersections of Fix (R_1) and $\psi_2\circ\phi\circ\psi_1(\text{Fix }(R_2))$, and so countably many symmetric periodic orbits. It is also easy to see that these periodic orbits are asymptotically π/ω apart in the time of passage from Σ_2 to Σ_1. They are also transversal intersections, and so we may continue them as we vary the parameter λ. Applying the Implicit Function Theorem and a rescaling of the parameter shows that for $|\lambda|$ sufficiently small, symmetric periodic solutions are given by the equation

$$\lambda + y^{\rho/\mu} \sin\left(\frac{\omega}{\mu}\ln\left(\frac{\hat{z}_L}{d}\right) + \Phi_2\right) + O(y^{(\min\{1+(\rho/\mu), 2\rho/\mu\})}) = 0,$$

and so the set of symmetric periodic solutions forms a one parameter family, parametrised by period. This family is parametrised along the spiral that is the image of Fix R_2 in Σ_1 under $\psi_2\circ\phi\circ\psi_1$. The effect of perturbing the parameter λ is effectively to move this spiral transversally through Fix R_1, and so by oscillating the parameter λ about zero we can follow the spiral into

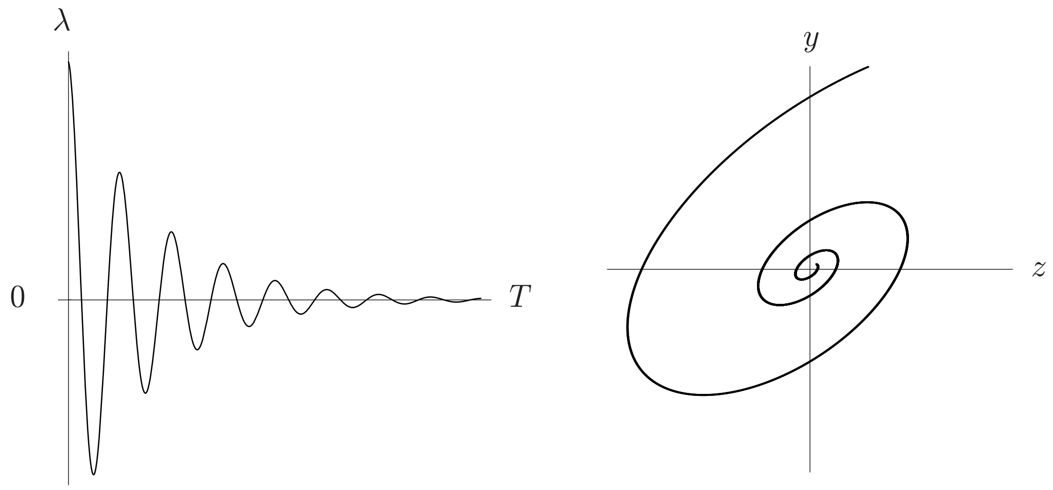

Figure 4.4: Symmetric periodic orbits plotted with parameter λ against period T. The interval between zeros of this function are asymptotically equal to π/ω. Also shown is the image of Fix R_2 in Σ_1.

the centre, where the period tends to infinity, see Figure 4.4. Clearly as the period tends to infinity, the periodic orbit converges to the 1-heteroclinic cycle.

We have studied symmetric 1-periodic orbits close to the heteroclinic cycle formed by $q_1(t)$, $q_2(t)$. As we shall see, there are countably many more heteroclinic cycles that exist at different parameter values in any neighbourhood of $\lambda = 0$. Clearly this same result may be applied to any one of these heteroclinic cycles, and so we obtain a countable infinity of one parameter families of symmetric periodic orbits, each parametrised by period, which converges to the given heteroclinic cycle as the period approaches infinity. $\square$

4.4.3 1D heteroclinic orbits and homoclinic orbits

Recall the characterization of symmetric heteroclinic orbits given in Lemma 4.4.1. In fact, it is easy to see by uniqueness that 1D heteroclinic orbits must always be symmetric. Also, at most one such connection can occur for each parameter value. Similar to the 2D heteroclinic orbits, we have a shortest

1D connection $q_1(t)$, formed by the coincidence of $W^u(p_2)$ and $W^s(p_1)$, which exists only at $\lambda = 0$. This heteroclinic orbit is the unique 1-1D heteroclinic orbit.

Homoclinic orbits to p_1 and p_2 in contrast must be asymmetric, and they occur in pairs. We will search for homoclinic orbits to the point p_2. We call a solution an n-homoclinic if it traces n consecutive loops through Σ_1 (or Σ_2).

Sketch Proof of Theorems 4.1.3 and 4.1.4. For $\lambda \neq 0$ the local and global maps will change slightly, but not significantly to affect our analysis. What is more important is that for $\lambda \neq 0$, $W^s(p_1)$ and $W^u(p_2)$ no longer coincide. In order to study the 1D heteroclinic orbits, for each $\lambda \neq 0$, we shall study the straight line ζ in Σ_1 that passes through the traces of $W^s(p_1)$ and $W^u(p_2)$. (In fact, any transversal line would do.) The tangent vectors to this line lie in Fix $(-R_1)$. We will parametrise this line by λ such that $\zeta(0)$ is the point where it crosses $W^s(p_1)$, and $\zeta(\lambda')$ is the point where it crosses $W^u_{\lambda'}(p_2)$, see Figure 4.5. Note that as λ varies this line has a possible translation in the direction of Fix (R_1), but this is unimportant for our analysis. In Σ_1, the parametrisation of ζ by λ is approximately a multiplicative factor away from the parametrisation of the locus of $W^u(p_2)$ (or $W^s(p_1)$) in Σ_1 as λ is varied. Therefore exponential accumulation in ζ corresponds to exponential accumulation in the true parameter space with the same exponential rate.

By studying ζ under the return maps, we are in fact studying the unstable manifold of p_2 for each parameter value λ close to zero. By studying intersections with Fix $(R_2) \cup$ Fix (R_1) (resp. $W^s(p_2)$), we will find 1D heteroclinic orbits (resp. homoclinic orbits).

First we map ζ under ψ_2'. Then ζ appears in σ_1' as a line segment, satisfying the hypotheses of Lemma 4.3.4. Applying Lemma 4.3.4, ζ then maps under ϕ' to a countable set of exponentially accumulating lines to $z_L' = 0$ in σ_2'. Choosing one line sufficiently close to z_L', we may map this line to Σ_2 such that it intersects

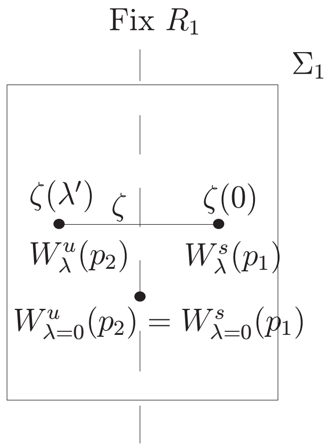

Figure 4.5: The line ζ through the traces of $W^s_\lambda(p_1)$ and $W^u_\lambda(p_0)$.

both Fix (R_2) and $W^s(p_2)$ transversally. Since there are a countably infinite number of lines with z'_L sufficiently small, there is a countable infinity of 2-1D heteroclinic orbits and 1-homoclinic orbits, exponentially accumulating to $\lambda = 0$ in parameter space from both sides.

Now take one of the lines in σ'_2 sufficiently close to $z'_L = 0$, and map it under $\psi_1 \circ \psi'_1$. This appears in σ_2 as a line segment satisfying the hypotheses of Lemma 4.3.1. Applying Lemma 4.3.1 then shows that this line maps to σ_1 as a logarithmic spiral, which in turn maps to Σ_1 diffeomorphically. Now, this spiral is not centred on $W^s(p_1)$ in Σ_1, but we may take it to be as close to the centre as we wish for λ close to zero. Then there will still be an arbitrarily large finite number of intersections of this spiral with Fix (R_1) for λ sufficiently close to zero. Therefore there will be a countable infinity of 3-1D heteroclinic orbits exponentially accumulating to $\lambda = 0$.

Then, mapping this spiral to σ'_1 we obtain a logarithmic spiral that does not quite satisfy the conditions of Lemma 4.3.2 as it not centred on $W^s(p_1)$, but is a small perturbation away from it. If this perturbation is sufficiently small (for λ close enough to zero), any finite number of the intersections of this spiral with the pre-image of (y'_L, z'_L) for fixed y'_L will persist, as in the proof of the Lemma. Then we may conclude that for λ close enough to zero, we may map the spiral into σ_2' as a finite set of lines which may get as close to $z_L' = 0$ as we like for λ close to zero. Then we can map any of these lines under ψ_1' to Σ_2 to find (for λ close to zero) transverse intersections with both Fix (R_2) and $W^s(p_2)$.

We can repeat this procedure again indefinitely to reveal a countably infinite number of n-1D heteroclinic orbits for $n \geq 2$ and n-homoclinic orbits for $n \geq 1$, occurring for unique parameter points, all accumulating exponentially to $\lambda = 0$ in parameter space from both sides. Moreover, since all intersections are transverse, these heteroclinic and homoclinic orbits are 'generic' in the sense that the unstable manifold of p_2 passes through Fix R or $W^s(p_2)$ with positive speed with respect to the parameter.

This concludes the proofs of Theorems 4.1.3 and 4.1.4. $\square$

4.5 The Symmetric Horseshoe

It is well known, that under certain eigenvalue conditions, a homoclinic orbit such as the ones found in Theorem 4.1.4 may give rise to chaotic dynamics [45, 36, 97, 98]. With our notation, this condition is $\rho < \mu$. However, under generic (open and dense) conditions, in our situation at $\lambda = 0$ there is another set of horseshoes which arises specifically due to the 1-heteroclinic cycle. This is an R-invariant, indecomposable, hyperbolic invariant set which is topologically conjugate to a full shift on n symbols, for any $n \in \mathbb{N}$. In the case $\rho/\mu < 1$, this set may be thought of as a bifurcation point of all the horseshoes that arise due to the homoclinic orbits.

First, we take an open set B_2 in Σ_2 such that one side of B_2 coincides with $W^s(p_2)$, and such that if we map this strip to σ_2 by ψ_1, it appears as the set

$$\psi_1(S) = \{(y_L, z_L) \ : \ 0 < z_L < \varepsilon_1, y^* - \varepsilon_2 < y_L < y^* + \varepsilon_2\}, \tag{4.26}$$

for some small $\varepsilon_2 \gg \varepsilon_1 > 0$. B_2 appears in Σ_2 as a thin strip along $W^s(p_2)$. By Lemma 4.3.1 $\psi_1(B_2)$ is mapped to a 'thickened' logarithmic spiral in σ_1, which in turn is mapped diffeomorphically by ψ_2 to a logarithmic spiral $\mathcal{S}_2$ in Σ_1. Now consider $B_1 := R_2 \circ B_2$, this strip lies along $W^u(p_1)$ in Σ_2. Note that the leaves of B_2, defined as the pre-image of the lines $\{(y_L, z_L) : y_L = \text{constant}\}$ in Σ_0, generically intersect the leaves of B_1 (defined similarly, or simply by letting R_2 act on the leaves on B_2) transversally everywhere.

By the reversibility, the map $(\psi_2')^{-1} \circ (\phi')^{-1} \circ (\psi_1')^{-1}$ acts on B_1 to produce a thickened spiral $\mathcal{S}_1$ in Σ_1, which is the R_1 image of $\mathcal{S}_2$, see Fig 4.6.

Define the leaves of $\mathcal{S}_2$ to be the leaves of B_2 under the map $\psi_2 \circ \phi \circ \psi_1$. Similarly for the leaves of $\mathcal{S}_1$. Similar arguments to those used in the proof of Lemma 4.3.2 can be used to show that for $\varepsilon_1, \varepsilon_2$ sufficiently small, any two leaves of $\mathcal{S}_2$ and $\mathcal{S}_1$ intersect each other in countably many points, and under generic conditions, each intersection is transverse. We may define a countable set M_i ($i \in \mathbb{N}$) of consecutive disjoint areas where the two spirals intersect, where M_i approaches the centre of the spirals as $i \to \infty$, and M_i, M_{i+1} are approximately π apart from each other in the angle coordinate. Define also

$$H_i := \psi_1^{-1} \circ \phi^{-1} \circ \psi_2^{-1}(M_i), \tag{4.27}$$

$$V_i := \psi_1' \circ \phi' \circ \psi_2'(M_i). \tag{4.28}$$

Consider a finite number of the M_i, H_i and V_i for i sufficiently large. It is clear that $F_2(H_i) = V_i$. Also, if we consider $B := B_1 \cap B_2$ as a topological square $B = \{(\overline{y}, \overline{z}) \in \mathbb{R}^2 \mid 0 < \overline{y} < 1, 0 < \overline{z} < 1\}$ then H_i and V_i can be considered 'horizontal' and 'vertical' strips in B respectively, according to the definitions in [50, section 5.2]. Following the exposition in [50], we would like to prove the following Proposition.

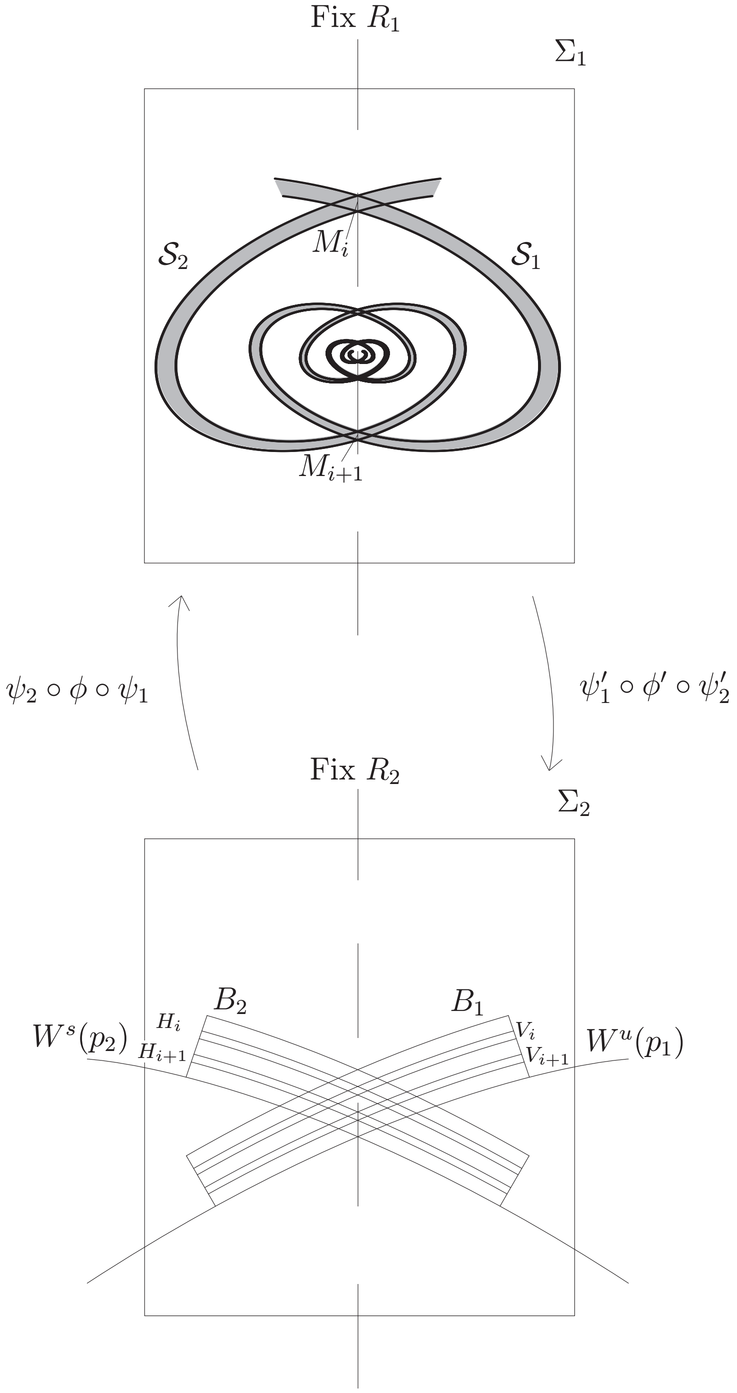

Figure 4.6: The symmetric horseshoe, with horizontal strips H_i and vertical strips V_i.

Proposition 4.5.1.
- *There exist sector bundles* $S^u(\overline{y},\overline{z}) = \{(\xi,\eta) \mid |\xi| < k|\eta|\}$ *defined over the union of all the* V_i, *and* $S^s(\overline{y},\overline{z}) = \{(\xi,\eta) \mid |\eta| < k|\xi|\}$ *defined over all the* H_i *with* $0 < k < 1$ *such that* $DF_2(S^u(\overline{y},\overline{z})) \subset S^u(F_2(\overline{y},\overline{z}))$ *and* $DF_2^{-1}(S^s(\overline{y},\overline{z})) \subset S^s(F_2^{-1}(\overline{y},\overline{z}))$.

- *Let* $DF_2(\xi_0,\eta_0) = (\xi_1,\eta_1)$ *and* $DF_2^{-1}(\xi_0,\eta_0) = (\xi_{-1},\eta_{-1})$. *Then* $|\eta_1| \geq (1/k)|\eta_0|$ *and* $\xi_{-1} \geq (1/k)|\xi_0|$.

In order to verify the above, we need to use the derivative of the map $F_2 : \Sigma_2 \to \Sigma_2$. In our case we require a generic condition to ensure the existence of hyperbolic horseshoes. This condition is not necessary for the Shil'nikov homoclinic case [4, 116], given that the eigenvalue condition $\rho/\mu < 1$ is satisfied.

Proof. We first study the map $\psi_2 \circ \phi \circ \psi_1(H_i)$ more closely. We can write this map down as

$$\psi_2 \circ \phi \circ \psi_1 \begin{pmatrix} y \\ z \end{pmatrix} = B \begin{pmatrix} y_L(\frac{z_L}{d})^{\rho/\mu} \sin(\frac{\omega}{\mu}\ln(\frac{z_L}{d})) \\ y_L(\frac{z_L}{d})^{\rho/\mu} \cos(\frac{\omega}{\mu}\ln(\frac{z_L}{d})) \end{pmatrix} + \cdots, \tag{4.29}$$

where here

$$\begin{pmatrix} y_L \\ z_L \end{pmatrix} = \psi_1 \begin{pmatrix} y \\ z \end{pmatrix} = \begin{pmatrix} y^* \\ 0 \end{pmatrix} + A \begin{pmatrix} y \\ z \end{pmatrix} + \cdots,$$

and the ellipsis in (4.29) denotes terms of higher order in (y,z) (and hence also $(y_L - y*, z_L)$). As $i \to \infty$, H_i becomes C^1 close to $W^s(p_2)$ in Σ_2, and hence $\psi_1(H_i)$ gets C^1 close to the line $z_L = 0$ in σ_2. Now we consider the mapping

$$D\psi_2 \circ \phi \begin{pmatrix} y_L \\ z_L \end{pmatrix} = \begin{pmatrix} y_L(\frac{z_L}{d})^{\rho/\mu}(b_1 \sin(\frac{\omega}{\mu}\ln(\frac{z_L}{d})) + b_2 \cos(\frac{\omega}{\mu}\ln(\frac{z_L}{d}))) \\ y_L(\frac{z_L}{d})^{\rho/\mu}(b_3 \cos(\frac{\omega}{\mu}\ln(\frac{z_L}{d})) + b_4 \sin(\frac{\omega}{\mu}\ln(\frac{z_L}{d}))) \end{pmatrix},$$

where $B = \begin{bmatrix} b_1 & b_2 \\ b_3 & b_4 \end{bmatrix}$. We may write

$$D\psi_2 \circ \phi \begin{pmatrix} y_L \\ z_L \end{pmatrix} = \begin{pmatrix} y_L(\frac{z_L}{d})^{\rho/\mu}(b_1^2 + b_2^2)^{1/2} \sin(\frac{\omega}{\mu}\ln(\frac{z_L}{d}) + \Phi_1) \\ y_L(\frac{z_L}{d})^{\rho/\mu}(b_3^2 + b_4^2)^{1/2} \sin(\frac{\omega}{\mu}\ln(\frac{z_L}{d}) + \Phi_2) \end{pmatrix},$$

where $\Phi_1 = \tan^{-1}\left(\frac{b_1}{b_2}\right)$, $\Phi_2 = \tan^{-1}\left(\frac{b_3}{b_4}\right)$. It may be verified that the angle that $D\psi_2 \circ \phi \begin{pmatrix} \hat{y_L} \\ z_L \end{pmatrix}$ (where $\hat{y_L}$ is a constant close to y^*) intersects the line $z = 0$ is equal to

$$\Theta_0 := \tan^{-1}\left(\frac{(b_3^2 + b_4^2)^{1/2}\sin(n\pi - \Phi_2 + \Phi_4)}{(b_1^2 + b_2^2)^{1/2}\sin(n\pi - \Phi_2 + \Phi_3)}\right)$$

where $z_L = d\exp(\frac{\mu}{\omega}(n\pi - \Phi_2))$, $n \in \mathbb{N}$, $\Phi_3 = \tan^{-1}\left(\frac{b_1\rho - b_2\omega}{b_1\omega + b_2\rho}\right)$ and $\Phi_4 = \tan^{-1}\left(\frac{b_3\rho - b_4\omega}{b_3\omega + b_4\rho}\right)$. It may also be shown that the map $D\psi_2 \circ \phi$ maps lines $z_L =$ constant to radial lines in the (y, z) plane. It is clear now that $\Theta_0 \neq 0$, and we may make the generic assumption that $\Theta_0 \neq \frac{\pi}{2}, \pm\tan^{-1}\left(\frac{a_3}{a_4}\right)$. We will use this assumption when studying the eigenvalues and eigenvectors of the linearised return map. This condition is an open and dense condition on the first derivatives of the return maps, and since we have used C^1 linearisation, the condition is C^k open and dense in general.

The derivative of the map $\phi : \sigma_2 \to \sigma_1$ is given by

$$D\phi(y_L, z_L) = y_L\left(\frac{z_L}{d}\right)^{\rho/\mu} \cdot \left[\begin{array}{cc} \frac{1}{y_L}\sin\left(\frac{\omega}{\mu}\ln\left(\frac{z_L}{d}\right)\right) & \dfrac{\omega\cos\left(\frac{\omega}{\mu}\ln\left(\frac{z_L}{d}\right)\right) + \rho\sin\left(\frac{\omega}{\mu}\ln\left(\frac{z_L}{d}\right)\right)}{\mu z_L} \\ \frac{1}{y_L}\cos\left(\frac{\omega}{\mu}\ln\left(\frac{z_L}{d}\right)\right) & \dfrac{\rho\cos\left(\frac{\omega}{\mu}\ln\left(\frac{z_L}{d}\right)\right) - \omega\sin\left(\frac{\omega}{\mu}\ln\left(\frac{z_L}{d}\right)\right)}{\mu z_L} \end{array}\right]. \quad (4.30)$$

Then the derivative map $D(\psi_2 \circ \phi \circ \psi_1)$ is given by

$$D(\psi_2 \circ \phi \circ \psi_1)(y, z) = \tilde{y}_L\left(\frac{\tilde{z}_L}{d}\right)^{\rho/\mu} B. \left[\begin{array}{cc} \frac{1}{\tilde{y}_L}\sin\left(\frac{\omega}{\mu}\ln\left(\frac{\tilde{z}_L}{d}\right)\right) & \dfrac{\omega\cos\left(\frac{\omega}{\mu}\ln\left(\frac{\tilde{z}_L}{d}\right)\right) + \rho\sin\left(\frac{\omega}{\mu}\ln\left(\frac{\tilde{z}_L}{d}\right)\right)}{\mu\tilde{z}_L} \\ \frac{1}{\tilde{y}_L}\cos\left(\frac{\omega}{\mu}\ln\left(\frac{\tilde{z}_L}{d}\right)\right) & \dfrac{\rho\cos\left(\frac{\omega}{\mu}\ln\left(\frac{\tilde{z}_L}{d}\right)\right) - \omega\sin\left(\frac{\omega}{\mu}\ln\left(\frac{\tilde{z}_L}{d}\right)\right)}{\mu\tilde{z}_L} \end{array}\right] A, \quad (4.31)$$

where $(\tilde{y}_L, \tilde{z}_L) = \psi_1(y, z)$, $B = D\psi_2(\phi \circ \psi_1(y, z))$ and $A = D\psi_1(y, z)$. Equation (4.31) may be rewritten in the form

$$\tilde{z}_L^{(-1+\rho/\mu)} C \left[\begin{array}{cc} \tilde{z}_L & 0 \\ 0 & \tilde{y}_L \end{array}\right] A, \quad (4.32)$$

where

$$C = d^{-\rho/\mu} B \begin{bmatrix} \sin\left(\frac{\omega}{\mu}\ln\left(\frac{\tilde{z}_L}{d}\right)\right) & -\cos\left(\frac{\omega}{\mu}\ln\left(\frac{\tilde{z}_L}{d}\right)\right) \\ \cos\left(\frac{\omega}{\mu}\ln\left(\frac{\tilde{z}_L}{d}\right)\right) & \sin\left(\frac{\omega}{\mu}\ln\left(\frac{\tilde{z}_L}{d}\right)\right) \end{bmatrix} \begin{bmatrix} 1 & \frac{\rho}{\mu} \\ 0 & -\frac{\omega}{\mu} \end{bmatrix}. \tag{4.33}$$

Note that the regions M_i, M_{i+1} have the property that their pre-images (under $\psi_2 \circ \phi$) have $\tilde{z}_L$ values in σ_2 (respectively $\tilde{z}_L^i$, $\tilde{z}_L^{i+1}$) that satisfy $(\omega/\mu)(\ln \tilde{z}_L^i - \ln \tilde{z}_L^{i+1}) \approx \pi$, where $j \in \mathbb{N}$. Consider the strips $\mathcal{Z}_i$ in Σ_2 which are formed by the pre-images of the M_i. (We shall also denote by $\mathcal{Z}_i$ the pre-images of M_i in σ_2 where the meaning is clear.) In these strips the value of the matrix C varies approximately by multiplication by

$$-I = \begin{bmatrix} -1 & 0 \\ 0 & -1 \end{bmatrix}.$$

We shall denote

$$C = \begin{bmatrix} c_1 & c_2 \\ c_3 & c_4 \end{bmatrix}, \quad A = \begin{bmatrix} a_1 & a_2 \\ a_3 & a_4 \end{bmatrix}.$$

From our previous calculation, we observe that the image of the line $y = -\frac{a_2}{a_1}z$ under $D(\psi_2 \circ \phi \circ \psi_1)$ intersects the line $z = 0$ at an angle $\Theta_0 \neq 0, \frac{\pi}{2}, \tan^{-1}\left(-\frac{a_3}{a_4}\right)$, in the regions M_i, asymptotically as $i \to \infty$. These conditions control the image under C of the least contracting eigenvector of

$$\tilde{z}_L^{(-1+\rho/\mu)} \begin{bmatrix} \tilde{z}_L & 0 \\ 0 & \tilde{y}_L \end{bmatrix} A.$$

They ensure that this eigenvector is not mapped in the direction of Fix R, Fix $(-R)$ or parallel to the most contracting eigenvector. These conditions ensure that $c_2, c_4 \neq 0$ and $a_3c_2 + a_4c_4 \neq 0$.

A direct calculation shows that the eigenvalues of (4.32) are

$$\lambda_1 = ((a_3c_2 + a_4c_4)\tilde{y}_L)^{-1}(\det A)(\det C)\tilde{y}_L\tilde{z}_L^{\rho/\mu} + O(\tilde{z}_L^{1+\rho/\mu})$$

and

$$\lambda_2 = (a_3c_2 + a_4c_4)\tilde{y}_L\tilde{z}_L^{-1+\rho/\mu} + O(\tilde{z}_L),$$

with respective eigenvectors

$$\left(-\frac{a_4}{a_3} + O(\tilde{z}_L), 1\right) \quad \text{and} \quad \left(\frac{c_2}{c_4} + O(\tilde{z}_L), 1\right).$$

This is consistent with the fact that the tangent space to the stable manifold $W^s(p_2)$ in Σ_2 at the intersection of the heteroclinic orbit $q_2(t)$ with Σ_2 is given by $x = -(a_3/a_4)y$. Also by our generic assumptions λ_2 is nonzero ($\tilde{y}_L \approx y^*$ as $i \to \infty$), and the eigenvectors are distinct. It is important to note that by the transversality hypothesis [H3], both $a_4, a_3 \neq 0$.

We deduce that for $(y, z) \in H_i$ in Σ_2 with i sufficiently large, the derivative map $D(\psi_2 \circ \phi \circ \psi_1)$ to Σ_1 is hyperbolic, with eigenvalues close to 0 and $\tilde{z}_L^{(-1+\rho/\mu)}(a_3c_2 + a_4c_4)\tilde{y}_L$, and distinct eigenvectors, which are both bounded away (in the C^1 sense) from the y-axis and the z-axis. In the case $\rho/\mu < 1$ the second eigenvalue grows without bound as $\tilde{z}_L \to 0$. In the case $\rho/\mu \geq 1$ the second eigenvalue is also small and the map $D(\psi_2 \circ \phi \circ \psi_1)$ is a stable node.

By the reversibility, it is clear that the linear map $R \circ D(\psi_2 \circ \phi \circ \psi_1)^{-1} \circ R$ is also hyperbolic, with eigenvalues $1/\lambda_1$, $1/\lambda_2$, whose eigenvectors are the R-images of those for λ_1, λ_2 respectively. It can be verified that the map $DF_2 = R \circ D(\psi_2 \circ \phi \circ \psi_1)^{-1} \circ R \circ D(\psi_2 \circ \phi \circ \psi_1)$ is given by

$$DF_2 = \frac{1}{\text{Det } A \text{ Det } C \ \tilde{y}_L \tilde{z}_L} \begin{bmatrix} 2a_3a_4c_2c_4\tilde{y}_L^2 + O(\tilde{z}_L) & 2a_4^2c_2c_4\tilde{y}_L + O(\tilde{z}_L) \\ 2a_3^2c_2c_4\tilde{y}_L + O(\tilde{z}_L) & 2a_3a_4c_2c_4\tilde{y}_L^2 + O(\tilde{z}_L) \end{bmatrix},$$

and that when $a_3, a_4, c_2, c_4 \neq 0$, the eigenvalues are $\lambda_1' = O(\tilde{z}_L)$, $\lambda_2' = O(1/\tilde{z}_L)$, with corresponding eigenvectors $(-a_4/a_3 + O(\tilde{z}_L), 1)$ and $(a_4/a_3 + O(\tilde{z}_L), 1)$. Thus the map DF_2 is hyperbolic for i sufficiently large, with eigenvalues tending to zero and infinity respectively as $i \to \infty$. Now it is clear that we may construct sector bundles S^s and S^u that satisfy the properties in Proposition 4.5.1. $\square$

We have shown the existence of countable many horseshoes at the critical parameter value $\lambda = 0$. This implies the existence of a uniformly hyperbolic invariant set which is topologically conjugate to a full shift on n symbols for any $n \in \mathbb{N}$, the symbols are represented by i. It is important to note that the closure of all these sets is not hyperbolic, since the heteroclinic cycle itself is necessarily not hyperbolic. This does not contradict the strong uniform hyperbolicity of any finite number of horseshoes since our return map is not C^1 at the singularity.

Note that this result also gives an explanation for the phenomenon observed in the Michelson system in [57]; that periodic orbits that appear to oscillate with period tending to infinity have regions of hyperbolicity where the Floquet multipliers are of the form M, $1/M$, where M is extremely large. The result in this chapter would suggest that this is due to a symmetric horseshoe that exists at $c \approx 0.8495$, and so the hyperbolic regions of these periodic orbits would in fact have eigenvalues tending to zero and to infinity as the period tends to infinity.

4.5.1 Summary

Many of the results here are characteristic of the possible chaotic behaviour in the neighbourhood of a single homoclinic orbit to a hyperbolic equilibrium, although the dynamics in our case is much more complicated, and there are interesting differences. Firstly, the presence of complicated dynamics does not depend on the ratio of eigenvalues of the fixed points. This is an important difference and is due to the fixed points having different index. Even without the generic hypotheses we have made here to ensure hyperbolicity of the symmetric horseshoe, complicated dynamics would still be present.

We note that this complicated dynamical phenomena is not dependent on the reversing symmetry—Bykov [16, 17] has studied the codimension two case of the same heteroclinic cycle in general (non-symmetric) systems. The heteroclinic cycle bifurcation has also been studied in the context of a model of the long Josephson junction by van den Berg *et. al.* [108]. These studies have obtained some of the results presented here for the non-symmetric case, including the existence of countably many periodic orbits at the critical parameter value, and bifurcation of heteroclinic and homoclinic orbits. From the analysis presented here, we may expect that there also exists countable sets of horseshoes in the non-symmetric case, which act as organising centres for the complicated dynamics.

It is interesting also to compare results obtained here with previous results for reversible systems. If we extend the phase space by the inclusion of the parameter λ, then the system becomes 4-dimensional with a 2-dimensional fixed point subspace for the reversing symmetry. This is clearly a degenerate example of such a system, but it is interesting to note that results on blue sky catastrophe [32] still hold in this situation, where the one parameter family of periodic orbits found in section 4.4.2 become the periodic orbit family with 'period blow-up' as they approach the heteroclinic cycle.

Chapter 5

Heteroclinic Cycle Bifurcation: Lin's Method

5.1 Introduction

In the previous chapter we analyzed the dynamics close to a heteroclinic cycle using geometrical methods, and have found the dynamics to be very rich. This chapter contains an alternative treatment for the same heteroclinic cycle bifurcation, using Lin's method. The advantages of such an alternative analysis are that the approach is more direct, and we avoid many of the technical difficulties involved in the geometrical analysis. The technical proofs that are present in the implementation of Lin's method are very much true in every application; once these have been established, new heteroclinic/homoclinic bifurcation problems may be approached more directly.

In this thesis we include the steps and proofs that are required to implement Lin's method in the general case, in order to be self-contained. The material up to the derivation of the bifurcation equations, and also in chapter 6 is contained in [94], and in [65] for discrete systems, except for the amendments required to take into consideration the effect of the reversing symmetry. However, the bifurcation analysis contained in section 5.6 is particular to this problem, and is original [66]. Here we combine the application of Lin's method with the reversing symmetry to analyse our problem. The main results are contained in Theorem 5.6.2. As we shall see, the geometric information that is given by the study of the return maps is also present in the bifurcation equations resulting from the current method. Also the results of this analysis are more easily generalised to higher dimensions.

Lin's method is an approach (similar in spirit to Liapunov Schmidt Reduction and Melnikov's method) to analysing the dynamics close to a heteroclinic or homoclinic cycle in the system

$$\dot{x} = F(x, \mu), \qquad F : \mathbb{R}^n \times \mathbb{R}^k \to \mathbb{R}^n. \tag{5.1}$$

In Lin's original paper [74], the method was developed for a *heteroclinic chain*: let p_i ($i \in \mathbb{Z}$) be a set of hyperbolic (saddle) fixed points, and for each i, suppose that at $\mu = \mu_0$ there is a heteroclinic connection $q_i(t)$ connecting p_{i-1} to p_i. This configuration allows any p_i to be not necessarily different from each other. The outline of the method now is to construct section planes Σ_i, which are transverse to $q_i(t)$ at some point, say (without loss of generality) at $q_i(0)$. We study the tangent spaces $T_{q_i(0)}W^u(p_{i-1})$ and $T_{q_i(0)}W^s(p_i)$ at the point $q_i(0)$ in Σ_i, and introduce subspaces Z_i such that

$$\mathbb{R}^n = Z_i \oplus (T_{q_i(0)}W^u(p_{i-1}) + T_{q_i(0)}W^s(p_i)).$$

These spaces Z_i are central to the principles of Lin's method. We now search (in a neighbourhood of the solutions $q_i(t)$) for piecewise continuous orbits $x_i^{\pm}(t)$; these are orbits that are solutions to the differential equation (5.1) (with $x_i^{\pm}(0) \in \Sigma_i$), except in the sections Σ_i where these orbits are allowed a discontinuity—a 'jump' in the direction of Z_i. Suppose that for each $i \in \mathbb{Z}$ we prescribe a sufficiently large time $2\omega_{i+1}$ for a piecewise continuous orbit $\{x_i^{\pm}(t)\}_{i\in\mathbb{Z}}$ to take to travel from the section Σ_i to the section Σ_{i+1} (passing close to p_i), with possible jumps in each Σ_i in the direction of Z_i, see Figure

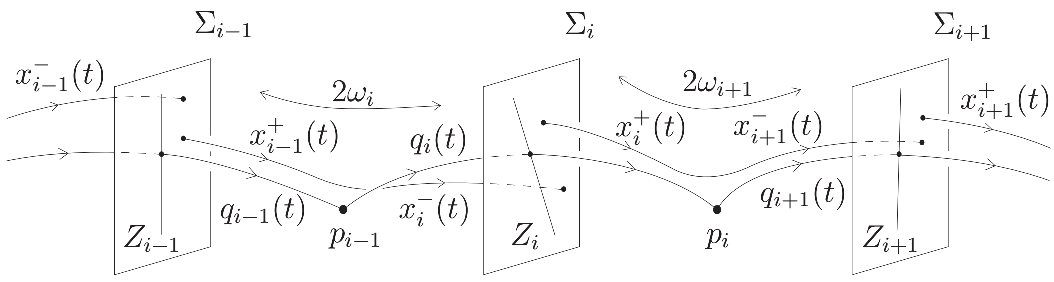

Figure 5.1: A heteroclinic chain between hyperbolic fixed points p_i for $\mu = \mu_0$, with sections Σ_i and subspaces Z_i indicated.

5.1. We find that such piecewise continuous orbits exist and are unique. We may then derive explicit expressions for the jumps Ξ_i^ω (where $\omega = \{\omega_i\}_{i\in\mathbb{Z}}$) depending on the times ω_i, whose zero set will give the set of real (continuous) orbits that exist close to the heteroclinic chain. As the time ω_{j+1} increases, $x_j^+(t)$, $x_{j+1}^-(t)$ become closer to solutions in the stable/unstable manifolds near p_j. In fact, we may set any of the times ω_{j+1} equal to infinity in the equations Ξ_i^ω, in which case we will obtain precisely pieces of solutions in $W^s(p_j)$, $W^u(p_j)$.

It is important to note that a heteroclinic chain as described above is not structurally stable, and will generically occur only in k-parameter families, for some k. (In fact, in Lin's paper [74], the method was applied in the case where each heteroclinic connection was structurally unstable, and the subspace Z_i was one-dimensional for each i. In this case, each equation Ξ_i^ω would be one-dimensional. However, the method may easily be applied to the more general case, as it is in this chapter.) We suppose then that the original heteroclinic chain exists at $\mu = \mu_0$, ($\mu \in \mathbb{R}^k$). For each $||\mu - \mu_0||$ sufficiently small we still find existence and uniqueness of piecewise continuous solutions $x_i^\pm(t)$, depending on the times ω_i. Now the jump equations also depend on the parameter μ, $\Xi_i^\omega = \Xi_i^\omega(\mu)$. In his PhD thesis [94], Sandstede divided the process of Lin's method into two main steps, separating the dependence of the jump on ω and μ. By doing this it is possible to derive the leading order terms of the equation $\Xi_i^\omega(\mu)$.

The first step of Lin's method is to study the splitting of the manifolds $W^u(p_i)$, $W^s(p_i)$ with respect to μ. This step is the content of the paper by Vanderbauwhede [111] and the paper by Knobloch [63], where the bifurcation set of a degenerate homoclinic orbit is studied. This is where there exists a homoclinic orbit to a hyperbolic fixed point, and the tangent spaces of the stable and unstable manifolds of the fixed point intersect in a two dimensional subspace along the homoclinic orbit. Vanderbauwhede shows that this is a codimension three bifurcation, and derives the bifurcation equation $\xi^\infty(\mu)$ whose zero set is the set of bifurcating homoclinic orbits. (Here there is no subscript i since there is only one hyperbolic fixed point.) In general, we search for solutions in the stable/unstable manifolds of each fixed point p_i with a possible jump in each section Σ_i in the direction Z_i—this is the case where above, each $\omega_i = \infty$. This produces the orbits $q_i^\pm(\mu)(t)$ in the stable and unstable manifolds (the superscript $\pm$ indicates that the orbit has a possible discontinuity at $t = 0$ in the section Σ_i), and the bifurcation equation

$$\xi^\infty(\mu) := q_i^+(\mu)(0) - q_i^-(\mu)(0),$$

whose zero set is the bifurcating set of real homoclinic/heteroclinic orbits.

The second step of Lin's method is to search for piecewise continuous orbits $x_i^\pm(\mu, \omega)(t)$ that are perturbations of the orbits $q_i^\pm(\mu)(t)$. These orbits have the prescribed times $2\omega_i$ from Σ_i to Σ_{i+1}. This step is separated into two stages: the first is to find 'uncoupled' solutions $\tilde{x}_i^\pm(\mu, -\omega_i, \omega_{i+1})(t)$ that lie close to $q_i^\pm(\mu)(t)$. These solutions do not travel from Σ_i to Σ_{i+1}, but from close to the fixed point p_{i-1}, through Σ_i, to close to the fixed point p_i. We assume that $\tilde{x}_i^\pm(\mu, -\omega_i, \omega_{i+1})(0) \in \Sigma_i$, $\tilde{x}_i^+(\mu, -\omega_i, \omega_{i+1})(0) - \tilde{x}_i^-(\mu, -\omega_i, \omega_{i+1})(0) \in Z_i$, and given times $-\omega_i$, ω_{i+1}, assume that projections of $\tilde{x}_i^+(\mu, -\omega_i, \omega_{i+1})(\omega_{i+1})$, $\tilde{x}_i^-(\mu, -\omega_i, \omega_{i+1})(-\omega_i)$ onto unstable, respectively stable subspaces are given. This condition is made clearer in section 5.4. We prove the existence and uniqueness of the orbits $\tilde{x}_i^\pm(\mu, -\omega_i, \omega_{i+1})(t)$ under these hypotheses. The second stage is then to show that we can couple these solutions, to find the piecewise continuous orbits $x_i^{\pm}(\mu, \omega)(t)$ that depend only on μ and the ω_i. We can then derive an expression for the jump $\xi_i^{\omega}(\mu)$, which is given by

$$\xi_i^{\omega}(\mu) := x_i^+(\mu, \omega)(0) - x_i^-(\mu, \omega)(0) - q_i^+(\mu)(0) + q_i^-(\mu)(0)).$$

Therefore we have decomposed the jump $\Xi_i^{\omega}(\mu)$ into the form

$$\Xi_i^{\omega}(\mu) = \xi_i^{\infty}(\mu) + \xi_i^{\omega}(\mu),$$

which illustrates the separation of the procedure into two steps.

Further results have been obtained using Lin's method. Vanderbauwhede and Fiedler [112] proved the existence of a blue sky catastrophe phenomenon in reversible and conservative systems using Lin's method. In this paper the authors did not derive an explicit expression for $\Xi_i^{\omega}(\mu)$ but instead exploited the structure of the system to find the required periodic solutions. Lin's method has been implemented in a numerical algorithm by Oldeman *et. al.* [86] to study bifurcation of homoclinic orbits. The principles have also been applied to the case of homoclinic orbits to non-hyperbolic fixed points [62, 114]. Finally, Knobloch [64] has generalised Lin's method to the study of discrete systems, where the connecting orbit was also assumed to be degenerate.

5.2 Setting of the Problem

We consider a k-parameter family of vector fields $f : \mathbb{R}^3 \times \mathbb{R}^k \to \mathbb{R}^3$:

$$\dot{x} = f(x, \mu), \tag{5.2}$$

where $x \in \mathbb{R}^3$, $\mu \in \mathbb{R}^k$. We suppose that the family is reversible with respect to a linear involution R, thus $R \circ f = -f \circ R$, and we assume that dim Fix $R = 1$. Also at $\mu = \mu_0$ there are two asymmetric fixed points p_1 and p_2, which lie in the same group orbit, that is $R(p_1) = p_2$. Both fixed points are hyperbolic and are of saddle-focus type. p_1 has a 1-dimensional stable manifold, and a

2-dimensional unstable (focus) manifold, and *vice versa* for p_2. Finally, at $\mu = 0$ there exists a heteroclinic cycle consisting of a symmetric heteroclinic orbit $q_1(t)$ lying in the coincidence of the 1-dimensional manifolds, and another symmetric heteroclinic orbit $q_2(t)$ lying in the transversal intersection of the 2-dimensional manifolds, see Figure 5.2. In chapter 3 we saw that such a heteroclinic cycle appears generically for an open set of unfoldings of the 'Hopf-zero' bifurcation in vector fields with involutory reversing symmetry.

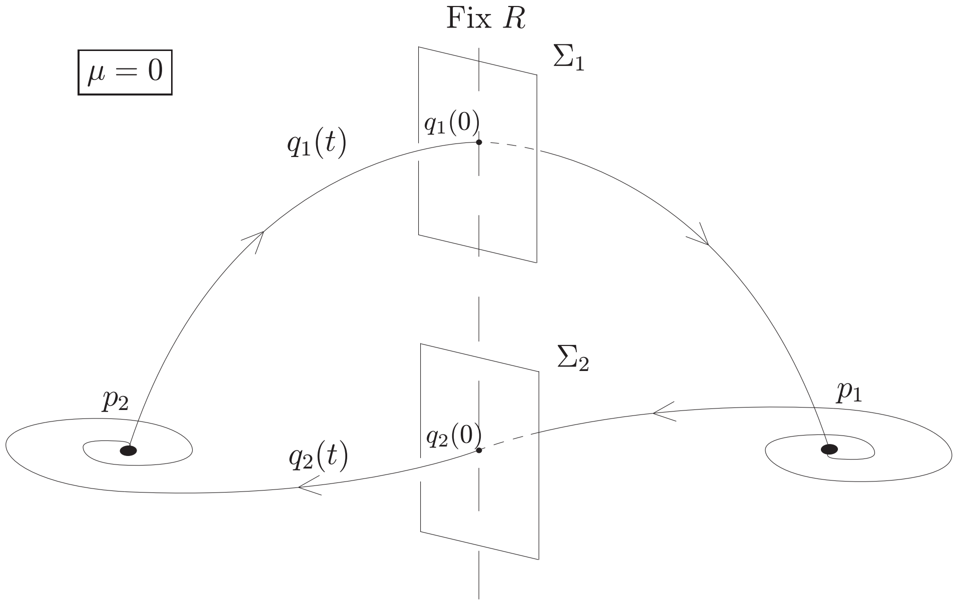

Figure 5.2: The heteroclinic cycle at $\mu = 0$.

To begin, fix the heteroclinic solutions so that $q_1(0), q_2(0) \in \text{Fix } R$. Construct a plane section Σ_1 transverse to the flow at $q_1(0)$ that is R-invariant. Similarly construct a plane section Σ_2 transverse to the flow at $q_2(0)$ that is R-invariant. Define subspaces Y_1, Y_2 by

$$\Sigma_1 = \{q_1(0) + y : y \in Y_1\}, \tag{5.3}$$

$$\Sigma_2 = \{q_2(0) + y : y \in Y_2\}. \tag{5.4}$$

Then

$$\mathbb{R}^3 = Y_1 \oplus (T_{q_1(0)}W^s(p_1) \cap T_{q_1(0)}W^u(p_2)), \tag{5.5}$$

$$\mathbb{R}^3 = Y_2 \oplus (T_{q_2(0)}W^u(p_1) \cap T_{q_2(0)}W^s(p_2)), \tag{5.6}$$

Also, consistent with the standard theory, we define subspaces $Z_1 \subset Y_1$, $Z_2 \subset Y_2$ such that

$$\begin{aligned}
\mathbb{R}^3 &= Z_1 \oplus (T_{q_1(0)}W^s(p_1) + T_{q_1(0)}W^u(p_2)), \qquad (5.7)\\
\mathbb{R}^3 &= Z_2 \oplus (T_{q_2(0)}W^u(p_1) + T_{q_2(0)}W^s(p_2)). \qquad (5.8)
\end{aligned}$$

However, note that in our case $Z_2 = \{0\}$, and $Z_1 = Y_1$. Hence we shall write $Z = Z_1$. Then $\dim Z = 2$.

In the k-parameter family (5.2) the fixed points p_1, p_2 will persist and will remain hyperbolic for all $|\mu - \mu_0|$ sufficiently small. Using C^∞ bump function transformations we can make $p_1(\mu), p_2(\mu)$ constant. Hence we shall assume this (R-invariant) transformation has been carried out and write $(p_1(\mu), p_2(\mu)) = (p_1, p_2)$ for all $|\mu - \mu_0|$ sufficiently small.

A further change of coordinates that we will make to simplify the analysis, is to flatten the local stable/unstable manifolds of the fixed points p_1, p_2; that is:

$$W^s_{loc}(p_i, \mu) \subset T_{p_i}W^s(p_i, \mu_0), \quad W^u_{loc}(p_i, \mu) \subset T_{p_i}W^u(p_i, \mu_0). \qquad (5.9)$$

We can bring the local stable/unstable manifolds into this form by means of a R-reversible, C^∞ bump function transformation, with disjoint supports, based around each of the fixed points p_i.

To begin our analysis, we make the change of variables

$$x(t) = q_i(t) + z_i(t), \qquad i = 1, 2.$$

under which (5.2) is transformed to

$$\dot{z}_i = A_i(t)z_i + g_i(t, z_i, \mu), \qquad (5.10)$$

where $A_i(t) = D_x f(q_i(t), \mu_0)$, and

$$g_i(t, z_i, \mu) = f(q_i(t) + z_i, \mu) - f(q_i(t), \mu_0) - A_i(t)z_i. \qquad (5.11)$$

Notation. It will be convenient later on to lift our heteroclinic cycle to a 'heteroclinic chain' as in [74], such that $p_{2i} = p_2$, $p_{2i+1} = p_1$, $A_{2i}(t) = A_2(t)$,

$A_{2i+1}(t) = A_1(t)$ etc., where $i \in \mathbb{Z}$. We shall exploit such notation throughout without specific reference.

5.3 Step 1 - Splitting of the Manifolds

The first step of Lin's method is to study the splitting of the manifolds with respect to the parameter μ. To be precise, for each μ we look for solutions $q_i^+(t)$ and $q_i^-(t)$ defined on $\mathbb{R}^+$ and $\mathbb{R}^-$ respectively, such that

1. $q_i^+(t)$ and $q_i^-(t)$ are close to $q_i(t)$,
2. $\lim_{t\to\infty} q_1^+(t) = p_1$, $\lim_{t\to-\infty} q_1^-(t) = p_2$, and *vice versa* for $q_2^{\pm}$.
3. $q_i^{\pm}(0)$ are close to $q_i(0)$,
4. $q_i^+(0) - q_i^-(0) \in Z_i$.

Note that for $q_2^{\pm}$, the last condition means $q_2^+(0) = q_2^-(0)$. With the above setting, we are looking for bounded solutions $z_i^+(t)$, $z_i^-(t)$ (defined on $\mathbb{R}^+$, $\mathbb{R}^-$ respectively) satisfying $z_i^+(0) - z_i^-(0) \in Z_i$, with $||z_i||_\infty := \max\left\{\sup_{t\in\mathbb{R}^+} ||z_i^+(t)||, \sup_{t\in\mathbb{R}^-} ||z_i^-(t)||\right\}$ finite and close to zero. By the theory of stable and unstable manifolds, $x_i^{\pm}(t) := q_i^{\pm}(t) + z_i^{\pm}(t)$ is in the desired stable/unstable manifold.

5.3.1 Solutions in the Stable/Unstable Manifolds

An important role is played by the properties of the linear nonautonomous equations

$$\dot{z}_i = A_i(t) z_i. \tag{5.12}$$

Denote by $\Phi_i(t,s)$ the transition matrix for (5.12). We have that $\lim_{t\to\infty} q_1(t) = \lim_{t\to-\infty} q_2(t) = p_1$, so then $\lim_{t\to\infty} A_1(t) = \lim_{t\to-\infty} A_2(t) = D_x f(p_1, \mu_0)$.

Similarly $\lim_{t\to-\infty} A_1(t) = \lim_{t\to\infty} A_2(t) = D_x f(p_2, \mu_0)$. Also $D_x f(p_1, \mu) = -R \circ D_x f(p_2, \mu)$.

By the theory of exponential dichotomies [23], due to the fact that p_1, p_2 are hyperbolic, the equations $\dot{z}_i = D_x f(p_1, \mu_0) z_i$ and $\dot{z}_i = D_x f(p_2, \mu_0) z_i$ have an exponential dichotomy on $\mathbb{R}$. Using the roughness theorem (see [23, Lecture 4, Proposition 1]), equations (5.12) have an exponential dichotomy on $\mathbb{R}_+$ and $\mathbb{R}_-$. That means there exist constants $K_i \geq 1$, $\alpha_i > 0$, and projections $P_{i,+} : \mathbb{R}_+ \to \mathcal{L}(\mathbb{R}^3)$, $Q_{i,-} : \mathbb{R}_- \to \mathcal{L}(\mathbb{R}^3)$ such that:

1. $P_{i,+}^2(t) = P_{i,+}(t)$ for $t \geq 0$ and $Q_{i,-}^2(t) = Q_{i,-}(t)$ for $t \leq 0$,
2. $P_{i,+}(t)\Phi_i(t,s) = \Phi_i(t,s)P_{i,+}(s) \quad \forall t, s \in \mathbb{R}_+$
   $Q_{i,-}(t)\Phi_i(t,s) = \Phi_i(t,s)Q_{i,-}(s) \quad \forall t, s \in \mathbb{R}_-$
3. $||\Phi_i(t,s)P_{i,+}(s)|| \leq K_i e^{-\alpha_i(t-s)} \quad 0 \leq s \leq t$
   $||\Phi_i(t,s)Q_{i,+}(s)|| \leq K_i e^{-\alpha_i(s-t)} \quad 0 \leq t \leq s$
   $||\Phi_i(t,s)Q_{i,-}(s)|| \leq K_i e^{-\alpha_i(s-t)} \quad t \leq s \leq 0$
   $||\Phi_i(t,s)P_{i,-}(s)|| \leq K_i e^{-\alpha_i(t-s)} \quad s \leq t \leq 0$
   where $Q_{i,+} = I - P_{i,+}$, $P_{i,-} = I - Q_{i,-}$.

In fact,

$$\text{Im } P_{1,+}(t) = T_{q_1(t)} W^s(p_1), \quad \text{Im } Q_{1,-}(t) = T_{q_1(t)} W^u(p_2)$$

and similarly for $P_{2,+}$, $Q_{2,-}$. See Figure 5.3 for a sketch of the images of these projections.

Where it is useful we can use the constant $\alpha := \min\{\alpha_1, \alpha_2\}$ in the estimates for the exponential dichotomies independent of i. There is some freedom in our choice of the projections $P_{i,+}$, $Q_{i,-}$ in that only the range is necessarily fixed. In order to simplify the analysis then, we choose $P_{i,+}$ and $Q_{i,-}$ such that $\text{Im } Q_{1,+}(0) = \text{Im } P_{1,-}(0) = Y_1$, and $\text{Im } Q_{2,+}(0), \text{Im } P_{2,-}(0) \subset Y_2$ with $\text{Im } Q_{2,+}(0) \subset \text{Im } Q_{2,-}(0)$ and $\text{Im } P_{2,-}(0) \subset \text{Im } P_{2,+}(0)$.

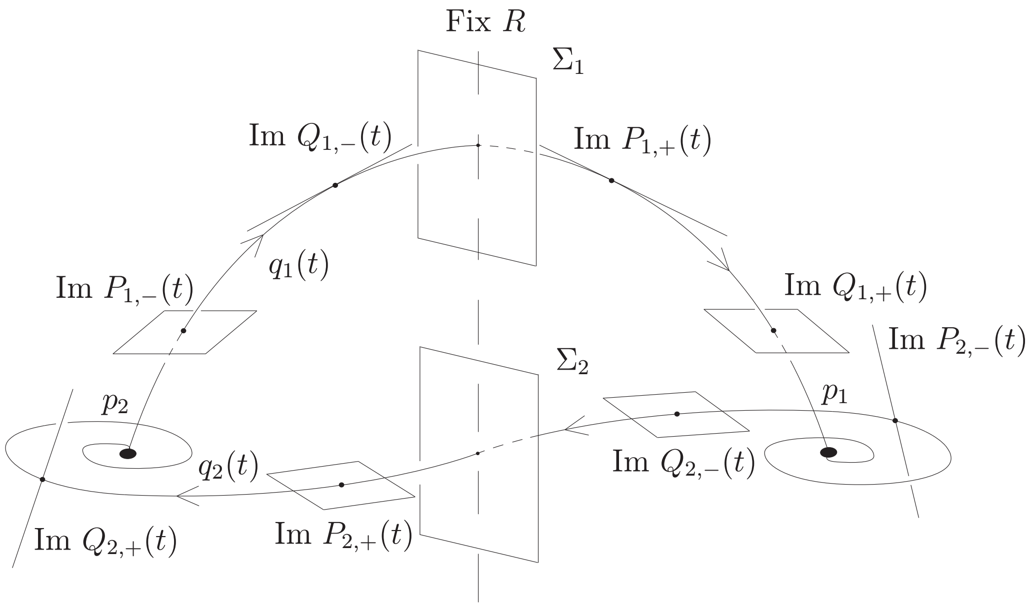

Figure 5.3: Schematic diagram of the images of the projections $P_{i,\pm}(t)$, $Q_{i,\pm}(t)$, here the value of t is different for each of the pairs of complementary images shown.

We also make a phase condition to fix the solutions $z_i^{\pm}$ by requiring that $z_i^{\pm}(0) \in Y_i$, and so $x_i(0) \in \Sigma_i$. Therefore we are looking for points $z_i^{+}(0)$ in the set $Y_i \cap W_0^{s,\varepsilon}(\mu)$, and $z_i^{-}(0)$ in the set $Y_i \cap W_0^{u,\varepsilon}(\mu)$, where

$$W_0^{s,\varepsilon}(\mu) := \{z_i^{+}(0) \in \mathbb{R}^3 : \sup_{t\geq 0}||z_i^{+}(t)|| < \varepsilon\},$$

for some ε sufficiently small, and similarly for $W_0^{u,\varepsilon}(\mu)$.

The variation of constants formula for (5.10) gives (see e.g. [52])

$$z_i^{+}(t) = \Phi_i(t,0)z_i^{+}(0) + \int_0^t \Phi_i(t,s)g_i(s, z_i^{+}(s), \mu)ds, \tag{5.13}$$

and we have that

$$\Phi_i(0,t)Q_{i,+}(t)z_i^{+}(t) = Q_{i,+}(0)z_i^{+}(0) + \int_0^t \Phi(0,s)Q_{i,+}(s)g_i(s, z_i^{+}(s), \mu)ds$$

then using the properties of the exponential dichotomy, and the fact that q_i, and hence $||g_i||$ is bounded (see (5.11)), we obtain

$$Q_{i,+}(0)z_i^{+}(0) = -\int_0^{\infty} \Phi_i(0,s)Q_{i,+}(s)g_i(s, z_i^{+}(s), \mu)ds$$

Therefore we see that $z_i^+(t)$ is a solution if and only if there is $\nu_i = P_{i,+}(0)z_i^+(0)$ such that

$$\begin{aligned} z_i^+(t) &= \Phi(t,0)\nu_i + \int_0^t \Phi_i(t,s)P_{i,+}(s)g_i(s,z_i^+(s),\mu)ds \\ &\quad - \int_t^\infty \Phi_i(t,s)Q_{i,+}(s)g_i(s,z_i^+(s),\mu)ds \qquad (5.14) \end{aligned}$$

It can be shown in a similar way that $z_i^-(t)$ is a solution if and only if there is $\eta_i = Q_{i,-}(0)z_i^-(0)$ such that

$$\begin{aligned} z_i^-(t) &= \Phi_i(t,0)\eta_i + \int_{-\infty}^t \Phi_i(t,s)P_{i,-}(s)g_i(s,z_i^-(s),\mu)ds \\ &\quad - \int_t^0 \Phi_i(t,s)Q_{i,-}(s)g_i(s,z_i^-(s),\mu)ds \qquad (5.15) \end{aligned}$$

Note that in case $i = 1$, we have that $\nu_1 = P_{1,+}(0)z_1^+(0) = \eta_1 = Q_{1,-}(0)z_1^-(0) = \{0\}$. However, in both cases the right hand side of (5.14) defines a mapping from

$$C_b^0(\mathbb{R}^+,\mathbb{R}^3) := \{z \in C^0(\mathbb{R}^+,\mathbb{R}^3) \mid \sup_{t\geq 0}||z(t)|| < \infty\}$$

into itself. Let us consider then $i = 2$; this equation has the solution $z_2^+(t) \equiv 0$ for $\nu_2 = 0$, $\mu = \mu_0$. By (5.11), the derivative of the right hand side with respect to z is zero at $(\nu_2,\mu) = (0,\mu_0)$. By the Implicit Function Theorem, we can solve the equation for $z_2^+(\nu_2,\mu)(t)$ for (ν_2,μ) close to $(0,\mu_0)$. Then

$$z_2^+(\nu_2,\mu)(0) = \nu_2 - Q_{2,+}(0)\int_0^\infty \Phi_2(0,s)g_2(s,z_2^+(\nu_2,\mu)(s),\mu)ds \qquad (5.16)$$

Similarly, we can solve (5.15) to find $z_2^-(\eta_2,\mu)(t)$ for (η_2,μ) close to $(0,\mu_0)$. In the case $i = 1$, we can solve (5.14) and (5.15) for μ close to μ_0. We find

$$\begin{aligned} z_2^-(\eta_2,\mu)(0) &= \eta_2 + P_{2,-}(0)\int_{-\infty}^0 \Phi_2(0,s)g_2(s,z_2^-(\eta_2,\mu)(s),\mu)ds \qquad (5.17) \\ z_1^+(\mu)(0) &= -Q_{1,+}(0)\int_0^\infty \Phi_1(0,s)g_1(s,z_1^+(\mu)(s),\mu)ds \qquad (5.18) \\ z_1^-(\mu)(0) &= P_{1,-}(0)\int_{-\infty}^0 \Phi_1(0,s)g_1(s,z_1^-(\mu)(s),\mu)ds \qquad (5.19) \end{aligned}$$

As before, for the remainder of the chapter we will describe heteroclinic connections that lie in the intersection of the two 2-dimensional manifolds of p_1, p_2

as 2D heteroclinic connections. Similarly, heteroclinic connections lying in the coincidence of the 1-dimensional manifolds are 1D heteroclinic connections. See also Definition 5.6.1.

5.3.2 Persistent 2D Symmetric Heteroclinic Connections

We will write $z_2^+(\nu_2,\mu)(0) = \nu_2 - h_2^+(\nu_2,\mu)$ and $z_2^-(\eta_2,\mu)(0) = \eta_2 + h_2^-(\eta_2,\mu)$, where $h_2^+(\nu_2,\mu)$, $h_2^-(\eta_2,\mu)$ are given by (5.16), (5.17). It is easily checked that

$$D_{\nu_2} h_2^+(0,\mu_0) = 0, \qquad D_{\eta_2} h_2^-(0,\mu_0) = 0. \tag{5.20}$$

Now

$$z_2^+(\nu_2,\mu)(0) - z_2^-(\eta_2,\mu)(0) = \nu_2 - \eta_2 - h_2^+(\nu_2,\mu) - h_2^-(\eta_2,\mu). \tag{5.21}$$

The above equation is zero at $(\nu_2,\eta_2,\mu) = (0,0,\mu_0)$. If we look for solutions such that $z_2^+(\nu_2,\mu)(0) - z_2^-(\eta_2,\mu)(0) = 0$, then from the above equation, and using the projections $Q_{2,+}(0)$, $P_{2,-}(0)$, we obtain

$$\begin{aligned} \nu_2 &= h_2^-(\eta_2,\mu) \\ \eta_2 &= -h_2^+(\nu_2,\mu) \end{aligned}$$

By the hypothesis that $W^u(p_1)$ and $W^s(p_2)$ are transversal along $q_2(t)$, ν_2 and η_2 are linearly independent in Y_2. Then by (5.20) and the Implicit Function Theorem the above equations can be solved to find $(\nu_2(\mu),\eta_2(\mu))$ for μ close to μ_0.

Now from (5.14), and using the fact that $R\Phi_2(t,s) = \Phi_2(-t,-s)R$, $RP_{2,+}(t) =$

$Q_{2,-}(-t)R$ and $RQ_{2,+}(t) = P_{2,-}(-t)R$, we have

$$\begin{aligned}
Rz_2^+(\nu_2(\mu),\mu)(t) &= \Phi_2(-t,0)R\nu_2(\mu) \\
&\quad + \int_0^t \Phi_2(-t,-s)Q_{2,-}(-s)Rg_2(s, z_2^+(\nu_2(\mu),\mu)(s),\mu)ds \\
&\quad - \int_t^\infty \Phi_2(-t,-s)P_{2,-}(-s)Rg_2(s, z_2^+(\nu_2(\mu),\mu)(s),\mu)ds \\
&= \Phi_2(-t,0)R\nu_2(\mu) \\
&\quad - \int_0^t \Phi_2(-t,-s)Q_{2,-}(-s)g_2(-s, Rz_2^+(\nu_2(\mu),\mu)(s),\mu)ds \\
&\quad + \int_t^\infty \Phi_2(-t,-s)P_{2,-}(-s)g_2(-s, Rz_2^+(\nu_2(\mu),\mu)(s),\mu)ds
\end{aligned}$$

The last equality follows from (5.11). Notice that $R\nu_2(\mu) \in \mathrm{Im}\ Q_{2,-}(0)$. Now substituting $\tau = -s$,

$$\begin{aligned}
Rz_2^+(\nu_2(\mu),\mu)(t) &= \Phi_2(-t,0)R\nu_2(\mu) \\
&\quad - \int_{-t}^0 \Phi_2(-t,\tau)Q_{2,-}(\tau)g_2(\tau, Rz_2^+(\nu_2(\mu),\mu)(-\tau),\mu)d\tau \\
&\quad - \int_{-\infty}^{-t} \Phi_2(-t,\tau)P_{2,-}(\tau)g_2(\tau, Rz_2^+(\nu_2(\mu),\mu)(-\tau),\mu)d\tau,
\end{aligned}$$

and so

$$Rz_2^+(\nu_2(\mu),\mu)(t) = z_2^-(R\nu_2(\mu),\mu)(-t). \tag{5.22}$$

It follows then that $\nu_2(\mu) = R\eta_2(\mu)$. So if we set

$$z_2(\mu)(t) := \begin{cases} z_2^-(\eta_2(\mu),\mu)(t), & t \le 0, \\ z_2^+(\nu_2(\mu),\mu)(t), & t \ge 0, \end{cases}$$

then $q_2(\mu)(t) := q_2(t) + z_2(\mu)(t)$ is the unique heteroclinic connection close to $q_2(t)$ for $|\mu - \mu_0|$ sufficiently small, and it is symmetric. Also $q_2(\mu_0)(t) = q_2(t)$.

5.3.3 Splitting of the 1D Heteroclinic Orbit

We will now correspondingly consider the case $i = 1$. Similar to the previous section, from (5.18), (5.19) we see that

$$\begin{aligned}
R(z_1^+(\mu)(0)) &= -RQ_{1,+}(0)\int_0^\infty \Phi_1(0,s)g_1(s, z_1^+(\mu)(s),\mu)ds \\
&= P_{1,-}(0)\int_{-\infty}^0 \Phi_1(0,s)g_1(s, Rz_1^+(-s),\mu)ds
\end{aligned}$$

and so

$$R(z_1^+(\mu)(0)) = z_1^-(\mu)(0) \tag{5.23}$$

Then we have

$$R(z_1^+(\mu)(0) - z_1^-(\mu)(0)) = -(z_1^+(\mu)(0) - z_1^-(\mu)(0))$$

Therefore the jump $\xi_1^\infty(\mu) := z_1^+(\mu)(0) - z_1^-(\mu)(0)$ is in Fix $(-R)$. Now let ψ_1, ψ_2 be an orthonormal basis for Z, such that Fix $R = \text{span}\{\psi_1\}$ and Fix $(-R) = \text{span}\{\psi_2\}$. Set

$$\psi_j(t) := \Phi_1^*(t,0)\psi_j \qquad \forall t \in \mathbb{R}, j = 1,2 \tag{5.24}$$

where $\Phi_i^*(s,t)$ is the adjoint operator of $\Phi_i(t,s)$, whose definition is given by

$$< \psi, \Phi_i(t,s)z > = < \Phi_i^*(s,t)\psi, z >, \quad z \in \mathbb{R}^3, \psi \in \mathbb{R}^{3*}, \quad i = 1,2.$$

Here and throughout the inner product $< \cdot, \cdot >$ is chosen to be R-invariant, and such that $(\text{Im } Q_{i,\pm}(0))^\perp = \text{Im } P_{i,\pm}(0)$. Note that this is consistent with the definitions of Section 5.3.1. The operator $\Phi_i^*(s,t)$ has an exponential dichotomy on $\mathbb{R}^+$, $\mathbb{R}^-$ (see also section 6.4.1), with the the projections $P_{i,+}^*(t)$, $Q_{i,+}^*(t)$, $Q_{i,-}^*(t)$, $P_{i,+}^*(t)$ being the adjoint operators of the projections for $\Phi_i(t,s)$:

1. ${P_{i,+}^*}^2(t) = P_{i,+}^*(t)$ for $t \geq 0$ and ${Q_{i,-}^*}^2(t) = Q_{i,-}^*(t)$ for $t \leq 0$,

2. $P_{i,+}^*(t)\Phi_i^*(t,s) = \Phi_i^*(t,s)P_{i,+}^*(s) \quad \forall t,s \in \mathbb{R}_+$
   $Q_{i,-}^*(t)\Phi_i^*(t,s) = \Phi_i^*(t,s)Q_{i,-}^*(s) \quad \forall t,s \in \mathbb{R}_-$

3. $||\Phi_i^*(t,s)P_{i,+}^*(s)|| \leq K_i e^{-\alpha_i(t-s)} \quad 0 \leq s \leq t$
   $||\Phi_i^*(t,s)Q_{i,+}^*(s)|| \leq K_i e^{-\alpha_i(s-t)} \quad 0 \leq t \leq s$
   $||\Phi_i^*(t,s)Q_{i,-}^*(s)|| \leq K_i e^{-\alpha_i(s-t)} \quad t \leq s \leq 0$
   $||\Phi_i^*(t,s)P_{i,-}^*(s)|| \leq K_i e^{-\alpha_i(t-s)} \quad s \leq t \leq 0$
   again $Q_{i,+}^* = I - P_{i,+}^*$, $P_{i,-}^* = I - Q_{i,-}^*$.

It follows then that $\psi_j(t)$ are exponentially bounded according to the above exponential dichotomy.

$$\begin{aligned}
\xi_1^{\infty}(\mu) &= \Sigma_{j=1}^{2}\psi_j\left[< \psi_j, -Q_{1,+}(0)\int_{-\infty}^{\infty}\Phi_1(0,s)g_1(s,z_1(\mu)(s)\mu)ds >\right] \\
&= \psi_2\int_{-\infty}^{\infty} < \psi_2(s), g_1(s,z_1(\mu)(s),\mu) > ds
\end{aligned}$$

where

$$z_1(\mu)(t) := \begin{cases} z_1^-(\mu)(t), & t \le 0, \\ z_1^+(\mu)(t), & t > 0. \end{cases}$$

Note that the possible discontinuity of $z_1(\mu)(t)$ at $t = 0$ is unimportant as the function is under an integral sign. Thus the choice of definition of $z_1(\mu)(t)$ at $t = 0$ is arbitrary. Then

$$\begin{aligned}
D_\mu\xi_1^{\infty}(\mu_0) &= \psi_2\int_{-\infty}^{\infty} < \psi_2(s), D_\mu g_1(s,0,\mu_0) > ds \\
&= \psi_2\int_{-\infty}^{\infty} < \psi_2(s), D_\mu f(q_1(s),\mu_0) > ds.
\end{aligned}$$

This follows from (5.11). Then we make the hypothesis

(H1) $$\int_{-\infty}^{\infty} < \psi_2(s), D_\mu f(q_1(s),\mu_0) > ds \neq 0$$

This is precisely the condition that says that the manifolds $(q_1^-(t), q_1^+(t))$ which, at $\mu = \mu_0$ form the 1D heteroclinic connection, split with positive speed with respect to the parameter μ. We see now from $\xi_1^{\infty}(\mu)$ that under the generic hypothesis **(H1)** our reversible heteroclinic cycle bifurcation is a 1-parameter problem. Then we may assume $\mu \in \mathbb{R}$, and by applying the implicit function theorem, we write

$$\xi_1^{\infty}(\mu) = \psi_2(\mu - \mu_0). \tag{5.25}$$

As before, we will write $q_1^-(\mu)(t) := q_1(t) + z_1^-(\mu)(t)$, $q_1^+(\mu)(t) := q_1(t) + z_1^+(\mu)(t)$ as the unique orbits comprising the unstable (resp. stable) manifolds of p_2 (resp. p_1) close to $q_1(t)$, and they are symmetric images of each other. Also $q_1(t)$ is the concatenation of $q_1^-(\mu_0)(t)$ with $q_1^+(\mu_0)(t)$.

5.4 Step 2 - Finite Time Solutions

The second step in the method is to search for orbits $x_i^{\pm}(t)$ which are perturbations of the orbits $q_i^{\pm}(\mu)(t)$, and which are allowed to have a jump in the sections Σ_i. We will find that with well defined allowed jumps, there exist unique such solutions, depending only on μ and the time the orbit takes between sections. To begin, we look for solutions of the form

$$x_i^{\pm}(t) = q_i^{\pm}(\mu)(t) + z_i^{\pm}(t) \tag{5.26}$$

Then

$$\dot{z_i}^{\pm} = A_i^{\pm}(t,\mu)z_i^{\pm} + g_i^{\pm}(t, z_i^{\pm}, \mu) \tag{5.27}$$

where $A_i^{\pm}(t,\mu) = D_x f(q_i^{\pm}(\mu)(t),\mu)$, and

$$g_i^{\pm}(t, z_i^{\pm}, \mu) = f(q_i^{\pm}(\mu)(t) + z_i^{\pm}, \mu) - f(q_i^{\pm}(\mu)(t), \mu) - A_i^{\pm}(t,\mu)z_i^{\pm}. \tag{5.28}$$

In case $i = 2$ we may omit the superscripts $\pm$. We still require that $q_i^{\pm}(\mu)(0) \in \Sigma_i$, and note that our previous definitions of Y_i, Z_i still hold and make sense. Let $\Phi_{i,\pm}(\mu, t, s)$ be the transition matrix for the equation

$$\dot{z}^{\pm} = A_i^{\pm}(t,\mu)z^{\pm} \tag{5.29}$$

As before, these operators have an exponential dichotomy on $\mathbb{R}^+$ and $\mathbb{R}^-$ with corresponding projections $P_{i,+}(\mu,t)$, $Q_{i,+}(\mu,t)$, $Q_{i,-}(\mu,t)$ and $P_{i,-}(\mu,t)$.

5.4.1 Uncoupled Solutions

In this section we begin looking for solutions $z_2^{\pm}(t)$ of the above form, which for given $a_2^+ \in \text{Im } Q_{2,+}, a_2^- \in \text{Im } P_{2,-}$, and given $\omega_1, \omega_2 > 0$, the following conditions hold:

1. $Q_{2,+}(\mu,\omega_1)z_2^+(\omega_1) = a_2^+$,
   $P_{2,-}(\mu,-\omega_2)z_2^-(-\omega_2) = a_2^-$,

2. $z_2^{\pm}(0) \in Y_2$,

3. $z_2^{+}(0) - z_2^{-}(0) \in Z_2$.

Then $z_2^+ \in C^0([0,\omega_1],\mathbb{R}^3)$, and $z_2^- \in C^0([-\omega_2,0],\mathbb{R}^3)$. Note the last condition in this case means $z_2^+(0) = z_2^-(0)$, but it is written as it is for consistency. We shall prove that under the above conditions, the solutions $z_2^{\pm}(t)$ exist and are unique.

Before considering this boundary value problem for (5.27), we will first study the same boundary value problem for the inhomogeneous linear equation

$$\dot{z}_i^{\pm} = A_i^{\pm}(t,\mu) z_i^{\pm} + h_i^{\pm}(t). \tag{5.30}$$

Thus, for $z_2^{\pm}(t)$, we are looking for solutions to the equations

$$\begin{aligned} z_2^{\pm}(t) &= \Phi_{2,\pm}(\mu,t,0) z_2^{\pm}(0) + \int_0^t \Phi_{2,\pm}(\mu,t,s) h_2^{\pm}(s) ds & (5.31)\\ & Q_{2,+}(\omega_1) z_2^+(\omega_1) = a_2^+, & (5.32)\\ & P_{2,-}(-\omega_2) z_2^-(-\omega_2) = a_2^-. & (5.33) \end{aligned}$$

Now

$$\begin{aligned} Q_{2,+}(\mu,0) z_2^+(0) &= \Phi_{2,+}(\mu,0,\omega_1) a_2^+ \\ &\quad - \int_0^{\omega_1} \Phi_{2,+}(\mu,0,s) Q_{2,+}(\mu,s) h_2^+(s) ds, & (5.34)\\ P_{2,-}(\mu,0) z_2^-(0) &= \Phi_{2,-}(\mu,0,-\omega_2) a_2^- \\ &\quad + \int_{-\omega_2}^{0} \Phi_{2,-}(\mu,0,s) P_{2,-}(\mu,s) h_2^-(s) ds, & (5.35) \end{aligned}$$

and since, for example, $z_2^+(0) \in Y_2$, $Q_{2,+}(\mu,0) z_2^+(0) = Q_{2,-}(\mu,0) z_2^+(0)$. Then we can add the two equations above to solve for $z_2^+(0) = z_2^-(0) =: z_2(0)$.

Substituting this into (5.31) then gives the solutions:

$$\begin{aligned} z_2^+(t) &= \Phi_{2,+}(\mu,t,0)P_{2,+}(\mu,0)z_2(0) + \Phi_{2,+}(\mu,t,\omega_1)a_2^+ \\ &\quad + \int_0^t \Phi_{2,+}(\mu,t,s)P_{2,+}(\mu,s)h_2^+(s)ds \\ &\quad - \int_t^{\omega_1} \Phi_{2,+}(\mu,t,s)Q_{2,+}(\mu,s)h_2^+(s)ds \qquad (5.36) \\ z_2^-(t) &= \Phi_{2,-}(\mu,t,0)Q_{2,-}(\mu,0)z_2(0) + \Phi_{2,-}(\mu,t,-\omega_2)a_2^- \\ &\quad - \int_t^0 \Phi_{2,-}(\mu,t,s)Q_{2,-}(\mu,s)h_2^-(s)ds \\ &\quad + \int_{-\omega_2}^t \Phi_{2,-}(\mu,t,s)P_{2,-}(\mu,s)h_2^-(s)ds \qquad (5.37) \end{aligned}$$

These functions are clearly in the spaces $C^0([0,\omega_1],\mathbb{R}^3)$, $C^0([-\omega_2,0],\mathbb{R}^3)$ respectively, and they depend on μ, ω_2, ω_1, a_2^-, a_2^+, h_2^-, h_2^+. We denote this solution by

$$\tilde{z}_2(t;\mu,\omega_2,\omega_1,a_2^-,a_2^+,h_2^-,h_2^+) := \begin{cases} z_2^-(t), & t \le 0, \\ z_2^+(t), & t > 0. \end{cases}$$

Note that this is a continuous solution. We would also like to consider the symmetry properties of these orbits. In the following we drop the subscripts/superscripts $+,-$, where the meaning is clear. We have from (5.34), (5.35), (5.36) and (5.37):

$$\begin{aligned} z_2(t) &= \Phi_2(\mu,t,-\omega_2)a_2^- + \Phi_2(\mu,t,\omega_1)a_2^+ \\ &\quad + \int_{-\omega_2}^t \Phi_2(\mu,t,s)P_2(\mu,s)h_2(s)ds - \int_t^{\omega_1} \Phi_2(\mu,t,s)Q_2(\mu,s)h_2(s)ds \\ Rz_2(t) &= \Phi_2(\mu,-t,\omega_2)Ra_2^- + \Phi_2(\mu,-t,-\omega_1)Ra_2^+ \\ &\quad - \int_{-t}^{\omega_2} \Phi_2(\mu,-t,s)Q_2(\mu,s)h_2(s)ds + \int_{-\omega_1}^{-t} \Phi_2(\mu,-t,s)P_2(\mu,s)h_2(s)ds \end{aligned}$$

Therefore $R\tilde{z}_2(t;\mu,\omega_2,\omega_1,a_2^-,a_2^+,h_2^-,h_2^+) = \tilde{z}_2(-t;\mu,\omega_1,\omega_2,Ra_2^+,Ra_2^-,h_2^-,h_2^+)$. Clearly then, if $a_2^+ = Ra_2^-$ and $\omega_1 = \omega_2$, $\tilde{z}_2(t;\mu,\omega_2,\omega_1,a_2^-,a_2^+,h_2^-,h_2^+)$ is symmetric. In general, $\tilde{z}_2(t)$ is symmetric if and only if

$$\begin{aligned} &\Phi_2(\mu,t,-\omega_2)a_2^- + \Phi_2(\mu,t,\omega_1)a_2^+ - \textstyle\int_{\omega_2}^{\omega_1} \Phi_2(\mu,t,s)Q_2(\mu,s)h_2(s)ds \\ &\quad = \Phi_2(\mu,t,\omega_2)Ra_2^- + \Phi_2(\mu,t,-\omega_1)Ra_2^+ + \textstyle\int_{-\omega_1}^{-\omega_2} \Phi_2(\mu,t,s)P_2(\mu,s)h_2(s)ds \end{aligned}$$

Using projections $P_2(\mu,t), Q_2(\mu,t)$:

$$\Phi_2(\mu,t,\omega_1)a_2^+ - \int_{\omega_2}^{\omega_1} \Phi_2(\mu,t,s)Q_2(\mu,s)h_2(s)ds = \Phi_2(\mu,t,\omega_2)Ra_2^-$$

$$\Rightarrow a_2^+ = \Phi_2(\mu,\omega_1,\omega_2)Ra_2^- - \int_{\omega_1}^{\omega_2} \Phi_2(\mu,\omega_1,s)Q_2(\mu,s)h_2(s)ds, \tag{5.38}$$

or equivalently:

$$a_2^- = \Phi_2(\mu,-\omega_2,-\omega_1)Ra_2^+ + \int_{-\omega_1}^{-\omega_2} \Phi_2(\mu,-\omega_2,s)P_2(\mu,s)h_2(s)ds, \tag{5.39}$$

This is the necessary and sufficient condition for $\tilde{z}_2(t;\mu,\omega_2,\omega_1,a_2^-,a_2^+,h_2^-,h_2^+)$ to be symmetric.

Remark 5.4.1. *We can, similar to section 5.3, find solutions in the case for ω_1 or ω_2 equal to infinity. This means that a_2^+ or a_2^- is zero. We obtain the desired solutions by equations similar to (5.14), (5.15). By equations analogous to (5.16), (5.17) we modify (5.34), (5.35) to*

$$\begin{aligned} Q_{2,+}(\mu,0)z_2^+(0) &= -\int_0^\infty \Phi_{2,+}(\mu,0,s)Q_{2,+}(\mu,s)h_2(s)ds, \\ P_{2,-}(\mu,0)z_2^-(0) &= \int_{-\infty}^0 \Phi_{2,-}(\mu,0,s)P_{2,-}(\mu,s)h_2(s)ds. \end{aligned}$$

Correspondingly, we look for solutions $z_1^\pm(t)$ to the inhomogeneous linear equation (5.30) satisfying the following for given $a_1^+ \in \text{Im } Q_{1,+}$, $a_1^- \in \text{Im } P_{1,-}$, and $\omega_1, \omega_2 > 0$:

1. $Q_{1,+}(\mu,\omega_2)z_1^+(\omega_2) = a_1^+$,
   $P_{1,-}(\mu,-\omega_1)z_1^-(-\omega_1) = a_1^-$,
2. $z_1^\pm(0) \in Y_1$,
3. $z_1^+(0) - z_1^-(0) \in Z_1$.

As before, we have

$$z_1^\pm(t) = \Phi_{1,\pm}(\mu,t,0)z_1^\pm(0) + \int_0^t \Phi_{1,\pm}(\mu,t,s)h_1(s)ds \tag{5.40}$$

and

$$\begin{aligned}
z_1^+(0) &= Q_{1,+}(\mu,0)z_1^+(0) \\
&= \Phi_{1,+}(\mu,0,\omega_2)a_1^+ - \int_0^{\omega_2} \Phi_{1,+}(\mu,0,s)Q_{1,+}(\mu,s)h_1(s)ds, \qquad (5.41)\\
z_1^-(0) &= P_{1,-}(\mu,0)z_1^-(0) \\
&= \Phi_{1,-}(\mu,0,-\omega_1)a_1^- + \int_{-\omega_1}^{0} \Phi_{1,-}(\mu,0,s)P_{1,-}(\mu,s)h_1(s)ds, \qquad (5.42)
\end{aligned}$$

Plugging these back into (5.40) then yields solutions $\tilde{z}_1^{\pm}(t;\mu,\omega_1,\omega_2,a_1^-,a_1^+,h_1^-,h_1^+)$.

Remark 5.4.2. *As before, we can find solutions in the case for ω_1 or ω_2 equal to infinity; in this case a_2^+ or a_2^- is zero. In this case we find in place of (5.41), (5.42):*

$$\begin{aligned}
z_1^+(0) &= -\int_0^{\infty} \Phi_{1,+}(\mu,0,s)Q_{1,+}(\mu,s)h_1(s)ds,\\
z_1^-(0) &= \int_{-\infty}^{0} \Phi_{1,-}(\mu,0,s)P_{1,-}(\mu,s)h_1(s)ds.
\end{aligned}$$

Remark 5.4.3. *Similar to $\tilde{z}_2(t)$, it can be shown that $R\tilde{z}_1^+(t) = \tilde{z}_1^-(-t)$ if and only if*

$$a_2^+ = \Phi_1(\mu,\omega_2,\omega_1)Ra_1^- - \int_{\omega_2}^{\omega_1} \Phi_1(\mu,\omega_2,s)Q_1(\mu,s)h_1(s)ds.$$

Remark 5.4.4. *It is easy to see that the solutions $\tilde{z}_2(t;\mu,\omega_2,\omega_1,a_2^-,a_2^+,h_2^-,h_2^+)$ and*
$\tilde{z}_1^{\pm}(t;\mu,\omega_1,\omega_2,a_1^-,a_1^+,h_1^-,h_1^+)$ depend linearly on $(a_i^+,a_i^-,h_i^+,h_i^-)$.

5.4.2 Coupling Projections

In the next section we will show how it is possible to couple the solutions found in section 5.4.1 near the hyperbolic fixed points p_1, p_2. We will need the following Lemma.

Lemma 5.4.5. *There exist constants $\overline{\omega} > 0$ and $M > 0$ such that for all $\omega_i \geq \overline{\omega}$,*

$$\mathbb{R}^3 = Im\ P_{i,-}(-\omega_i) \oplus Im\ Q_{i-1,+}(\omega_i),$$

and $||\tilde{P}_{i,\omega_i}(\mu)|| \leq M$, $||\tilde{Q}_{i,\omega_i}(\mu)|| \leq M$ *with* $\tilde{P}_{i,\omega_i}(\mu)$ *and* $\tilde{Q}_{i,\omega_i}(\mu) = I - \tilde{P}_{i,\omega_i}(\mu)$ *complementary projections on respectively Im* $P_{i,-}(\mu, -\omega_i)$, *Im* $Q_{i-1,+}(\mu, \omega_i)$.

Proof. Let $P_0(p_1)$, $Q_0(p_1)$ be the complementary projections on the stable, resp. unstable subspaces of $D_x f(p_1, \mu)$. Similarly for $P_0(p_2)$, $Q_0(p_2)$. Then note that Im $P_0(p_1) = R \circ \text{Im } Q_0(p_2)$, and Im $Q_0(p_1) = R \circ \text{Im } P_0(p_2)$.

Take $\tilde{M} := \max \{||P_0(p_1)||, ||Q_0(p_1)||, ||P_0(p_2)||, ||Q_0(p_2)||\} \geq 1$.

Using the fact that

$$\lim_{t\to\infty} ||P_{i-1,+}(\mu, t) - P_0(p_{i-1})|| = 0,$$

and similar expressions for $Q_{i,-}$, $P_{i,-}$, $Q_{i-1,+}$, we can find $\overline{\omega}$ such that

$$\sup_{\omega\geq\overline{\omega}} ||P_{i-1,+}(\mu, \omega) - P_0(p_{i-1})|| \leq \frac{1}{4\tilde{M}},$$

and similarly for $Q_{i,-}$, $P_{i,-}$, $Q_{i-1,+}$ for all i. Now, for

$\omega \geq \overline{\omega}$, we set

$$\begin{aligned} S_{i,\omega} &:= (P_0(p_{i-1}) + (P_{i,-}(\mu, -\omega) - P_0(p_{i-1})))P_0(p_{i-1}) \\ &\quad + (Q_0(p_{i-1}) + (Q_{i-1,+}(\mu, \omega) - Q_0(p_{i-1})))Q_0(p_{i-1}) \\ &= I + (P_{i,-}(\mu, -\omega) - P_0(p_{i-1}))P_0(p_{i-1}) \\ &\quad + (Q_{i-1,+}(\mu, \omega) - Q_0(p_{i-1}))Q_0(p_{i-1}) \end{aligned}$$

Since

$$||(P_{i,-}(\mu, -\omega) - P_0(p_{i-1}))P_0(p_{i-1})|| + (Q_{i-1,+}(\mu, \omega) - Q_0(p_{i-1}))Q_0(p_{i-1}) \leq \frac{1}{2},$$

the eigenvalues of $S_{i,\omega}$ must have modulus $\geq 1/2$, and hence $S_{i,\omega}$ is invertible.

Now we define $\tilde{P}_{i,\omega}(\mu)$ by

$$\tilde{P}_{i,\omega}(\mu) := S_{i,\omega} P_0(p_{i-1}) S_{i,\omega}^{-1}$$

for $\omega \geq \overline{\omega}$. It is easy to see that $\tilde{P}_{i,\omega}(\mu)$ is a projection. Also

$$\tilde{P}_{i,\omega}(\mu) S_{i,\omega} = S_{i,\omega} P_0(p_{i-1}) = P_{i,-}(\mu, -\omega) P_0(p_{i-1}),$$

so Im $\tilde{P}_{i,\omega}(\mu) = \text{Im } P_{i,-}(\mu, -\omega)P_0(p_{i-1}) = \text{Im } P_{i,-}(\mu, -\omega)$. This follows since

$$\lim_{\omega\to\infty} P_{i,-}(\mu, -\omega) = P_0(p_{i-1})$$

and so $P_{i,-}(\mu, -\omega)$ is injective on Im $P_0(p_{i-1})$ for $\omega \geq \overline{\omega}$ sufficiently large. These two projections have the same dimension on their image, so equality follows.

It is easy to check that $||S_{i,\omega}|| \leq 2$ and $||S_{i,\omega}^{-1}|| \leq 2$, so $||\tilde{P}_{i,\omega}(\mu)|| \leq 4||P_0(p_{i-1})|| \leq 4\tilde{M}$. Taking $M = 4\tilde{M}$ now proves the Lemma. □

Remark 5.4.6. *By the reversibility, the projections $\tilde{P}_{i,\omega}(\mu)$, $\tilde{Q}_{i,\omega}(\mu)$ are chosen to have the property that $R\tilde{P}_{i,\omega}(\mu) = \tilde{Q}_{i+1,\omega}(\mu)$. (Note that the subscript i on these projections is taken modulo 2.)*

5.4.3 Coupled Solutions

We would now like to couple the solutions

$$\tilde{x}_i^{\pm}(t; \mu, \omega_i, \omega_{i+1}, a_i^-, a_i^+, h_i^-, h_i^+) := q_i^{\pm}(\mu)(t) + \tilde{z}_i^{\pm}(t; \mu, \omega_i, \omega_{i+1}, a_i^-, a_i^+, h_i^-, h_i^+),$$

close to the fixed points p_i. We require that, for ω_i sufficiently large for all i, we can find unique $(a_i^+, a_i^-) \in \text{Im } Q_{i,+}(\mu, \omega_{i+1}) \times \text{Im } P_{i,-}(\mu, -\omega_i)$ such that

$$\tilde{x}_{i-1}^+(\omega_i; \mu, \omega_{i-1}, \omega_i, a_{i-1}^-, a_{i-1}^+, h_{i-1}^-, h_{i-1}^+) = \tilde{x}_i^-(-\omega_i; \mu, \omega_i, \omega_{i+1}, a_i^-, a_i^+, h_i^-, h_i^+).$$

This would provide existence and uniqueness of a piecewise continuous solution that spends a given time between sections Σ_i, and which have a possible jump in each Σ_i in the direction Z_i, for every μ close to μ_0.

If then we define

$$d_i := q_i^-(\mu)(-\omega_i) - q_{i-1}^+(\mu)(\omega_i),$$

our problem reduces to finding (a_i^+, a_i^-) for all i such that

$$\tilde{z}_{i-1}^+(\omega_i; \mu, \omega_{i-1}, \omega_i, a_{i-1}^-, a_{i-1}^+, h_{i-1}^-, h_{i-1}^+) - \tilde{z}_i^-(-\omega_i; \mu, \omega_i, \omega_{i+1}, a_i^-, a_i^+, h_i^-, h_i^+) = d_i. \tag{5.43}$$

As before

$$\begin{aligned} P_{i,-}(\mu,-\omega_i)\tilde{z}_i^-(-\omega_i) &= a_i^-, \quad (5.44)\\ Q_{i-1,+}(\mu,\omega_i)\tilde{z}_{i-1}^+(\omega_i) &= a_{i-1}^+, \quad (5.45)\end{aligned}$$

where $\tilde{z}_i^\pm(t)$ is shorter notation for $\tilde{z}_i^\pm(t;\mu,\omega_{i-1},\omega_i,a_i^-,a_i^+,h_i^-,h_i^+)$. Combining (5.43), (5.44), (5.45), we find that

$$a_{i-1}^+ - a_i^- = d_i - P_{i-1,+}(\mu,\omega_i)\tilde{z}_{i-1}^+(\omega_i) + Q_{i,-}(\mu,-\omega_i)\tilde{z}_i^-(-\omega_i). \quad (5.46)$$

Using projections $\tilde{P}_{i,\omega_i}$ and $\tilde{Q}_{i,\omega_i}$ as defined in section 5.4.2, we obtain the following fixed point equations for (a_i^-,a_{i-1}^+):

$$\begin{aligned} a_i^- &= -\tilde{P}_{i,\omega_i}\left(d_i - P_{i-1,+}(\mu,\omega_i)\tilde{z}_{i-1}^+(\omega_i) + Q_{i,-}(\mu,-\omega_i)\tilde{z}_i^-(-\omega_i)\right) \quad (5.47)\\ a_{i-1}^+ &= \tilde{Q}_{i,\omega_i}\left(d_i - P_{i-1,+}(\mu,\omega_i)\tilde{z}_{i-1}^+(\omega_i) + Q_{i,-}(\mu,-\omega_i)\tilde{z}_i^-(-\omega_i)\right) \quad (5.48)\end{aligned}$$

Note that $-P_{i-1,+}(\mu,\omega_i)\tilde{z}_{i-1}^+(\omega_i) + Q_{i,-}(\mu,-\omega_i)\tilde{z}_i^-(-\omega_i)$ is linear in $(a_{i-1}^+,a_i^-,h_{i-1}^+,h_i^-)$ (cf. Remark 5.4.4). Then we may write

$$\mathbf{a} = L_1(\mu)\mathbf{a} + L_2(\mu)\mathbf{h} + L_3(\mu)\mathbf{d} \quad (5.49)$$

with $\mathbf{a} := (a_{i-1}^+,a_i^-)_{i\in\mathbb{Z}} \in l^\infty_{\mathbb{R}^3\times\mathbb{R}^3}$, similarly for $\mathbf{h}$ and $\mathbf{d}$, where l^∞_X denotes the space of all bounded sequences $\mathbf{x} := (x_i)_{i\in\mathbb{Z}}, x_i \in X$. l^∞_X is equipped with the supremum norm/metric. The $L_j(\mu)$, $j = 1,2,3$, are linear operators depending smoothly on μ. The estimate (6.5) supplied in section 6.1.3 ensures that we can choose again some $\overline{\omega}$ even larger such that $\omega_i \geq \overline{\omega}$ implies that the linear operator $(id - L_1(\mu))$ is invertible. Then we can uniquely solve equation (5.49) for $\mathbf{a} = \mathbf{a}(\mu,\mathbf{h},\mathbf{d})$, where $\mathbf{a}$ is linear in $(\mu,\mathbf{h},\mathbf{d})$ and also linear in $(\mathbf{h},\mathbf{d})$. Then we find the solutions $\tilde{z}_i^\pm(t;\mu,\mathbf{h},\mathbf{d},\omega)$. This shows that we can uniquely couple the solutions $\tilde{x}_i^\pm(t;\mu,\omega_i,\omega_{i+1},a_i^-,a_i^+,h_i^-,h_i^+)$ for each μ, depending only on a prescribed sequence ω such that the time spent between $\tilde{x}_{i-1}^+(0;\mu,\omega_{i-1},\omega_i,a_{i-1}^-,a_{i-1}^+,h_{i-1}^-,h_{i-1}^+) \in \Sigma_{i-1}$ and $\tilde{x}_i^-(0;\mu,\omega_i,\omega_{i+1},a_i^-,a_i^+,h_i^-,h_i^+) \in \Sigma_i$ is precisely $2\omega_i$. Thus we may write the solution as $\tilde{x}_i^{\pm}(t;\mu,\mathbf{h},\mathbf{d},\omega)$. Recall that $\tilde{x}_i^{\pm}(t;\mu,\mathbf{h},\mathbf{d},\omega)$ has a possible jump at $t=0$ in the direction of Z_i.

Remark 5.4.7. *The case for when some $\omega_j=\infty$ can similarly be dealt with, in this case $a_{j-1}^{+}=a_j^{-}=d_j=0$, and we require $lim_{t\to\infty}z_{j-1}^{+}(t)=0$ and $lim_{t\to-\infty}z_j^{-}(t)=0$. Note then that the equations (5.47) and (5.48) are automatically satisfied for $i=j$. The solutions $\tilde{z}_i^{\pm}(t;\mu,\omega_i,\omega_{i+1},a_i^{-},a_i^{+},h_i^{-},h_i^{+})$ used in the proof of this section then are precisely those described at the end of section 5.4.1 and we may couple the solutions at $z_j^{+}(\omega_{j+1})$ and $z_{j-1}^{-}(-\omega_{j-1})$ in the same way.*

Remark 5.4.8. *It is clear by uniqueness that $\tilde{z}_i^{\pm}(t;\mu,\omega_i,\omega_{i+1},a_i^{-},a_i^{+},h_i^{-},h_i^{+})$ is symmetric if and only if the sequence $\{\omega_i\}_{i\in\mathbb{Z}}$ is symmetric, that is, $\omega_{i-j}=\omega_{i+j+1}$, where $j=0,1,2,\ldots$. In this case, we have*

$$R(\tilde{z}_i^{+}(0;\omega,\mu)-\tilde{z}_i^{-}(0;\omega,\mu)) \quad = \quad -(\tilde{z}_i^{+}(0;\omega,\mu)-\tilde{z}_i^{-}(0;\omega,\mu)),$$

and so $\tilde{z}_i^{+}(0;\omega,\mu)-\tilde{z}_i^{-}(0;\omega,\mu)\in Fix\,(-R)$.

We now consider the problem of solving the boundary value problem for the nonlinear equation (5.27):

$$\dot{z}_i^{\pm}=A_i^{\pm}(t,\mu)z_i^{\pm}+g_i^{\pm}(t,z_i^{\pm},\mu), \tag{5.50}$$

$$z_{i-1}^{+}(\omega_i)-z_i^{-}(-\omega_i)=d_i. \tag{5.51}$$

We first make the following definitions.

Definition 5.4.9. *Given a sequence $\omega=\{\omega_i\}_{i\in\mathbb{Z}}$, denote by $\mathcal{Z}_\omega$ the space of all sequences $\mathbf{z}\in(C^0([0,\omega_{i+1}],\mathbb{R}^3),C^0([-\omega_i,0],\mathbb{R}^3))_{i\in\mathbb{Z}}$. This space has the norm $||\mathbf{z}||:=max\,\{sup_{i\in\mathbb{Z}}||z_i^{+}||,sup_{i\in\mathbb{Z}}||z_i^{-}||\}$. $\omega_i=\infty$ is allowed for bounded continuous functions.*

Definition 5.4.10. *Let $\mathcal{G}:\mathcal{Z}_\omega\times\mathbb{R}\to\mathcal{Z}_\omega$ be defined by*

$$\mathcal{G}(\mathbf{z},\mu)(t)=(g_i^{+}(t,z_i^{+}(t),\mu),g_i^{-}(t,z_i^{-}(t),\mu))_{i\in\mathbb{Z}},$$

where $\mathbf{z}:=(z_i^{+},z_i^{-})_{i\in\mathbb{Z}}$.

The boundary value problem (5.50), (5.51) can then be rewritten as the fixed point problem

$$\mathbf{z} = \tilde{\mathbf{z}}(\mu, \mathcal{G}(\mathbf{z},\mu), \mathbf{d}(\omega,\mu), \omega) := \mathcal{F}(\mu, \mathbf{z}, \omega), \tag{5.52}$$

where $\tilde{\mathbf{z}}(\mu, \mathbf{h}, \mathbf{d}, \omega) = (\tilde{z}_i^+(t; \mu, \mathbf{h}, \mathbf{d}, \omega), \tilde{z}_i^-(t; \mu, \mathbf{h}, \mathbf{d}, \omega))_{i\in\mathbb{Z}} \in \mathcal{Z}_\omega$. The following Lemma provides solutions to the fixed point problem.

Lemma 5.4.11. *For ω_i sufficiently large, and $|\mu|$ sufficiently small, the fixed point problem (5.52) has a unique solution $\overline{\mathbf{z}}(\omega,\mu) = (\overline{z}_i^+(\cdot;\omega,\mu), \overline{z}_i^-(\cdot;\omega,\mu))_{i\in\mathbb{Z}}$ (given $\mathbf{z}$ sufficiently close to 0 in $(C^0([0,\omega_{i+1}],\mathbb{R}^3), C^0([-\omega_i,0],\mathbb{R}^3))_{i\in\mathbb{Z}} =: \mathcal{Z}_\omega$). For fixed ω the mapping $\mu \to \overline{\mathbf{z}}(\omega,\mu)$ is smooth.*

Proof. We show first that there is an $\mathcal{F}$-invariant closed neighbourhood of 0 in $\mathcal{Z}_\omega$. From (6.6) we see that

$$||\mathcal{F}(\omega, \mathbf{z}, \mu)|| \leq \hat{K}(||\mathbf{d}|| + ||\mathcal{G}||)$$

From (5.28), $\mathcal{G}(0,0) = 0$. Then by the Mean Value Theorem:

$$\begin{aligned} ||\mathcal{G}(\mathbf{z},\mu)|| &= \left|\left|\left(\int_0^1 D\mathcal{G}(s(\mathbf{z},\mu))ds\right)(\mathbf{z},\mu)\right|\right| \\ &\leq \int_0^1 ||D_{\mathbf{z}}\mathcal{G}(s(\mathbf{z},\mu))||ds||\mathbf{z}|| + \int_0^1 ||D_\mu\mathcal{G}(s(\mathbf{z},\mu))||ds||\mu|| \end{aligned}$$

Now, if $||\mathbf{z}||, ||\mu - \mu_0|| < \epsilon$, there is a constant C_2 such that

$$\int_0^1 ||D_\mu\mathcal{G}(s(\mathbf{z},\mu))||ds < C_2.$$

Again from (5.28), $D_{\mathbf{z}}\mathcal{G}(0,0) = 0$. Then for $||\mathbf{z}||, ||\mu - \mu_0|| < \overline{\epsilon} \leq \epsilon$ small enough, we have $||D_{\mathbf{z}}\mathcal{G}(s(\mathbf{z},\mu))|| \leq (4\hat{K})^{-1}$ for $\hat{K}$ arbitrarily large and so

$$\int_0^1 ||D_{\mathbf{z}}\mathcal{G}(s(\mathbf{z},\mu))||ds \leq \frac{1}{4\hat{K}}$$

Now choose $\epsilon_\mu \leq \overline{\epsilon}$ small enough so that $C_2\epsilon_\mu \leq \overline{\epsilon}/(4\hat{K})$. Then it follows that for $||\mathbf{z}|| \leq \overline{\epsilon}$ and $||\mu - \mu_0|| \leq \epsilon_\mu$, we have $||\mathcal{G}(\mathbf{z},\mu)|| \leq \overline{\epsilon}/(2\hat{K})$.

Since $q_i^\pm(\mu)(\cdot) \to q_i^\pm(\mu_0)(\cdot)$ in the space $C_b^0(\mathbb{R}^\pm, \mathbb{R}^3)$ as $\mu - \mu_0 \to 0$, there is an $\overline{\omega}$ sufficiently large such that for all $\omega_1, \omega_2 > \overline{\omega}$ we have $||q_i^+(\mu)(\omega_1) -$

$q_{i+1}^{-}(\mu)(-\omega_2)|| < \overline{\epsilon}/(8\hat{K})$. In this case we can write $||\mathbf{d}|| \leq \overline{\epsilon}/(2\hat{K})$. Then if $||\mu - \mu_0|| < \epsilon_\mu$ and ω_i are sufficiently large, $\mathcal{F}$ leaves the ball centred on 0 with radius $\overline{\epsilon}$, $B(0, \overline{\epsilon}) \subset \mathcal{Z}_\omega$, invariant.

We also have (using (6.6)):

$$||D_{\mathbf{z}}\mathcal{F}(\omega, \mathbf{z}, \mu)|| \leq ||D_{\mathbf{h}}\mathbf{z}(\mu, \mathcal{G}(\mathbf{z}, \mu), \mathbf{d}, \omega)|| \cdot ||D_{\mathbf{z}}\mathcal{G}(\mathbf{z}, \mu)|| = \hat{K}\frac{1}{4\hat{K}} = \frac{1}{4}.$$

Applying the Mean Value Theorem to $\mathcal{F}$ now implies that $\mathcal{F}$ is a contraction on $B(0, \epsilon)$, and we can use the Banach fixed point theorem to deduce the existence and uniqueness of the solution $\tilde{z}(\omega, \mu)$. □

Thus we have solved the nonlinear boundary value problem (5.50), (5.51) to find the solution $\overline{\mathbf{z}}(\omega, \mu) = (\overline{z}_i^+(\cdot; \omega, \mu), \overline{z}_i^-(\cdot; \omega, \mu))_{i \in \mathbb{Z}}$. We may also write $\overline{z}_i^\pm(0; \omega_i, \omega_{i+1}, \mu)$.

5.5 The Bifurcation Equations

Consider the form (5.26). We would now like to derive a representation of the 'jump'

$$\Xi_i^\omega(\mu) := \xi_i^\infty(\mu) + \xi_i^\omega(\mu), \tag{5.53}$$

where

$$\xi_i^\omega(\mu) = \overline{z}_i^+(0; \omega_i, \omega_{i+1}, \mu) - \overline{z}_i^-(0; \omega_i, \omega_{i+1}, \mu). \tag{5.54}$$

Equations (5.53) and (5.54) will both be equal to zero if i is even, for any prescribed sequence ω. Thus we will assume that i is odd, and we will focus on the jump $\xi_i^\omega(\mu)$ in the section Σ_1.

$$\xi_i^\omega(\mu) = \sum_{j=1}^{2} \psi_j < \psi_j, \xi_i^\omega(\mu) >$$

As in section 5.3.3, ψ_1, ψ_2 are an orthonormal basis for Z, such that Fix $R =$ Sp$\{\psi_1\}$ and Fix $(-R) =$ Sp$\{\psi_2\}$. We can write

$$\xi_i^\omega(\mu) = \sum_{j=1}^{2} \psi_j \left\{ < \psi_j, Q_{1,+}(\mu,0)\overline{z}_i^+(0;\omega,\mu) > - < \psi_j, P_{1,-}(\mu,0)\overline{z}_i^-(0;\omega,\mu) > \right\}$$

Now (cf. (5.41))

$$\begin{aligned} Q_{1,+}(\mu,0)\overline{z}_i^+(\omega,\mu)(0) &= \Phi_1^+(\mu,0,\omega_{i+1})a_i^+(\mu,\omega_{i+1}) \\ &\quad - \int_0^{\omega_{i+1}} \Phi_1^+(\mu,0,s)Q_{1,+}(\mu,s)g_1(s,\overline{z}_i^+(s;\omega,\mu),\mu)ds \end{aligned} \tag{5.55}$$

Recall that

$$\begin{aligned} Q_{1,+}(\mu,\omega_{i+1})\overline{z}_i^+(\omega_{i+1};\omega,\mu) &= a_i^+ \\ P_{2,-}(\mu,-\omega_{i+1})\overline{z}_{i+1}^-(-\omega_{i+1};\omega,\mu) &= a_{i+1}^- \end{aligned}$$

Then

$$\begin{aligned} a_i^+ - a_{i+1}^- &= q_{i+1}^-(\mu)(-\omega_{i+1}) - q_i^+(\mu)(\omega_{i+1}) + Q_{2,-}(\mu,-\omega_{i+1})\overline{z}_{i+1}^-(-\omega_{i+1};\omega,\mu) \\ &\quad - P_{1,+}(\mu,\omega_{i+1})\overline{z}_i^+(\omega_{i+1};\omega,\mu) \\ a_{i+1}^+ &= \tilde{Q}_{i+1,\omega_{i+1}}(\mu)\left\{ q_{i+1}^-(\mu)(-\omega_{i+1}) - q_i^+(\mu)(\omega_{i+1}) \right. \\ &\quad \left. + Q_{2,-}(\mu,-\omega_{i+1})\overline{z}_{i+1}^-(-\omega_{i+1},\omega,\mu) - P_{1,+}(\mu,\omega_{i+1})\overline{z}_i^+(\omega_{i+1},\omega,\mu) \right\} \end{aligned}$$

Plugging the above back into equation (5.55) gives

$$\begin{aligned} Q_{1,+}(\mu,0)\overline{z}_i^+(0;\omega,\mu) &= \Phi_1^+(\mu,0,\omega_{i+1})Q_{1,+}(\mu,\omega_{i+1}) \circ \\ &\quad \tilde{Q}_{i+1,\omega_{i+1}}(\mu)\left\{ q_{i+1}^-(\mu)(-\omega_{i+1}) - q_i^+(\mu)(\omega_{i+1}) \right. \\ &\quad + Q_{2,-}(\mu,-\omega_{i+1})\overline{z}_{i+1}^-(-\omega_{i+1},\omega,\mu) \\ &\quad \left. - P_{1,+}(\mu,\omega_{i+1})\overline{z}_i^+(\omega_{i+1},\omega,\mu) \right\} \\ &\quad - \int_0^{\omega_{i+1}} \Phi_1^+(\mu,0,s)Q_{1,+}(\mu,s)g_1(s,\overline{z}_i^+(s;\omega,\mu),\mu)ds, \end{aligned}$$

and we can obtain a similar expression for $P_{1,-}(\mu,0)\overline{z}_i^-(0;,\omega,\mu)$. Now we can rewrite the jump $\xi_i^\omega(\mu)$ in the form

$$
\begin{aligned}
\xi_i^\omega(\mu) \;=\; & \sum_{j=1}^{2}\psi_j\,\{<\Phi_{1,+}^*(\mu,0,\omega_{i+1})Q_{1,+}^*(\mu,0)\psi_j,\\
& \quad \tilde{Q}_{i+1,\omega_{i+1}}(\mu)\left[q_{i+1}^-(\mu)(-\omega_{i+1})-q_i^+(\mu)(\omega_{i+1})\right.\\
& +Q_{2,-}(\mu,-\omega_{i+1})\overline{z}_{i+1}^-(-\omega_{i+1};\omega,\mu)-P_{1,+}(\mu,\omega_{i+1})\overline{z}_i^+(\omega_{i+1};\omega,\mu)\left.\right]>\\
& -<\psi_j,\int_0^{\omega_{i+1}}\Phi_1^+(\mu,0,s)Q_{1,+}(\mu,s)g_1(s,\overline{z}_i^+(s;\omega,\mu),\mu)ds>\\
& -<\Phi_{1,-}^*(\mu,0,-\omega_i)P_{1,-}^*(\mu,0)\psi_j,\\
& \quad \tilde{P}_{i,\omega_i}(\mu)\left[q_{i-1}^+(\mu)(\omega_i)-q_i^-(\mu)(-\omega_i)\right.\\
& +P_{2,+}(\mu,\omega_i)\overline{z}_{i-1}^+(\omega_i;\omega,\mu)-Q_{1,-}(\mu,-\omega_i)\overline{z}_i^-(-\omega_i;\omega,\mu)\left.\right]>\\
& -<\psi_j,\int_{-\omega_i}^{0}\Phi_1^-(\mu,0,s)P_{1,-}(\mu,s)g_1(s,\overline{z}_i^-(s;\omega,\mu),\mu)ds>\Big\}
\end{aligned}
\tag{5.56}
$$

In the above, A^* is the adjoint of A with respect to the inner product $<\cdot,\cdot>$. In section 6.4 we estimate each term in the above expression, and find that the leading order term is

$$
\begin{aligned}
\sum_{j=1}^{2}\psi_j\Big\{ & <\Phi_{1,+}^*(\mu,0,\omega_{i+1})Q_{1,+}^*(\mu,0)\psi_j,\tilde{Q}_{i+1,\omega_{i+1}}(\mu)q_{i+1}^-(\mu)(-\omega_{i+1})>\\
& -<\Phi_{1,-}^*(\mu,0,-\omega_i)P_{1,-}^*(\mu,0)\psi_j,\tilde{P}_{i,\omega_i}(\mu)q_{i-1}^+(\mu)(\omega_i)>\Big\}
\end{aligned}
\tag{5.57}
$$

We have the following representation of the above terms, due to Theorems 6.3.1 and 6.3.3:

$$
\begin{aligned}
\Phi_{1,+}^*(\mu,0,\omega_{i+1})Q_{1,+}^*(\mu,0)\psi_j &= \Psi_{p_1}(\mu,\omega_{i+1},0)\eta^+(\psi_j,\mu)+\cdots\\
\Phi_{1,-}^*(\mu,0,-\omega_i)P_{1,-}^*(\mu,0)\psi_j &= \Psi_{p_2}(\mu,-\omega_i,0)\eta^-(\psi_j,\mu)+\cdots\\
\tilde{Q}_{i+1,\omega_{i+1}}(\mu)q_2^-(\mu)(-\omega_{i+1}) &= \Phi_{p_1}(\mu,-\omega_{i+1},0)\eta^u(q_2^-(\mu)(0),\mu)+\cdots\\
\tilde{P}_{i,\omega_i}(\mu)q_2^+(\mu)(\omega_i) &= \Phi_{p_2}(\mu,\omega_i,0)\eta^s(q_2^+(\mu)(0),\mu)+\cdots
\end{aligned}
$$

where the dots denote terms of higher order than $\exp(-\rho(\mu)\omega)$, $\Psi_{p_i}(\mu,t,s)$ is the transition matrix of the equation $\dot{\psi}=-(D_xf(p_i,\mu))^*\psi$, and $\Phi_{p_i}(\mu,t,s)$ is the transition matrix of the equation $\dot{x} = D_x f(p_i, \mu)x$. From Theorems 6.3.1, 6.3.3, $\eta^+(\psi_j, \mu)$ (resp. $\eta^-(\psi_j, \mu)$) is an eigenvector of $-(D_x f(p_1, \mu))^*$ (resp. $-(D_x f(p_2, \mu))^*$) with respect to the eigenvalues $-\rho(\mu) \pm i\phi(\mu)$ (resp. $\rho(\mu) \pm i\phi(\mu)$). Similarly $\eta^u(q_2^-(\mu)(0), \mu)$ (resp. $\eta^s(q_2^+(\mu)(0), \mu)$) is an eigenvector of $D_x f(p_1, \mu)$ (resp. $D_x f(p_2, \mu)$) with respect to the eigenvalues $\rho(\mu) \pm i\phi(\mu)$ (resp. $-\rho(\mu) \pm i\phi(\mu)$). Now we have

$$\Psi_{p_1}(\mu, \omega_{i+1}, 0)\eta^+(\psi_j, \mu) = G_\mu e^{-\Lambda^* \omega_{i+1}} G_\mu^{-1} \eta^+(\psi_j, \mu),$$

where G_μ is a nonsingular matrix, and $-\Lambda^*$ is the block diagonalisation of $-(D_x f(p_1, \mu))^*$ with respect to the inner product $< \cdot, \cdot >$. Also

$$\Phi_{p_1}(\mu, -\omega_{i+1}, 0)\eta^u(q_2^-(\mu)(0), \mu) = (G_\mu^*)^{-1} e^{-\Lambda \omega_{i+1}} G_\mu^* \eta^u(q_2^-(\mu)(0), \mu),$$

with Λ the block diagonalisation of $D_x f(p_1, \mu)$. By construction, $G_\mu^{-1}\eta^+(\psi_j, \mu)$ and $G_\mu^* \eta^u(q_2^-(\mu)(0), \mu)$ are in the stable space of $e^{-\Lambda^* t}$ and unstable space of $e^{\Lambda t}$ respectively. Similar expressions also hold for the other terms. Now by using the equality $< A^{-1}x, A^*\psi > = < x, \psi >$ for a nonsingular matrix A, we may write

$$\begin{aligned}
&< \Psi_{p_1}(\mu, \omega_{i+1}, 0)\eta^+(\psi_j, \mu), \Phi_{p_1}(\mu, -\omega_{i+1}, 0)\eta^u(q_2^-(\mu)(0), \mu) > \\
&\qquad = < G_\mu e^{-\Lambda^* \omega_{i+1}} G_\mu^{-1} \eta^+(\psi_j, \mu), (G_\mu^*)^{-1} e^{-\Lambda \omega_{i+1}} G_\mu^* \eta^u(q_2^-(\mu)(0), \mu) > \\
&\qquad = < e^{-\Lambda^* \omega_{i+1}} G_\mu^{-1} \eta^+(\psi_j, \mu), e^{-\Lambda \omega_{i+1}} G_\mu^* \eta^u(q_2^-(\mu)(0), \mu) > \\
&= e^{-2\rho(\mu)\omega_{i+1}} \left\langle \begin{bmatrix} \cos(\phi(\mu)\omega_{i+1}) & -\sin(\phi(\mu)\omega_{i+1}) & 0 \\ \sin(\phi(\mu)\omega_{i+1}) & \cos(\phi(\mu)\omega_{i+1}) & 0 \\ 0 & 0 & e^{(\lambda(\mu)+\rho(\mu))\omega_{i+1}} \end{bmatrix} \begin{bmatrix} \eta_1^+(\mu) \\ \eta_2^+(\mu) \\ 0 \end{bmatrix}, \right. \\
&\qquad \left. \begin{bmatrix} \cos(\phi(\mu)\omega_{i+1}) & \sin(\phi(\mu)\omega_{i+1}) & 0 \\ -\sin(\phi(\mu)\omega_{i+1}) & \cos(\phi(\mu)\omega_{i+1}) & 0 \\ 0 & 0 & e^{(\lambda(\mu)+\rho(\mu))\omega_{i+1}} \end{bmatrix} \begin{bmatrix} \eta_1^u(\mu) \\ \eta_2^u(\mu) \\ 0 \end{bmatrix} \right\rangle
\end{aligned} \tag{5.58}$$

where

$$\left\langle \begin{bmatrix} \eta_1^+(\mu) \\ \eta_2^+(\mu) \\ 0 \end{bmatrix}, \begin{bmatrix} \eta_1^u(\mu) \\ \eta_2^u(\mu) \\ 0 \end{bmatrix} \right\rangle = \left\langle G_\mu^{-1}\eta^+(\psi_j,\mu), G_\mu^*\eta^u(q_2^-(\mu)(0),\mu)\right\rangle$$
$$= \left\langle \eta^+(\psi_j,\mu), \eta^u(q_2^-(\mu)(0),\mu)\right\rangle$$

Then the scalar product (5.58) gives

$$e^{-2\rho(\mu)\omega_{i+1}}(\eta_1^+(\mu)\eta_2^u(\mu) - \eta_2^+(\mu)\eta_1^u(\mu))\sin(2\phi(\mu)\omega_{i+1})$$
$$+(\eta_1^+(\mu)\eta_1^u(\mu) + \eta_2^+(\mu)\eta_2^u(\mu))\cos(2\phi(\mu)\omega_{i+1})). \tag{5.59}$$

Since $(\eta_1^+(\mu),\eta_2^+(\mu)) \neq (0,0)$, $(\eta_1^u(\mu),\eta_2^u(\mu)) \neq (0,0)$ and the standard scalar product between $(\eta_2^u(\mu), -\eta_1^u(\mu))$ and $(\eta_1^u(\mu),\eta_2^u(\mu))$ is zero, we have that $(\eta_1(\mu),\eta_2(\mu)) := (\eta_1^+(\mu)\eta_2^u(\mu)-\eta_2^+(\mu)\eta_1^u(\mu), \eta_1^+(\mu)\eta_1^u(\mu)+\eta_2^+(\mu)\eta_2^u(\mu)) \neq (0,0)$.

Now, using Lemma 6.4.1 we observe that

$$R\Phi_{1,+}^*(\mu,0,\omega_{i+1})Q_{1,+}^*(\mu,0)\psi_j = \Phi_{1,-}^*(\mu,0,-\omega_{i+1})P_{1,-}^*(\mu,0)R\psi_j,$$
$$R\tilde{Q}_{i+1,\omega_{i+1}}(\mu)q_{i+1}^-(\mu)(-\omega_{i+1}) = \tilde{P}_{i,\omega_{i+1}}(\mu)q_{i-1}^+(\mu)(\omega_{i+1})$$

Then we see that if $\omega_i = \omega_{i+1}$, we have

$$< \Phi_{1,+}^*(\mu,0,\omega_{i+1})Q_{1,+}^*(\mu,0)\psi_1, \tilde{Q}_{i+1,\omega_{i+1}}(\mu)q_{i+1}^-(\mu)(-\omega_{i+1}) >$$
$$- < \Phi_{1,-}^*(\mu,0,-\omega_i)P_{1,-}^*(\mu,0)\psi_1, \tilde{P}_{i,\omega_i}(\mu)q_{i-1}^+(\mu)(\omega_i) >$$
$$=< \Phi_{1,+}^*(\mu,0,\omega_i)Q_{1,+}^*(\mu,0)R\psi_1, R\tilde{P}_{i,\omega_i}(\mu)q_{i-1}^+(\mu)(\omega_i) >$$
$$- < R\Phi_{1,-}^*(\mu,0,-\omega_i)P_{1,-}^*(\mu,0)\psi_1, R\tilde{P}_{i,\omega_i}(\mu)q_{i-1}^+(\mu)(\omega_i) >$$
$$=< R\Phi_{1,-}^*(\mu,0,-\omega_i)P_{1,-}^*(\mu,0)\psi_1, R\tilde{P}_{i,\omega_i}(\mu)q_{i-1}^+(\mu)(\omega_i) >$$
$$- < R\Phi_{1,-}^*(\mu,0,-\omega_i)P_{1,-}^*(\mu,0)\psi_1, R\tilde{P}_{i,\omega_i}(\mu)q_{i-1}^+(\mu)(\omega_i) >$$
$$= 0.$$

In fact, from section 5.4.3 (see Remark 5.4.8), we see that if $\omega_{i-j} = \omega_{i+j+1}$ $(j = 0,1,2,\ldots)$ all the terms in the jump $\xi_i^\omega(\mu)$ are zero in the direction of ψ_1

(Fix R). Using the expression (5.59) (similar for the other terms), we obtain

$$\begin{aligned}
&\sum_{j=1}^{2}\psi_j \Big\{< \Phi^*_{1,+}(\mu,0,\omega_{i+1})Q^*_{1,+}(\mu,0)\psi_j, \tilde{Q}_{i+1,\omega_{i+1}}(\mu)q^-_{i+1}(\mu)(-\omega_{i+1}) > \\
&\qquad\qquad - < \Phi^*_{1,-}(\mu,0,-\omega_i)P^*_{1,-}(\mu,0)\psi_j, \tilde{P}_{i,\omega_i}(\mu)q^+_{i-1}(\mu)(\omega_i) >\Big\} \\
&= \sum_{j=1}^{2}\psi_j \left\{e^{-2\rho(\mu)\omega_{i+1}}\left(\eta^j_{1,+}(\mu)\sin(2\phi(\mu)\omega_{i+1}) + \eta^j_{2,+}(\mu)\cos(2\phi(\mu)\omega_{i+1})\right)\right. \\
&\qquad \left. -e^{-2\rho(\mu)\omega_i}\left(\eta^j_{1,-}(\mu)\sin(2\phi(\mu)\omega_i) + \eta^j_{2,-}(\mu)\cos(2\phi(\mu)\omega_i)\right)\right\} + \cdots,
\end{aligned}$$

where $\eta^1_{1,+} = \eta^1_{1,-}$ and $\eta^1_{2,+} = \eta^1_{2,-}$. It can similarly be shown that $\eta^2_{1,+} = -\eta^2_{1,-}$ and $\eta^2_{2,+} = -\eta^2_{2,-}$. This follows from properties of $\Phi^*_{1,\pm}$, $\tilde{Q}$, $\tilde{P}$ when premultiplied by R, and that $< \cdot,\cdot >$ is R-invariant, $\psi_1 \in \text{Fix } R$, $\psi_2 \in \text{Fix } (-R)$.

There is an angle $\varphi^j_\pm$ such that

$$\begin{aligned}
\sin\varphi^j_\pm &= \eta^j_{1,\pm}/(\sqrt{(\eta^j_{1,\pm})^2 + (\eta^j_{2,\pm})^2}) \\
\cos\varphi^j_\pm &= \eta^j_{2,\pm}/(\sqrt{(\eta^j_{1,\pm})^2 + (\eta^j_{2,\pm})^2}).
\end{aligned} \tag{5.60}$$

Then

$$\begin{aligned}
\xi^\omega_i(\mu) &= \sum_{j=1}^{2}\psi_j \left\{e^{-2\rho(\mu)\omega_{i+1}}\left(\sqrt{(\eta^j_{1,+})^2 + (\eta^j_{2,+})^2}\sin(2\phi(\mu)\omega_{i+1} + \varphi^j_+)\right)\right. \\
&\qquad \left. -e^{-2\rho(\mu)\omega_i}\left(\sqrt{(\eta^j_{1,-})^2 + (\eta^j_{2,-})^2}\sin(2\phi(\mu)\omega_i + \varphi^j_-)\right)\right\} + \cdots,
\end{aligned}$$

with $\varphi^1_+ = \varphi^1_-$ and $\varphi^2_+ = \varphi^2_- + \pi$. Finally, combining the above together with (5.25) we obtain the following representation of $\Xi^\omega_i(\mu)$:

$$\begin{aligned}
\Xi^\omega_i(\mu) &= \psi_1\left\{c_1(\mu)e^{-2\rho(\mu)\omega_{i+1}}\sin(2\phi(\mu)\omega_{i+1} + \varphi^1)\right. \\
&\qquad \left. -c_1(\mu)e^{-2\rho(\mu)\omega_i}\sin(2\phi(\mu)\omega_i + \varphi^1) + o(e^{-2\rho(\mu)\min\{\omega_i,\omega_{i+1}\}})\right\} \\
&\quad +\psi_2\left\{(\mu-\mu_0) + c_2(\mu)e^{-2\rho(\mu)\omega_{i+1}}\sin(2\phi(\mu)\omega_{i+1} + \varphi^2)\right. \\
&\qquad \left. +c_2(\mu)e^{-2\rho(\mu)\omega_i}\sin(2\phi(\mu)\omega_i + \varphi^2) + o(e^{-2\rho(\mu)\min\{\omega_i,\omega_{i+1}\}})\right\},
\end{aligned} \tag{5.61}$$

with $c_1(\mu)$, $c_2(\mu)$ constants that do not equal zero for μ close enough to μ_0, and φ^1, φ^2 constants. It follows that we must have $\varphi^1 - \varphi^2 \neq \pi \pmod{2\pi}$ since otherwise equations (5.60) would imply that all $\eta^j_{i,\pm} = 0$. Equation (5.61) is the bifurcation equation for our problem.

Remark 5.5.1. *It is important to note that by reversibility and uniqueness, (5.61) has the property that if we permute the sequence* $\{\omega_i\}_{i\in\mathbb{Z}}$ *by the rule*

$$\omega^{new}_{i-k} = \omega_{i+k+1}, \qquad k \in \mathbb{Z},$$

then the sign of the ψ_1 *(Fix R) coordinate changes, where the terms in the* ψ_2 *coordinate remain identical.*

One way of viewing equation (5.61) (ignoring the higher order terms) is to think of it as the equations for two logarithmic spirals $\mathcal{S}^1$, $\mathcal{S}^2$ in the plane (spanned by the basis ψ_1, ψ_2), parametrised separately by ω_{i+1}, ω_i:

$$\mathcal{S}^1 : \qquad \begin{array}{c} c_1(\mu)e^{-2\rho(\mu)\omega_{i+1}}\sin(2\phi(\mu)\omega_{i+1}+\varphi^1)\psi_1 \\ +c_2(\mu)e^{-2\rho(\mu)\omega_{i+1}}\sin(2\phi(\mu)\omega_{i+1}+\varphi^2)\psi_2, \end{array}$$

$$\mathcal{S}^2 : \qquad \begin{array}{c} -c_1(\mu)e^{-2\rho(\mu)\omega_{i}}\sin(2\phi(\mu)\omega_{i}+\varphi^1)\psi_1 \\ +c_2(\mu)e^{-2\rho(\mu)\omega_{i}}\sin(2\phi(\mu)\omega_{i}+\varphi^2)\psi_2. \end{array}$$

These spirals have opposite winding direction. This is in direct analogy to the analysis carried out in chapter 4, and shows the geometrical meaning of equation (5.61). Similar to chapter 4, we would like these spirals to intersect each other transversally along Fix R. A simple calculation shows that these intersections are tangent if and only if $\varphi^1 - \varphi^2 = \tan^{-1}(\phi(\mu)/\rho(\mu)) \pmod{\pi}$. Therefore the analogous hypothesis to that in chapter 4 that we shall make is

$$\textbf{(H2)} \qquad \varphi^1 - \varphi^2 \neq \tan^{-1}\left(\frac{\phi(\mu)}{\rho(\mu)}\right) \pmod{\pi}.$$

This hypothesis is required to find locally unique solutions in the next section, but we emphasise that without this condition the intersections along Fix R of these two spirals still persist. In section 5.6 we shall effectively solve for the intersections of the two spirals in the search for orbits found in Theorem 5.6.2. We will focus on the intersections that are present independent of the constants in equation (5.61), but there may be many more intersections (and hence many more solutions) as we sketch here.

Figure 5.4 shows the two possibilities for the topology of the spirals corresponding to the two cases $0 < \varphi^1 - \varphi^2 < \tan^{-1}(\phi(\mu)/\rho(\mu))$, $\tan^{-1}(\phi(\mu)/\rho(\mu)) < \varphi^1 - \varphi^2 < \pi$. In the second case the spirals have more (asymmetric) intersections, see also section 4.3 and Figure 4.3. However, in each case there may be many more intersections, depending on the ratio $\rho(\mu)/\phi(\mu)$, see Figure 5.5. This ratio acts as a damping term for the spirals. We note again that these extra intersections are asymmetric, and the number of intersections do not depend on the constants $c_1(\mu)$, $c_2(\mu)$. It is interesting to remark that in the unfolding of the reversible Hopf-zero bifurcation as in chapter 3, the ratio $\rho(\mu)/\phi(\mu)$ will be arbitrarily small in a neighbourhood of the singularity, and so heteroclinic cycle bifurcations occuring in the unfolding will have an arbitrarily large number of extra intersections of the spirals $\mathcal{S}_0$ and $\mathcal{S}_1$, leading to increasingly rich dynamics in the neighbourhood of the heteroclinic cycle bifurcations as the singularity is approached.

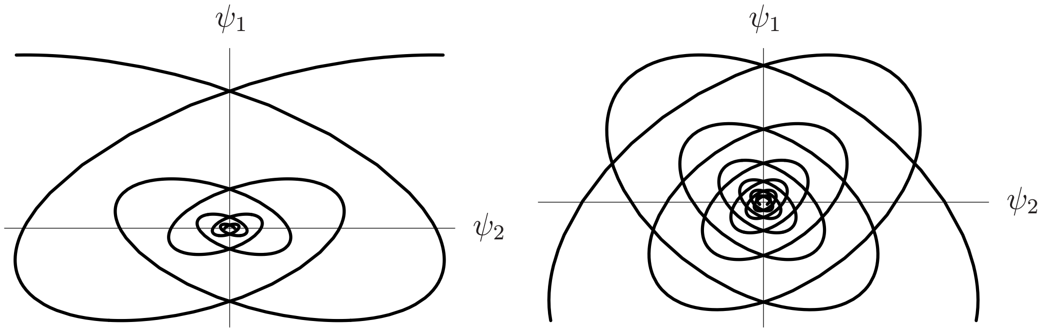

Figure 5.4: The spirals $\mathcal{S}^1$, $\mathcal{S}^2$, shown first for $\tan^{-1}(\phi(\mu)/\rho(\mu)) < \varphi^1 - \varphi^2 < \pi$ (mod π), and second for $0 < \varphi^1 - \varphi^2 < \tan^{-1}(\phi(\mu)/\rho(\mu))$ (mod π).

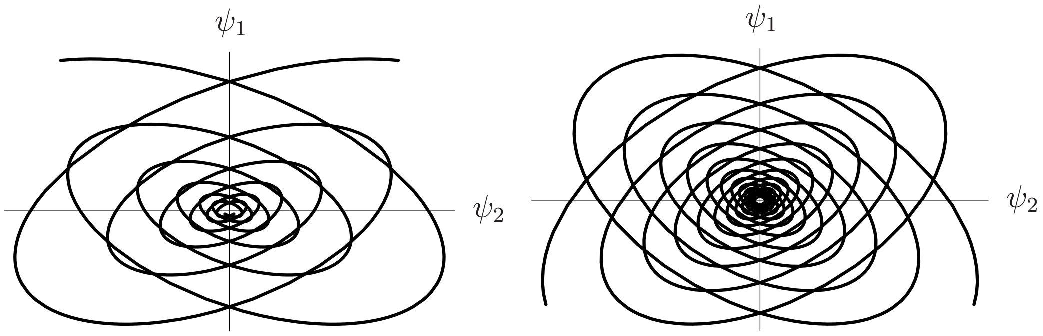

Figure 5.5: The spirals $\mathcal{S}^1$, $\mathcal{S}^2$ shown for lower values of the ratio $\rho(\mu)/\phi(\mu)$. Again, the case $\tan^{-1}(\phi(\mu)/\rho(\mu)) < \varphi^1 - \varphi^2 < \pi$ (mod π) is shown first, and the case $0 < \varphi^1 - \varphi^2 < \tan^{-1}(\phi(\mu)/\rho(\mu))$ (mod π) is shown second.

5.6 Bifurcation Analysis

In this section we shall study equation (5.61) to analyse the nearby dynamics of the heteroclinic cycle. Let us first recover some terminology.

Definition 5.6.1.

- *A periodic orbit is said to have index k (or it is a k-periodic orbit) if it passes through Σ_1 (or Σ_2) k times.*
- *A homoclinic orbit to p_i is said to have index k (or it is a k-homoclinic orbit) if it passes through Σ_1 (or Σ_2) k times.*
- *A heteroclinic orbit connecting p_2 to p_1 is called a 1D heteroclinic orbit.*

A 1D heteroclinic orbit that passes k times through Σ_1 is called a 1D heteroclinic orbit of index k (or a k-1D heteroclinic orbit).

- *A heteroclinic orbit connecting p_1 to p_2 is called a 2D heteroclinic orbit. A 2D heteroclinic orbit that passes k times through Σ_2 is called a 2D heteroclinic orbit of index k (or a k-2D heteroclinic orbit).*

The main results are summarised in the following Theorem.

Theorem 5.6.2. *1. There is a 1 parameter family of symmetric 1-periodic orbits close to the heteroclinic cycle. The family is parametrised by period, and the periodic orbits converge to the heteroclinic cycle as the period tends to infinity.*

2. *There is a countable set of parameter values, converging exponentially to $\mu = \mu_0$ from both sides, for which there exists a k-homoclinic orbit to each fixed point p_i, for each $k \in \mathbb{N}$.*

3. *There is a countable set of parameter values, converging exponentially to $\mu = \mu_0$ from both sides, for which there exists a k-1D heteroclinic orbit, for $k \geq 2$.*

4. *There is a countable set of parameter values, converging exponentially to $\mu = \mu_0$ from both sides, for which there exists a k-2D heteroclinic orbit, for $k \geq 2$.*

5. *At $\mu = \mu_0$, there exists an invariant set which is topologically conjugate to a full shift on n symbols, for any n. Each set is indecomposable, and setwise symmetric. The collection of all these sets exists only for $\mu = \mu_0$, although each set is individually structurally stable.*

5.6.1 Periodic Orbits Of Index 1

To find 1-periodic orbits from equation (5.61) we have to solve the equations

$$\Xi_1^\omega(\mu) = 0$$

That is,

$$\begin{aligned} c_1(\mu)e^{-2\rho(\mu)\omega_2}\sin(2\phi(\mu)\omega_2+\varphi^1) - c_1(\mu)e^{-2\rho(\mu)\omega_1}\sin(2\phi(\mu)\omega_1+\varphi^1) & \\ +o(e^{-2\rho(\mu)\min\{\omega_1,\omega_2\}}) &= 0 \end{aligned} \tag{5.62}$$

$$\begin{aligned} (\mu-\mu_0) + c_2(\mu)e^{-2\rho(\mu)\omega_2}\sin(2\phi(\mu)\omega_2+\varphi^2) & \\ +c_2(\mu)e^{-2\rho(\mu)\omega_1}\sin(2\phi(\mu)\omega_1+\varphi^2) + o(e^{-2\rho(\mu)\min\{\omega_1,\omega_2\}}) &= 0 \end{aligned} \tag{5.63}$$

We first consider symmetric 1-periodic orbits. A 1-periodic orbit is symmetric if and only if $\omega_1 = \omega_2$, and we note that by Remark 5.5.1, this implies that (5.62) is automatically satisfied. Then the bifurcation equation for symmetric 1-periodic orbits reduces down to a 1-dimensional equation:

$$(\mu-\mu_0) + 2c_2(\mu)e^{-2\rho(\mu)\omega}\sin(2\phi(\mu)\omega+\varphi^2) + o(e^{-2\rho(\mu)\omega}) = 0 \tag{5.64}$$

By (5.64) and using the Implicit Function Theorem, we have that at $\mu = \mu_0$, there is a countably infinite set of 1-periodic orbits, with difference in period asymptotically tending to $\pi/2\phi(\mu)$. For $\mu \neq \mu_0$ there are finitely many 1-periodic orbits. With the addition of the parameter to the phase space these periodic orbits form a 1 parameter family parametrised by period, see Figure 5.6.

Remark 5.6.3. *Strictly, we have to solve a system of equations in $l^\infty_{\mathbb{R}\times\mathbb{R}}$ and use uniqueness to find periodic orbits. This system would consist of infinitely many copies of equations (5.62), (5.63).*

The oscillatory behaviour exhibited in Figure 5.6 is characteristic of the Shil'nikov homoclinic orbit to a saddle-focus under certain eigenvalue conditions, where there exists chaotic dynamics [40]. This represents a marked

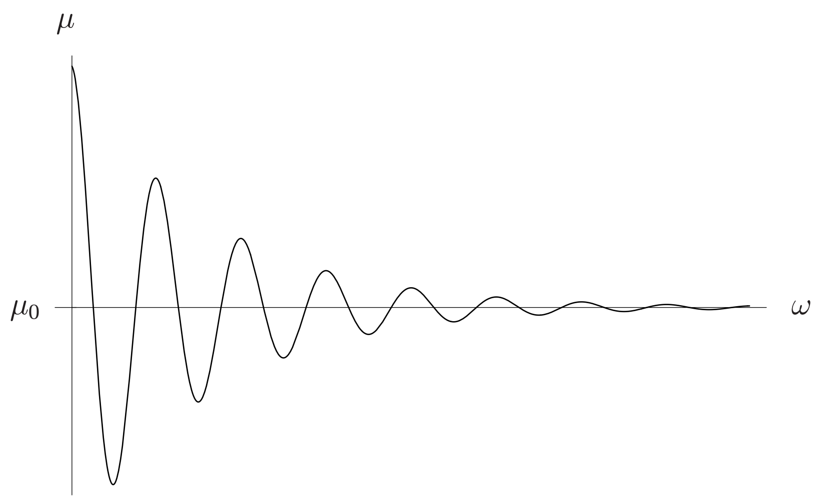

Figure 5.6: Bifurcation diagram for 1-periodic orbits.

difference in our analysis: we do not require any eigenvalue condition to have this oscillatory behaviour. This is due to the fact that only the real part of the complex eigenvalues of p_i appears in the bifurcation equations; $\lambda(\mu)$ does not appear. This is an important consequence of the two fixed points having different indices. We will see that in addition, there must also automatically be chaotic dynamics present in our situation, see section 5.6.5.

We also note that equations (5.62), (5.63) can be solved to find more families of 1-periodic orbits where $\omega_1 \neq \omega_2$, and that equations (5.62), (5.63) might also possibly be solved to find more families of 1-periodic orbits at $\mu = \mu_0$ where $\omega_1 \neq \omega_2$. These are asymmetric periodic orbits that exist for $|\mu - \mu_0|$ sufficiently small. As previously mentioned, the existence of these asymmetric orbits is guaranteed if the condition $0 < \varphi^1 - \varphi^2 < \tan^{-1}(\phi(\mu)/\rho(\mu)) \pmod{\pi}$ is satisfied. We may also obtain asymmetric 1-periodic orbits if the damping ratio $\rho(\mu)/\phi(\mu)$ is small enough, although we omit the details here.

Such asymmetric 1-periodic orbits are associated to the families of homoclinic orbits to each fixed point, see section 5.6.4. In the infinite-period limit, they may be continued to a homoclinic orbit that exists for some $\mu \neq \mu_0$.

5.6.2 1D Heteroclinic Orbits

It is clear that there can only be at most one 1D heteroclinic orbit for each parameter value, and furthermore this such a connection must be symmetric. From $\xi_1^\infty(\mu)$ we already saw that there is just one 1-1D heteroclinic orbit, and this is the original connection that exists at $\mu = \mu_0$. We can recover the equation for $\xi_1^\infty(\mu)$ by setting $\omega = \infty$ in equation (5.64). Actually, this gives the bifurcation equation for heteroclinic cycles consisting of a 1-1D heteroclinic and a 1-2D heteroclinic, but by section 5.3.2 the original 1-2D heteroclinic connection is stable and unique, and so we really recover $\xi_1^\infty(\mu)$.

Now we will search for k-1D heteroclinic orbits for $k > 1$. In order to analyse such connections using equation (5.61), we will in fact search for heteroclinic cycles, always using the connection $q_2(\mu)(t)$ to complete the cycle. To find these heteroclinic cycles we will set $\omega_2 = \omega_3 = \infty$, and we will make the sequence $\{\omega_i\}_{i\in\mathbb{Z}}$ $2k$-periodic. In this case setting $\Xi_1^\omega(\mu) = 0$, $\Xi_3^\omega(\mu) = 0$ gives

$$-c_1(\mu)e^{-2\rho(\mu)\omega_1}\sin(2\phi(\mu)\omega_1 + \varphi^1) + o(e^{-2\rho(\mu)\omega_1}) = 0 \quad (5.65)$$

$$(\mu - \mu_0) + c_2(\mu)e^{-2\rho(\mu)\omega_1}\sin(2\phi(\mu)\omega_1 + \varphi^2) + o(e^{-2\rho(\mu)\omega_1}) = 0 \quad (5.66)$$

$$c_1(\mu)e^{-2\rho(\mu)\omega_4}\sin(2\phi(\mu)\omega_4 + \varphi^1) + o(e^{-2\rho(\mu)\omega_4}) = 0 \quad (5.67)$$

$$(\mu - \mu_0) + c_2(\mu)e^{-2\rho(\mu)\omega_4}\sin(2\phi(\mu)\omega_4 + \varphi^2) + o(e^{-2\rho(\mu)\omega_4}) = 0 \quad (5.68)$$

We first consider (5.65). The $o(e^{-2\rho(\mu)\omega_1})$ term can be made arbitrarily small with respect to the leading order terms by taking ω_1 sufficiently large. It is easy to see that the equation

$$-c_1(\mu)e^{-2\rho(\mu)\omega_1}\sin(2\phi(\mu)\omega_1 + \varphi^1) = 0$$

can be solved to give $\omega_1 = (n\pi - \varphi^1)/2\phi(\mu)$ for $n \in \mathbb{N}$ sufficiently large. Now we may use the Implicit Function Theorem to show that equation (5.65) has, for each μ close to μ_0, countably many solutions $\omega^1_\mu(n)$, $n \in \mathbb{N}$ sufficiently large, where $\omega^1_\mu(n) \approx (n\pi - \varphi^1)/2\phi(\mu)$ as $n \to \infty$. The superscript 1 appears since the other ω_i appear in equation (5.65) in the higher order terms. Substituting this into equation (5.66) now gives (asymptotically):

$$(\mu - \mu_0) + (-1)^n c'_2(\mu) \exp(-\frac{\rho(\mu)}{\phi(\mu)}(n\pi - \varphi^1)) + \cdots = 0, \tag{5.69}$$

where $c'_2(\cdot)$ is a constant which does not equal zero for μ close enough to μ_0, and the ellipsis denotes arbitrarily small terms. From equation (5.69) we see that each $\omega^1_\mu(n)$ solves equations (5.65), (5.66) for a discrete set of parameter values, which accumulate exponentially to $\mu = \mu_0$ from both sides as $n \to \infty$. Call this sequence $\mu(n)$. Note that this sequence does in fact depend also on all the other ω_i, since these are contained in the higher order terms.

Similarly we can independently solve equations (5.67), (5.68) for $\omega_4 = \omega^3_\mu(n)$, where $\omega^3_\mu(n)$ are the zeros of (5.67), $n \in \mathbb{Z}$. Clearly we can only simultaneously solve equations (5.65)–(5.68) if equation (5.65) is identical to equation (5.67) (apart from a change of sign), and (5.66) is identical to (5.68). By Remark 5.5.1 we deduce that this is true if and only if the entire sequence $\{\omega_i\}_{i\in\mathbb{Z}}$ satisfies the following condition:

$$\omega_{k+l} = \omega_{k+j}, \qquad l, j \in \mathbb{Z}, \quad l + j = 5 \pmod{2k}. \tag{5.70}$$

In this case $\omega^1_\mu(n) = \omega^3_\mu(n)$. Condition (5.70) confirms that the desired 1D connection is symmetric.

If we would like to find 2-1D heteroclinic orbits then we solve the system of equations in $l^\infty_{\mathbb{R}\times\mathbb{R}}$ consisting of infinitely many copies of equations (5.65)–(5.68). Then the 2-1D heteroclinic orbits exist for a countable set of parameter values $\mu(n)(n \in \mathbb{Z})$ which accumulate exponentially to $\mu = \mu_0$, given by (5.69). These parameter values can be parametrised by the return times on the second loop. Suppose $\omega_1 = \omega_4 = \omega^1_\mu(n_1)$, then $\mu = \mu(n_1)$. Note that the 2-1D heteroclinic orbits intersect Fix R in the section Σ_2 close to $q_2(\mu)(0)$ since $\overline{z}_0(t; \omega^1_\mu(n_1), \omega^1_\mu(n_1), \mu)$ here is symmetric.

If we would now like to find k-1D heteroclinic orbits, then we need to solve equations (5.65)–(5.68), and also the system

$$\Xi_i^\omega(\mu) = 0, \qquad i = 5, 7, 9, \ldots, 2k-1. \tag{5.71}$$

These equations are decoupled over i, and they have the form

$$\begin{aligned} c_1(\mu)e^{-2\rho(\mu)\omega_{i+1}}\sin(2\phi(\mu)\omega_{i+1}+\varphi^1) - c_1(\mu)e^{-2\rho(\mu)\omega_i}\sin(2\phi(\mu)\omega_i+\varphi^1) & \\ +o(e^{-2\rho(\mu)\min\{\omega_i,\omega_{i+1}\}}) &= 0, \end{aligned} \tag{5.72}$$

$$\begin{aligned} (\mu-\mu_0) + c_2(\mu)e^{-2\rho(\mu)\omega_{i+1}}\sin(2\phi(\mu)\omega_{i+1}+\varphi^2) & \\ +c_2(\mu)e^{-2\rho(\mu)\omega_i}\sin(2\phi(\mu)\omega_i+\varphi^2) + o(e^{-2\rho(\mu)\min\{\omega_i,\omega_{i+1}\}}) &= 0. \end{aligned} \tag{5.73}$$

Consider the case when k is odd. Then the 1D heteroclinic orbit will intersect Fix R in Σ_1. Condition (5.70) says that $\omega_{k+2} = \omega_{k+3}$ and the equations for Ξ_{k+2} reduces to the one dimensional equation

$$(\mu-\mu_0) + 2c_2(\mu)e^{-2\rho(\mu)\omega_{k+2}}\sin(2\phi(\mu)\omega_{k+2}+\varphi^2) + o(e^{-2\rho(\mu)\omega_{k+2}}) = 0. \tag{5.74}$$

Recall we can solve equations (5.65)–(5.68) to obtain the parameter value $\mu(n_1)$ (depending on the value of the ω_i). It is clear that for ω_1, ω_4 large enough, the above equation can be solved to find (finitely many) $\omega_{k+2} = \omega_{k+3}$ for a given $\mu(n_1)$. As $n_1 \to \infty$, ω_{k+2} tends to some $\omega_\mu^{k+2}(n_{k+2})$, where $\omega_\mu^{k+2}(n_{k+2})$ is a zero of (5.74) at $\mu = \mu_0$.

Now we have to solve the remaining equations in the system (5.71). Due to the symmetry properties of the sequence $\{\omega_i\}_{i\in\mathbb{Z}}$, we have that in addition to equations (5.72) and (5.73), the equations for $\Xi_{4-i}^\omega(\mu)$ (the subscript taken mod $2k$) yield

$$c_1(\mu)e^{-2\rho(\mu)\omega_i}\sin(2\phi(\mu)\omega_i+\varphi^1)-c_1(\mu)e^{-2\rho(\mu)\omega_{i+1}}\sin(2\phi(\mu)\omega_{i+1}+\varphi^1) +o(e^{-2\rho(\mu)\min\{\omega_i,\omega_{i+1}\}}) = 0, \tag{5.75}$$

$$(\mu-\mu_0)+c_2(\mu)e^{-2\rho(\mu)\omega_i}\sin(2\phi(\mu)\omega_i+\varphi^2) +c_2(\mu)e^{-2\rho(\mu)\omega_{i+1}}\sin(2\phi(\mu)\omega_{i+1}+\varphi^2)+o(e^{-2\rho(\mu)\min\{\omega_i,\omega_{i+1}\}}) = 0. \tag{5.76}$$

It is important to note that if we suppose $\omega_i \neq \omega_{i+1}$, the higher order terms in these equations are different to those in equations (5.72), (5.73). Therefore we cannot solve equations (5.72) and (5.75) by choosing different values for ω_i and ω_{i+1} such that

$$c_1(\mu)e^{-2\rho(\mu)\omega_i}\sin(2\phi(\mu)\omega_i+\varphi^1)-c_1(\mu)e^{-2\rho(\mu)\omega_{i+1}}\sin(2\phi(\mu)\omega_{i+1}+\varphi^1)=0$$

and use the Implicit Function Theorem. However if we set first $\omega_i=\omega_{i+1}$ then we satisfy the above equation and we can solve (5.72), (5.75) using the Implicit Function Theorem to find ω_i almost equal to ω_{i+1}. Using again Remark 5.5.1 and (5.70), equations (5.73) and (5.76) can then be trivially solved (recall $\mu=\mu(n_1)$, some n_1) to find finitely many $\omega_i \approx \omega_{i+1}$. We have that ω_i, $\omega_{i+1}\approx\omega_\mu^i(n_i)$ (zeros of (5.73) at $\mu=\mu_0$) as $n_1\to\infty$.

It remains to consider the case when k is even. In this case the 1D heteroclinic orbit will intersect Fix R in Σ_2. As before, using (5.70) and Remark 5.5.1 we find that

$$\left.\begin{array}{l}\omega_{k+2-2j}\approx\omega_{k+1-2j}\\ \omega_{k+4+2j}\approx\omega_{k+3+2j}\end{array}\right\}\quad j=0,\ldots,(k-4)/2.$$

The equations (5.72) and (5.73) are solved in the same way to obtain (finitely many) solutions ω_i, ω_{i+1}, where each ω_i, ω_{i+1} tends to some $\omega_\mu^i(n_i)$ as $n_1\to\infty$.

This completes the proof of the existence of k-1D heteroclinic orbits, for any k.

5.6.3 2D Heteroclinic Orbits

As noted in the previous section, by section 5.3.2 there is a unique, stable 1-2D heteroclinic connection for μ close to μ_0. Then we will search for k-2D heteroclinic connections for $k \geq 2$. To find these from equations (5.61) we will search for 'cycles' that consist of the k-2D heteroclinic connections together with the solutions $q_1^{\pm}(\mu)(t)$. Then we set $\omega_1 = \omega_2 = \infty$ and $\omega_3, \omega_4 \neq \infty$, and make the sequence $\{\omega_i\}_{i\in\mathbb{Z}}$ $2k$-periodic. In this case the equations $\Xi_1^{\omega}(\mu)$ become those for $\xi_1^{\infty}(\mu)$. We are not interested here in setting $\Xi_1^{\omega}(\mu) = 0$ (this would yield only the solution $\mu = \mu_0$). To find k-2D heteroclinic orbits then we need to solve the equations

$$\Xi_i^{\omega}(\mu) = 0, \qquad i = 3, 5, \ldots, 2k-1. \tag{5.77}$$

This system is identical to equations (5.72) and (5.73). We will first search for 2D heteroclinic orbits that exist at $\mu = \mu_0$.

We first study 2-2D heteroclinic orbits, in this case we only have to solve (5.77) for $i = 3$. Consider first equation (5.72). We see that we can first solve the following equation for a continuous choice of values for ω_i and ω_{i+1}:

$$e^{-2\rho(\mu)\omega_{i+1}} \sin(2\phi(\mu)\omega_{i+1} + \varphi^1) - e^{-2\rho(\mu)\omega_i} \sin(2\phi(\mu)\omega_i + \varphi^1) = 0. \tag{5.78}$$

Provided that not both ω_i, ω_{i+1} are at turning points of the sine functions, we can solve then use the Implicit Function Theorem to solve equation (5.72). Clearly as ω_i, ω_{i+1} tend to infinity their true values converge to the solutions of (5.78). Consider now equation (5.73) and set $\mu = \mu_0$. If we choose values of ω_i, ω_{i+1} such that $\omega_i = \omega_{i+1}$ in (5.78) (before using the Implicit Function Theorem) then we can solve equation (5.73) to find ω_i, ω_{i+1} close to $\omega_{\mu}^i(n_i)$. Recall $k = 2$, then by Remark 5.5.1 and uniqueness of the Implicit Function Theorem we see that in fact ω_i precisely equals ω_{i+1}. Thus these 2-2D heteroclinic orbits that exist at $\mu = \mu_0$ are symmetric, and they intersect Fix R in Σ_1, close to $q_1(\mu_0)(0)$. We can use the Implicit Function Theorem again to show that such heteroclinic connections persist for μ close to μ_0. Similar to the 1-periodic orbits, depending on the constants $\varphi^1, \varphi^2, \rho(\mu), \phi(\mu)$ we may also be able to find asymmetric 2-2D heteroclinic connections.

Now we will study k-2D heteroclinic orbits for $k \geq 3$. We solve equations (5.77) in the same way, to find the ω_i, ω_{i+1} close to $\omega_\mu^i(n_i)$ ($j = 3, 4, \ldots, 2k-1$). In the case $k \geq 3$ we can always have symmetric and asymmetric 2D heteroclinic orbits. This depends only on the choice of the $\omega_\mu^i(n_i)$; if the sequence satisfies the condition

$$\omega_\mu^{k+l}(n_{k+l}) = \omega_\mu^{k+j}(n_{k+j}), \qquad l, j \in \mathbb{Z}, \quad l + j = 3 \pmod{2k}, \tag{5.79}$$

then the corresponding k-2D heteroclinic orbit is symmetric. Otherwise it is not. To see this we need Remark 5.5.1 and uniqueness of the Implicit Function Theorem. We can similarly show that all these heteroclinic connections are stable under perturbation of the parameter. The precise structure of the set of k-2D heteroclinic orbits will again depend on the constants $\varphi^1, \varphi^2, \rho(\mu), \phi(\mu)$.

We have solved (5.72), (5.73) at $\mu = \mu_0$ and found that we may always solve for $\omega_i \approx \omega_{i+1}$ (possibly exactly equal). Consider now equations (5.72), (5.73) at $\mu \neq \mu_0$. Then we may, for example, take first $\omega_3 \neq \omega_4$ to solve (5.78) and use the Implicit Function Theorem to solve (5.72). Then these values will solve (5.73) for some $\mu \neq \mu_0$. We can then certainly solve the remaining equations (5.77) in the same way as before, to find additional k-2D heteroclinic orbits for $k \geq 2$. We expect that the complete set of bifurcating 2D heteroclinic orbits for $\mu \neq \mu_0$ would be very complicated, and may depend sensitively on the precise unfolding of the heteroclinic cycle. However there will be countably many bifurcating heteroclinic orbits for each $k \geq 2$. Arguments similar to those used in the study of the 1D heteroclinic orbits imply that such 2D heteroclinic connections must in fact be asymmetric. Note that if (5.79) is satisfied and $\omega_i = \omega_{i+1}$, $i = 3, 5, \ldots, 2k-1$, then the corresponding heteroclinic orbit will be the continuation of one found at $\mu = \mu_0$. We can also deduce that these heteroclinic connections are sequentially removed in tangent bifurcations as μ varies from μ_0.

This completes the proof of the existence of the k-2D heteroclinic orbits, for any k.

5.6.4 Homoclinic Orbits

Unlike the heteroclinic connections, homoclinic orbits to either p_1 or p_2 cannot be symmetric, however they must occur in symmetric pairs. We will consider then only homoclinic orbits to the fixed point p_2. If we first study 1-homoclinic orbits, then we must set $\omega_1 = \infty$, and we obtain:

$$c_1(\mu)e^{-2\rho(\mu)\omega_2}\sin(2\phi(\mu)\omega_2 + \varphi^1) + o(e^{-2\rho(\mu)\omega_2}) = 0 \quad (5.80)$$

$$(\mu - \mu_0) + c_2(\mu)e^{-2\rho(\mu)\omega_2}\sin(2\phi(\mu)\omega_2 + \varphi^2) + o(e^{-2\rho(\mu)\omega_2}) = 0 \quad (5.81)$$

First we solve the first equation (using the Implicit Function Theorem) to show that $\omega_2 = (n\pi - \varphi^1)/2\phi(\mu)$, for $n \in \mathbb{N}$ larger than some positive integer N_0, asymptotically as $n \to \infty$. Substituting in the second equation gives:

$$(\mu - \mu_0) + (-1)^n c_2'(\mu)\exp(-\frac{\rho(\mu)}{\phi(\mu)}(n\pi - \varphi^1)) + \cdots = 0 \quad (5.82)$$

Then there are a countable infinity of 1-homoclinic orbits in parameter space, each at discrete parameter values accumulating exponentially from both sides to $\mu = \mu_0$.

From previous studies we would expect that each such 1-homoclinic orbit would infer the existence of a one parameter family of periodic orbits, parametrised by period and lying asymptotic to the homoclinic orbit in period-parameter space. Consider again equations (5.62), (5.63). As mentioned before, as well as the family of symmetric periodic orbits ($\omega_1 = \omega_2$), these equations may be solved to find asymmetric periodic orbits. As before, we first solve

$$e^{-2\rho(\mu)\omega_2}\sin(2\phi(\mu)\omega_2 + \varphi^1) - e^{-2\rho(\mu)\omega_1}\sin(2\phi(\mu)\omega_1 + \varphi^1) = 0 \quad (5.83)$$

to find some $\omega_1 \neq \omega_2$, and solve (5.62) using the Implicit Function Theorem. Substituting these values into (5.63) then gives a value for $\mu \neq \mu_0$. As before, (5.83) can be solved for a continuous set of ω_1, ω_2 and in fact we may think of fixing ω_2 around $(n_2\pi - \varphi^1)/2\phi(\mu)$ ($n_2 \in \mathbb{Z}$ sufficiently large) and continuing ω_1 to infinity. This provides a smooth variation in μ and thus continues the periodic orbit to the corresponding homoclinic orbit found above. It is well known that the ratio of the (leading) expanding and contracting eigenvalues of the fixed point of such a homoclinic orbit determines the manner of approach for the local one parameter family of periodic orbits. That is, the periodic orbit could oscillate to homoclinicity (as in Figure 5.6), or approach monotonically as the period goes to infinity. But equations (5.62), (5.63) have no information about the ratio of eigenvalues of the fixed points; at least the real eigenvalue $\lambda(\mu)$ is not present in the leading order terms.

We may solve (5.62) as mentioned before, for a continuous set of values for ω_1, ω_2 as $\omega_1 \to \infty$. Then we can obtain a function $\omega_2 = \omega_2(\omega_1)$ that solves (5.62). It is easy to see that $\omega_2(\omega_1) \sim e^{-2\rho(\mu)\omega_1}$. Then if we substitute this function into (5.63), we obtain a function $\mu = \mu(\omega_1)$, which would determine the nature of the approach of the periodic orbit to homoclinicity. However, clearly now the higher order terms become important in this equation, and the leading order terms are no longer dominant as $\omega_1 \to \infty$. Therefore the behaviour of the periodic orbit is determined by the higher order terms, as we should expect.

We would now like to similarly study the existence of k-homoclinic orbits. Then in addition to (5.80), (5.81), we need to solve the following equations:

$$\Xi_i^\omega(\mu) = 0, \qquad i = 3, 5, \ldots, 2k-1. \tag{5.84}$$

These equations are again identical to (5.72) and (5.73). Similar to before, we first solve equation (5.78) for a continuous choice of values of ω_i, ω_{i+1} and solve (5.72) using the Implicit Function Theorem. To solve (5.73), we first note that μ is given (for a discrete set of points) by equation (5.82). For any value of μ we can solve (5.73) by first setting $\omega_i = \omega_{i+1}$ in (5.78) to find (using the Implicit Function Theorem) solutions $\omega_i \approx \omega_{i+1}$ to (5.72), (5.73). As ω_2 gets large, ω_i, ω_{i+1} converge to some $\omega^i_\mu(n_i)$ $(n_i \in \mathbb{Z})$; $\omega^i_\mu(n_i)$ are defined to be the zeros of (5.73) for $\mu = \mu_0$. As before, the set of solutions to (5.72), (5.73) depend on the constants $\varphi^1, \varphi^2, \rho(\mu), \phi(\mu)$.

For a given value of μ (sufficiently close to μ_0), and for all the ω_i, ω_{i+1} sufficiently large, there is some $\omega_i \neq \omega_{i+1}$ that solve (5.78) such that we can also solve (5.72), (5.73) (using the Implicit Function Theorem). This gives an additional countably infinite family of homoclinic orbits. As for the asymmetric 2D heteroclinic orbits that do not exist at $\mu = \mu_0$, the structure of this family is complicated and may depend sensitively on the unfolding parameter.

5.6.5 Symbolic Dynamics

We now finally use the representation (5.61) to deduce the existence of symbolic dynamics. Recall again the equations for $\Xi^\omega_i(\mu) = 0$ (i an odd integer):

$$\begin{aligned} c_1(\mu)e^{-2\rho(\mu)\omega_{i+1}}\sin(2\phi(\mu)\omega_{i+1} + \varphi^1) - c_1(\mu)e^{-2\rho(\mu)\omega_i}\sin(2\phi(\mu)\omega_i + \varphi^1) & \\ + o(e^{-2\rho(\mu)\min\{\omega_i,\omega_{i+1}\}}) &= 0, \end{aligned} \tag{5.85}$$

$$\begin{aligned} (\mu - \mu_0) + c_2(\mu)e^{-2\rho(\mu)\omega_{i+1}}\sin(2\phi(\mu)\omega_{i+1} + \varphi^2) & \\ + c_2(\mu)e^{-2\rho(\mu)\omega_i}\sin(2\phi(\mu)\omega_i + \varphi^2) + o(e^{-2\rho(\mu)\min\{\omega_i,\omega_{i+1}\}}) &= 0. \end{aligned} \tag{5.86}$$

Here we will set $\mu = \mu_0$, and search for bounded solutions that are not homoclinic or heteroclinic connections. As in previous arguments, at $\mu = \mu_0$ we can solve (5.85) by first choosing $\omega_i = \omega_{i+1}$ to solve

$$e^{-2\rho(\mu)\omega_{i+1}}\sin(2\phi(\mu)\omega_{i+1} + \varphi^1) - e^{-2\rho(\mu)\omega_i}\sin(2\phi(\mu)\omega_i + \varphi^1) = 0, \tag{5.87}$$

$$e^{-2\rho(\mu)\omega_{i+1}}\sin(2\phi(\mu)\omega_{i+1} + \varphi^2) + e^{-2\rho(\mu)\omega_i}\sin(2\phi(\mu)\omega_i + \varphi^2) = 0, \tag{5.88}$$

and then using the Implicit Function Theorem to solve (5.85), (5.86). This provides solutions $\omega_i \approx \omega_{i+1}$. These values for ω_i, ω_{i+1} will be close to $\omega_\mu(n)$ ($n \in \mathbb{Z}$), which here we define to be the zeros of

$$e^{-2\rho(\mu)\omega} \sin(2\phi(\mu)\omega + \varphi^2). \tag{5.89}$$

In fact, for any choice of $\omega_\mu(n)$, there are unique solutions $\omega_i, \omega_{i+1} \approx \omega_\mu(n)$ to (5.85), (5.86). Now choose any finite number of $\omega_\mu(n)$, say $n = 1, 2, \ldots, N$, and prescribe a sequence $\{\omega_j\}_{j\in\mathbb{Z}}$, where $\omega_i, \omega_{i+1} = \omega_\mu(n_i)$, $n_i \in \{1, 2, \ldots, N\}$. Then ω_i, ω_{i+1} solve (5.87), (5.88) for all i. Now we would like to use the Implicit Function Theorem to solve equations (5.85), (5.86) for all i, in $l^\infty_{\mathbb{R}\times\mathbb{R}}$. Since there are finitely many ω_i, we see that for the $\omega_\mu(n)$ large enough, the higher order terms are bounded for all i, and can be made arbitrarily small. Then we can use the Implicit Function Theorem to solve each of the equations (5.85), (5.86) to find solutions $\omega_i, \omega_{i+1} \approx \omega_\mu(n_i)$. We see that if the sequence $\{\omega_\mu(n_i)\}$ is periodic, then the equations (5.85), (5.86) will also be periodic (this follows from uniqueness of the Implicit Function Theorem), and the corresponding orbit will be a periodic orbit, with the same period (thus the $\{\omega_j\}_{j\in\mathbb{Z}}$ will be periodic).

We would like to now study the symmetry properties of this set. Suppose that $\omega_j \approx \omega_\mu(n_j)$, where $j \in \mathbb{Z}$. (Note that if j is odd, then $\omega_\mu(n_j) = \omega_\mu(n_{j+1})$.) Similar to before, we can prove (using Remark 5.5.1 and uniqueness of the Implicit Function Theorem) that if we choose the sequence $\{\omega_\mu(n_j)\}_{j\in\mathbb{Z}}$ such that there is an integer j_0 where the following condition is satisfied:

$$\omega_\mu(n_{j_0-p}) = \omega_\mu(n_{j_0+1+p}), \quad p = 0, 1, 2, \ldots, \tag{5.90}$$

then the orbit corresponding to that sequence is symmetric. If j_0 is odd, then the orbit intersects Fix R in Σ_1; if j_0 is even, then the orbit intersects Fix R in Σ_2, both between times $\omega_\mu(n_{j_0})$ and $\omega_\mu(n_{j_0+1})$. Any sequence can have this property in a maximum of 2 distinct ways—if the orbit intersects Fix R twice, then it is a symmetric periodic orbit. Moreover, any periodic orbit must intersect Fix R either twice or not at all.

As before, depending on the constants $\varphi^1, \varphi^2, \rho(\mu), \phi(\mu)$ there may be many more orbits present, corresponding to the presence of countably many more 'symbols'. In this case we solve (5.85), (5.86) in the same way as before to find these orbits.

Thus we have proved the existence of dynamics which is topologically conjugate to a full shift on n symbols, for any n. This invariant set is setwise-symmetric and indecomposable. Moreover, we see that if we take any corresponding invariant set up to a given n symbols, this set is persistent under small perturbations in μ. However, the union of all sets exists only for $\mu = \mu_0$.

Chapter 6

Appendix

Here we present proofs of the various estimates needed throughout the implementation of the method.

6.1 Estimates for $\tilde{z}_i(t; \mu, \omega_i, \omega_{i+1}, a_i^-, a_i^+, h_i^-, h_i^+)$

For ease of notation in the working we shall write simply $z_i^{\pm}(t)$. In the proofs of the estimates the properties of the exponential dichotomies are used extensively throughout.

6.1.1 $||\tilde{z}_i^{\pm}(0; \mu, \omega_i, \omega_{i+1}, a_i^-, a_i^+, h_i^-, h_i^+)|| \leq K(e^{-\alpha_i \omega_{i+1}}||a_i^+|| + e^{-\alpha_i \omega_i}||a_i^-|| + ||h_i||)$

We will consider separately the cases $i = 1, 2$. Consider first $i = 1$, from equations (5.41) and (5.42), and recalling that $a_1^+ = Q_{1,+}(\mu, \omega_2)a_1^+$ and $a_1^- = P_{1,-}(\mu, -\omega_1)a_1^-$;

$$\begin{aligned} ||z_1^+(0)|| &\leq Ke^{-\alpha_1 \omega_2}||a_1^+|| + \int_0^{\omega_2} Ke^{-\alpha_1 \tau}||h_1^+||d\tau \\ &\leq K(e^{-\alpha_1 \omega_2}||a_1^+|| + ||h_1^+||) \end{aligned} \tag{6.1}$$

Similarly we obtain

$$||z_1^-(0)|| \leq K(e^{-\alpha_1\omega_1}||a_1^-|| + ||h_1^-||). \tag{6.2}$$

The corresponding equations for $||z_2^+(0)||$ and $||z_2^-(0)||$ are equations (5.34) and (5.35). As in section 5.4.1 we will add the two equations to solve for $z_2(0)$, then similar to the above we have

$$\begin{aligned} ||z_2(0)|| &\leq Ke^{-\alpha_2\omega_1}||a_2^+|| + Ke^{-\alpha_2\omega_2}||a_2^-|| \\ &\quad + \int_0^{\omega_1} Ke^{-\alpha_2\tau}||h_2||d\tau + \int_{-\omega_2}^{0} Ke^{\alpha_2\tau}||h_2||d\tau \\ &\leq K(e^{-\alpha_2\omega_1}||a_2^+|| + e^{-\alpha_2\omega_2}||a_2^-|| + ||h_2||). \end{aligned}$$

Then together we have

$$||\tilde{z}_i^{\pm}(0;\mu,\omega_i,\omega_{i+1},a_i^-,a_i^+)|| \leq K(e^{-\alpha_i\omega_{i+1}}||a_i^+|| + e^{-\alpha_i\omega_i}||a_i^-|| + ||h_i||). \tag{6.3}$$

6.1.2 $||\tilde{z}_i(t;\mu,\omega_i,\omega_{i+1},a_i^-,a_i^+,h_i^-,h_i^+)|| \leq K(||a_i^+|| + ||a_i^-|| + ||h_i||)$

Recall from section 5.4.1 (cf (5.37)):

$$\begin{aligned} z_i^-(t) &= \Phi_i^-(\mu,t,0)Q_{i,-}(\mu,0)z_i^-(0) + \Phi_i^-(\mu,t,-\omega_i)a_i^- \\ &\quad - \int_t^0 \Phi_i^-(\mu,t,s)Q_{i,-}(\mu,s)h_i^-(s)ds + \int_{-\omega_i}^t \Phi_i^-(\mu,t,s)P_{i,-}(\mu,s)h_i^-(s)ds, \end{aligned}$$

$$\begin{aligned} P_{i,-}(\mu,t)z_i^-(t) &= \Phi_i^-(\mu,t,-\omega_i)P_{i,-}(\mu,-\omega_i)a_i^- \\ &\quad + \int_{-\omega_i}^t \Phi_i^-(\mu,t,s)P_{i,-}(\mu,s)h_i^-(s)ds, \\ Q_{i,-}(\mu,t)z_i^-(t) &= \Phi_i^-(\mu,t,-\omega_i)Q_{i,-}(\mu,0)z_i^-(0) \\ &\quad - \int_t^0 \Phi_i^-(\mu,t,s)Q_{i,-}(\mu,s)h_i^-(s)ds. \end{aligned}$$

We will use sup norms as the norms for functions here.

$$\begin{aligned}
||z_i^-(t)|| &\leq ||P_{i,-}(\mu,t)z_i^-(t)|| + ||Q_{i,-}(\mu,t)z_i^-(t)|| \\
&\leq ||\Phi_i^-(\mu,t,-\omega_i)P_{i,-}(\mu,-\omega_i)a_i^-|| \\
&\quad + \int_{-\omega_i}^{t} ||\Phi_i^-(\mu,t,s)P_{i,-}(s)h_i^-(s)||ds \\
&\quad +||\Phi_i^-(\mu,t,0)Q_{i,-}(\mu,0)z_i^-(0)|| \\
&\quad + \int_t^0 ||\Phi_i^-(\mu,t,s)Q_{i,-}(\mu,s)h_i^-(s)||ds \\
&\leq Ke^{-\alpha_{i-1}(t+\omega_i)}||a_i^-|| + \int_{-\omega_i}^{t} Ke^{-\alpha_{i-1}(t-\tau)}||h_i||d\tau \\
&\quad +Ke^{\alpha_{i-1}t}||z_i^-(0)|| + \int_t^0 Ke^{-\alpha_{i-1}(\tau-t)}||h_i||d\tau \\
&\leq K(||a_i^-|| + ||h_i||).
\end{aligned}$$

For the last inequality we have used (6.2). Here (and throughout) the constants K are not necessarily the same. Similarly we prove

$$||z_i^+(t)|| \leq K(||a_i^+|| + ||h_i||).$$

Then we obtain

$$||\tilde{z}_i(t;\mu,\omega_i,\omega_{i+1},a_i^-,a_i^+)|| \leq K(||a_i^+|| + ||a_i^-|| + ||h_i||). \tag{6.4}$$

6.1.3 $||P_{i-1,+}(\mu,\omega_i)\tilde{z}_{i-1}(\omega_i;\mu,\omega_{i-1},\omega_i,a_{i-1}^-,a_{i-1}^+,h_i^-,h_i^+)|| + ||Q_{i,-}(\mu,-\omega_i)\tilde{z}_i(-\omega_i;\mu,\omega_i,\omega_{i+1},a_i^-,a_i^+,h_i^-,h_i^+)|| \leq K(e^{-2\alpha\overline{\omega}}||\mathbf{a}|| + ||\mathbf{h}||)$

In the above estimate $\overline{\omega}$ is chosen as in Lemma 5.4.5 and all the $\omega_i \geq \overline{\omega}$. Also $\alpha := \min\{\alpha_1,\alpha_2\}$ as in section 5.3. We have

$$\begin{aligned}
P_{i-1,+}(\mu,t)z_{i-1}^+(t) &= \Phi_{i-1}^+(\mu,t,0)P_{i-1,+}(\mu,0)z_{i-1}^+(0) \\
&\quad + \int_0^t \Phi_{i-1}^+(\mu,t,\tau)P_{i-1,+}(\mu,\tau)h_{i-1}(\tau)d\tau, \\
Q_{i,-}(\mu,t)z_i^-(t) &= \Phi_i^-(\mu,t,0)Q_{i,-}(\mu,0)z_i^-(0) \\
&\quad + \int_0^t \Phi_i^+(\mu,t,\tau)Q_{i,-}(\mu,\tau)h_i(\tau)d\tau.
\end{aligned}$$

Considering only $P_{i-1,+}(\mu,t)z_{i-1}^+(t)$;

$$\begin{aligned} P_{i-1,+}(\mu,\omega_i)z_{i-1}^+(\omega_i) &= \Phi_{i-1}^+(\mu,\omega_i,0)P_{i-1,+}(\mu,0)z_{i-1}^+(0) \\ &\quad + \int_0^{\omega_i} \Phi_{i-1}^+(\mu,\omega_i,\tau)P_{i-1,+}(\mu,\tau)h_{i-1}(\tau)d\tau, \end{aligned}$$

$$\begin{aligned} ||P_{i-1,+}(\mu,\omega_i)z_{i-1}^+(\omega_i)|| &\leq Ke^{-\alpha_{i-1}\omega_i}||z_{i-1}^+(0)|| + \int_0^{\omega_i} Ke^{-\alpha_{i-1}(\omega_i-\tau)}||h_{i-1}||d\tau \\ &\leq Ke^{-\alpha_{i-1}\omega_i}||z_{i-1}^+(0)|| + K||h_{i-1}||. \end{aligned}$$

Now using equation (6.3), we can write

$$||P_{i-1,+}(\mu,\omega_i)z_{i-1}^+(\omega_i)|| \leq K(e^{-\alpha_{i-1}\omega_i}||a_{i-1}^+|| + e^{-\alpha_{i-1}\omega_{i-1}}||a_{i-1}^-|| + ||h_{i-1}||).$$

Similarly

$$||Q_{i,-}(\mu,-\omega_i)z_i^-(-\omega_i)|| \leq K(e^{-\alpha_i\omega_{i+1}}||a_i^+|| + e^{-\alpha_i\omega_i}||a_i^-|| + ||h_i||).$$

Combining the above two estimates then yields

$$\begin{aligned} &||P_{i-1,+}(\mu,\omega_i)\tilde{z}_{i-1}(\omega_i;\mu,\omega_{i-1},\omega_i,a_{i-1}^-,a_{i-1}^+,h_i^-,h_i^+)|| \\ &\quad + ||Q_{i,-}(\mu,-\omega_i)\tilde{z}_i(-\omega_i;\mu,\omega_i,\omega_{i+1},a_i^-,a_i^+,h_i^-,h_i^+)|| \leq K(e^{-2\alpha\overline{\omega}}||\mathbf{a}|| + ||\mathbf{h}||). \end{aligned} \tag{6.5}$$

6.1.4 $||\tilde{z}_i(t;\mu,\omega_i,\omega_{i+1},a_i^-,a_i^+,h_i^-,h_i^+)|| \leq K(||\mathbf{d}|| + ||\mathbf{h}||)$

From estimate (6.4) we have

$$||\tilde{z}_i(t;\mu,\omega_i,\omega_{i+1},a_i^-,a_i^+,h_i^-,h_i^+)|| \leq K(||\mathbf{a}|| + ||\mathbf{h}||).$$

Now from (5.49) and section 5.4.3 we have $||\mathbf{a}|| \leq K(||\mathbf{d}|| + ||\mathbf{h}||)$. Then together we prove

$$||\tilde{z}_i(t;\mu,\omega_i,\omega_{i+1},a_i^-,a_i^+,h_i^-,h_i^+)|| \leq K(||\mathbf{d}|| + ||\mathbf{h}||). \tag{6.6}$$

6.2 Estimates for $\tilde{P}$ and $\tilde{Q}$

In section 5.4.2 we defined the projections $\tilde{P}_{i,\omega}$ and $\tilde{Q}_{i,\omega}$ as follows:

$$\begin{aligned}
\tilde{P}_{i,\omega} &:= S_\omega P_0(p_{i-1}) S_\omega^{-1}, \\
\tilde{Q}_{i,\omega} &:= S_\omega (I - P_0(p_{i-1})) S_\omega^{-1} \\
&= S_\omega Q_0(p_{i-1}) S_\omega^{-1},
\end{aligned}$$

where $P_0(p_{i-1})$, $Q_0(p_{i-1})$ are the complementary projections on the stable, resp. unstable subspaces of $D_x f(p_{i-1}, \mu)$, and where

$$\begin{aligned}
S_{i,\omega} &:= (P_0(p_{i-1}) + (P_{i,-}(\mu, -\omega) - P_0(p_{i-1})))P_0(p_{i-1}) \\
&\quad +(Q_0(p_{i-1}) + (Q_{i-1,+}(\mu, \omega) - Q_0(p_{i-1})))Q_0(p_{i-1}).
\end{aligned}$$

Let the (leading) eigenvalues of the fixed point p_1 be $-\lambda(\mu)$ and $\rho(\mu) \pm i\phi(\mu)$, with $\lambda(\mu), \rho(\mu) > 0$. Then by the reversibility, the (leading) eigenvalues of the fixed point p_2 must be $\lambda(\mu)$, $-\rho(\mu) \pm i\phi(\mu)$. We choose constants α_i^s, α_i^{ss}, α_i^u, α_i^{uu} such that

$$\{\sigma_1^{ss}(\mu)\} < \alpha_1^{ss} < -\lambda(\mu) < \alpha_1^s < 0 < \alpha_1^u < \rho(\mu) < \alpha_1^{uu} < \{\sigma_1^{uu}\},$$

where $\{\sigma_1^{ss}(\mu)\}$ (resp. $\{\sigma_1^{uu}(\mu)\}$) represents the strong stable (resp. strong unstable) eigenvalues of the fixed point p_1. Also define the analogous constants for p_2: $\alpha_2^s = -\alpha_1^u$, $\alpha_2^{ss} = -\alpha_1^{uu}$, $\alpha_2^{uu} = -\alpha_1^{ss}$ and $\alpha_2^u = -\alpha_1^s$.

6.2.1 $||S_{i,\omega} - I|| \leq K e^{-(\mathbf{min}\{-\alpha_{i-1}^s, \alpha_{i-1}^u\})\omega}$

By the definition of $S_{i,\omega}$:

$$\begin{aligned}
||S_{i,\omega} - I|| &\leq ||Q_{i,-}(\mu, -\omega)P_0(p_{i-1})|| + ||P_{i-1,+}(\mu, \omega)Q_0(p_{i-1})|| \\
&= ||(Q_{i,-}(\mu, -\omega) - Q_0(p_{i-1}))P_0(p_{i-1})|| \\
&\quad +||(P_{i-1,+}(\mu, \omega) - P_0(p_{i-1}))Q_0(p_{i-1})|| \\
&\leq ||Q_{i,-}(\mu, -\omega) - (I - P_0(p_{i-1}))||\ ||P_0(p_{i-1})|| \\
&\quad +||P_{i-1,+}(\mu, \omega) - P_0(p_{i-1})||\ ||I - P_0(p_{i-1})||.
\end{aligned}$$

From [89] (Lemma 3.4), we have that

$$\lim_{t\to\infty}||P_{i-1,+}(\mu,t) - P_0(p_{i-1})|| = 0. \tag{6.7}$$

Also, from [113] (Theorem 7.1) we know that for $x_0 \in W^s(p_{i-1})$,

$$||\varphi(t,x_0) - p_{i-1}|| < K_1 e^{\alpha^s_{i-1}t}, \tag{6.8}$$

for some constant K_1, where $\varphi(\cdot,\cdot)$ denotes the flow of (5.2) (with appropriate C^∞ transformations carried out as in section 5.2). The same estimate works also for complex eigenvalues, see also section 6.3 on the leading terms in approach to equilibrium. Using the Mean Value Theorem, we get

$$||Df(\varphi(t,x_0)) - Df(p_{i-1})|| < K_2 e^{\alpha^s_{i-1}t}.$$

Together, this implies the estimate

$$||P_{i-1,+}(\mu,t) - P_0(p_{i-1})|| < C e^{\alpha^s_{i-1}t}.$$

The above estimate can be used for both $||Q_{i,-}(\mu,-\omega) - (I - P_0(p_{i-1}))||$ and $||P_{i-1,+}(\mu,\omega) - P_0(p_{i-1})||$, yielding

$$||S_{i,\omega} - I|| \leq K e^{-(\min\{-\alpha^s_{i-1},\alpha^u_{i-1}\})\omega}. \tag{6.9}$$

Also, we can derive a similar estimate for $||S^{-1}_{i,\omega} - I||$. Since the mapping $GL(n,\mathbb{R}) \to GL(n,\mathbb{R}) : A \to A^{-1}$ is continuous (with suitable norm), then together with (6.9), we have

$$\lim_{\omega\to\infty} S^{-1}_{i,\omega} = I.$$

Also

$$||S^{-1}_{i,\omega} - I|| \leq ||S^{-1}_{i,\omega}||\, ||S_{i,\omega} - I||.$$

Together this shows

$$||S^{-1}_{i,\omega} - I|| \leq \tilde{K} e^{(\min\{\alpha^s_{i-1},-\alpha^u_{i-1}\})\omega}. \tag{6.10}$$

6.2.2 $||\tilde{Q}_{i,\omega} - Q_0(p_{i-1})|| \leq Ke^{-(\mathbf{min}\{-\alpha_i^s,\alpha_i^u\})\omega}$

By definition, we have

$$\begin{aligned}
||\tilde{Q}_{i,\omega} - Q_0(p_{i-1})|| &= ||(S_{i,\omega} - I + I)(I - P_0(p_{i-1}))(S_{i,\omega}^{-1} - I + I) \\
&\quad -(I - P_0(p_{i-1}))|| \\
&\leq ||(S_{i,\omega} - I)(I - P_0(p_{i-1}))(S_{i,\omega}^{-1} - I)|| \\
&\quad +||(S_{i,\omega} - I)(I - P_0(p_{i-1}))|| \\
&\quad +||(I - P_0(p_{i-1}))(S_{i,\omega}^{-1} - I)||.
\end{aligned}$$

Now by (6.9) and (6.10), we have

$$||\tilde{Q}_{i,\omega} - Q_0(p_{i-1})|| \leq Ke^{-(\min\{-\alpha_i^s,\alpha_i^u\})\omega}. \tag{6.11}$$

6.2.3 $||\tilde{Q}_{i,\omega}v^s|| \leq Ce^{-(\mathbf{min}\{-\alpha_i^s,\alpha_i^u\})\omega}||v^s||$

Here $v^s \in T_{p_{i-1}}W^s(p_{i-1}) = \text{Im } P_0(p_{i-1})$. Then we have the following:

$$||\tilde{Q}_{i,\omega}v^s|| = ||\tilde{Q}_{i,\omega}v^s - Q_0(p_{i-1})v^s||.$$

Now from (6.11), we have

$$||\tilde{Q}_{i,\omega}v^s|| \leq Ce^{-(\min\{-\alpha_i^s,\alpha_i^u\})\omega}||v^s||. \tag{6.12}$$

In a similar way we can prove

$$||\tilde{Q}_{i,\omega}v^u - v^u|| \leq Ce^{-(\min\{-\alpha_i^s,\alpha_i^u\})\omega}||v^u||, \tag{6.13}$$

whenever $v^u \in T_{p_{i-1}}W^u(p_{i-1}) = \text{Ker } P_0(p_{i-1})$.

6.3 Leading Terms In Approach To Equilibrium

This section provides some crucial estimates for an accurate representation of the jump $\xi_i^\omega(\mu)$. It provides the leading terms of an orbit approaching an equilibrium in the weak stable manifold. Throughout we assume that the leading eigenvalue of the equilibrium is simple. We will consider the cases when the leading eigenvalue is real and when it is complex together, as the proof of the following theorem is identical in both cases.

Suppose $x = 0$ is an asymptotically stable fixed point of a smooth C^2 vector field $f(\cdot, \mu) : \mathbb{R}^k \to \mathbb{R}^k$, $\mu \in \mathbb{R}^p$. When the leading eigenvalue is real, let the spectrum be $\sigma(Df(0, \mu)) = \lambda^s(\mu) \cup \sigma^{ss}(\mu)$. When it is complex, then the leading eigenvalue is $\lambda^s(\mu) \pm i\theta(\mu)$. Choose constants α^{ss} and α^s as before such that

$$\{\sigma^{ss}(\mu)\} < \alpha^{ss} < \lambda(\mu) < \alpha^s < 0.$$

Further, we require that $2|\alpha^s| > |\lambda(\mu)|$ for sufficiently small μ. Still then we can apply Theorem 7.1 from [113] with the constant α^s; that is, given initial condition x_0, there exist constants C, t_0, δ such that $||x_0|| < \delta$ implies

$$||x(t)|| \leq C||x_0||e^{\alpha^s(t-t_0)}, \quad t \geq t_0, \tag{6.14}$$

where $x(t)$ is the solution to $\dot{x} = f(x, \mu)$ with $x(0) = x_0$.

The following Theorem appears in [94] Lemma 1.7, but we include it here to be reasonably self-contained. It is concerned with the leading order terms of an orbit of the system $\dot{x} = f(x, \mu)$ that approaches equilibrium in the weak stable manifold, see Figure 6.1.

Theorem 6.3.1. *Let the previous assumptions hold. Then there exists a constant $\delta > 0$ such that for all solutions $x(\cdot)$ of*

$$\dot{x} = f(x, \mu)$$

with $||x(0)|| < \delta$ the limit

$$\eta(x(0), \mu) := lim_{t\to\infty}\Phi(\mu, 0, t)P_s(\mu)x(t)$$

exists, where $\Phi(\mu, t, 0)$ is the transition matrix of

$$\dot{x} = Df(0, \mu)x$$

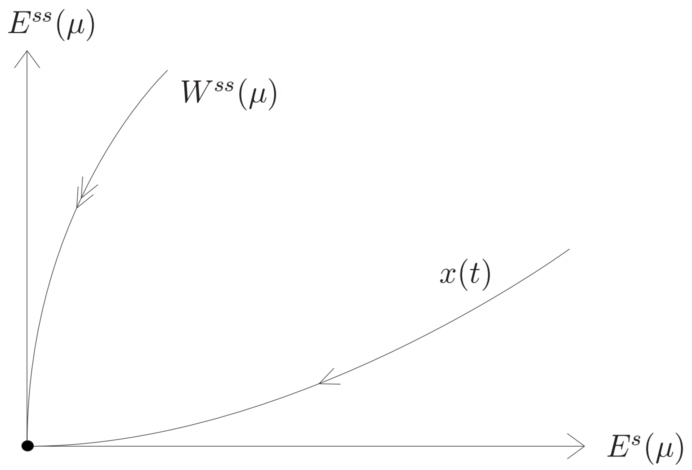

Figure 6.1: The orbit $x(t)$ approaching equilibrium in the weak stable manifold $W^s(\mu)$.

from 0 *to* t *and* P_s *is the projection onto the stable subspace* $E^s(\mu)$ *along the strong stable subspace* $E^{ss}(\mu)$. *Further, there exists a constant* C *such that*

$$||x(t) - \Phi(\mu, t, 0)\eta(x(0), \mu)|| \leq Ce^{-min\{|\alpha^{ss}|, 2|\alpha^s|\}t}. \tag{6.15}$$

Proof. Define $A(\mu) := Df(0, \mu)$, and set

$$f(x, \mu) = A(\mu)x + g(x, \mu),$$

then $g(x, \mu) = O(x^2)$. By the variation of constants formula, the nonlinear equation is solved by

$$x(t) = \Phi(\mu, t, s)x(s) + \int_s^t \Phi(\mu, t, \tau)g(x(\tau), \mu)d\tau. \tag{6.16}$$

Now since $\Phi(\mu, t, 0)(E^s(\mu)) \subset E^s(\mu)$ and $\Phi(\mu, t, 0)(E^{ss}(\mu)) \subset E^{ss}(\mu)$, then we have

$$P_s(\mu)\Phi(\mu, t, 0) = \Phi(\mu, t, 0)P_s(\mu).$$

Hence

$$\Phi(\mu, 0, t)P_s(\mu)x(t) = \Phi(\mu, 0, s)P_s(\mu)x(s) + \int_s^t \Phi(\mu, 0, \tau)P_s(\mu)g(x(\tau), \mu)d\tau. \tag{6.17}$$

We would like to show that $\Phi(\mu, 0, t)P_s(\mu)x(t)$ converges as $t \to \infty$. We shall do this by showing that $(\Phi(\mu, 0, t_k)P_s(\mu)x(t_k))_{k\in\mathbb{N}}$ is a Cauchy sequence, when $\lim_{k\to\infty} t_k = \infty$.

Take $k, j \in \mathbb{N}$, $t_k > t_j$, then by (6.17):

$$\begin{aligned}
&||\Phi(\mu, 0, t_k)P_s(\mu)x(t_k) - \Phi(\mu, 0, t_j)P_s(\mu)x(t_j)|| \\
&\qquad\qquad \le \textstyle\int_{t_j}^{t_k} ||\Phi(\mu, 0, \tau)P_s(\mu)||\, ||g(x(\tau), \mu)||d\tau \\
&\qquad\qquad \le \textstyle\int_{t_j}^{t_k} Ke^{|\lambda^s(\mu)|\tau}.e^{2\alpha^s\tau}d\tau \qquad \forall ||x(0)|| < \delta.
\end{aligned}$$

Here the constant δ is chosen so we can invoke (6.14). The final inequality then follows from (6.14) and (perhaps shrinking δ) using the fact that $g(x, \mu) = O(x^2)$, $\forall x : ||x|| < \epsilon$. Recall that $2|\alpha^s| > \lambda^s(\mu)$, now it is clear that the sequence is Cauchy and therefore convergent. Then as in the statement of the theorem we define

$$\eta(x(0), \mu) := \lim_{t\to\infty}\Phi(\mu, 0, t)P_s(\mu)x(t).$$

Since $\Phi(\mu, 0, t)$ leaves $E^s(\mu)$ invariant and $E^s(\mu)$ is closed, $\eta(x(0), \mu) \in E^s(\mu)$.

Using the fact that $P_s(\mu)\Phi(\mu, t, s) = \Phi(\mu, t, s)P_s(\mu)$ we have

$$\begin{aligned}
P_s(\mu)x(t) &= \Phi(\mu, t, s)P_s(\mu)x(s) + \int_s^t \Phi(\mu, t, \tau)P_s(\mu)g(x(\tau), \mu)d\tau, \\
(I - P_s(\mu))x(t) &= \Phi(\mu, t, s)(I - P_s(\mu))x(s) \\
&\quad + \int_s^t \Phi(\mu, t, \tau)(I - P_s(\mu))g(x(\tau), \mu)d\tau.
\end{aligned}$$

Consider the first equation. With the previous result, both terms have a limit as $s \to \infty$:

$$P_s(\mu)x(t) = \Phi(\mu, t, 0)\eta(x(0), \mu) + \int_\infty^t \Phi(\mu, t, \tau)P_s(\mu)g(x(\tau), \mu)d\tau.$$

Together with the second equation, we get

$$\begin{aligned}
||x(t)-\Phi(\mu,t,0)\eta(x(0),\mu)|| &\leq ||\Phi(\mu,t,s)(I-P_s(\mu))x(s)|| \\
&\quad + \int_s^t ||\Phi(\mu,t,\tau)(I-P_s(\mu))g(x(\tau),\mu)||d\tau \\
&\quad + \int_\infty^t ||\Phi(\mu,t,\tau)P_s(\mu)g(x(\tau),\mu)||d\tau \\
&\leq K\left(e^{\alpha^{ss}(t-s)}||x(s)|| + \int_s^t e^{\alpha^{ss}(t-\tau)}||g(x(\tau),\mu)||d\tau \right.\\
&\quad \left. + \int_\infty^t e^{\alpha^{s}(t-\tau)}||g(x(\tau),\mu)||d\tau\right) \\
&\leq K\left(e^{\alpha^{ss}(t-s)}||x(s)|| \quad + \int_s^t e^{\alpha^{ss}(t-\tau)}||x(\tau)||^2 d\tau \right.\\
&\quad \left. + \int_\infty^t e^{\alpha^{s}(t-\tau)}||x(\tau)||^2 d\tau\right).
\end{aligned}$$

Now we have chosen δ small enough if to satisfy (6.14) and $||x(t)|| < \epsilon \ \forall t \in \mathbb{R}^+$. Then by (6.14) $||x(\tau)|| \leq Ce^{\alpha^s\tau}||x(0)||$. So then for fixed s the terms in the above inequality can be estimated as follows:

$$\begin{aligned}
e^{\alpha^{ss}(t-s)}||x(s)|| &\leq Ce^{\alpha^{ss}t}, \\
\int_s^t e^{\alpha^{ss}(t-\tau)}||x(\tau)||^2 d\tau &\leq Ce^{\alpha^{ss}t}\int_s^t e^{-\alpha^{ss}\tau+2\alpha^s\tau}d\tau \\
&\leq Ce^{\alpha^{ss}t}\left[\frac{1}{2\alpha^s-\alpha^{ss}}(e^{(2\alpha^s-\alpha^{ss})t}-e^{(2\alpha^s-\alpha^{ss})s})\right] \\
&\leq Ce^{2\alpha^s t}, \\
\int_\infty^t e^{\alpha^{s}(t-\tau)}||x(\tau)||^2 d\tau &\leq Ce^{\alpha^{s}t}\int_\infty^t e^{\alpha^s\tau}d\tau \\
&\leq Ce^{\alpha^s t}\left[\frac{1}{\alpha^s}(e^{\alpha^s t})\right] \\
&\leq Ce^{2\alpha^s t}.
\end{aligned}$$

Hence we obtain

$$\begin{aligned}
||x(t)-\Phi(\mu,t,0)\eta(x(0),\mu)|| &\leq K\left(e^{\alpha^{ss}t}+e^{2\alpha^s t}\right) \\
&\leq Ke^{-\min\{|\alpha^{ss}|,2|\alpha^s|\}t},
\end{aligned}$$

and the theorem is proved. □

Remark 6.3.2. *If 0 is a hyperbolic fixed point then Theorem 6.3.1 describes the behaviour of trajectories in the stable manifold. By reversing time we can derive a similar expression for trajectories in the unstable manifold. Note in the above that $\eta(x(0),\mu)$ is zero if and only if $x(t)$ lies in the strong stable manifold.*

We shall also need the following theorem, which makes the same assertion as Theorem 6.3.1 for non-autonomous perturbed linear systems.

Theorem 6.3.3. *Let $x = 0$ be a hyperbolic fixed point of a C^2 vector field*

$$\dot{x} = A(\mu)x + B(t,\mu)x, \tag{6.18}$$

where $A(\mu), B(\cdot,\mu) \in GL(k,\mathbb{R})$, $\mu \in \mathbb{R}^p$. Suppose the fixed point has leading stable eigenvalue $\lambda^s(\mu)$ (if it is real) or $\lambda^s(\mu) \pm i\theta^s(\mu)$ (if it is complex), similarly the leading unstable eigenvalue is $\lambda^u(\mu)$ or $\lambda^u(\mu) \pm \theta^u(\mu)$. Then we introduce constants α^{ss}, α^s, α^{uu}, α^u such that

$$\{\sigma^{ss}(\mu)\} < \alpha^{ss} < \lambda^s(\mu) < \alpha^s < 0 < \alpha^u < \lambda^u(\mu) < \alpha^{uu} < \{\sigma^{uu}(\mu)\},$$

where $\{\sigma^{ss}(\mu)\}$ denotes the strong stable eigenvalues of the fixed point, $\{\sigma^{uu}(\mu)\}$ denotes the strong unstable eigenvalues. Suppose also there is a constant $\beta \in (-\infty, 0)$ such that $||B(t,\mu)|| < e^{\beta t}$ and $|\alpha^s + \beta| > |\lambda^s(\mu)|$ for small μ. Let $E^s(\mu)$, $E^{ss}(\mu)$ and $E^u(\mu)$ be the stable, strong stable and unstable subspaces of $A(\mu)$ respectively. Also $P_s(\mu)$ is the projection onto $E^s(\mu)$ along $E^{ss}(\mu) \oplus E^u(\mu)$.

Now suppose $x(t)$ is a solution of (6.18) which tends to zero as $t \to \infty$. Then the following limit exists:

$$\eta(x(0),\mu) := \lim_{t\to\infty} \Phi(\mu,0,t)P_s(\mu)x(t),$$

where $\Phi(\mu,t,0)$ is the transition matrix of $\dot{x} = A(\mu)x$ from 0 to t. Furthermore there exists a constant C such that

$$||x(t) - \Phi(\mu,t,0)\eta(x(0),\mu)|| \leq Ce^{-\min\{|\alpha^{ss}|,|\alpha^s+\beta|\}t}.$$

Proof. The proof is similar to that of Theorem 6.3.1. The stable solutions of (6.18) are given by bounded solutions of the form

$$\begin{aligned} x(t) &= \Phi(\mu,t,s)(I-P_u(\mu))x(s)+\int_s^t \Phi(\mu,t,\tau)(I-P_u(\mu))B(\tau,\mu)x(\tau)d\tau \\ &\quad -\int_t^\infty \Phi(t,\tau)P_u(\mu)B(\tau,\mu)x(\tau)d\tau, \end{aligned} \tag{6.19}$$

$P_u(\mu)$ is the projection onto $E^u(\mu)$ along $E^s(\mu)\oplus E^{ss}(\mu)$, coming from the exponential dichotomy of $\dot{x}=A(\mu)x$. Note that $P_u(\mu)$ and $P_s(\mu)$ commute. Compare with section 5.3, and equation (5.14).

We would again like to show that $(\Phi(\mu,0,t_k)P_s(\mu)x(t_k))_{k\in\mathbb{N}}$ is a Cauchy sequence, when $\lim_{k\to\infty}t_k=\infty$. We have

$$\begin{aligned} \Phi(\mu,0,t_k)P_s(\mu)x(t_k) &= \Phi(\mu,0,s)P_s(\mu)x(s) \\ &\quad +\int_s^{t_k}\Phi(\mu,0,\tau)P_s(\mu)B(\tau,\mu)x(\tau)d\tau. \end{aligned}$$

Then, by using the estimates of $B(t,\mu)$ assumed in the statement of the theorem, and the estimates of $x(t)$ produced by the exponential dichotomy of 6.18, similar inequalities follow as before to show that the sequence $(\Phi(\mu,0,t_k)P_s(\mu)x(t_k))_{k\in\mathbb{N}}$ is Cauchy, and that the limit

$$\eta(x(0),\mu):=\lim_{t\to\infty}\Phi(\mu,0,t)P_s(\mu)x(t)$$

exists. In fact, we may choose the constant in the exponential dichotomy of (6.18) to be α^s (see [23], Chapter 4, Proposition 1). Here we have also used the fact that $|\alpha^s+\beta|>|\lambda^s(\mu)|$.

As before, we rewrite (6.19) as

$$\begin{aligned} P_s(\mu)x(t) &= \Phi(\mu,t,s)P_s(\mu)x(s)+\int_s^t\Phi(\mu,t,\tau)P_s(\mu)B(\tau,\mu)x(\tau)d\tau, \\ (I-P_s(\mu))x(t) &= \Phi(\mu,t,s)(I-P_s(\mu))(I-P_u(\mu))x(s) \\ &\quad +\int_s^t\Phi(\mu,t,\tau)(I-P_s(\mu))(I-P_u(\mu))B(\tau,\mu)x(\tau)d\tau \\ &\quad -\int_t^\infty\Phi(\mu,t,\tau)P_u(\mu)B(\tau,\mu)x(\tau)d\tau. \end{aligned}$$

By letting $s \to \infty$ as before in the first equation and then combining the two equations, we get

$$\begin{aligned}
||x(t) - \Phi(\mu,t,0)\eta(x(0),\mu)|| &\leq ||\Phi(\mu,t,s)(I-P_s(\mu))(I-P_u(\mu))x(s)|| \\
&+ \int_s^t ||\Phi(\mu,t,\tau)(I-P_s(\mu))(I-P_u(\mu))B(\tau,\mu)x(\tau)||d\tau \\
&+ \int_\infty^t ||\Phi(\mu,t,\tau)P_u(\mu)B(\tau,\mu)x(\tau)||d\tau \\
&+ \int_\infty^t ||\Phi(\mu,t,\tau)P_s(\mu)B(\tau,\mu)x(\tau)||d\tau.
\end{aligned}$$

This differs from the analogous inequality from the proof of Theorem 6.3.1 in that here we have an extra term. This extra term can be estimated as follows:

$$\begin{aligned}
\int_\infty^t ||\Phi(\mu,t,\tau)P_u(\mu)B(\tau,\mu)x(\tau)||d\tau &\leq \int_\infty^t Ke^{-\alpha^u(\tau-t)}.e^{\beta\tau}.e^{\alpha^s\tau}d\tau \\
&\leq Ke^{(\beta+\alpha^s)t}.
\end{aligned}$$

The remaining terms can be estimated similarly, as before. Note that $(I - P_s(\mu))(I - P_u(\mu))$ is the projection onto $E^{ss}(\mu)$ along $E^s(\mu) \oplus E^u(\mu)$. This provides us with the estimate

$$||x(t) - \Phi(\mu,t,0)\eta(x(0),\mu)|| \leq Ce^{-\min\{|\alpha^{ss}|,|\alpha^s+\beta|\}t}.$$

This completes the proof. □

6.4 Estimates for $\xi_i^\omega(\mu)$

Here we collect all the estimates needed to determine the leading order term in (5.56). Throughout this section all solutions $z_i^\pm(t)$ are in fact $\overline{z}_i^\pm(t)$ but we have dropped the bar for notational convenience.

6.4.1 Estimate for $\Phi_{1,+}^*(\mu,0,\omega_{i+1})Q_{1,+}^*(\mu,0)\psi_j$

Lemma 6.4.1. *Let $\Phi_{i,\pm}(\mu,t,s)$ be the transition matrix of $\dot{x} = A_i^\pm(t,\mu)x$ as before (see (5.29)). Define $\Psi_{i,\pm}(\mu,s,t) := \Phi_{i,\pm}^*(\mu,t,s)$, where $\Phi_{i,\pm}^*(\mu,t,s)$ is* *the adjoint of $\Phi_{i,\pm}(\mu,t,s)$, defined by*

$$< \psi, \Phi_{i,\pm}(t,s)x > = < \Phi^*_{i,\pm}(t,s)\psi, x > . \tag{6.20}$$

Then $\Psi_{i,\pm}(\mu,s,t)$ is the transition matrix of

$$\dot{\psi} = -(A_i^\pm(t,\mu))^*\psi,$$

the adjoint of the variational equation along $q_i^\pm(\mu)(t)$.

Furthermore, we have $R(A_i^\pm(t,\mu))^* = -(A_i^\mp(-t,\mu))^*R$ and $R\Psi_{i,\pm}(\mu,s,t) = \Psi_{i,\pm}(\mu,-s,-t)R$.

Proof. $x(t) = \Phi_{i,\pm}(\mu,t,s)x(s)$ solves the equation $\dot{x} = A_i^\pm(t,\mu)x$. Then

$$\begin{aligned} \Phi_{i,\pm}(\mu,s,t)x(t) &= x(s), \\ \dot{\Phi}_{i,\pm}(\mu,s,t)x(t) + \Phi_{i,\pm}(\mu,s,t)\dot{x}(t) &= 0, \end{aligned}$$

$$\dot{\Phi}_{i,\pm}(\mu,s,t)\Phi_{i,\pm}(\mu,t,s)x(s) + \Phi_{i,\pm}(\mu,s,t)A_i^\pm(t,\mu)\Phi_{i,\pm}(\mu,t,s)x(s) = 0,$$

but $x(s)$ is arbitrary, so

$$\dot{\Phi}_{i,\pm}(\mu,s,t) = -\Phi_{i,\pm}(\mu,s,t)A_i^\pm(t,\mu).$$

Now set $\psi(t) = \Psi_{i,\pm}(\mu,t,s)\psi(s) = \Phi^*_{i,\pm}(\mu,s,t)\psi(s)$. Then

$$\begin{aligned} \dot{\psi}(t) &= \dot{\Phi}^*_{i,\pm}(\mu,s,t)\psi(s) \\ &= -(\Phi_{i,\pm}(\mu,s,t)A_i^\pm(t,\mu))^*\psi(s) \\ &= -(A_i^\pm(t,\mu))^*\Phi^*_{i,\pm}(\mu,s,t)\psi(s) \\ &= -(A_i^\pm(t,\mu))^*\psi(t). \end{aligned}$$

To prove the final equalities, since the inner product is R-invariant,

$$\begin{aligned} < -A_i^\mp(-t,\mu)Rx, R\psi > &= < Rx, RA_i^\pm(t,\mu))^*\psi >, \\ < A_i^\pm(t,\mu)Rx, R\psi > &= < Rx, -RA_i^\mp(-t,\mu))^*\psi > \\ &= < Rx, A_i^\pm(t,\mu))^*R\psi >, \end{aligned}$$

but x, ψ are arbitrary, so $RA_i^{\pm}(t,\mu))^* = -A_i^{\mp}(-t,\mu))^* R$. It follows then that $R\Psi_{i,\pm}(\mu,s,t) = \Psi_{i,\pm}(\mu,-s,-t)R$. □

Then, recalling the definition of ψ_j, we have that $\Phi_{1,\pm}^*(\mu,0,\omega_{i+1})Q_{1,+}^*(\mu,0)\psi_j = \Phi_{1,\pm}^*(\mu,0,\omega_{i+1})\psi_j$ solves $\dot\psi = -(A_1^{\pm}(t,\mu))^*\psi$. This equation has an exponential dichotomy on $\mathbb{R}_+$, $\mathbb{R}_-$, with projections $P_{1,\pm}^*(\mu,t)$, $Q_{1,\pm}^*(\mu,t)$. Also

$$\{w : \sup_{t\in\mathbb{R}_+}||\Psi_{1,+}(\mu,t,0)w|| < \infty\} \;=\; (T_{q_1^+(\mu)(0)}W_\mu^s(p_1))^\perp,$$

and $\operatorname{Im} Q_{1,+}^*(\mu,t) = (T_{q_1^+(\mu)(0)}W_\mu^s(p_1))^\perp$. By reversibility, we have that $\sigma(-(D_xf(p_1,\mu))^*) = \sigma(D_xf(p_2,\mu))$. Then by Theorem 6.3.3,

$$\psi_j^+(t) = \Psi_{p_1}(\mu,t,0)\eta^+(\psi^+(0),\mu) + \mathcal{O}(\exp(-\min\{|\alpha_1^{uu}|, 2|\alpha_1^u|\}t)),$$

where α_1^{uu}, α_1^u are as in section 6.2, and $\Psi_{p_i}(\mu,t,0)$ is the transition matrix of the equation $\dot\psi = -(D_xf(p_i,\mu))^*\psi$. $\eta^+(\psi^+(0),\mu)$ is as given in Theorem 6.3.3, and is contained in the stable subspace of $\Psi_{p_1}(\mu,\cdot,\cdot)$.

Hence we obtain

$$\begin{aligned}\Phi_{1,+}^*(\mu,0,\omega_{i+1})Q_{1,+}^*(\mu,0)\psi_j &= \Phi_{1,+}^*(\mu,0,\omega_{i+1})\psi_j \\ &= \Psi_{p_1}(\mu,\omega_{i+1},0)\eta^+(\psi_j,\mu) \\ &\quad +\mathcal{O}(\exp(-\min\{|\alpha_1^{uu}|, 2|\alpha_1^u|\}\omega_{i+1})). \qquad (6.21)\end{aligned}$$

Similarly we also obtain

$$\begin{aligned}\Phi_{1,-}^*(\mu,0,-\omega_i)P_{1,-}^*(\mu,0)\psi_j &= \Phi_{1,-}^*(\mu,0,-\omega_i)\psi_j \\ &= \Psi_{p_2}(\mu,-\omega_i,0)\eta^-(\psi_j,\mu) \\ &\quad +\mathcal{O}(\exp(-\min\{|\alpha_2^{ss}|, 2|\alpha_2^s|\}\omega_i)), \qquad (6.22)\end{aligned}$$

with $\eta^-(\psi_j,\mu)$ in the unstable subspace of $\Psi_{p_2}(\mu,\cdot,\cdot)$.

6.4.2 Estimate for $\tilde{Q}_{i+1,\omega_{i+1}}(\mu)\left[q_{i+1}^{-}(\mu)(-\omega_{i+1}) - q_i^{+}(\mu)(\omega_{i+1})\right]$

By Theorem 6.3.1,

$$\begin{aligned} q_1^+(\mu)(t) &= \Phi_{p_1}(\mu,t,0)\eta_1^s(q_1^+(\mu)(0),\mu) \\ &\qquad +\mathcal{O}(\exp(-\min\{|\alpha_1^{ss}|,2|\alpha_1^s|\}t), \qquad (6.23) \\ q_2^-(\mu)(-t) &= \Phi_{p_1}(\mu,-t,0)\eta_1^u(q_2^-(\mu)(0),\mu) \\ &\qquad +\mathcal{O}(\exp(-\min\{|\alpha_1^{uu}|,2|\alpha_1^u|\}t), \qquad (6.24) \end{aligned}$$

where $\Phi_{p_i}(\mu,\cdot,\cdot)$ is the transition matrix operator of the equation $\dot{x} = D_xf(p_i,\mu)x$, $\eta_1^s(q_1^+(\mu)(0),\mu)$ (resp. $\eta_1^u(q_2^-(\mu)(0),\mu)$) is in the stable (resp. unstable) subspace of $D_xf(p_1,\mu)$. Recalling estimates (6.12), (6.13) then, we have

$$\begin{aligned} \tilde{Q}_{i+1,\omega_{i+1}}(\mu)(q_1^+(\mu)(\omega_{i+1})) &= +\mathcal{O}(\exp((-\min\{-\alpha_1^s,\alpha_1^u\}-\lambda(\mu))\omega_{i+1}) \\ &\qquad +\mathcal{O}((\exp(-\min\{-\alpha_1^s,\alpha_1^u\}-\min\{|\alpha_1^{ss}|,2|\alpha_1^s|\})\omega_{i+1}), \\ &\qquad (6.25) \\ \tilde{Q}_{i+1,\omega_{i+1}}(\mu)(q_2^-(\mu)(-\omega_{i+1})) &= \Phi_{p_1}(\mu,-\omega_{i+1},0)\eta_1^u(q_2^-(\mu)(0),\mu) \\ &\qquad +\mathcal{O}(\exp((-\min\{-\alpha_1^s,\alpha_1^u\}-\rho(\mu))\omega_{i+1}) \\ &\qquad +\mathcal{O}((\exp(-\min\{-\alpha_1^s,\alpha_1^u\}-\min\{\alpha_1^{uu},2\alpha_1^u\})\omega_{i+1}). \\ &\qquad (6.26) \end{aligned}$$

In a similar way we show

$$\begin{aligned} \tilde{P}_{i,\omega_i}(\mu)(q_2^+(\mu)(\omega_i)) &= \Phi_{p_2}(\mu,\omega_i,0)\eta_2^s(q_2^+(\mu)(0),\mu) \\ &\qquad +\mathcal{O}(\exp((-\min\{-\alpha_2^s,\alpha_2^u\}-\rho(\mu))\omega_i) \\ &\qquad +\mathcal{O}((\exp(-\min\{-\alpha_2^s,\alpha_2^u\}-\min\{\alpha_2^{uu},2\alpha_2^u\})\omega_i), \\ &\qquad (6.27) \\ \tilde{P}_{i,\omega_i}(\mu)(q_1^-(\mu)(-\omega_i)) &= +\mathcal{O}(\exp((-\min\{-\alpha_2^s,\alpha_2^u\}-\lambda(\mu))\omega_i) \\ &\qquad +\mathcal{O}((\exp(-\min\{-\alpha_2^s,\alpha_2^u\}-\min\{|\alpha_2^{ss}|,2|\alpha_1^s|\})\omega_i). \\ &\qquad (6.28) \end{aligned}$$

6.4.3 Estimate for $\tilde{Q}_{i+1,\omega_{i+1}}(\mu)\left[Q_{2,-}(\mu,-\omega_{i+1})z_{i+1}^-(-\omega_{i+1}) - P_{1,+}(\mu,\omega_{i+1})z_i^+(\omega_{i+1})\right]$

From (6.5) we have

$$||P_{1,+}(\mu,\omega_{i+1})z_i^+(\omega_{i+1})|| + ||Q_{2,-}(\mu,-\omega_{i+1})z_{i+1}^-(-\omega_{i+1})|| \leq K(e^{-2\alpha\overline{\omega}}||\mathbf{a}|| + ||\mathbf{g}||),$$

where all the $\omega_i \geq \overline{\omega}$. In fact, we can write

$$\begin{aligned} &||P_{1,+}(\mu,\omega_{i+1})z_i^+(\omega_{i+1})|| + ||Q_{2,-}(\mu,-\omega_{i+1})z_{i+1}^-(-\omega_{i+1})|| \\ &\quad \leq K(\exp(-2\min\{\alpha_1^u,-\alpha_1^s\}\omega_{i+1}||\mathbf{a}|| + ||g_i^-|| + ||g_{i-1}^+||)), \end{aligned} \tag{6.29}$$

Now from (6.6) we have

$$||z_i^\pm(t)|| \leq K(||\mathbf{d}|| + ||\mathbf{g}||).$$

In fact, we will use the following Lemma, which decouples estimate (6.6) over i.

Lemma 6.4.2. $||(\tilde{z}_i^+(t), \tilde{z}_{i+1}^-(t))|| \leq K(||d_{i+1}|| + ||(h_i^+, h_{i+1}^-)||)$.

Proof. We follow the same arguments as in section 6.1, but we will keep track of only $\tilde{z}_i^+(t)$ and $\tilde{z}_{i+1}^-(t)$. Identically to section 6.1.1 we find

$$\begin{aligned} ||\tilde{z}_i^+(0)|| &\leq K(e^{-\alpha_i\omega_{i+1}}||a_i^+|| + ||h_i^+||), \\ ||\tilde{z}_{i+1}^-(0)|| &\leq K(e^{-\alpha_{i+1}\omega_{i+1}}||a_{i+1}^-|| + ||h_{i+1}^-||). \end{aligned} \tag{6.30}$$

Now, we follow the same arguments as in section 6.1.3 to show the estimates

$$\begin{aligned} ||P_{i,+}(\mu,\omega_i)\tilde{z}_i^+(\omega_i)|| &\leq K(e^{-\alpha_i\omega_{i+1}}||\tilde{z}_i^+(0)|| + ||h_i^+||), \\ ||Q_{i+1,+}(\mu,\omega_i)\tilde{z}_{i+1}^-(\omega_{i+1})|| &\leq K(e^{-\alpha_{i+1}\omega_{i+1}}||\tilde{z}_{i+1}^-(0)|| + ||h_{i+1}^-||), \end{aligned}$$

and together with (6.30) we show

$$\begin{aligned} ||P_{i,+}(\mu,\omega_i)\tilde{z}_i^+(\omega_i)|| &\leq K(e^{-\alpha_i\omega_{i+1}}||a_i^+|| + ||h_i^+||), \\ ||Q_{i+1,+}(\mu,\omega_i)\tilde{z}_{i+1}^-(\omega_{i+1})|| &\leq K(e^{-\alpha_{i+1}\omega_{i+1}}||a_{i+1}^-|| + ||h_{i+1}^-||). \end{aligned} \tag{6.31}$$

Now, from (5.46) we have

$$a_i^+ - a_{i+1}^- = d_{i+1} - P_{i,+}(\mu,\omega_{i+1})\tilde{z}_i^+(\omega_{i+1}) + Q_{i+1,-}(\mu,-\omega_{i+1})\tilde{z}_{i+1}^-(-\omega_{i+1}).$$

Using the projections $\tilde{P}_{i+1,\omega_{i+1}}$, $\tilde{Q}_{i+1,\omega_{i+1}}$:

$$\begin{aligned} a_i^+ &= \tilde{Q}_{i+1,\omega_{i+1}}(d_{i+1} - P_{i,+}(\mu,\omega_{i+1})\tilde{z}_i^+(\omega_{i+1}) \\ &\qquad + Q_{i+1,-}(\mu,-\omega_{i+1})\tilde{z}_{i+1}^-(-\omega_{i+1})), \\ a_{i+1}^- &= -\tilde{P}_{i+1,\omega_{i+1}}(d_{i+1} - P_{i,+}(\mu,\omega_{i+1})\tilde{z}_i^+(\omega_{i+1}) \\ &\qquad + Q_{i+1,-}(\mu,-\omega_{i+1})\tilde{z}_{i+1}^-(-\omega_{i+1})). \end{aligned}$$

The terms $-P_{i,+}(\mu,\omega_{i+1})\tilde{z}_i^+(\omega_{i+1}) + Q_{i+1,-}(\mu,-\omega_{i+1})\tilde{z}_{i+1}^-(-\omega_{i+1})$ depend linearly on $(a_i^+, a_{i+1}^-, h_i^+, h_{i+1}^-)$. Then we may write

$$(a_i^+, a_{i+1}^-) = L_1'(\mu)(a_i^+, a_{i+1}^-) + L_2'(\mu)(h_i^+, h_{i+1}^-) + L_3'(\mu)d_{i+1},$$

where the $L_j'(\mu)$, $j = 1,2,3$, are linear operators depending smoothly on μ. Now the estimates (6.31) ensure that we can choose ω_{i+1} large enough so that the operator $(I - L_1(\mu))$ is invertible. Then we find that (a_i^+, a_{i+1}^-) is a linear function of d_{i+1} and (h_i^+, h_{i+1}^-).

From section 6.1.2 we have that

$$\begin{aligned} ||\tilde{z}_i^+(t)|| &\leq K(||a_i^+|| + ||h_i^+||), \\ ||\tilde{z}_{i+1}^-(t)|| &\leq K(||a_{i+1}^-|| + ||h_{i+1}^-||), \end{aligned}$$

and we can now use the linear dependence of (a_i^+, a_{i+1}^-) on d_{i+1} and (h_i^+, h_{i+1}^-) to prove the Lemma. □

From Lemma 6.4.2 we see that we may write

$$||(\tilde{z}_i^+(t), \tilde{z}_{i+1}^-(t))|| \leq K(||d_{i+1}|| + ||(g_i^+, g_{i+1}^-)||).$$

Now, it follows from the definition that $g_i^\pm = \mathcal{O}(||z_i^\pm||^2)$ and hence for $||\mathbf{z}||$ small enough, we have

$$K||(g_i^+, g_{i+1}^-)|| \leq \frac{1}{2}||(z_i^+(t), z_{i+1}^-(t)||,$$

and then

$$||(z_i^+(t), z_{i+1}^-(t))|| \leq K||d_{i+1}||.$$

Recall that the definition of d_{i+1} was given by $d_{i+1} := q_{i+1}^-(\mu)(-\omega_{i+1}) - q_i^+(\mu)(\omega_{i+1})$ and from (6.23) and (6.24) we obtain the estimate

$$||(z_i^+(t), z_{i+1}^-(t))|| = \mathcal{O}(\exp(-\min\{-\alpha_1^s, \alpha_1^u\}\omega_{i+1})), \tag{6.32}$$

and since $g_i^\pm = \mathcal{O}(||z_i^\pm||^2)$ we have

$$||(g_i^+, g_{i+1}^-)|| = \mathcal{O}(\exp(-2\min\{-\alpha_1^s, \alpha_1^u\}\omega_{i+1})),$$

We can now combine this with equation (6.29) to provide

$$\begin{aligned} Q_{2,-}(\mu, -\omega_{i+1})z_{i+1}^-(-\omega_{i+1}) - P_{1,+}(\mu, \omega_{i+1})z_i^+(\omega_{i+1}) & \\ = \quad \mathcal{O}(\exp(-2\min\{-\alpha_1^s, \alpha_1^u\}\omega_{i+1})). & \end{aligned} \tag{6.33}$$

Now by Lemma 5.4.5 we obtain the final estimate

$$\begin{aligned} \tilde{Q}_{i+1,\omega_{i+1}}(\mu)\left[Q_{2,-}(\mu, -\omega_{i+1})z_{i+1}^-(-\omega_{i+1}) - P_{1,+}(\mu, \omega_{i+1})z_i^+(\omega_{i+1})\right] & \\ = \mathcal{O}(\exp(-2\min\{-\alpha_1^s, \alpha_1^u\}\omega_{i+1})). & \end{aligned} \tag{6.34}$$

Similarly we can show

$$\begin{aligned} \tilde{P}_{i,\omega_i}(\mu)\left[P_{2,+}(\mu, \omega_i)z_{i-1}^+(\omega_i) - Q_{1,-}(\mu, -\omega_i)z_i^-(-\omega_i)\right] & \\ = \mathcal{O}(\exp(-2\min\{-\alpha_2^s, \alpha_2^u\}\omega_i)). & \end{aligned} \tag{6.35}$$

6.4.4 Estimate for $\int_0^{\omega_{i+1}} \Phi_1^+(\mu, 0, s)Q_{1,+}(\mu, s)g_1^+(s, z_i^+(s; \omega, \mu), \mu)ds$

First define

$$\begin{aligned} z_i^{+,u}(t) &:= Q_{i,+}(\mu, t)z_i^+(t), \\ z_i^{+,s}(t) &:= P_{i,+}(\mu, t)z_i^+(t), \end{aligned}$$

so $z_i^+(t) = z_i^{+,s}(t) + z_i^{+,u}(t)$. Recall from (5.28):

$$g_1^+(t, z_i^+(t), \mu) = f(q_1^+(\mu)(t) + z_i^+(t), \mu) - f(q_1^+(\mu)(t), \mu) - D_x f(q_1^+(\mu)(t), \mu)z_i^+(t).$$

Then we write

$$\begin{aligned} Q_{1,+}(\mu,s)g_1^+(s,z_i^+(s),\mu) &= Q_{1,+}(\mu,s)\left[f(q_1^+(\mu)(s)+z_i^{+,s}(s)+z_i^{+,u}(s),\mu)\right. \\ &\quad \left. -f(q_1^+(\mu)(s),\mu)-D_xf(q_1^+(\mu)(s),\mu)(z_i^{+,s}(s)+z_i^{+,u}(s))\right]. \end{aligned}$$

By the Mean Value Theorem, we can write for fixed s;

$$f(q_1^+(\mu)(s)+z,\mu)-f(q_1^+(\mu)(s),\mu)=\left(\int_0^1 D_xf(q_1^+(\mu)(s)+\tau z,\mu)d\tau\right)z.$$

Substituting this into the above gives

$$\begin{aligned} &Q_{1,+}(\mu,s)g_1^+(s,z_i^{+,s}(s)+z_i^{+,u}(s),\mu) \\ &\quad = Q_{1,+}(\mu,s)\left[\int_0^1 (D_xf(q_1^+(\mu)(s)+\tau(z_i^{+,s}(s)+z_i^{+,u}(s)),\mu)\right. \\ &\qquad \left. -D_xf(q_1^+(\mu)(s),\mu)(z_i^{+,s}(s)+z_i^{+,u}(s)))d\tau\right](z_i^{+,s}(s)+z_i^{+,u}(s)) \\ &\quad = \left[\int_0^1\left(\frac{\partial}{\partial z_i^{+,s}}Q_{1,+}(\mu,s)f(q_1^+(\mu)(s)+\tau(z_i^{+,s}(s)+z_i^{+,u}(s)),\mu)\right.\right. \\ &\qquad \left.\left.-\frac{\partial}{\partial z_i^{+,s}}Q_{1,+}(\mu,s)f(q_1^+(\mu)(s),\mu)\right)d\tau\right]z_i^{+,s}(s) \\ &\qquad +\left[\int_0^1\left(\frac{\partial}{\partial z_i^{+,u}}Q_{1,+}(\mu,s)f(q_1^+(\mu)(s)+\tau(z_i^{+,s}(s)+z_i^{+,u}(s)),\mu)\right.\right. \\ &\qquad \left.\left.-\frac{\partial}{\partial z_i^{+,u}}Q_{1,+}(\mu,s)f(q_1^+(\mu)(s),\mu)\right)d\tau\right]z_i^{+,u}(s). \end{aligned}$$

We apply the Mean Value Theorem again to the two terms in the last equation:

$$\begin{aligned} &Q_{1,+}(\mu,s)g_1^+(s,z_i^{+,s}(s)+z_i^{+,u}(s),\mu) \\ &\quad = \left[\int_0^1\int_0^1 \frac{\partial^2}{\partial(z_i^{+,s})^2}Q_{1,+}(\mu,s)f(q_1^+(\mu)(s)\right. \\ &\qquad \left.+\tau_1\tau_2(z_i^{+,s}(s)+z_i^{+,u}(s)),\mu)d\tau_1d\tau_2\right](z_i^{+,s}(s),z_i^{+,s}(s)) \\ &\qquad +2\left[\int_0^1\int_0^1 \frac{\partial^2}{\partial z_i^{+,s}\partial z_i^{+,u}}Q_{1,+}(\mu,s)f(q_1^+(\mu)(s)\right. \\ &\qquad \left.+\tau_1\tau_2(z_i^{+,s}(s)+z_i^{+,u}(s)),\mu)d\tau_1d\tau_2\right](z_i^{+,s}(s),z_i^{+,u}(u)) \\ &\qquad +\left[\int_0^1\int_0^1 \frac{\partial^2}{\partial(z_i^{+,u})^2}Q_{1,+}(\mu,s)f(q_1^+(\mu)(s)\right. \\ &\qquad \left.+\tau_1\tau_2(z_i^{+,s}(s)+z_i^{+,u}(s)),\mu)d\tau_1\tau_2\right](z_i^{+,u}(s),z_i^{+,u}(s)). \end{aligned} \tag{6.36}$$

We now recall that the stable/unstable manifolds of the fixed points p_i are locally flat, see (5.9). Note that Im $P_{1,+}(\mu,s)=T_{q_1^+(\mu)(s)}W^s(p_i,\mu)\supset W^s_{loc}(p_i,\mu)$.

Then if we consider $||z_i^{+,s}(s)|| < \epsilon$ sufficiently small, s sufficiently large, then $z_i^{+,s}(s) \in W^s(p_i,\mu) \cap B(q_1^+(\mu)(s),\epsilon)$, where $B(x,\epsilon)$ is a ball centred on x, radius ϵ. Now, since $W^s(p_i,\mu)$ is f-invariant, we have

$$Q_{1,+}(\mu,s)f(q_1^+(\mu)(s)+z_i^{+,s}(s),\mu)=0,$$

and we also have

$$\frac{\partial^2}{\partial(z_i^{+,s})^2}Q_{1,+}(\mu,s)f(q_1^+(\mu)(s)+z^s,\mu)=0$$

for all $z^s \in W^s(p_i,\mu)\cap B(q_1^+(\mu)(s),\epsilon)$. This means we may rewrite the first term on the right hand side of (6.36) as

$$\begin{aligned}
&\Big[\int_0^1\int_0^1 \frac{\partial^2}{\partial(z_i^{+,s})^2}Q_{1,+}(\mu,s)f(q_1^+(\mu)(s)\\
&\quad+\tau_1\tau_2(z_i^{+,s}(s)+z_i^{+,u}(s)),\mu)d\tau_1 d\tau_2\Big]\left(z_i^{+,s}(s),z_i^{+,s}(s)\right)\\
&\quad= \Big[\int_0^1\int_0^1 \frac{\partial^2}{\partial(z_i^{+,s})^2}Q_{1,+}(\mu,s)f(q_1^+(\mu)(s)+\tau_1\tau_2(z_i^{+,s}(s)+z_i^{+,u}(s)),\mu)d\tau_1 d\tau_2\\
&\qquad -\int_0^1\int_0^1 \frac{\partial^2}{\partial(z_i^{+,s})^2}Q_{1,+}(\mu,s)f(q_1^+(\mu)(s)\\
&\qquad\qquad +\tau_1\tau_2 z_i^{+,s}(s),\mu)d\tau_1 d\tau_2\Big]\left(z_i^{+,s}(s),z_i^{+,s}(s)\right).
\end{aligned}$$

Now we again may apply the Mean Value Theorem, and we obtain

$$\begin{aligned}
&\Big[\int_0^1\int_0^1 \frac{\partial^2}{\partial(z_i^{+,s})^2}Q_{1,+}(\mu,s)f(q_1^+(\mu)(s)\\
&\quad+\tau_1\tau_2(z_i^{+,s}(s)+z_i^{+,u}(s)),\mu)d\tau_1 d\tau_2\Big]\left(z_i^{+,s}(s),z_i^{+,s}(s)\right)\\
&\quad= \Big[\int_0^1\int_0^1\int_0^1 \frac{\partial^3}{\partial(z_i^{+,s})^2\partial z_i^{+,u}}Q_{1,+}(\mu,s)f(q_1^+(\mu)(s)\\
&\qquad +\tau_1\tau_2 z_i^{+,s}(s)+\tau_1\tau_2\tau_3 z_i^{+,u}(s),\mu)d\tau_1 d\tau_2 d\tau_3\Big]\left(z_i^{+,s}(s),z_i^{+,s}(s),z_i^{+,u}(s)\right).
\end{aligned}$$

Using the fact that $z_i^{+,s/u}$ and the partial derivatives of $Q_{1,+}(\mu,s)f(\cdots)$ are bounded, we have

$$||Q_{1,+}(\mu,s)g_1^+(s,\tilde{z}_i^+(s;\omega,\mu)|| \le C||z_i^{+,u}(s)||(||z_i^{+,s}(s)||+||z_i^{+,u}(s)||). \quad (6.37)$$

Now, it is easy to see that

$$\begin{aligned}
&\left|\left|\int_0^{\omega_{i+1}}\Phi_1^+(\mu,0,s)Q_{1,+}(\mu,s)g_1^+(s,z_i^+(s),\mu)ds\right|\right|\\
&\quad\le \exp(-\alpha_1^u\omega_{i+1})\omega_{i+1}\left(\sup_{s\in[0,\omega_{i+1}]}\{K\exp(\alpha_1^u(\omega_{i+1}-s)).\right.\\
&\qquad\qquad \left.||Q_{1,+}(\mu,s)g_1^+(s,z_i^+(s),\mu)||\}\right). \quad (6.38)
\end{aligned}$$

Now choose $\delta < 0$ such that $\delta + \alpha_1^u > 0$ and ω_{i+1} so large that $e^{\delta\omega_{i+1}}\omega_{i+1} < 1$. Then we multiply the right hand side of (6.38) by $e^{(\delta-\delta)\omega_{i+1}}$ and combine together with (6.37) to obtain

$$\begin{aligned}&\left|\left|\int_0^{\omega_{i+1}} \Phi_1^+(\mu,0,s)Q_{1,+}(\mu,s)g_1^+(s,z_i^+(s),\mu)ds\right|\right|\\&\quad\leq \exp(-(\delta+\alpha_1^u)\omega_{i+1})C||z_i^+||\left(\sup_{s\in[0,\omega_{i+1}]}\{K\exp(\alpha_1^u(\omega_{i+1}-s))||z_i^{+,u}(s)||\}\right).\end{aligned}$$

Here $||z_i^+||$ is the sup norm. Using estimate (6.32):

$$\begin{aligned}&\left|\left|\int_0^{\omega_{i+1}} \Phi_1^+(\mu,0,s)Q_{1,+}(\mu,s)g_1^+(s,z_i^+(s),\mu)ds\right|\right|\\&\qquad\leq \exp(-(\delta+\alpha_1^u)\omega_{i+1})C\exp(-\min\{-\alpha_1^s,\alpha_1^u\}\omega_{i+1}).\\&\qquad\qquad\left(\sup_{s\in[0,\omega_{i+1}]}\{K\exp(\alpha_1^u(\omega_{i+1}-s))||z_i^{+,u}(s)||\}\right).\end{aligned}$$

We would now like to estimate $\sup_{s\in[0,\omega_{i+1}]}\{K\exp(\alpha_1^u(\omega_{i+1}-s))||z_i^{+,u}(s)||\}$. Recall again from section 5.4.1 (cf. 5.36);

$$\begin{aligned}Q_{1,+}(\mu,s)z_i^+(s) &= \Phi_1^+(\mu,s,\omega_{i+1})Q_{1,+}(\mu,s)a_i^+\\&\quad -\int_s^{\omega_{i+1}} \Phi_1^+(\mu,s,\tau)Q_{1,+}(\mu,\tau)g_1^+(\tau,z_i^+(\tau),\mu)d\tau.\end{aligned}$$

This gives

$$\begin{aligned}||z_i^{+,u}(s)|| &= ||Q_{1,+}(\mu,s)z_i^+(s)||\\&\leq ||\Phi_1^+(\mu,s,\omega_{i+1})Q_{1,+}(\mu,s)||.||a_i^+||\\&\quad+\left|\left|\int_s^{\omega_{i+1}} \Phi_1^+(\mu,s,\tau)Q_{1,+}(\mu,\tau)g_1^+(\tau,z_i^+(\tau),\mu)d\tau\right|\right|.\end{aligned}$$

Using again (6.37) and the exponential dichotomy for $\Phi_1^+(\mu,\cdot,\cdot)$;

$$\begin{aligned}&\exp(\alpha_1^u(\omega_{i+1}-s))||z_i^{+,u}(s)||\\&\quad\leq\quad K\exp(\alpha_1^u(\omega_{i+1}-s))\exp(-\alpha_1^u(\omega_{i+1}-s))||a_i^+||\\&\qquad\qquad +K\exp(\alpha_1^u(\omega_{i+1}-s))\int_s^{\omega_{i+1}}\exp(-\alpha_1^u(\tau-s)).\\&\qquad\qquad\qquad ||z_i^{+,u}(\tau)||(||z_i^{+,u}(\tau)||+||z_i^{+,s}(\tau)||)d\tau\\&\quad\leq\quad K||a_i^+||+K\omega_{i+1}\sup{}_{\tau\in[s,\omega_{i+1}]}\{\exp(-\alpha_1^u(\tau-\omega_{i+1})).\\&\qquad\qquad ||z_i^{+,u}(\tau)||(||z_i^{+,u}(\tau)||+||z_i^{+,s}(\tau)||)\}.\end{aligned}$$

Therefore

$$\begin{aligned}
&\sup{}_{s\in[0,\omega_{i+1}]} \exp(\alpha_1^u(\omega_{i+1}-s))||z_i^{+,u}(s)|| \\
&\quad\leq \quad K||a_i^+|| + K\omega_{i+1}\sup{}_{\tau\in[0,\omega_{i+1}]}\{\exp(-\alpha_1^u(\tau-\omega_{i+1}))||z_i^{+,u}(\tau)||\}. \\
&\qquad\qquad \sup{}_{\tau\in[0,\omega_{i+1}]}\{||z_i^{+,u}(\tau)|| + ||z_i^{+,s}(\tau)||\}. \qquad (6.39)
\end{aligned}$$

Note that $\sup{}_{\tau\in[0,\omega_{i+1}]}\{||z_i^{+,u}(\tau)|| + ||z_i^{+,s}(\tau)||\} \leq C||z_i^+||$, and that $||z_i^+||$ is converging exponentially to zero as ω_{i+1} tends to infinity

Then for ω_{i+1} large enough, we have

$$\sup{}_{\tau\in[0,\omega_{i+1}]}\{||z_i^{+,u}(\tau)|| + ||z_i^{+,s}(\tau)||\} < \frac{1}{2K}.$$

Now, together with (6.39) we prove that

$$\sup{}_{s\in[0,\omega_{i+1}]} \exp(\alpha_1^u(\omega_{i+1}-s))||z_i^{+,u}(s)|| \leq 2K||a_i^+||.$$

We estimate the term $||a_i^+||$ by using (5.48), (6.33), the definition of d_{i+1} and Theorem 6.3.1. Then we see that we may estimate $||a_i^+||$ by

$$||a_i^+|| \leq C\exp(-\min\,\{-\alpha_1^s, \alpha^u\}\omega_{i+1}),$$

so that

$$\sup{}_{s\in[0,\omega_{i+1}]} \exp(\alpha_1^u(\omega_{i+1}-s))||z_i^{+,u}(s)|| \leq C\exp(-\min\,\{-\alpha_1^s, \alpha^u\}\omega_{i+1}).$$

Finally then, we obtain the estimate

$$\begin{aligned}
&\left|\left|\int_0^{\omega_{i+1}} \Phi_1^+(\mu,0,s)Q_{1,+}(\mu,s)g_1^+(s,z_i^+(s),\mu)ds\right|\right| \\
&\qquad\qquad\qquad \leq\; C\exp(-2\min\,\{-\alpha_1^s, \alpha_1^u\}\omega_{i+1}). \qquad (6.40)
\end{aligned}$$

In a similar way we prove the estimate

$$\begin{aligned}
&\left|\left|\int_{-\omega_i}^0 \Phi_1^-(\mu,0,s)P_{1,-}(\mu,s)g_1^-(s,z_i^-(s),\mu)ds\right|\right| \\
&\qquad\qquad\qquad \leq\; C\exp(-2\min\,\{-\alpha_2^s, \alpha_2^u\}\omega_i). \qquad (6.41)
\end{aligned}$$

Chapter 7

Summary and Discussion

This thesis has studied generic dynamical phenomena that arise in three dimensional systems, specifically due to an involutory reversing symmetry. We have first examined numerically the bifurcation behaviour of the Michelson system,

$$\begin{aligned}\dot{x} &= y,\\ \dot{y} &= z,\\ \dot{z} &= c^2 - \frac{1}{2}x^2 - y,\end{aligned} \tag{$*$}$$

which is a reversible system with respect to the involution $R(x, y, z) = (-x, y, -z)$. We have examined the codimension one reversible 'Hopf-zero' bifurcation which occurs at $c = 0$, first through a general reversible normal form analysis, and also with a multiple time scale analysis for the Michelson system for small c. We have seen that these two approaches recover the same result. The formal normal form puts the system in an S^1 symmetric form, separating the angular component of the vector field. This is equivalent to the separation of solutions that evolve on different time scales, since the angular component of the vector field is approximately constant, whereas the remaining vector field components are of higher order. However, the multiple time scale analysis provides approximate analytic solutions for all of the bounded phase space trajectories in this parameter range for the Michelson system, which are of a relatively simple form, due to the simple form of equations ($*$). This analysis demonstrates the near integrable behaviour of the Michelson system for small values of the parameter c, which is evident also from the normal form. Agreement between these approximate results and numerical simulations of the full system is excellent. However, this analysis is effectively only formal, and does not take into account higher order terms (the flat terms) that break the S^1 symmetry. We have also considered the effect of the addition of these terms, and found that we may expect many heteroclinic and homoclinic bifurcations to occur, leading to chaotic dynamics. The nature of this result infers that although numerical evidence can be given for the existence of chaotic dynamics, it cannot be checked in physical applications (such as the Michelson system) in any finite jet of the normal form.

We have further focused on analysing the heteroclinic cycle bifurcation, using the results from the normal form unfolding analysis as a partial motivation. There is also strong evidence that this heteroclinic cycle bifurcation occurs in the Michelson system at $c \approx 0.84952$, where it is known that a 1D heteroclinic connection exists [67]:

$$x(t) = \alpha(-9\tanh\beta t + 11\tanh^3\beta t), \tag{$\dagger$}$$

where $\alpha = 15\sqrt{\frac{11}{19^3}}$, $\beta = \frac{1}{2}\sqrt{\frac{11}{19}}$, and there is also numerical evidence for the existence of many 2D heteroclinic connections at the same parameter value, which combine with ($\dagger$) to form a heteroclinic cycle. Another motivation of studying this heteroclinic cycle is to further progress a current area of research, which is to try and reduce the study of heteroclinic/homoclinic bifurcation in reversible-equivariant systems to that of steady state bifurcation, using singularity theory. Lin's method appears to be a good tool for this study, and it is hoped that in the general reversible-equivariant case, it is possible to classify the different bifurcation equations that arise, and therefore also classify some of the main bifurcation properties these heteroclinic/homoclinic cycles possess. As is the case with Lin's method, the first step is to classify the splitting of invariant manifolds in reversible-equivariant systems by singularity theory. A final motivation for our study is that the heteroclinic cycle bifurcation is also used as a model with which to compare the two contrasting approaches to analyse heteroclinic/homoclinic cycle configurations—namely, the more standard geometric approach and Lin's method.

The bifurcation analysis contained in chapters 4 and 5 reveal very rich dynamical behaviour in a neighbourhood of the heteroclinic cycle, similar to that which appears close to a single homoclinic orbit to a hyperbolic saddle-focus. However, in our case the dynamics is much more complicated, and there are important differences from the homoclinic case, such as the fact that the presence of complicated dynamics does not depend on the ratio of eigenvalues of the fixed points. This is due to the fixed points having different index. An organising centre for the dynamics is shown to be a symmetric horseshoe which exists at the critical parameter value. We have made generic hypotheses to ensure hyperbolicity of the symmetric horseshoe and generic unfolding of the heteroclinic cycle, but even without these hypotheses, complicated dynamics would still be present.

It would be an interesting problem to see if it is possible to check that the generic hypotheses are satisfied in the Michelson system at the parameter value $c \approx 0.84952$, since there exists an analytic solution for a 1D heteroclinic connection (†). To do this, one would need to first check the hypothesis that the 1D heteroclinic connection breaks with positive speed with respect to the parameter. This could be checked by proving the value of a given integral is nonzero, as described in section 5.3.3. There is no known analytic solution for a 2D heteroclinic connection at this parameter value, although it is suspected that the simplest 2D heteroclinic connection $X_0(t)$ exists. One could perhaps perform a computer assisted proof that this orbit exists, and that it is a transversal heteroclinic orbit.

Finally, we would like to compare the two methods used in the study of the heteroclinic cycle bifurcation in chapters 4 and 5. The geometrical approach is maybe more intuitive, and builds a picture of the local dynamics, whereas Lin's method is perhaps somewhat less intuitive, and is compared to a Liapunov Schmidt reduction, where the dynamics of the system is discarded and solutions are sought simply as the zeros of functions. Both methods bring many technical difficulties—in the geometric case, these difficulties are manifest in the introduction of local coordinates, expressions for the composition of local and global maps, and non-differentiability of the return maps. In chapter 4 we have used C^1 linearisation about each fixed point, but the analysis is also made much more difficult if such a linearisation is either not possible, or one wishes to study higher derivatives of the return maps, for example to study local bifurcations. In this case one uses local C^k coordinates to put the system near the fixed points in a simpler form, see e.g. [2, 17, 87].

In the case of Lin's method, many estimates are needed to write down the leading order term of the jump $\Xi_i^\omega(\mu)$, but these technical details are standard in the application of Lin's method, and so for each new problem the derivation of the bifurcation equations is much simpler. In this thesis we have also tried to argue that the geometric picture is not entirely discarded through Lin's method: in this case, the times ω_i, ω_{i+1} parametrise the spirals in the section Σ_1, and where they intersect we find solutions. Therefore we can build up a complete topological picture of the return maps in this way. This is the same picture that is used in chapter 4 to analyse the local dynamics. In fact, the only information that is missing from the bifurcation equations of Lin's method when compared to the analysis in chapter 4 is the derivatives of the return map, which are used to establish hyperbolicity of the symmetric horseshoe.

However, it is maybe possible to prove hyperbolicity of the invariant set established by Lin's method, using the information supplied in $\Xi_i^\omega(\mu)$: we can establish the existence and uniqueness of certain periodic and aperiodic orbits from the bifurcation equations, as well as their persistence under an arbitrarily small perturbation. Then we may be able to prove hyperbolicity of this set by using this persistence property. This would yield the same description of the symmetric horseshoe as in section 4.5 in terms of topological structure and hyperbolicity.

Bibliography

[1] Abraham, R. & Robbin, J. (1967), *Transversal Mappings and Flows*, W. A. Benjamin, Inc., New York.

[2] Alekseeva, S. A. & Shil'nikov, L. P. (2000), 'On cusp-bifurcations of periodic orbits in systems with a saddle-focus homoclinic curve', *Amer. Math. Soc. Transl.* **200**, 23–34.

[3] Armbruster, D., Guckenheimer, J. & Holmes, P. (1989), 'Kuramoto-Sivashinsky Dynamics on the center-unstable manifold', *SIAM J. Appl. Math* **49**, No. 3, 676–691.

[4] Arn'old, V. I. (1994), *Dynamical Systems V/Bifurcation Theory and Catastrophe Theory*, Springer-Verlag, Berlin, London.

[5] Arn'old, V. I. & Sevryuk, M. B. (1986), 'Oscillations and bifurcations in reversible systems', *in*: Sagdeev, R. Z. (ed.), '*Nonlinear Phenomena in Plasma Physics and Hydrodynamics*', Mir, Moscow, 31–64.

[6] Artuso, R., Aurell, E. & Cvitanović, P. (1990), 'Recycling of strange sets: I. Cycle expansions', *Nonlinearity* **3**, 325–359.

[7] Artuso, R., Aurell, E. & Cvitanović, P. (1990), 'Recycling of strange sets: II. Applications', *Nonlinearity* **3**, 361–386.

[8] Belitskii, G. R. (1973), 'Functional equations and conjugacy of local diffeomorphisms of a finite smoothness class', *Func. Anal. Appl.* **7**, 268–277.

[9] Bochner, S. (1945), 'Compact groups of differentiable transformations', *Ann. of Math.* **(2) 46**, 372–381.

[10] Broer, H. W. (1979), *Bifurcations of singularities in volume preserving vector fields*, PhD Thesis, Groningen.

[11] Broer, H. W. (1980), 'Formal normal forms for vector fields and some consequences for bifurcations in the volume-preserving case', *in* Rand, D. A. & Young, L.-S. (eds.), '*Dynamical Systems and Turbulence*', Springer Lecture Notes in Mathematics 898, 54–74.

[12] Broer, H. W. (1980), 'Quasi periodic flow near a codimension one singularity of a divergence free vector field in dimension three', *in* Rand, D. A. & Young, L.-S. (eds.), '*Dynamical Systems and Turbulence*', Springer Lecture Notes in Mathematics 898, 75–89.

[13] Broer, H. W. & van Strien, S. J. (1983), 'Infinitely many moduli of strong stability in divergence free unfoldings of singularities of vector fields', *Geometric Dynamics*, Lect. Not. in Math. **1007**, Springer, Berlin, 39–59.

[14] Broer, H. W. & Vegter, G. (1983), 'Subordinate Sil'nikov bifurcations near some singularities of vector fields having low codimension', *Ergod. Th. & Dynam. Sys.* **4**, 509–525.

[15] Buzzi, C. A., Teixeira, M. A. & Yang, J. (2001), 'Hopf-zero bifurcations of reversible vector fields', *Nonlinearity* **14**, 623–638.

[16] Bykov, V. V. (1999), 'On systems with separatrix contour containing two saddle-foci', *J. Math. Sci.* **95** No. 5, 2513–2522.

[17] Bykov, V. V. (2000), 'Orbit structure in a neighborhood of a separatrix cycle containing two saddle-foci', *Amer. Math. Soc. Transl.* **200**, 87–97.

[18] Cardan, J. (1545), *Ars Magna*.

[19] Chang, H.-C. (1986), 'Travelling waves on fluid interfaces: normal form analysis of the Kuramoto-Sivashinsky equation', *Phys. Fluids* **29**, 3142–3147.

[20] Chang, H.-C. (1987), 'Evolution of nonlinear waves on vertically falling films–a normal form analysis', *Chem. Eng. Sci.* **47**, 515–533.

[21] Christiansen, F., Cvitanović, P. & Putkaradze, V. (1997), 'Hopf's last hope: spatiotemporal chaos in terms of unstable recurrent patterns', *Nonlinearity* **10**, 55–70.

[22] Coddington, E. A. & Levinson, N. (1955), *Theory of ordinary differential equations*, McGraw-Hill Book Company, Inc., New York-Toronto-London.

[23] Coppel, W. A. (1978), *Dichotomies in Stability Theory*, Lect. Not. in Math. **629**, Springer-Verlag.

[24] Christiansen, F., Cvitanović, P. & Putkaradze, V. (1997), 'Hopf's last hope: spatiotemporal chaos in terms of unstable recurrent patterns', *Nonlinearity* **10**, 55–70.

[25] Cvitanović, P. (1991), 'Periodic orbits as the skeleton of classical and quantum chaos', *Physica D* **51**, 138–151.

[26] Cvitanović, P., Gunaratne, G. H. & Procaccia, I. (1988), 'Topological and metric properties of Hénon type strange attractors', *Phys. Rev. A* **38**, 1503–1520.

[27] Dawson, S. P. & Mancho, A. M. (1997), 'Collections of heteroclinic cycles in the Kuramoto-Sivashinsky equation', *Physica D* **100**, No. 3–4, 231–256.

[28] Diekmann, O., van Gils, S. A., Verduyn Lunel, S. M. & Walther, H.-O. (1995), *Delay Equations*, Springer-Verlag, *Applied Math. Sciences* **110**.

[29] Delshams, A. & Martinez-Seara, M. T. (1989), 'On the existence of homoclinic orbits in a family of vector fields near an equilibrium point', *in*

Alsina, C., Llibre, J., Mira Ch., Simo, C., Targonski, G. & Thibault, R. (eds.), *European Conference on Iteration Theory*, World Scientific Publishers, 167–177.

[30] Demekhin, Y. A., Tokarev, G. Y. & Shkadov, V. Y. (1991), 'Hierarchy of bifurcations of space-periodic structures in a nonlinear model of active dissipative media', *Physica D* **52**, 338–361.

[31] Devaney, R. L. (1976), 'Reversible diffeomorphisms and flows', *Trans. of the Amer. Math. Soc.* **218**, 89–113.

[32] Devaney, R. L. (1977), 'Blue sky catastrophes in reversible and Hamiltonian systems', *Indiana Univ. Math. J.* **26**, 247–263.

[33] Doedel, E. (1986), AUTO: software for continuation and bifurcation problems in ODEs, (Technical Report, California Institute of Technology, Pasadena CA 91125).

[34] Elgin, J. N. & Wu, X. (1996), 'Stability of cellular states of the Kuramoto-Sivashinsky equation', *SIAM J. Appl. Math.* **56**, No. 6, 1621–1638.

[35] Elphick, C., Tirapegui E., Brachet M. E., Coullet P. & Iooss G. (1987), 'A simple characterization for normal forms of singular vector fields', *Physica D* **29**, 95; addendum (1988), *Physica D* **32**, 488.

[36] Feroe, J. A. (1993), 'Homoclinic orbits in a parametrized saddle-focus system', *Physica D* **62**, 254–262.

[37] Field, M. (1970), 'Equivariant dynamical systems', *Bull. AMS* **76**, 1314–1318.

[38] Foias, C., Nicolaenko, B., Sell, G. R. & Temam, R. (1988), 'Inertial manifolds for the Kuramoto-Sivashinsky equation and estimates of their dimensions', *J. Math. Pures Appl.* **67**, 197–226.

[39] Gaspard, P. (1993), 'Local birth of homoclinic chaos', *Physica D* **62**, 94–122.

[40] Glendinning, P. & Sparrow, C. (1984), ‘Local and global behaviour near homoclinic orbits’, *J. Stat. Phys.* **35**, 645–696.

[41] Golubitsky, M., Marsden, J. E., Stewart, I. & Dellnitz, M. (1995), ‘The constrained Liapunov-Schmidt procedure and periodic orbits’, *Fields. Inst. Commun.* **4**, 81–127.

[42] Golubitsky M. & Schaeffer, D. G. (1985), *Singularities and Groups in Bifurcation Theory Vol. 1*, Springer-Verlag, *Applied Math. Sciences* **51**.

[43] Golubitsky, M. & Stewart, I. (2003), *The Symmetry Perspective. From equilibrium to chaos in phase space and physical space*, Birkhäuser Verlag, Basel.

[44] Golubitsky M., Stewart, I. & Schaeffer, D. G. (1988), *Singularities and Groups in Bifurcation Theory Vol. 2*, Springer-Verlag, *Applied Math. Sciences* **69**.

[45] Gonchenko, S. V., Turaev, D. V., Gaspard, P. & Nicolis, G. (1997), ‘Complexity in the bifurcation structure of homoclinic loops to a saddle-focus’, *Nonlinearity* **10**, 409–423.

[46] Gratrix, S. (2003), WinAuto97—an Auto 97 Windows Environment, *http://gratrix.net/auto*.

[47] Gratrix, S., *Spatiotemporal Chaos Analysed Through Unstable Periodic States*, PhD Thesis, Imperial College of Science, Technology and Medicine, London, to appear.

[48] Greene, J. M., Mackay, R. S., Vivaldi, F. & Feigenbaum, M. J. (1986), ‘Universal behaviour in families of area-preserving maps’, *Physica D* **3**, 468–486.

[49] Guckenheimer, J. (1981), ‘On a codimension two bifurcation’, *in* Dynamical Systems and Turbulence (Warwick 1980), Lecture Notes in Mathematics, **898**, Springer, New York.

[50] Guckenheimer, J. & Holmes, P. (1983), *Nonlinear Oscillations, Dynamical Systems, and Bifurcations of Vector Fields*, Springer, *Applied Math. Sciences* **42**.

[51] Hirsch, M. W. (1976), *Differential Topology*, Springer-Verlag: New York, Heidelberg, Berlin.

[52] Hirsch, M. W. & Smale, S. (1974), *Differential equations, dynamical systems, and linear algebra*, Pure and Applied Mathematics, Vol. 60, Academic Press, New York-London.

[53] Hooper, A. P. & Grimshaw, R. (1988), 'Travelling wave solutions of the Kuramoto-Sivashinsky equation', *Wave Motion* **10**, 405–420.

[54] Hoveijn, I., Lamb, J. S. W. & Roberts, R. M. (2003), 'Normal forms and unfoldings of linear systems in the eigenspaces of (anti-)automorphisms of order two', *J. Differential Equations* **190**, 182–213.

[55] Hyman, J. M. & Nicolaenko, B. (1988), 'The Kuramoto-Sivashinsky Equation: A Bridge Between PDEs and Dynamical Systems', *Physica D* **18**, 113–126.

[56] Kelley, J. (1955), *General Topology*, Van Nostrand Co., Inc., Princeton, New Jersey.

[57] Kent, P. (1991), *Bifurcations of the travelling-wave solutions of the Kuramoto-Sivashinsky equation*, PhD Thesis, Imperial College of Science, Technology and Medicine, London.

[58] Kent, P. & Elgin, J. N. (1991), 'Noose bifurcation of periodic orbits', *Nonlinearity* **4**, 1045–1061.

[59] Kent, P. & Elgin, J. N. (1991), 'A Shil'nikov-type analysis in a system with symmetry', *Physics Letters A* **152**, 28–32.

[60] Kent, P. & Elgin, J. N. (1992), 'Travelling-wave solutions of the Kuramoto-Sivashinsky equation', *Nonlinearity* **5**, 899–919.

[61] Kevrekidis, I. G., Nicolaenko, B. & Scovel, J. C. (1990), 'Back in the saddle again: a computer assisted study of the Kuramoto-Sivashinsky equation', *SIAM J. Appl. Math.* **50**, No. 3, 760–790.

[62] Klaus, J. & Knobloch, J. (2003), 'Bifurcation of homoclinic orbits to a saddle center in reversible systems', to appear in *Int. J. Bif. and Chaos*, preprint TU Ilmenau No. M01/01.

[63] Knobloch, J. (1997), 'Bifurcation of degenerate homoclinics in reversible and conservative systems', *J. Dyn. Diff. Eq.* **9** No. 3, 427–444.

[64] Knobloch, J. (2000), 'Lin's method for discrete dynamical systems', *J. of Difference Eq. and Appl.* **6**, 577–623.

[65] Knobloch, J. (2003), 'Jump estimates for Lin's method', preprint TU Ilmenau No. M31/99.

[66] Knobloch, J., Webster, K. N. & Lamb, J. S. W. (2003), 'Studying Heteroclinic Cycle Bifurcation in Reversible Systems using Lin's Method', in preparation.

[67] Kuramoto, Y. & Tsuzuki, T. (1976), 'Persistent propagation of concentration waves in dissipative media far from thermal equilibrium', *Prog. Theor. Phys.* **55**, 356–369.

[68] Lamb, J. S. W. (1994), *Reversing Symmetries in Dynamical Systems*, PhD Thesis, Amsterdam.

[69] Lamb, J. S. W. & Melbourne, I. (1999), 'Bifurcation from discrete rotating waves', *Arch. Rational Mech. Anal.* **149**, 229–270.

[70] Lamb, J. S. W., Melbourne, I. & Wulff, C. (2003), 'Bifurcation from periodic solutions with spatiotemporal symmetry, including resonances and mode-interactions', *J. Differential Eq.* **191**, 377–407.

[71] Lamb, J. S. W. & Roberts, J. A. G. (1998), 'Time-reversal symmetry in dynamical systems: a survey', *Physica D* **112**, 1–39.

[72] Lamb, J. S. W., Teixeira, M. A. & Webster, K. N. (2003), 'Heteroclinic Cycles near Hopf-Zero Bifurcation in Reversible Vector Fields in $\mathbb{R}^3$', in preparation.

[73] Lau, Y.-T. (1992), 'The "Cocoon" bifurcations in three-dimensional systems with two fixed points', *Internat. J. Bifur. Chaos Appl. Sci. Engrg.* **2**, no. 3, 543–558.

[74] Lin, X.-B. (1990), 'Using Melnikov's Method to Solve Silnikov's Problems', *Proc. Roy. Soc. Edinburgh* **116A**, 295–325.

[75] MacKay, R. S. (1982), *Renormalisation in area-preserving maps*, PhD Thesis, Princeton.

[76] Mackay, R. S. (1987), 'Introduction to the dynamics of area-preserving maps', *in* Month, M. & Dienes, M. (eds.), '*Physics of Particle Accelerators*', American Institute of Physics Conference Proceedings 153, vol. 1, 534–602.

[77] Mackay, R. S. (1994), 'Transport in 3D volume-preserving flows', *J. Nonlinear Sci.* **4**, 329–354.

[78] McCord, C. K. (1986), 'Uniqueness of connecting orbits in the equation $Y^{(3)} = Y^2 - 1$', *J. Math. Anal. Appl.* **114**, 584–592.

[79] Meyer, K. (1970), 'Generic bifurcation of periodic orbits', *Transactions A.M.S.* **149**, 95–107.

[80] Michelson, D. (1986), 'Steady solutions of the Kuramoto-Sivashinsky equation', *Physica D* **19**, 89–111.

[81] Michelson, D. & Sivashinsky, G. I. (1977), 'Nonlinear analysis of hydrodynamic instability in laminar flames—II. Numerical experiments', *Acta Astronautica* **4**, 1207–1221.

[82] Montgomery, D. & Zippin, L. (1995), *Topological Transformation Groups*, New York: Interscience.

[83] Moser, J. (1967), 'Convergent series expansions for quasi-periodic motions', *Math. Ann.* **169**, 136–176.

[84] Myers, M., Holmes, P., Elezgaray, J. & Berkooz, G. (1995), 'Wavelet projections of the Kuramoto-Sivashinsky equation I. Heteroclinic cycles and modulated traveling waves for short systems', *Physica D* **86**, 396–427.

[85] Nicolaenko, B., Scheurer, B., & Temam, R. (1985), 'Some global dynamical properties of Kuramoto-Sivashinsky equations: Nonlinear stability and attractors', *Physica D* **16**, 155–183.

[86] Oldeman, B. E., Champneys, A. R. & Krauskopf, B. (2001), *Homoclinic branch switching: a numerical implementation of Lin's method*, Applied Nonlinear Mathematics Research Report 2001.11, University of Bristol.

[87] Ovsyannikov, I. M. & Shil'nikov, L. P. (1986), 'On systems with a saddle-focus homoclinic curve', *Mat. Sb.* **130 (172)** No. 4, 552–570, English transl., (1987) *Math. USSR-Sb.* **58**, 557–574.

[88] Palis, J. & de Melo, W. (1982), *Geometric Theory of Dynamical Systems*, translated by Manning, A. K., Springer-Verlag, New York, Heidelberg, Berlin.

[89] Palmer, K. J. (1984), 'Exponential Dichotomies and Transversal Homoclinic Points', *J. Diff. Eq.* **55**, 225–256.

[90] Peixoto, M. (1967), 'On an approximation theorem of Kupka and Smale', *Journal of Differential Equations* **3**, 214–227.

[91] Robinson, R. C. (1970), 'Generic properties of conservative systems I, II', *Amer. J. Math.* **92**, 562–603, 897–906.

[92] Robinson, C. (1968), 'A global approximation theorem for Hamiltonian systems', *Proc. AMS Summer Institute on Global Analysis*, Amer. Math. Soc., Providence, RI, 233–243.

[93] Ruelle, D. (1973), 'Bifurcations in the presence of a symmetry group', *Arch. Rat. Mech. Anal.* **51**, 136–152.

[94] Sandstede, B. (1993), *Verzweigungtheorie homokliner Verdopplungen*, PhD thesis, IAAS Report No. 7, University of Stuttgart.

[95] Sevryuk, M. B. (1986), 'Reversible systems', Lecture Notes in Mathematics, vol. 1211, Springer, Berlin.

[96] Sevryuk, M. B. (1998), 'The finite dimensional reversible KAM theory', *Physica D* **111**, 132–147.

[97] Shil'nikov, L. P. (1965), 'A case of the existence of a countable number of periodic motions', *Dokl. Akad. Nauk SSSR* **160**, 558–561, English translation (1965): *Soviet Math. Dokl.* **6**, 163–166.

[98] Shil'nikov, L. P. (1972), 'On the question of the structure of an extended neighbourhood of a rough saddle-node equilibrium', *Math. USSR. Sb.* **10**, 91–102.

[99] Sivashinsky, G. I. (1977), 'Nonlinear analysis of hydrodynamic instability in laminar flames—I. Derivation of basic equations', *Acta Astronautica* **4**, 1177–1206.

[100] Smale, S. (1967), 'Differentiable dynamical systems', *Bull. Amer. Math. Soc.* **73**, 747–817.

[101] Sparrow, C. (1982), *The Lorenz equations: bifurcations, chaos and strange attractors*, Springer-Verlag, New York.

[102] Szlenk, W. (1984), *An Introduction to the Theory of Smooth Dynamical Systems*, John Wiley & Sons.

[103] Takens, F. (1973), 'Normal forms for certain singularities of vector fields', *Ann. Inst. Fourier* **23**, 163–95.

[104] Takens, F. (1974), 'Forced oscillations and bifurcations', *Comm. Math. Inst. Univ. Utrecht* **3**, 1–59, also in *Global analysis of dynamical systems* (2001), Inst. Phys., Bristol, 1–61.

[105] Takens, F. (1974), 'Singularities of vector fields', *Publ. Math. I. H. E. S.* **43**, 48–100.

[106] Toland, J. F. (1988), 'Existence and uniqueness of heteroclinic orbits for the equation $\lambda u''' + u' = f(u)$', *Proc. Roy. Soc. Edinburgh A* **109**, 23–36.

[107] Troy, W. C. (1989), 'The existence of steady solutions of the Kuramoto-Sivashinsky equation', *J. Diff. Eqns.* **82**, 269–313.

[108] van den Berg, J. B., van Gils, S. A. & Visser, T. P. P. (2003), 'Parameter dependence of homoclinic solutions in a single long Josephson junction', *Nonlinearity* **16**, 707–717.

[109] Vanderbauwhede, A. (1990), *Local bifurcation and symmetry* **75**, Research Notes in Mathematics, London: Pitman.

[110] Vanderbauwhede, A. (1992), Branching of periodic solutions in time-reversible systems, *in* Broer, H. W. & Takens, F. (eds.), '*Geometry and analysis in nonlinear dynamics*', Burnt Mill, Harlow.

[111] Vanderbauwhede, A. (1992), 'Bifurcation of degenerate homoclinics', *Results in Mathematics* **21**, 211–223.

[112] Vanderbauwhede, A. & Fiedler, B. (1992), 'Homoclinic period blow-up in reversible and conservative systems', *Z. Angew. Math. Phys.* **43**, 292–318.

[113] Verhulst, F. (1996), *Nonlinear Differential Equations and Dynamical Systems*, Springer-Verlag: Berlin, Heidelberg, New York.

[114] Wagenknecht, T. (2001), *Reversible homoclinic pitchfork bifurcation*, Preprint No M14/01, TU Ilmenau.

[115] Webster, K. N. & Elgin, J. N. (2003), 'Asymptotic Analysis of the Michelson System', to appear in *Nonlinearity*.

[116] Wiggins, S. (1990), *Introduction to Applied Nonlinear Dynamical Systems and Chaos*, Springer-Verlag, New York, Berlin, Heidelberg.

[117] Wiklund, K. O. & Elgin, J. N. (1996), 'Multifractality of the Lorenz system', *Phys. Rev. E* **54**, 1111–1119.

[118] Wilczak, D. (2003), 'Chaos in the Kuramoto-Sivashinsky equations - a computer assisted proof', to appear in *J. Differential Eq.*.